TTI: BDL76

Texas Transportation Institute

COMPARISON OF RESILIENT MODULUS VALUES USED IN PAVEMENT DESIGN

Technical Report BDL76-1

TEXAS TRANSPORTATION INSTITUTE
THE TEXAS A&M UNIVERSITY SYSTEM
COLLEGE STATION, TEXAS

FLORIDA DEPARTMENT OF TRANSPORTATION

in cooperation with the
Federal Highway Administration and the
Florida Department of Transportation

Final Report

COMPARISON OF RESILIENT MODULUS VALUES USED IN PAVEMENT DESIGN

Research Project Title: Comparison of Resilient Modulus Values Used in Pavement Design
Contract No. BDL76

Submitted to:

Florida Department of Transportation
605 Suwannee Street
Tallahassee, FL 32399

TEXAS TRANSPORTATION INSTITUTE

Jeong Ho Oh
Emmanuel G. Fernando
Materials and Pavements Division
3135 TAMU
College Station, TX 77343-3135

January 2011

DISCLAIMER

The opinions, findings, and conclusions expressed in this publication are those of the authors and not necessarily those of the State of Florida Department of Transportation. This report does not constitute a standard, specification, or regulation, nor is it intended for construction, bidding, or permit purposes. The United States Government and the State of Florida do not endorse products or manufacturers. Trade or manufacturers' names appear herein solely because they are considered essential to the object of this report. The engineer in charge of the project was Dr. Emmanuel G. Fernando.

SI* (MODERN METRIC) CONVERSION FACTORS

APPROXIMATE CONVERSIONS TO SI UNITS

Symbol	When You Know	Multiply By	To Find	Symbol
	LENGTH			
in	inches	25.4	millimeters	mm
ft	feet	0.305	meters	m
yd	yards	0.914	meters	m
mi	miles	1.61	kilometers	km
	AREA			
in^2	square inches	645.2	square millimeters	mm^2
ft^2	square feet	0.093	square meters	m^2
yd^2	square yards	0.836	square meters	m^2
ac	acres	0.405	hectares	ha
mi^2	square miles	2.59	square kilometers	km^2
	VOLUME			
fl oz	fluid ounces	29.57	milliliters	ml
gal	gallons	3.785	liters	l
ft^3	cubic feet	0.028	cubic meters	m^3
yd^3	cubic yards	0.765	cubic meters	m^3
NOTE: Volumes greater than 1000 l shall be shown in m^3.				
	MASS			
oz	ounces	28.35	grams	g
lb	pounds	0.454	kilograms	kg
T	short tons (2000 lb)	0.907	megagrams	Mg
	TEMPERATURE (exact)			
°F	Fahrenheit temperature	5(F-32)/9 or (F-32)/1.8	Celcius temperature	°C
	ILLUMINATION			
fc	foot-candles	10.76	lux	l
fl	foot-Lamberts	3.426	candela/m^2	cd/m^2
	FORCE and PRESSURE or STRESS			
lbf	poundforce	4.45	newtons	N
psi	poundforce per square inch	6.89	kilopascals	kPa

APPROXIMATE CONVERSIONS FROM SI UNITS

Symbol	When You Know	Multiply By	To Find	Symbol
	LENGTH			
mm	millimeters	0.039	inches	in
m	meters	3.28	feet	ft
m	meters	1.09	yards	yd
km	kilometers	0.621	miles	mi
	AREA			
mm^2	square millimeters	0.0016	square inches	in^2
m^2	square meters	10.764	square feet	ft^2
m^2	square meters	1.195	square yards	yd^2
ha	hectares	2.47	acres	ac
km^2	square kilometers	0.386	square miles	mi^2
	VOLUME			
ml	milliliters	0.034	fluid ounces	fl oz
l	liters	0.264	gallons	gal
m^3	cubic meters	35.71	cubic feet	ft^3
m^3	cubic meters	1.307	cubic yards	yd^3
	MASS			
g	grams	0.035	ounces	oz
kg	kilograms	2.202	pounds	lb
Mg	megagrams	1.103	short tons (2000 lb)	T
	TEMPERATURE (exact)			
°C	Celcius temperature	1.8C + 32	Fahrenheit temperature	°F
	ILLUMINATION			
lx	lux	0.0929	foot-candles	fc
cd/m^2	candela/m^2	0.2919	foot-Lamberts	fl
	FORCE and PRESSURE or STRESS			
N	newtons	0.225	poundforce	lbf
kPa	kilopascals	0.145	poundforce per square inch	psi

* SI is the symbol for the International System of Units. Appropriate rounding should be made to comply with Section 4 of ASTM E380.

(Revised August 1992)

TECHNICAL REPORT DOCUMENTATION PAGE

1. Report No.	2. Government Accession No.	3. Recipient's Catalog No.
BDL76-1		

4. Title and Subtitle	5. Report Date
COMPARISON OF RESILIENT MODULUS VALUES USED IN PAVEMENT DESIGN	October 2010 Published: January 2011
	6. Performing Organization Code

7. Author(s)	8. Performing Organization Report No.
Jeong Ho Oh and Emmanuel G. Fernando	BDL76-1

9. Performing Organization Name and Address	10. Work Unit No. (TRAIS)
Texas Transportation Institute The Texas A&M University System College Station, Texas 77843-3135	11. Contract or Grant No. BDL76

12. Sponsoring Agency Name and Address	13. Type of Report and Period Covered
Florida Department of Transportation Research and Development Office 605 Suwannee Street, MS 30 Tallahassee, Florida 32399-0450	Technical Report August 2008 – January 2011
	14. Sponsoring Agency Code

15. Supplementary Notes

Research performed in cooperation with the Florida Department of Transportation.
Research Project Title: Comparison of Resilient Modulus Values Used in Pavement Design

16. Abstract

The Mechanistic-Empirical Pavement Design Guide (M-E PDG) requires the resilient modulus (M_R) of underlying materials for both new construction and rehabilitation projects. For the latter projects, the M-E PDG recommends using nondestructive test (NDT) methods such as the falling weight deflectometer (FWD) to characterize the in-situ resilient modulus of underlying materials. Considering that the performance models in the new guide were calibrated using resilient modulus data from laboratory tests, there is a need to convert the resilient modulus obtained from NDT tests to equivalent laboratory values for inputs to the M-E PDG program. In this project, Texas Transportation Institute researchers and engineers with the Florida Department of Transportation (FDOT) conducted a cooperative effort to evaluate correction factors for overlay design based on the M-E PDG. To evaluate correction factors for base, mechanically stabilized subgrade and embankment materials used on Florida pavements, researchers reviewed available data and findings from earlier projects to compile information that can be used for this evaluation. In consultation with FDOT engineers, researchers also developed field and laboratory test plans to collect additional data to fill gaps in the available information as identified from the literature review. Based on these plans, field and laboratory tests were conducted to characterize material properties of in-service pavement sections. Field tests included FWD, portable seismic pavement analyzer (PSPA), dynamic cone penetrometer, and material sampling of asphalt concrete cores and underlying materials to measure the field moisture contents at the time of tests. Laboratory tests included resilient modulus, dynamic modulus, dynamic shear rheometer, soil suction and extractions to characterize properties of asphalt concrete mixtures and underlying materials for evaluating correction factors and investigating the applicability of the PSPA for in-situ assessment of asphalt concrete layer modulus. Researchers analyzed the test data to determine correction factors and to evaluate the relationships between these factors and FWD backcalculated layer moduli. This report documents the efforts made to evaluate correction factors applicable to Florida pavement materials for flexible pavement overlay design based on the M-E PDG.

17. Key Word	18. Distribution Statement
M-E PDG program, Resilient modulus, Overlay design, Correction factor, Sensitivity analysis, Soil suction, Nondestructive testing, Falling weight deflectometer, Portable seismic pavement analyzer	

19. Security Classif. (of this report)	20. Security Classif. (of this page)	21. No. of Pages	22. Price
Unclassified	Unclassified	260	

Form DOT F 1700.7 (8-72) Reproduction of completed page authorized

ACKNOWLEDGMENTS

The work reported herein was conducted as part of a project sponsored by the Florida Department of Transportation (FDOT) to support its implementation of the Mechanistic-Empirical Pavement Design Guide originally developed in National Cooperative Highway Research Program (NCHRP) Project 1-37A. The authors gratefully acknowledge the steadfast support and technical guidance of the project manager, Mr. Charles Holzschuher, of the State Materials Office, Florida Department of Transportation. Mr. Holzschuher played a major role in planning and executing the test program conducted in this project to characterize pavement sections for the purpose of developing a database for evaluating correction factors. Dr. David Horhota also provided valuable technical guidance and resilient modulus test data to this study.

The project was truly a cooperative effort between researchers and the Florida Department of Transportation. Without the steadfast cooperation of FDOT engineers, it would not have been possible to execute the test program established in this project. The researchers are extremely grateful to the FDOT engineers, technical specialists, and consultants who participated in this effort, and would like to acknowledge and give them credit in this report:

- Shanna Johnson
- Hyung Lee
- Jason Noel
- Pat Upshaw
- Bruce Dietrich
- Ulas Toros
- Emmanuel Uwaibi
- Jonathan Moxley
- Jarrod Hunte
- Greg Sholar
- Jamie Greene
- Michael Suggs

Finally, researchers acknowledge the assistance provided by Dr. Soheil Nazarian of the University of Texas at El Paso who served as a consultant on the operation and application of the portable seismic pavement analyzer. Dr. Nazarian also provided training to FDOT personnel on the use of the PSPA in this project.

EXECUTIVE SUMMARY

The primary objectives of this project were (a) to recommend correction factors for determining equivalent laboratory modulus values given the corresponding base, stabilized subgrade, and embankment moduli from in-situ pavement testing, and (b) to evaluate nondestructive tests with the falling weight deflectometer (FWD) and the portable seismic pavement analyzer (PSPA) to recommend a procedure for characterizing existing pavement condition for flexible pavement overlay design based on the mechanistic-empirical pavement design guide (M-E PDG). To accomplish these objectives, researchers and FDOT engineers executed a comprehensive work plan that included the following tasks:

- Reviewed available data and findings from earlier projects to compile information that can be used to accomplish the study objectives;
- Developed field and laboratory test plans to collect additional data to fill gaps in the available information as identified from the literature review.
- Conducted field and laboratory tests to characterize material properties of in-service pavement sections.
- Analyzed test data to determine correction factors (CFs) and establish the relationships between these factors and FWD backcalculated moduli.
- Conducted a sensitivity analysis to examine the impact of proposed CFs on design of asphalt concrete overlays using the M-E PDG program.
- Investigated a procedure for frequency correction of asphalt concrete modulus determined from PSPA.

Based on the research conducted, the following findings are noted:

- Using the *MODULUS 6.1* program, researchers conducted backcalculations of pavement layer moduli using the FWD data collected on in-service pavement sections tested during this project. For these backcalculations, researchers aimed to be within an average absolute error per sensor of five percent. For the majority of cases, this criterion was met, with an overall average absolute error per sensor of about three percent across all test stations. Comparisons of measured and predicted deflections showed excellent correlations between measured and predicted values on all test sections with standard errors of estimate (SEE) below 0.5 mils.

- Seismic moduli from PSPA tests showed coefficients of variation (COV) ranging from 1.4 to 25.4 percent, with an overall average COV of 9.7 percent. Researchers recognized during field testing that special caution needs to be taken when using the PSPA on open-graded surfaces. In analyzing the PSPA data, researchers used the average PSPA modulus per station to compare with the corresponding FWD modulus and dynamic asphalt concrete (AC) modulus from laboratory tests.
- Researchers analyzed dynamic cone penetrometer (DCP) data to estimate in-situ moduli of underlying layers using a correlation equation incorporated into the M-E PDG program. From this analysis, researchers found that the base modulus determined from DCP measurements ranged from 30 to 70 ksi. The subgrade modulus varied from 20 to 50 ksi while the embankment modulus ranged from 15 to 35 ksi.
- During field tests, researchers collected underlying material samples to determine field moisture contents. These measurements were conducted so that comparisons between laboratory and FWD backcalculated moduli can be made based on the in-situ moisture condition at the time of the FWD test. From these measurements, researchers found that the base layer moisture content varied from 5.4 to 15 percent. District 6 base materials generally had lower moisture contents than other areas. Most groundwater table depths were found to be within 10 feet except for District 3 sections and test sections located in Alachua County in District 2.
- For characterizing the resilient modulus (M_R), researchers proposed a modified form of the M-E PDG resilient modulus model that includes a term to account for the effect of soil moisture based on the material's soil-water characteristic curve. Researchers fitted the resilient modulus and soil suction data to the proposed resilient modulus model, and found that the model fitted the test data reasonably well as indicated by the goodness-of-fit of the model predictions.
- Researchers generated charts showing the relationships between calculated correction factors for base, stabilized subgrade and embankment materials and the corresponding FWD backcalculated modulus. To quantify these relationships, researchers fitted a power law model to the data and found that the model gave a

reasonable fit to the data as indicated by the goodness-of-fit statistics from the regression analysis. Researchers also determined the 95 percent confidence interval bands of the fitted curves to account for the variability in calculated CFs.

- For a given material, researchers calculated correction factors at selected depths within the layer. For the base and stabilized subgrade, researchers found the CFs to be slightly higher at locations closest to the top of the layer compared to the calculated CFs at the lower depths. The higher CF is mainly attributed to the higher calculated bulk stress under the FWD load at the upper depths resulting in a higher resilient modulus. In contrast to the base and stabilized subgrade, the calculated CFs for the embankment tends to increase with depth due to the higher calculated gravimetric stresses within this layer and the diminished influence of the surface load.
- Comparison of CFs determined from the two approaches used in this project show the fitted CF curves based on NCHRP 1-28A recommended stresses to be generally higher than those calculated based on FWD load induced stresses. Researchers note that the NCHRP recommended bulk stress is close to the upper limit of the calculated bulk stresses based on the FWD load. A higher bulk stress would give a higher resilient modulus resulting in a higher correction factor. Researchers also found that the fitted CF curve based on calculated FWD load induced stresses generally lies between the fitted CF curve based on NCHRP recommended stresses and the lower bound of the 95 percent confidence interval for these CFs.
- Researchers conducted a sensitivity analysis to evaluate the potential impact of the calculated CFs on overlay designs using the M-E PDG program based on a performance criterion of 35 percent alligator cracking. The results from this analysis indicate that the required overlay thickness is most sensitive to the variation of CFs for the base material where a 1-inch difference in required overlay thickness was determined between CFs corresponding to the lower and upper bounds of the 95 percent confidence interval for the fitted CF curve. However, if the overlay thickness based on the fitted curve (corresponding to the mean CF) is used as the reference, the difference is half an inch in either direction. The sensitivity was found to be less for the stabilized subgrade where a maximum

difference of 0.5-inch was obtained. For the embankment material, the results show no differences in the required overlay thickness for the range of correction factors considered in the analysis. The sensitivity analysis also showed a maximum difference of 1.5 inches in required overlay thickness when the correction factors for base, stabilized subgrade and embankment were simultaneously varied from the respective lower bound values to the corresponding upper bound values.

- Researchers compared AC moduli determined from laboratory dynamic modulus tests with corresponding values determined from FWD and PSPA measurements. From these comparisons, researchers found a significant linear relationship between the FWD backcalculated AC moduli and laboratory dynamic moduli determined at corresponding FWD test frequencies. A significant linear relationship was also observed between laboratory dynamic moduli and frequency corrected PSPA AC moduli.
- To correct PSPA AC modulus, researchers investigated a procedure to determine a composite modulus based on properties of individual lifts using Odemark's equation. For this investigation, researchers used data obtained from dynamic modulus (DM), dynamic shear rheometer (DSR), and volumetric tests conducted on 14 cores taken from three of the field sections tested. Using data from DSR tests and extractions done on individual lifts, researchers performed frequency corrections of PSPA moduli using Odemark's equation. Researchers then compared the corrected PSPA moduli from this analysis with the corrected moduli based on data from laboratory dynamic modulus tests. Although the number of data points for this comparison is rather limited, the trend line shows a statistically reasonable agreement in adjusted PSPA modulus determined from the proposed approach when compared to the adjusted PSPA modulus based on DM test data that is regarded as the reference.
- To provide an approximate but simpler method of correcting the PSPA modulus determined from field testing, researchers also evaluated the relationship between the measured PSPA moduli and the corresponding moduli after correction. In this regard, researchers developed an equation for correcting the PSPA modulus based on the pavement temperature at the time of test. The resulting equation was found

to provide fairly good predictions of corrected PSPA moduli over the range of pavement temperatures at which PSPA tests were conducted. Researchers provide this equation as an alternative method for correcting PSPA modulus when DSR and volumetric test data are not readily available.

Given the above findings, researchers offer the following recommendations with respect to implementing the M-E PDG program for thickness design of flexible pavement overlays:

- From the evaluation of correction factors, researchers recommend that the fitted curves based on calculated FWD load induced stresses be considered for converting FWD backcalculated modulus to the equivalent laboratory resilient modulus for asphalt concrete overlay design based on the M-E PDG. Employing these fitted curves is expected to provide overlay thickness designs that are between the thickness designs based on the lower bound and fitted CFs obtained using NCHRP recommended stress levels. Using the fitted curve to the calculated CFs based on FWD load induced stresses is consistent with the recommended use of average input values for performance predictions using the M-E PDG program.
- The Florida DOT presently uses the FWD to estimate the embankment modulus. Researchers recommend that the Department consider expanding the application of the FWD for nondestructive assessment of pavement layer moduli by backcalculation. In this project, researchers used the MODULUS program to backcalculate pavement layer moduli from measured FWD deflections. In general, the predicted deflection basins from backcalculations done in this project using MODULUS provided a reasonable match with the measured basins for flexible pavement sections that covered the range of materials found in Florida. Based on this experience, researchers recommend that the Department consider using the MODULUS program for backcalculating pavement layer moduli from FWD deflections.
- Recognizing that ground penetrating radar, DCP and PSPA can support FWD data interpretation, researchers recommend that the Department adopt an integrated approach of collectively utilizing these pavement evaluation tools to provide supporting information needed for thickness design of flexible pavement overlays using the M-E PDG.

TABLE OF CONTENTS

LIST OF FIGURES

FIGURE Page

FIGURE Page

FIGURE Page

FIGURE Page

FIGURE Page

FIGURE Page

FIGURE Page

FIGURE Page

FIGURE Page

LIST OF TABLES

TABLE Page

TABLE Page

CHAPTER I. INTRODUCTION

BACKGROUND

The National Cooperative Highway Research Program (NCHRP) Project 1-37A delivered the *Mechanistic-Empirical Pavement Design Guide* (M-E PDG) and its companion software (Version 0.7) in 2004. The new M-E PDG requires the resilient modulus (M_R) of underlying materials for both new construction and rehabilitation projects. For the latter projects, the M-E PDG recommends using nondestructive test (NDT) methods such as the falling weight deflectometer (FWD) to characterize the in-situ resilient modulus of underlying materials. Considering that the performance models in the new guide were calibrated using resilient modulus data from laboratory tests, there is a need to convert the resilient modulus obtained from NDT tests to equivalent laboratory values for inputs to the M-E PDG program. To address this need, the present project aims to establish guidelines for using the FWD with other NDT methods to get comparable laboratory resilient modulus values for the base, stabilized subgrade, and embankment materials used by the Florida Department of Transportation (FDOT).

RESEARCH OBJECTIVES

The primary objectives of this project are:

- Recommend correction factors to convert in-situ resilient modulus from nondestructive tests to the equivalent laboratory modulus for overlay design based on the M-E PDG ; and
- Evaluate nondestructive tests with the FWD and the portable seismic pavement analyzer (PSPA) to recommend a procedure for characterizing existing pavement layer moduli for overlay design.

To accomplish these objectives, researchers conducted the following tasks:

- Reviewed available data and findings from earlier projects to compile information that can be used to accomplish the study objectives;
- Developed field and laboratory test plans to collect additional data to fill gaps in the available information as identified from the literature review;

- Conducted field and laboratory tests to characterize material properties of in-service pavement sections;
- Analyzed test data to determine correction factors (CFs) and establish the relationships between these factors and FWD backcalculated moduli;
- Conducted sensitivity analyses to examine the impact of proposed CFs on design of pavement overlays using the M-E PDG program; and
- Developed a procedure to correct asphalt concrete modulus determined from the PSPA to the corresponding FWD backcalculated modulus.

SCOPE OF RESEARCH REPORT

This report documents the efforts made to establish correction factors for overlay designs based on the M-E PDG. The report is organized into the following chapters:

- Chapter I provides the impetus for this project and states its objectives.
- Chapter II describes the review of available information related to this study.
- Chapter III presents the field and laboratory test plans to collect additional data to fill gaps in the available information as identified from the above review.
- Chapter IV documents the field and laboratory tests to characterize in-service pavement sections and the analysis of the test data.
- Chapter V presents the development of the correction factors.
- Chapter VI presents the procedure to correct PSPA asphalt concrete modulus.
- Chapter VII summarizes the findings from this project and presents recommendations for future efforts.

The appendices provide supporting material for the tasks conducted in this project that are documented in the different chapters of this report.

CHAPTER II. DEVELOPMENT OF TEST PROGRAM

This chapter describes the development of a test program for evaluating correction factors on flexible pavement materials based on the M-E PDG rehabilitation design procedure. Researchers first gathered available information from two previous FDOT projects conducted by the Florida State University (FSU) and the Texas Transportation Institute (TTI). Based on this review and discussions with the project advisory committee, researchers came up with a field and laboratory test program to fill gaps in the available data.

REVIEW OF FSU STUDY

Ping et al. (2000) conducted a study for evaluating the resilient moduli of Florida pavement soils based on field and laboratory tests. They conducted a field test program to characterize the in-situ bearing behavior of pavement layers on selected types of pavement soils in Florida. Figure 2.1 shows the distribution of the twenty sites that cover different soil and climatic conditions in the state. On each site, FSU researchers and FDOT personnel conducted FWD and plate bearing tests, field density and moisture content measurements, and trenching to establish the pavement layer profile and collect material samples for laboratory testing. On these samples, the State Materials Office (SMO) molded laboratory specimens to characterize the resilient moduli at optimum and field moisture contents and at different stress states.

The FSU project found FWD backcalculated moduli to be 1.5 – 1.9 times greater than laboratory resilient moduli. In addition, researchers reported that laboratory resilient moduli obtained at in-situ moisture content were more compatible with other field test results than the resilient moduli determined at optimum moisture content.

Table 2.1 summarizes the available data from the FSU project. Since this project was completed, the FSU test sites have either been rehabilitated, or been programmed for rehabilitation. Researchers also considered the aging that has occurred on the asphalt concrete materials at the sites over the 10-year period since the FSU study was completed. Therefore, the decision was made to conduct FWD tests on all sections to obtain more representative data, and to conduct PSPA and dynamic cone penetrometer (DCP) tests at

the same time. With respect to resilient modulus data, SMO conducted additional laboratory tests to fill gaps, particularly in the resilient modulus data at optimum moisture content for the base materials found on the FSU sections.

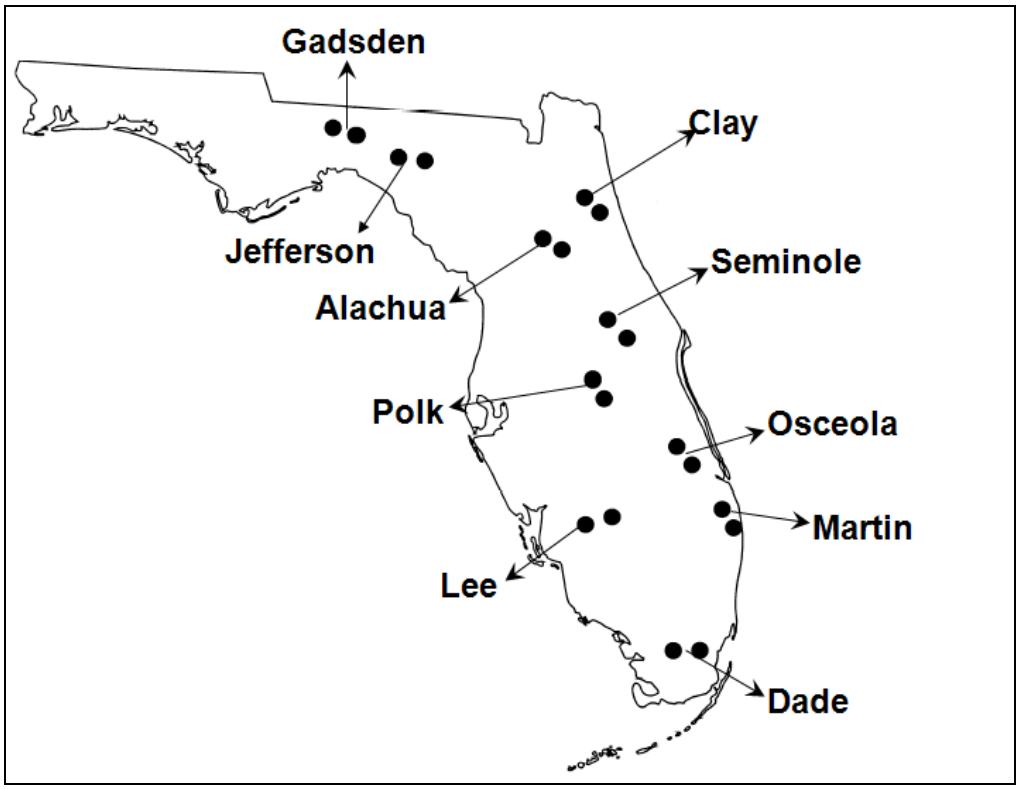

Figure 2.1. Sections Tested in FSU Project.

Table 2.1. Summary of Available Data from FSU Study.

County	Rdwy. ID	Route	FWD	Mr (optimum)			Mr (field)		
				Base	Sub.	Embank.	Base	Sub.	Embank.
Jefferson	5402000	US 27	•	N/A	N/A	N/A	•	N/A	•
Gadsden	5002000	US 27	•	N/A	•	•	•	•	•
Alachua	2606000	US 301	N/A	N/A	•	•	•	•	•
Clay	7102000	US 17	N/A	N/A	•	•	•	•	•
Seminole	7702000	SR 414	•	N/A	•	•	•	•	•
Osceola	9206000	US 441	•	N/A	•	•	•	•	•
Dade	8712000	US 41	•	N/A	•	•	•	N/A	N/A
Martin	8901000	US 1	•	N/A	•	•	•	•	•
Polk	1602000	US 17	•	N/A	•	•	N/A	•	•
Lee	1200500	SR 884	•	N/A	•	•	•	•	•

REVIEW OF TTI STUDY

Oh and Fernando (2008) conducted a Florida DOT project to develop thickness design tables based on the M-E PDG. In that project, TTI researchers and Florida DOT engineers conducted a cooperative effort to establish and characterize field test sections for the purpose of compiling a database of materials, geometric, and traffic-related design variables with which to calibrate the M-E PDG models to Florida conditions. Figure 2.2 illustrates the distribution of the M-E PDG test sites established from this earlier project. The test sites are spread throughout Florida. The numbers inside the parentheses on the map give, respectively, the counts of flexible and rigid pavement sections at a given site. A total of 15 hot-mix asphalt and 16 Portland cement concrete (PCC) sections were established during the previous project. Table 2.2 summarizes the available test data on the flexible pavement sections that are of relevance to the current project. In addition to the data identified in this table, researchers conducted soil suction tests, and SMO characterized asphalt concrete cores taken from field test sites to determine dynamic modulus, volumetric properties and binder temperature-viscosity relationships.

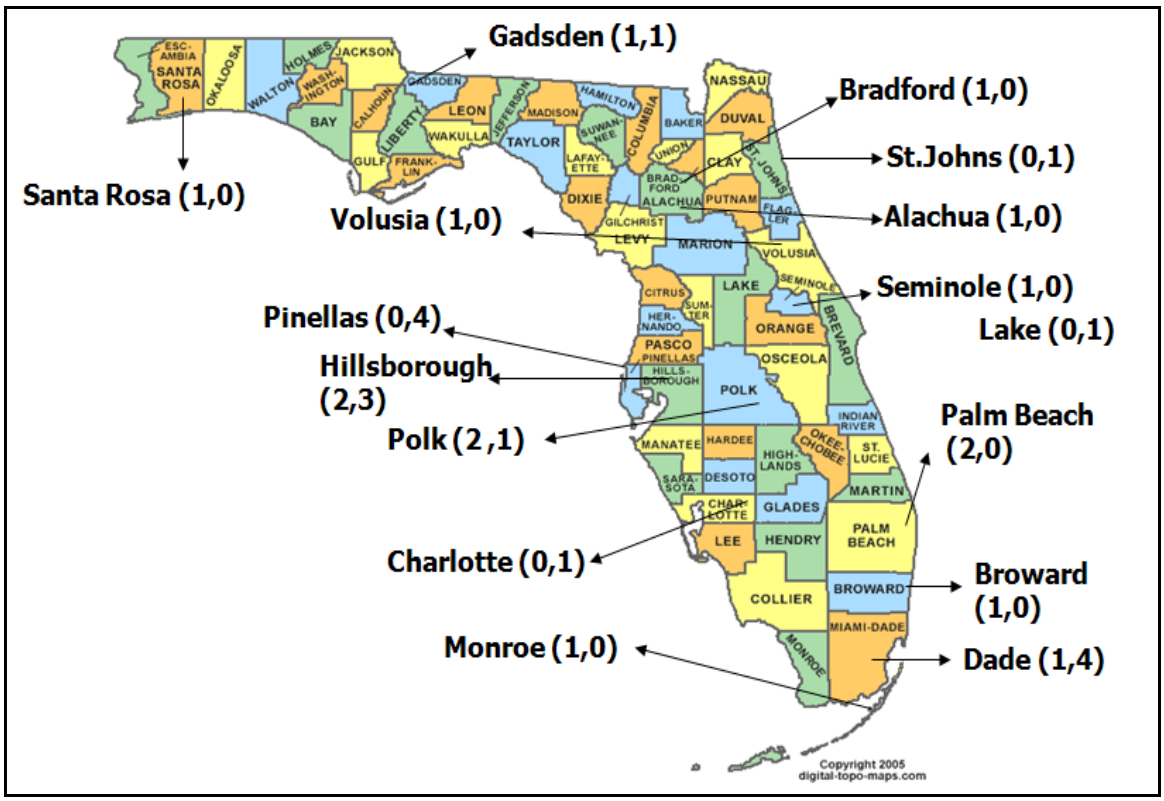

Figure 2.2. Sections Tested in M-E PDG Implementation Project.

Table 2.2. Summary of Available Data from TTI Study.

County	Rdwy. ID	Route	FWD	Mr (optimum)			Mr (field)		
				Base	Sub.	Emb ank.	Base	Sub.	Emb ank.
Alachua	26005000	SR 222	•	•	•	•	•	•	•
Bradford	28040000	SR 18	•	SBRM*	•	•	SBRM	N/A	•
Broward	86190000	SR 823	•	•	•	•	•	•	•
Dade	87060000	A1A	•	•	•	•	•	•	•
Gadsden	50010000	US 90	•	PCC	•	•	PCC	•	•
Hillsborough	10060000	US 41	•	•	•	•	•	•	•
	10160000	SR 60	•	•	•	•	•	•	•
Palm Beach	93100000	US27	•	•	•	•	N/A	N/A	N/A
	93310000	SR 710	•	•	•	•	•	•	•
Monroe	90060000	US 1	•	•	•	•	•	•	•
Polk	16003001	SR 563	•	•	•	•	•	•	•
	16250000	SR 37	•	PCC	•	•	PCC	•	•
Santa Rosa	58060000	SR 89	•	•	•	•	•	•	N/A
Seminole	77040000	SR 46	•	SBRM	•	•	SBRM	N/A	•
Volusia	79270000	SR 483	•	•	•	•	•	•	•

*Sand Bituminous Road Mix.

FIELD TEST PROGRAM

Based on the review of available information from previous projects and discussions with the project advisory committee, researchers established the field test program illustrated in Figure 2.3. Within each FSU and M-E PDG test site, researchers established a 100-ft segment centered about the trench where samples of the underlying materials were taken to characterize the resilient modulus during the earlier FSU and TTI projects. As shown in Figure 2.3, FWD, PSPA and DCP tests were conducted along the outer wheel path and between wheel paths of the selected test lane.

For the FWD data collection, SMO personnel applied two drops at 9,000 lb and one drop at 12,000 lb on the selected test stations shown in Figure 2.3. At each station, FWD full-time history data were collected along with measurements of pavement surface

temperatures. PSPA tests closely followed the FWD tests to minimize effects associated with temperature variations. Five PSPA modulus readings were obtained at each station.

After the FWD and PSPA tests, asphalt concrete (AC) cores were taken at the eight locations shown in Figure 2.3. Researchers measured the core thickness in the field. Cores were later tested in the laboratory to characterize AC mixture and binder properties.

SMO personnel also conducted DCP tests at the four locations shown in Figure 2.3. Researchers later processed the DCP data to estimate layer moduli from the DCP penetration rate according to the following equation:

$$M_r = 2555\left(\frac{292}{DCPI^{1.12}}\right)^{0.64} \quad (2.1)$$

where,

M_r = resilient modulus in psi, and

$DCPI$ = DCP index (penetration rate in mm/blow).

Equation (2.1) is provided as an option in the M-E PDG program for input of layer modulus when DCP data are available. On completion of DCP tests, researchers collected material samples to determine field moisture content in the laboratory.

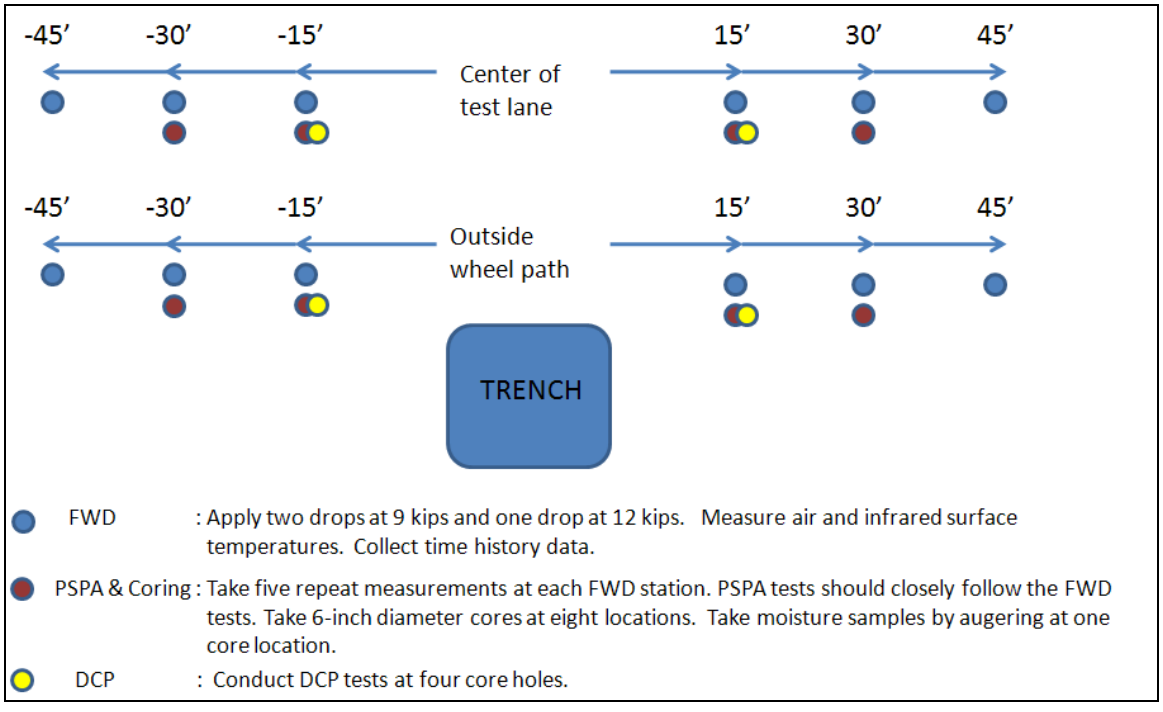

Figure 2.3. Field Test Plan on Test Sections.

LABORATORY TEST PROGRAM

Researchers established a laboratory test program to characterize the dynamic modulus of AC cores and to fill gaps in the available resilient modulus data. This program included the following laboratory tests conducted at the State Materials Office:

- resilient modulus at optimum moisture condition on samples considered representative of base materials found at the FSU test sites;
- extractions on AC cores to determine volumetric properties;
- dynamic modulus (DM) tests; and
- dynamic shear rheometer (DSR) tests on the binders extracted from AC cores to characterize temperature-viscosity relationships.

Characterizing AC samples is required to determine the master curve for correcting the PSPA seismic modulus to a value that corresponds to actual vehicle loading times. In this regard, the M-E PDG provides two options for establishing the master curve:

- Conduct dynamic modulus tests (AASHTO TP-62) on cores that meet the minimum height requirement of six inches specified in the test method; and
- Use the equation provided in the M-E PDG to predict dynamic modulus.

The latter approach requires running extractions to determine volumetric properties and DSR tests to characterize the temperature-viscosity relationship of the extracted binder. These properties are used in the M-E PDG program to predict dynamic modulus based on the following equation:

$$\log E^* = \delta + \frac{\alpha}{1 + e^{\beta + \gamma \log t_r}} \quad (2.2)$$

where t_r is the time of loading at the reference temperature, and the model coefficients δ, α, β, and γ are defined as follows:

$$\delta = 3.750 + 0.029\, p_{200} - 0.002\left(p_{200}\right)^2 - 0.003\, p_4 - 0.058 V_a - 0.802\left(\frac{V_{beff}}{V_{beff} + V_a}\right) \quad (2.3)$$

$$\alpha = 3.872 - 0.002\, p_4 + 0.004\, p_{38} - 0.000017\, p_{38}{}^2 + 0.005\, p_{34} \quad (2.4)$$

$$\beta = -0.603 - 0.394 \log \eta_T \quad (2.5)$$

$$\gamma = 0.313 \quad (2.6)$$

It is observed that δ and α are functions of volumetric mixture properties, specifically:

- air voids content V_a (%)
- effective bitumen content by volume V_{beff} (%),
- cumulative percent retained on ¾-inch sieve, p_{34},
- cumulative percent retained on 3/8-inch sieve, p_{38},
- cumulative percent retained on No. 4 sieve, p_4, and
- cumulative percent retained on No. 200 sieve.

The loading time t_r in Eq. (2.2) is related to the loading time t at the temperature of interest through the equation:

$$\log\frac{t_r}{t} = -1.256 \log\frac{\eta}{\eta_T} \quad (2.7)$$

In addition to the above, the laboratory test program also covered soil suction tests conducted at TTI to determine the soil-water characteristic curves of base materials considered representative of those found at the FSU test sites. Characterizing soil suction properties is crucial in assessing the resilient modulus and corresponding correction factor for the given field moisture conditions at the time of the FWD test. Researchers used the filter paper method (Bulut et al, 2001) to measure soil suction properties. From the test data, researchers determined the soil-water characteristic curve according to the following equations, which are used in the M-E PDG program.

$$V_w = C(h) \times \left[\frac{V_{sat}}{\left[\ln\left[\exp(1) + \left(\frac{S}{a_f} \right)^{b_f} \right] \right]^{c_f}} \right] \quad (2.8)$$

where,

$$C(h) = \left[1 - \frac{\ln(1 + \frac{S}{h_r})}{\ln\left(1 + \frac{1.45 \times 10^5}{h_r}\right)} \right] \tag{2.9}$$

V_w = volumetric water content,

V_{sat} = volumetric saturated water content,

S = soil suction in psi, and

a_f, b_f, c_f, & h_r = model parameters.

CHAPTER III. FIELD TEST DATA ANALYSIS

The field and laboratory test program presented in Chapter II was successfully completed with Florida DOT's assistance. The main objective of the field test program was to evaluate the supporting characteristics of pavement layers in-situ. This chapter documents how researchers analyzed the test data along with a brief description of how the data were collected. A complete set of data from tests in this project are presented in the appendices to this report.

FWD TEST DATA ANALYSIS AND RESULTS

FWD data on the FSU and M-E PDG sections were collected by SMO personnel. On each section, project personnel marked (within a 100-foot segment) 12 stations along the wheel path and between the wheel paths where FWD and PSPA measurements were taken as shown in Figure 3.1. As stated earlier, air and infrared surface temperatures were measured during FWD testing and full-time history data were collected. Researchers used the measured temperatures to estimate the AC mid-depth pavement temperature using FDOT's temperature correction procedure. Researchers used this mid-depth temperature as the test temperature to establish the master curve based on the laboratory data collected from tests on AC cores sampled from the FSU and M-E PDG sections. The FWD test frequency was determined from the full-time load history data.

Figure 3.1. Field Test Set-Up.

The objective of the FWD data processing is to assess the in-situ layer moduli. For this purpose, researchers used the *MODULUS 6.1* program (Scullion and Liu, 2001) based on their in-depth knowledge of program applications acquired from previous studies. Table 3.1 presents the results from the FWD modulus backcalculations. To check the accuracy of these results, researchers examined plots comparing measured and predicted deflections that are given in Appendix A of this report.

In backcalculating pavement layer moduli by deflection basin fitting, researchers aimed to be within an average absolute error per sensor of 5 percent. The MODULUS program determines this statistic as the average of the absolute differences between measured and predicted deflections on the first six FWD sensors. The results presented in Table 3.1 indicate that, for the majority of cases, the average absolute error per sensor is within the 5 percent tolerance. Across all test stations, researchers determined the overall average absolute error per sensor to be about 3 percent. As shown in the plots given in Appendix A, the modulus backcalculations achieved excellent correlations between measured and predicted deflections on all test sections with standard errors of estimate (SEE) below 0.5 mils.

PSPA TEST DATA ANALYSIS AND RESULTS

In this project, researchers investigated the application of the PSPA as an alternative method for in-situ characterization of asphalt concrete modulus, particularly on pavement sections with thin (< 3-inch thick) hot-mix surface layers. Backcalculating layer moduli from FWD deflections collected on thin AC pavements is a challenge since the predicted deflection basin is not sensitive to the asphalt concrete modulus. In this regard, the user needs additional information to assign an AC modulus that would yield realistic predictions of pavement response and performance. For example, researchers tried several backcalculations on section 12005000 in Lee County where the asphalt concrete layer is only 1.5 inches thick. Different solutions were obtained that covered a wide range of asphalt concrete modulus, with acceptable average errors per sensor of around 5 percent. In this case, the user should consider collecting additional information to decide which AC modulus is the most representative. For example, the user might review available data on the relationship between AC modulus and pavement temperature

for the particular asphalt mix tested in the field. Alternatively, the user might consider running the PSPA to determine a representative modulus value. The uncorrected in-situ PSPA AC modulus can be adjusted using the procedure or equation described later in Chapter 6 of this report. Another backcalculation can then be made where the AC modulus is fixed to the value obtained from the PSPA to determine the moduli of the underlying layers.

The operating principle of the PSPA is based on generating and observing stress waves in the pavement layers (Celaya and Nazarian, 2006). The Ultrasonic Surface Wave (USW) method is used for calculation of the seismic modulus. Using this method, the seismic modulus of the upper pavement layer, $E_{seismic}$, can be calculated using equation (3.1):

$$E_{seismic} = 2\rho\left[(1.13 - 0.16\nu)V_R\right]^2(1+\nu) \quad (3.1)$$

where V_R is the velocity of surface waves, υ is Poisson's ratio, and ρ is mass density. During this study, the Florida DOT purchased a PSPA unit that was used in the field tests conducted in this project. Training on the PSPA was provided by Dr. Soheil Nazarian of the University of Texas at El Paso. This training was conducted at the State Materials Office within the first year of the project.

On each FWD test station, researchers collected PSPA data on the same circular area where the FWD load was applied. Five measurements were taken on this area to determine an average seismic modulus per station. The PSPA data collection and analysis was achieved using the Version 3.2 SpaMgr program provided by Dr. Soheil Nazarian. Table 3.2 presents the PSPA test results along with statistics determined to check the repeatability of the PSPA measurements.

Researchers recognized during field testing that special caution needs to be taken when using the PSPA on open-graded surfaces. The coefficient of variation (COV) of the PSPA seismic modulus ranged from 1.4 to 25.4 percent, with an overall average COV of 9.8 percent. Celaya and Nazarian (2006) reported that the variability of PSPA is less than 3 percent when repeat measurements are made without moving the device and around 7 percent when the device is moved within a small area. Considering the different types of AC surface layers and the number of stations tested, researchers are of the

opinion that the PSPA measurements seem reasonable despite the higher COVs obtained at certain stations.

DCP TEST DATA ANALYSIS AND RESULTS

The automated dynamic cone penetrometer (ADCP) test was performed from the top of the base layer after cores were taken on a given section. During data collection, researchers were not able to complete the test at several locations where the penetration rate was too low (around 0.05 in/blow) indicating the presence of a very stiff base material. At these locations, SMO personnel aborted the test. These locations are on sections 93310000 in Palm Beach County, 86190000 in Broward County, 92060000 in Osceola County, 87120000 and 87060000 in Dade County, and 90060000 in Monroe County.

Researchers used a Microsoft Excel spreadsheet program provided by the Florida DOT to process the DCP data. Researchers first plotted the measured penetration depth against the number of blows. From this plot, the penetration rate was determined for each layer, and the layer modulus was calculated using equation (2.1). Figures 3.2 and 3.3 show processed DCP data on section 54020000 in Jefferson County. This example captures different slopes indicating the presence of different layers. The layer moduli based on the DCP data collected from this location were generally higher than the corresponding FWD backcalculated moduli presented in Table 3.1. Data for other sections are presented in Appendix B. From the DCP data processing, researchers found that the base modulus determined from DCP measurements ranged from 30 to 70 ksi. The subgrade modulus varied from 20 to 50 ksi while the embankment modulus ranged from 15 to 35 ksi.

Table 3.1. Summary of FWD Modulus Backcalculation Results.

District	County	State road	Station		Load (lbs)	Backcalculated Modulus (ksi)					Thickness (in.)		
						Surface	Base	Subgrade	Embankment	ERR/Sens	Surface	Base	Subgrade
1	Polk (16020)	US17 OWP	1A	-30	8,905	239.8	51.8	48.0	29.0	3.3	4.5	9.0	13.0
			2A	-15	8,916	266.2	49.5	48.0	25.7	3.3	4.5	9.0	13.0
			3A	15	8,861	274.6	70.8	48.0	22.3	4.0	4.5	9.0	13.0
			4A	30	8,982	262.3	72.8	48.0	21.8	3.5	4.6	9.0	13.0
		US17 Center	1B	-30	8,905	233.3	54.7	50.0	32.7	4.6	5.0	9.0	13.0
			2B	-15	8,960	227.5	54.9	50.0	27.4	3.7	5.0	9.0	13.0
			3B	15	8,839	233.8	64.5	50.0	25.5	6.4	4.5	9.0	13.0
			4B	30	8,850	268.3	65.9	50.0	21.7	3.3	4.6	9.0	13.0
1	Polk (16003)	SR563 OWP	1A	-30	8,938	419.5	50.0	35.8	29.6	3.9	4.0	10.0	24.0
			2A	-15	8,828	468.3	50.0	38.5	12.6	3.5	4.3	10.0	24.0
			3A	15	8,938	479.8	50.0	32.7	22.1	1.6	4.5	10.0	24.0
			4A	30	8,817	640.1	50.0	49.9	22.6	1.6	4.5	10.0	24.0
		SR563 Center	1B	-30	8,861	674.6	50.0	45.0	34.3	2.2	3.8	10.0	24.0
			2B	-15	8,817	472.1	50.0	42.4	14.4	3.3	4.5	10.0	24.0
			3B	15	8,861	679.3	50.0	40.8	16.0	1.9	4.3	10.0	24.0
			4B	30	8,905	693.0	50.3	50.0	17.5	2.4	4.3	10.0	24.0
1	Lee (12005)	SR884 OWP	1A	-30	8,883	800.0	62.2	20.0	21.6	5.6	1.5	11.5	12.0
			2A	-15	8,894	800.0	58.0	20.0	20.7	6.2	1.5	11.5	12.0
			3A	15	8,883	800.0	50.2	20.0	20.9	5.1	1.5	11.5	12.0
			4A	30	8,938	800.0	53.6	20.0	24.6	5.5	1.5	11.5	12.0
		SR884 Center	1B	-30	9,135	535.8	50.0	34.9	17.2	1.3	4.5	8.5	12.0
			2B	-15	9,146	502.4	50.0	36.3	16.2	1.8	4.5	8.5	12.0
			3B	15	9,058	593.2	51.2	23.3	16.5	0.3	4.5	8.5	12.0
			4B	30	9,058	498.0	50.0	27.4	17.6	1.7	4.3	8.5	12.0

Table 3.1. Summary of FWD Modulus Backcalculation Results (continued).

District	County	State road	Station		Load (lbs)	Backcalculated Modulus (ksi)					Thickness (in.)		
						Surface	Base	Subgrade	Embankment	ERR/Sens	Surface	Base	Subgrade
2	Alachua (26060)	US301 OWP	1A	-30	9,190	692.0	35.0	25.0	16.1	4.0	4.0	9.0	8.0
			2A	-15	9,245	850.0	40.0	30.0	18.0	3.9	4.0	9.0	8.0
			3A	15	9,168	665.0	20.0	20.0	12.0	5.0	3.2	9.0	8.0
			4A	30	9,091	680.0	20.0	20.0	9.7	4.4	3.1	9.0	8.0
		US301 Center	1B	-30	9,025	701.4	48.9	26.7	14.5	0.3	4.3	9.0	8.0
			2B	-15	9,255	930.0	45.0	30.0	15.3	3.5	4.2	9.0	8.0
			3B	15	9,190	807.0	35.0	30.0	19.8	4.3	3.3	9.0	8.0
			4B	30	9,058	840.0	40.0	24.5	17.9	4.9	3.0	9.0	8.0
2	Clay (71020)	US17 OWP	1A	-30	8,894	776.0	90.0	76.5	14.5	5.6	3.2	7.0	14.0
			2A	-15	8,719	1018.8	90.0	71.9	15.1	4.6	3.6	7.0	14.0
			3A	15	8,883	1040.0	140.0	64.1	13.3	5.6	3.5	7.0	14.0
			4A	30	8,861	796.0	140.0	47.7	9.7	4.9	4.5	7.0	14.0
		US17 Center	1B	-30	8,916	977.9	51.3	31.2	27.8	0.3	9.1	7.0	14.0
			2B	-15	8,905	1117.7	38.1	29.7	27.4	1.1	8.3	7.0	14.0
			3B	15	8,763	1014.4	100.0	64.0	23.3	4.7	4.5	7.0	14.0
			4B	30	8,916	1085.9	34.7	26.2	23.0	0.5	8.7	7.0	14.0
2	Alachua (26005)	SR222 OWP	1A	-30	9,047	800.0	55.0	40.0	15.0	4.6	4.8	15.0	30.0
			2A	-15	9,091	950.0	59.0	44.2	15.2	0.7	4.9	15.0	30.0
			3A	15	9,124	800.0	50.0	41.5	13.8	3.3	5.0	15.0	30.0
			4A	30	9,113	850.0	50.0	39.7	12.5	3.5	4.8	15.0	30.0
		SR222 Center	1B	-30	9,113	725.0	58.8	39.8	15.0	0.4	4.7	15.0	30.0
			2B	-15	9,135	736.8	54.6	33.3	16.4	0.6	4.9	15.0	30.0
			3B	15	9,135	732.2	50.0	49.5	13.9	1.0	4.9	15.0	30.0
			4B	30	9,058	731.0	61.2	38.2	16.1	0.1	4.9	15.0	30.0

Table 3.1. Summary of FWD Modulus Backcalculation Results (continued).

District	County	State road	Station		Load (lbs)	Backcalculated Modulus (ksi)					Thickness (in.)		
						Surface	Base	Subgrade	Embankment	ERR/Sens	Surface	Base	Subgrade
3	Jefferson (54020)	US27 OWP	1A	-30	8,861	504.3	31.0	29.4	8.5	1.5	5.0	7.5	11.5
			2A	-15	8,872	722.2	36.0	33.0	13.4	4.1	4.8	7.5	11.5
			3A	15	8,938	409.2	30.0	24.2	6.2	4.7	4.6	7.5	11.5
			4A	30	8,938	281.2	32.0	20.6	10.7	3.7	5.0	7.5	11.5
		US27 Center	1B	-30	8,916	526.8	43.0	37.4	14.3	1.8	4.8	7.5	11.5
			2B	-15	8,927	579.4	40.0	37.9	14.0	3.2	5.0	7.5	11.5
			3B	15	8,894	343.5	43.2	29.7	11.7	1.3	4.6	7.5	11.5
			4B	30	8,861	221.0	38.0	33.6	6.7	5.5	5.0	7.5	11.5
3	Gadsden (50020)	US27 OWP	1A	-30	8,883	543.8	21.8	20.0	14.0	0.6	7.0	8.5	23.0
			2A	-15	8,861	397.3	26.8	22.4	6.1	0.9	5.0	8.5	23.0
			3A	15	8,905	352.3	31.3	15.7	11.2	1.4	4.8	8.5	23.0
			4A	30	8,894	475.0	30.0	16.4	6.8	1.3	4.5	8.5	23.0
		US27 Center	1B	-30	8,916	536.9	28.4	23.8	10.3	1.1	6.0	8.5	23.0
			2B	-15	8,872	327.5	39.5	15.1	10.8	4.0	5.0	8.5	23.0
			3B	15	8,872	575.3	25.0	21.3	4.4	2.2	4.5	8.5	23.0
			4B	30	8,806	375.2	38.4	14.7	12.5	1.6	4.5	8.5	23.0
3	Santa Rosa (58060)	SR89 OWP	1A	-30	9,014	651.0	55.6	44.4	21.7	1.0	6.0	10.0	10.0
			2A	-15	9,004	464.5	57.6	20.0	17.5	0.5	6.0	10.0	10.0
			3A	15	8,993	448.7	54.8	50.0	22.9	2.1	6.0	10.0	10.0
			4A	30	8,993	370.7	32.0	25.6	14.3	4.5	6.0	10.0	10.0
		SR89 Center	1B	-30	8,894	664.2	47.1	32.6	20.8	0.9	6.0	10.0	10.0
			2B	-15	8,894	606.1	44.0	16.7	16.5	0.8	6.0	10.0	10.0
			3B	15	9,036	742.1	50.7	49.1	22.8	0.7	6.0	10.0	10.0
			4B	30	8,916	525.5	41.0	39.0	12.5	4.4	6.0	10.0	10.0

Table 3.1. Summary of FWD Modulus Backcalculation Results (continued).

District	County	State road	Station		Load (lbs)	Backcalculated Modulus (ksi)					Thickness (in.)		
						Surface	Base	Subgrade	Embankment	ERR/Sens	Surface	Base	Subgrade
4	Martin (89010)	US 1 OWP	1A	-30	8,982	1164.2	67.2	55.0	35.7	3.6	3.0	10.0	16.0
			2A	-15	9,058	871.2	90.3	70.0	32.4	2.9	3.3	10.0	16.0
			3A	15	9,014	670.2	116.3	55.0	46.4	5.8	3.0	10.0	16.0
			4A	30	8,993	838.3	106.8	80.0	42.4	4.9	2.8	10.0	16.0
		US 1 Center	1B	-30	8,883	1155.8	77.2	60.0	35.8	1.7	3.0	10.0	16.0
			2B	-15	8,916	1136.1	94.5	60.0	33.2	2.3	3.3	10.0	16.0
			3B	15	8,839	1023.2	128.2	60.0	38.8	3.5	3.0	10.0	16.0
			4B	30	8,905	665.0	139.5	60.0	40.1	4.0	3.0	10.0	16.0
4	Palm Beach (93310)	SR710 OWP	1A	-30	8,960	214.3	74.0	50.0	41.7	2.5	8.0	14.0	12.0
			2A	-15	8,982	227.9	63.9	50.0	31.2	2.8	7.5	14.0	12.0
			3A	15	8,993	233.7	72.8	50.0	39.3	2.8	8.3	14.0	12.0
			4A	30	8,916	201.3	80.3	50.0	40.5	2.7	8.0	14.0	12.0
		SR710 Center	1B	-30	8,916	212.2	84.2	50.0	45.8	3.3	8.0	14.0	12.0
			2B	-15	8,949	200.0	72.5	50.0	44.8	4.7	7.8	14.0	12.0
			3B	15	8,938	245.7	86.3	50.0	44.0	2.6	8.0	14.0	12.0
			4B	30	8,949	218.8	82.6	50.0	47.1	3.2	8.0	14.0	12.0
4	Palm Beach (93100)	US27 OWP	1A	-30	8,982	400.0	35.4	62.2	65.4	9.3	2.5	16.0	12.0
			2A	-15	8,916	400.0	33.8	43.5	71.1	6.9	2.5	16.0	12.0
			3A	15	9,124	400.0	29.8	63.7	63.7	6.8	2.5	16.0	12.0
			4A	30	8,938	400.0	27.9	34.5	75.6	5.9	2.5	16.0	12.0
		US27 Center	1B	-30	8,949	582.7	200.0	80.0	67.7	10.5	2.5	16.0	12.0
			2B	-15	8,763	517.6	154.8	110.0	83.0	8.2	2.5	16.0	12.0
			3B	15	9,004	531.6	193.8	110.0	102.6	7.1	2.5	16.0	12.0
			4B	30	8,795	423.2	154.9	110.0	78.3	5.3	2.5	16.0	12.0

Table 3.1. Summary of FWD Modulus Backcalculation Results (continued).

District	County	State road	Station		Load (lbs)	Backcalculated Modulus (ksi)					Thickness (in.)		
						Surface	Base	Subgrade	Embankment	ERR/Sens	Surface	Base	Subgrade
4	Broward (86190)	SR823 OWP	1A	-30	8,938	643.2	123.7	100.0	77.0	6.4	4.0	8.0	12.0
			2A	-15	8,850	507.5	139.1	100.0	82.0	6.2	4.0	8.0	12.0
			3A	15	8,730	389.7	179.2	100.0	84.6	6.3	4.0	8.0	12.0
			4A	30	8,971	522.5	112.8	100.0	68.3	6.6	4.0	8.0	12.0
		SR823 Center	1B	-30	8,949	582.7	200.0	80.0	67.7	10.5	4.3	8.0	12.0
			2B	-15	8,763	517.6	154.8	110.0	83.0	8.2	4.0	8.0	12.0
			3B	15	9,004	531.6	193.8	110.0	102.6	7.1	4.0	8.0	12.0
			4B	30	8,795	423.2	154.9	110.0	78.3	5.3	4.0	8.0	12.0
5	Seminole (77002)	SR414 OWP	1A	-30	8,927	615.4	56.2	50.0	10.0	2.8	5.3	12.0	12.0
			2A	-15	8,872	564.6	71.5	50.0	9.0	3.0	5.5	12.0	12.0
			3A	15	8,905	589.3	50.1	50.0	8.1	1.5	6.0	12.0	12.0
			4A	30	8,883	667.0	70.4	50.0	8.2	1.9	6.0	12.0	12.0
		SR414 Center	1B	-30	8,894	427.0	72.4	50.0	10.4	1.9	5.5	12.0	12.0
			2B	-15	8,883	504.3	71.6	50.0	9.8	2.8	5.8	12.0	12.0
			3B	15	8,806	551.1	69.9	50.0	8.1	1.2	6.0	12.0	12.0
			4B	30	8,850	388.3	77.6	50.0	8.2	1.5	6.0	12.0	12.0
5	Osceola (92060)	US441 OWP	1A	-30	8,850	495.3	108.6	50.0	12.8	2.6	8.3	11.0	18.0
			2A	-15	8,894	456.2	169.4	50.0	11.8	4.2	8.0	11.0	18.0
			3A	15	8,872	654.3	200.0	42.6	6.7	2.9	8.0	11.0	18.0
			4A	30	8,828	579.0	200.0	27.6	10.1	4.5	8.0	11.0	18.0
		US441 Center	1B	-30	8,949	309.3	120.7	50.0	14.8	3.2	8.5	11.0	18.0
			2B	-15	8,850	243.8	172.9	50.0	12.9	3.2	8.0	11.0	18.0
			3B	15	8,916	372.9	200.0	28.5	7.3	2.8	8.5	11.0	18.0
			4B	30	8,883	418.8	200.0	25.8	9.5	3.8	8.0	11.0	18.0

Table 3.1. Summary of FWD Modulus Backcalculation Results (continued).

District	County	State road	Station		Load (lbs)	Backcalculated Modulus (ksi)					Thickness (in.)		
						Surface	Base	Subgrade	Embankment	ERR/Sens	Surface	Base	Subgrade
5	Volusia (79270)	SR483 OWP	1A	-30	8,806	587.0	42.5	30.0	14.6	8.6	2.5	13.0	12.0
			2A	-15	8,784	533.0	44.6	30.0	15.6	8.7	2.5	13.0	12.0
			3A	15	8,784	621.0	45.3	35.0	15.2	7.8	2.5	13.0	12.0
			4A	30	8,828	600.0	47.4	40.0	14.5	8.4	2.5	13.0	12.0
		SR483 Center	1B	-30	8,763	627.0	48.6	40.4	17.7	7.2	2.5	13.0	12.0
			2B	-15	8,784	550.0	45.1	40.0	18.4	6.9	2.5	13.0	12.0
			3B	15	8,784	725.0	49.7	35.0	18.3	7.5	2.5	13.0	12.0
			4B	30	8,850	590.0	49.6	40.0	15.1	8.7	2.5	13.0	12.0
6	Dade (87120)	US41 OWP	1A	-30	8,806	652.3	100.0	87.0	85.2	4.4	3.8	9.5	12.5
			2A	-15	8,773	815.0	100.0	94.8	88.1	4.6	3.5	9.5	12.5
			3A	15	8,916	794.1	100.0	75.3	66.5	3.6	4.0	9.5	12.5
			4A	30	8,850	472.1	100.0	76.1	70.4	5.6	4.0	9.5	12.5
		US41 Center	1B	-30	9,025	594.7	130.0	107.2	85.6	4.2	4.0	9.5	12.5
			2B	-15	8,916	819.3	130.0	128.1	99.2	2.8	3.5	9.5	12.5
			3B	15	8,883	752.9	130.0	106.6	67.0	3.2	3.5	9.5	12.5
			4B	30	8,839	456.6	130.0	85.3	65.5	4.8	4.0	9.5	12.5
6	Dade (87060)	A1A OWP	1A	-30	8,971	820.0	95.0	30.0	24.0	1.5	8.0	14.0	16.0
			2A	-15	8,993	820.0	84.7	30.0	21.1	1.5	8.0	14.0	16.0
			3A	15	9,036	810.0	80.0	31.0	24.1	1.1	8.0	14.0	16.0
			4A	30	9,025	820.0	81.7	31.0	25.8	2.0	8.0	14.0	16.0
		A1A Center	1B	-30	8,982	790.0	63.0	40.0	18.3	0.5	8.0	14.0	16.0
			2B	-15	8,982	773.0	68.7	42.9	17.0	0.3	8.0	14.0	16.0
			3B	15	9,004	791.0	80.6	37.6	18.4	0.9	8.0	14.0	16.0
			4B	30	8,971	791.0	61.5	43.2	16.7	0.2	8.0	14.0	16.0

Table 3.1. Summary of FWD Modulus Backcalculation Results (continued).

District	County	State road	Station		Load (lbs)	Backcalculated Modulus (ksi)					Thickness (in.)		
						Surface	Base	Subgrade	Embankment	ERR/Sens	Surface	Base	Subgrade
6	Monroe (90060)	US1 OWP	1A	-30	8,828	486.4	20.0	0.0	14.2	9.4	4.0	24.0	-
			2A	-15	8,883	422.8	20.0	0.0	8.2	7.5	4.0	24.0	-
			3A	15	8,982	516.5	20.0	0.0	13.1	6.8	4.0	24.0	-
			4A	30	8,883	448.7	20.0	0.0	12.1	8.7	4.0	24.0	-
		US1 Center	1B	-30	9,014	650.0	19.9	0.0	18.7	7.0	4.0	24.0	-
			2B	-15	8,894	650.0	20.0	0.0	12.1	4.0	4.0	24.0	-
			3B	15	8,916	656.3	20.0	0.0	14.5	3.4	4.0	24.0	-
			4B	30	8,927	532.8	20.0	0.0	12.4	4.4	4.0	24.0	-
7	Hillsborough (10060)	US41 OWP	1A	-30	8,905	379.2	30.0	25.9	17.4	2.1	3.8	9.0	16.0
			2A	-15	8,828	380.0	37.2	23.8	19.7	2.4	3.5	9.0	16.0
			3A	15	8,905	380.0	27.0	24.8	13.7	3.0	4.0	9.0	16.0
			4A	30	8,850	383.4	27.0	22.3	16.0	1.0	4.0	9.0	16.0
		US41 Center	1B	-30	9,069	580.0	41.0	31.0	29.6	3.8	4.0	9.0	16.0
			2B	-15	9,058	580.0	46.5	32.6	30.5	1.1	3.5	9.0	16.0
			3B	15	9,047	580.0	41.9	32.3	25.8	0.6	3.5	9.0	16.0
			4B	30	9,036	580.0	41.0	31.0	23.6	2.0	4.0	9.0	16.0
7	Hillsborough (10160)	SR580 OWP	1A	-30	8,894	835.2	50.3	43.3	21.7	0.7	6.5	10.0	16.0
			2A	-15	8,828	840.0	39.5	31.0	29.1	2.3	9.0	10.0	16.0
			3A	15	8,839	809.8	40.0	37.8	21.5	1.4	5.0	10.0	16.0
			4A	30	8,806	788.5	40.0	34.3	20.5	0.8	5.5	10.0	16.0
		SR580 Center	1B	-30	8,883	500.0	47.7	44.0	35.0	4.3	6.0	10.0	16.0
			2B	-15	8,806	874.8	60.0	32.0	29.0	4.2	5.5	10.0	16.0
			3B	15	8,894	500.0	40.0	28.1	23.0	4.5	5.5	10.0	16.0
			4B	30	8,850	850.0	42.2	30.0	30.3	4.9	5.3	10.0	16.0

Table 3.2. Summary of PSPA Seismic Modulus Data.

District	County	State road	Station		PSPA Seismic Modulus(ksi) 1	2	3	4	5	Average (ksi)	STDEV (ksi)	COV %
1	Polk (16020)	US17 OWP	1A	-30	1350	1100	1060	1060	930	1100	153.8	14.0
			2A	-15	1210	1540	1060	1460	1317	1317.4	192.1	14.6
			3A	15	1155	1330	1255	1370	1277	1277.4	81.9	6.4
			4A	30	1100	1150	1520	1610	1350	1346	223.0	16.6
		US17 Center	1B	-30	1450	1020	1450	1660	1395	1395	232.9	16.7
			2B	-15	1480	1370	1510	1460	1230	1410	113.4	8.0
			3B	15	1560	1430	1400	1070	1000	1292	243.5	18.8
			4B	30	910	1210	1130	1410	1220	1176	180.8	15.4
1	Polk (16003)	SR563 OWP	1A	-30	1090	1200	1290	1200	1250	1206	75.0	6.2
			2A	-15	1200	1350	1380	1310	1410	1330	81.5	6.1
			3A	15	1370	1280	1350	1330	1550	1376	102.9	7.5
			4A	30	1010	1360	1020	1460	1040	1178	215.0	18.3
		SR563 Center	1B	-30	1580	1460	1660	1650	1760	1622	111.0	6.8
			2B	-15	1780	1660	1660	1850	1760	1742	82.0	4.7
			3B	15	1590	1570	1610	1560	1510	1568	37.7	2.4
			4B	30	1550	1580	1340	1340	1360	1434	120.3	8.4
1	Lee (12005)	SR884 OWP	1A	-30	1770	1910	1400	1470	1430	1596	229.5	14.4
			2A	-15	1650	1770	1470	1180	1620	1538	226.9	14.8
			3A	15	1290	1630	1710	1690	1580	1580	170.0	10.8
			4A	30	1560	1980	1960	1780	1630	1782	189.3	10.6
		SR884 Center	1B	-30	1350	1940	1470	1590	1560	1582	220.8	14.0
			2B	-15	2000	1900	1760	1680	1835	1835	123.6	6.7
			3B	15	2100	2070	2090	1710	1700	1934	209.4	10.8
			4B	30	1810	2150	1420	1670	1740	1758	264.0	15.0

Table 3.2. Summary of PSPA Seismic Modulus Data (continued).

District	County	State road	Station		PSPA Seismic Modulus(ksi) 1	2	3	4	5	Average (ksi)	STDEV (ksi)	COV %
1	Polk (16020)	US17 OWP	1A	-30	1350	1100	1060	1060	930	1100	153.8	14.0
			2A	-15	1210	1540	1060	1460	1317	1317.4	192.1	14.6
			3A	15	1155	1330	1255	1370	1277	1277.4	81.9	6.4
			4A	30	1100	1150	1520	1610	1350	1346	223.0	16.6
		US17 Center	1B	-30	1450	1020	1450	1660	1395	1395	232.9	16.7
			2B	-15	1480	1370	1510	1460	1230	1410	113.4	8.0
			3B	15	1560	1430	1400	1070	1000	1292	243.5	18.8
			4B	30	910	1210	1130	1410	1220	1176	180.8	15.4
1	Polk (16003)	SR563 OWP	1A	-30	1090	1200	1290	1200	1250	1206	75.0	6.2
			2A	-15	1200	1350	1380	1310	1410	1330	81.5	6.1
			3A	15	1370	1280	1350	1330	1550	1376	102.9	7.5
			4A	30	1010	1360	1020	1460	1040	1178	215.0	18.3
		SR563 Center	1B	-30	1580	1460	1660	1650	1760	1622	111.0	6.8
			2B	-15	1780	1660	1660	1850	1760	1742	82.0	4.7
			3B	15	1590	1570	1610	1560	1510	1568	37.7	2.4
			4B	30	1550	1580	1340	1340	1360	1434	120.3	8.4
1	Lee (12005)	SR884 OWP	1A	-30	1770	1910	1400	1470	1430	1596	229.5	14.4
			2A	-15	1650	1770	1470	1180	1620	1538	226.9	14.8
			3A	15	1290	1630	1710	1690	1580	1580	170.0	10.8
			4A	30	1560	1980	1960	1780	1630	1782	189.3	10.6
		SR884 Center	1B	-30	1350	1940	1470	1590	1560	1582	220.8	14.0
			2B	-15	2000	1900	1760	1680	1835	1835	123.6	6.7
			3B	15	2100	2070	2090	1710	1700	1934	209.4	10.8
			4B	30	1810	2150	1420	1670	1740	1758	264.0	15.0

Table 3.2. Summary of PSPA Seismic Modulus Data (continued).

District	County	State road	Station		PSPA Seismic Modulus (ksi) 1	2	3	4	5	Average (ksi)	STDEV (ksi)	COV %
3	Jefferson (54020)	US27 OWP	1A	-30	1970	2090	1870	2560	2480	2194	308.9	14.1
			2A	-15	2340	1990	2500	2120	2360	2262	204.0	9.0
			3A	15	2080	2200	1980	2290	2100	2130	118.7	5.6
			4A	30	2660	1990	2080	2150	2410	2258	273.8	12.1
		US27 Center	1B	-30	2020	1630	1860	1530	1950	1798	209.9	11.7
			2B	-15	1870	1370	1870	1670	1480	1652	226.1	13.7
			3B	15	1700	1750	1420	1480	1490	1568	146.9	9.4
			4B	30	1750	1700	1600	1620	1590	1652	69.8	4.2
3	Gadsden (50020)	US27 OWP	1A	-30	1330	1220	1250	1450	1630	1376	167.6	12.2
			2A	-15	930	980	950	950	880	938	37.0	3.9
			3A	15	1480	1350	1530	1160	1540	1412	159.9	11.3
			4A	30	1360	1310	1270	1610	1550	1420	151.0	10.6
		US27 Center	1B	-30	2050	1910	1700	1740	1600	1800	179.0	9.9
			2B	-15	1050	950	990	960	1040	998	45.5	4.6
			3B	15	1110	1190	1230	1440	1630	1320	211.9	16.1
			4B	30	1400	1280	1540	1370	1240	1366	117.0	8.6
3	Santa Rosa (58060)	SR89 OWP	1A	-30	2320	2080	2330	2230	2400	2272	123.3	5.4
			2A	-15	1990	1910	2150	2040	1830	1984	122.4	6.2
			3A	15	2190	2300	2200	1710	2490	2178	288.0	13.3
			4A	30	2290	2060	2280	1980	2320	2186	154.9	7.1
		SR89 Center	1B	-30	2260	2280	2080	2460	2300	2276	135.2	5.9
			2B	-15	2260	2250	2390	2300	2320	2304	55.9	2.4
			3B	15	2400	2340	2310	2230	2200	2296	81.4	3.5
			4B	30	2060	2300	2270	2330	2090	2210	125.5	5.7

Table 3.2. Summary of PSPA Seismic Modulus Data (continued).

District	County	State road	Station		PSPA Seismic Modulus (ksi) 1	2	3	4	5	Average (ksi)	STDEV (ksi)	COV %
4	Martin (89010)	US 1 OWP	1A	-30	1670	1770	1920	1850	1975	1837	120.9	6.6
			2A	-15	2480	2010	2160	2380	2290	2264	184.5	8.1
			3A	15	1940	2130	1820	1800	1970	1932	132.9	6.9
			4A	30	1790	1870	1730	1910	2290	1918	219.4	11.4
		US 1 Center	1B	-30	1710	1680	1600	1850	1710	1710	90.3	5.3
			2B	-15	2020	1820	1860	2000	2060	1952	105.5	5.4
			3B	15	1640	1600	1700	1740	1710	1678	56.7	3.4
			4B	30	1430	1990	1530	1460	1610	1604	226.7	14.1
4	Palm Beach (93310)	SR710 OWP	1A	-30	950	970	980	940	1190	1006	104.1	10.3
			2A	-15	1020	1040	1110	1310	1240	1144	126.6	11.1
			3A	15	1310	1300	1200	1320	1100	1246	94.8	7.6
			4A	30	1020	920	1070	1150	980	1028	87.6	8.5
		SR710 Center	1B	-30	1030	1010	1210	1100	900	1050	114.7	10.9
			2B	-15	1050	1120	890	850	1050	992	115.8	11.7
			3B	15	1030	1010	1080	1110	1270	1100	103.0	9.4
			4B	30	1070	1040	1020	1070	1230	1086	83.3	7.7
4	Broward (86190)	SR823 OWP	1A	-30	1090	990	960	920	1290	1050	148.2	14.1
			2A	-15	1220	1320	1230	1240	1340	1270	55.7	4.4
			3A	15	950	1070	1070	1100	980	1034	65.0	6.3
			4A	30	1200	1010	1000	1180	1200	1118	103.5	9.3
		SR823 Center	1B	-30	1060	1050	1180	1200	1150	1128	69.1	6.1
			2B	-15	1300	1060	1060	1380	1040	1168	159.7	13.7
			3B	15	1150	1350	1250	1440	1420	1322	121.5	9.2
			4B	30	1480	1330	1080	1200	1250	1268	149.2	11.8

Table 3.2. Summary of PSPA Seismic Modulus Data (continued).

District	County	State road	Station		PSPA Seismic Modulus (ksi) 1	2	3	4	5	Average (ksi)	STDEV (ksi)	COV %
4	Palm Beach (93100)	US 27 OWP	1A	-30	1010	780	890	1060	780	904	129.0	14.3
			2A	-15	890	950	1130	1150	980	1020	114.5	11.2
			3A	15	1220	1240	1320	1540	1360	1336	127.6	9.6
			4A	30	620	680	940	770	640	730	130.8	17.9
		US27 Center	1B	-30	1090	1070	1150	1240	1240	1158	80.4	6.9
			2B	-15	1000	1120	990	940	980	1006	67.7	6.7
			3B	15	1010	940	730	1260	1050	998	191.5	19.2
			4B	30	1440	1030	1240	1350	1310	1274	154.4	12.1
5	Seminole (77002)	SR414 OWP	1A	-30	1900	1780	1660	2000	1930	1854	134.5	7.3
			2A	-15	1750	1830	1790	1690	1670	1746	66.9	3.8
			3A	15	1470	1500	1510	1520	1680	1536	82.6	5.4
			4A	30	1470	1450	1410	1280	1070	1336	166.1	12.4
		SR414 Center	1B	-30	1310	1500	1340	1320	1310	1356	81.4	6.0
			2B	-15	1800	2090	2130	1550	1450	1804	307.4	17.0
			3B	15	1280	1410	1580	1360	1620	1450	145.3	10.0
			4B	30	1330	1520	1070	1310	1630	1372	215.2	15.7
5	Osceola (92060)	US441 OWP	1A	-30	1590	1730	1390	1420	1440	1514	143.3	9.5
			2A	-15	1400	1440	1870	1770	1490	1594	211.7	13.3
			3A	15	1450	1460	1730	1640	1590	1574	119.7	7.6
			4A	30	1570	1450	1340	1390	1400	1430	87.5	6.1
		US441 Center	1B	-30	1070	1040	1060	1100	1100	1074	26.1	2.4
			2B	-15	1100	1100	1000	1010	1100	1062	52.2	4.9
			3B	15	1020	1080	1000	1000	1030	1026	32.9	3.3
			4B	30	960	1090	1020	1020	1040	1026	46.7	4.6

Table 3.2. Summary of PSPA Seismic Modulus Data (continued).

District	County	State road	Station		PSPA Seismic Modulus (ksi) 1	2	3	4	5	Average (ksi)	STDEV (ksi)	COV %
5	Volusia (79270)	SR483 OWP	1A	-30	1460	1480	1430	1570	1430	1474	57.7	3.9
			2A	-15	1510	1370	1270	1330	1390	1374	88.8	6.5
			3A	15	1650	1810	1440	1530	1470	1580	151.7	9.6
			4A	30	1320	1310	1360	1390	1370	1350	33.9	2.5
		SR483 Center	1B	-30	1440	1320	1370	1420	1590	1428	101.8	7.1
			2B	-15	1580	1120	1470	1550	1450	1434	183.7	12.8
			3B	15	1610	1710	1880	2310	1620	1826	291.4	16.0
			4B	30	1600	1500	1550	1550	1690	1578	71.9	4.6
6	Dade (87120)	US41 OWP	1A	-30	1380	1680	2080	1610	1980	1746	284.2	16.3
			2A	-15	1270	1070	1460	1630	1520	1390	221.5	15.9
			3A	15	1510	1750	1700	1400	1340	1540	180.4	11.7
			4A	30	1410	1620	1460	1930	1420	1568	219.2	14.0
		US41 Center	1B	-30	1620	1810	1670	1590	1670	1672	84.4	5.0
			2B	-15	1940	1690	1420	1700	1790	1708	189.7	11.1
			3B	15	1560	1560	1240	1450	1520	1466	134.1	9.1
			4B	30	1470	1340	1410	1650	1500	1474	115.9	7.9
6	Dade (87060)	A1A OWP	1A	-30	2490	1810	2700	1810	1850	2132	429.4	20.1
			2A	-15	2040	1950	2170	2070	2270	2100	123.3	5.9
			3A	15	1800	1510	1980	2010	1690	1798	207.8	11.6
			4A	30	2050	2260	2230	2200	1720	2092	223.1	10.7
		A1A Center	1B	-30	1280	1560	1360	1250	1400	1370	122.1	8.9
			2B	-15	1880	1890	2090	1870	1490	1844	217.9	11.8
			3B	15	1620	1880	2040	1660	1790	1798	170.4	9.5
			4B	30	2090	1650	1680	1660	1810	1778	185.9	10.5

Table 3.2. Summary of PSPA Seismic Modulus Data (continued).

District	County	State road	Station		PSPA Seismic Modulus (ksi) 1	2	3	4	5	Average (ksi)	STDEV (ksi)	COV %
6	Monroe (90060)	US1 OWP	1A	-30	1100	1620	1250	1020	1210	1240	231.0	18.6
			2A	-15	1600	1370	1340	1820	1130	1452	264.7	18.2
			3A	15	1200	1170	1250	1020	1380	1204	130.5	10.8
			4A	30	1050	980	1180	1070	1140	1084	78.3	7.2
		US1 Center	1B	-30	1420	1470	1140	1290	1440	1352	137.0	10.1
			2B	-15	1400	1220	1050	1280	1230	1236	126.2	10.2
			3B	15	1060	1120	1250	1130	1080	1128	74.0	6.6
			4B	30	1140	1200	1110	970	940	1072	112.1	10.5
7	Hillsborough (10060)	US41 OWP	1A	-30	1220	1140	1260	1230	1200	1210	44.7	3.7
			2A	-15	1100	1020	1070	1120	1040	1070	41.2	3.9
			3A	15	1220	1170	980	1120	870	1072	144.1	13.4
			4A	30	1250	1290	1250	1320	1350	1292	43.8	3.4
		US41 Center	1B	-30	1170	1230	980	980	1090	1090	112.0	10.3
			2B	-15	1690	1250	1220	1140	1310	1322	214.6	16.2
			3B	15	1250	1450	1380	1300	1540	1384	115.9	8.4
			4B	30	1200	1240	1220	1010	1020	1138	113.3	9.9
7	Hillsborough (10160)	SR580 OWP	1A	-30	2150	2150	2200	2120	2130	2150	30.8	1.4
			2A	-15	2250	2060	1850	1920	2040	2024	153.1	7.6
			3A	15	1800	1670	1740	1820	1690	1744	65.8	3.8
			4A	30	1930	2090	1890	2000	1900	1962	83.5	4.3
		SR580 Center	1B	-30	1620	1500	1500	1740	1610	1594	99.9	6.3
			2B	-15	1640	1600	1640	1710	1740	1666	57.3	3.4
			3B	15	1510	1560	1530	1790	1870	1652	165.9	10.0
			4B	30	2270	1790	2110	2200	2200	2114	189.8	9.0

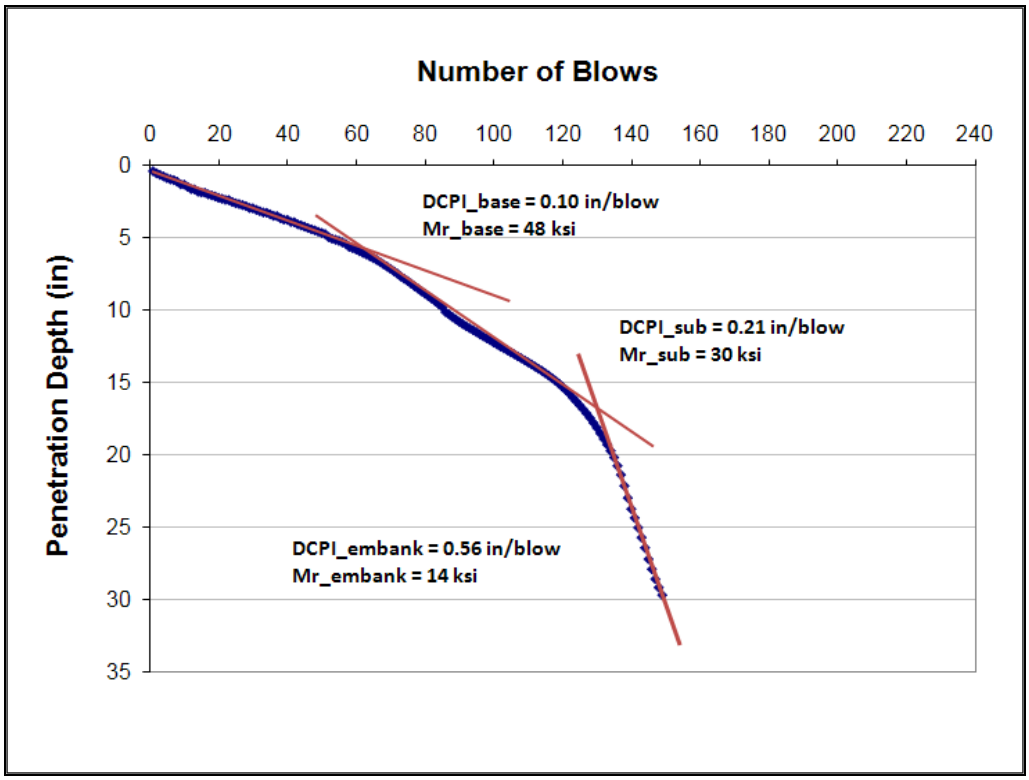

Figure 3.2. DCP Data Analysis on Section 54020000-2A.

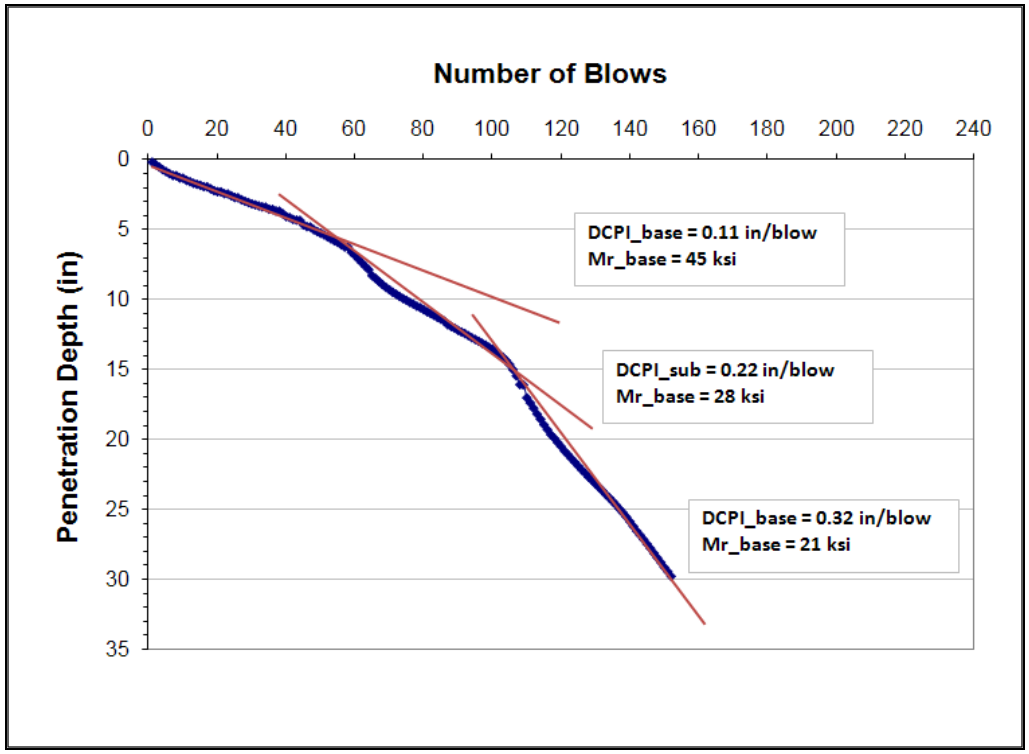

Figure 3.3. DCP Data Analysis on Section 54020000-3A.

DCP data are useful to enhance backcalculation results in cases where the layer thickness is uncertain or the underlying layer moduli backcalculated from FWD deflections do not seem to be reasonable. For example, researchers modified the initial backcalculated subgrade modulus of section 79270000 in Volusia County using DCP data shown in Figures B29 and B30. The initial backcalculation gave a subgrade modulus that was 3.7 times higher than limerock base modulus. Researchers considered this result as unrealistic given that the subgrade was mechanically stabilized and based on prior experience with interpreting FWD data collected on Florida pavements. The DCP data indicated that the penetration index and calculated modulus tend to gradually decrease with greater penetration depth. Consequently, researchers made another backcalculation using MODULUS where the search range for the mechanically stabilized subgrade was selected to be consistent with DCP data interpretation. The results from this backcalculation gave a higher modulus value for the limerock compared to the mechanically stabilized subgrade.

MEASUREMENTS OF FIELD MOISTURE CONTENT AND GROUNDWATER TABLE DEPTH

As part of the field tests, researchers collected underlying material samples to determine field moisture contents in the laboratory. These measurements were conducted so that comparisons between laboratory and FWD backcalculated moduli can be made based on the in-situ moisture condition at the time of the FWD test. Table 3.3 presents the field moisture contents and groundwater table (GWT) depths on the test sections. The groundwater table depth in this table is referred from the pavement surface.

The measurements show that the base layer moisture content varied from 5.4 to 15 percent. District 6 base materials generally had lower moisture contents than other areas. Most groundwater table depths were found to be within 10 feet except for District 3 sections and test sections located in Alachua County in District 2.

Table 3.3. Field Moisture Contents and Groundwater Table Depths.

District	County	Project #	Material	W (%)_Field	G.W.T (ft)
1	Polk	16020	Base	10.8	7'
			Sub	8.4	
			Emb	8.8*	
1	Polk	16003001	Base	11.0	7'2"
			Sub	10.8	
			Emb	11.8*	
1	Lee	12005000	Base	11.1	6'5"
			Sub	13.0*	
			Emb	11.8*	
2	Alachua	26005000	Base	8.9	14'2"
			Sub	7.5*	
			Emb	10.6*	
2	Alachua	26060000	Base	10.4	17'
			Sub	10.0*	
			Emb	10.0*	
2	Clay	71020000	Base	12.5	5'
			Sub	8.9*	
			Emb	10.0*	
3	Gadsden	50020000	Base	10.8	19'
			Sub	9.9	
			Emb	9.0	
3	Jefferson	54020000	Base	15.0	>20'
			Sub	9.3	
			Emb	10.5	
3	Santa Rosa	58060000	Base	7.7	>20'
			Sub	7.3	
			Emb	8.5	
4	Palm Beach	93100000	Base	11.1	N/A (9' based on M-E PDG project data)
			Sub	10.6	
			Emb	13.0*	
4	Palm Beach	93310000	Base	8.0	8'7"
			Sub	4.6	
			Emb	9.0*	
4	Broward	86190000	Base	4.6	8'
			Sub	6.0*	
			Emb	9.8*	

*****No field samples obtained. Moisture content was estimated.

Table 3.3 Field Moisture Contents and Groundwater Table Depths (continued).

District	County	Project #	Material	W (%)_Field	G.W.T (ft)
4	Martin	89010000	Base	6.4	>20'
			Sub	7.5*	
			Emb	8.0*	
5	Seminole	77002000	Base	8.7	6'
			Sub	9.3	
			Emb	10.1	
5	Volusia	79270000	Base	9.8	5'1"
			Sub	11.1	
			Emb	8.4	
5	Osceola	92060000	Base	6.3	11'5"
			Sub	7.0	
			Emb	7.3	
6	Dade	87060000	Base	5.4	7'5"
			Sub	6.0*	
			Emb	6.0*	
6	Dade	87120000	Base	6.3	7'7"
			Sub	7.5*	
			Emb	7.5*	
6	Monroe	90060000	Base	6.8	9'4"
			Emb	6.8	
7	Hillsborough	10060000	Base	11.9	6'10"
			Sub	7.9	
			Emb	6.5*	
7	Hillsborough	10160000	Base	15.0	8'10"
			Sub	9.1	
			Emb	9.0*	

*****No field samples obtained. Moisture content was estimated.

CHAPTER IV. LABORATORY TEST DATA ANALYSIS

Characterizing resilient modulus properties is crucial to assess the correction factors between modulus values determined from laboratory and field testing. In addition, characterizing AC materials is essential for correcting the PSPA seismic modulus to a test frequency that is representative of loading times used in pavement design. As noted in Chapter II, the State Materials Office conducted laboratory resilient modulus tests on base materials, dynamic modulus tests on asphalt concrete cores, extractions to determine volumetric properties, and dynamic shear rheometer tests to characterize binder viscosity-temperature relationships. In addition, TTI researchers conducted soil suction tests to determine the soil-water characteristic curves of the same base materials on which resilient modulus tests were conducted at SMO. This chapter documents the analysis of the laboratory test data researchers performed as part of evaluating the relationship between laboratory resilient modulus and FWD backcalculated modulus to develop correction factors for flexible pavement rehabilitation design based on the M-E PDG. Detailed laboratory test data are presented in the appendices of this report.

RESILIENT MODULUS TEST RESULTS

The State Materials Office collected samples of materials from six source locations that are considered representative of the base materials placed on the FSU study test sites in terms of geographical area and moisture-density properties. SMO personnel conducted resilient modulus tests (AASHTO T 307) on these base samples to characterize the resilient modulus at the optimum moisture content. Table 4.1 summarizes the resilient modulus test results.

Researchers compiled available laboratory data from previous projects to determine resilient modulus properties. The M-E PDG incorporates the resilient modulus model that considers the stress dependency of unbound pavement materials according to equation (4.1).

$$M_R = k_1 P_a \left(\frac{\theta}{P_a} \right)^{k_2} \left(\frac{\tau_{oct}}{P_a} + 1 \right)^{k_3} \quad (4.1)$$

where θ = bulk stress, τ_{oct} = octahedral shear stress, P_a = atmospheric pressure (14.5 psi), and k_1,k_2,k_3 are regression coefficients. More details on determining resilient modulus properties along with soil suction properties will be presented in subsequent sections.

Table 4.1. Summary of Resilient Modulus Tests.

Mine No.	Pit Name	Corresponding Ping's Site	Material	Max. Density	W_{opt} (%)	M_R @(1) θ=20psi	M_R @(1) θ=40psi
03-037	VULCAN	Lee (12005)	LIMEROCK	120.7	10.3%	21,108	32,031
						20,646	29,856
26-098	LIMEROCK IND	Alachua (26060) Clay (71020)	LIMEROCK	118.2	11.9%	19,547	28,052
						18,458	27,498
36-527	COUNTS	Seminole (77002)	LIMEROCK	120.8	11.0%	24,136	33,530
						23,672	33,014
87-089	CEMEX	Dade (87120) Martin (89010)	LIMEROCK	130.6	7.7%	19,918	28,594
						19,440	29,292
94-209	Florida Rock	Osceola (92060)	CEMENTED COQUINA	130.3	6.4%	23,145	34,000
						21,784	32,015
38-627	CABBAGE GROVE	Gadsden (50020) Jefferson (54020)	LIMEROCK	123.4	9.4%	19,786	29,170
						19,725	28,769

(1) Resilient modulus values (two replicates) corresponding to bulk stress of 20 and 40 psi based on k-θ model ($M_R = k^1 \theta^{k2}$).

SOIL SUCTION TEST RESULTS

Researchers conducted soil suction tests to establish the soil-water characteristic curves (SWCC) of the base materials listed in Table 4.1. These tests were performed in accordance with the filter paper method described by Bulut, Lytton, and Wray (2001). Figures 4.1 to 4.6 show SWCCs for the base materials identified in Table 4.1. Researchers performed nonlinear regression analysis to fit equations (2.8) and (2.9) to the soil suction test data. As observed in Figures 4.1 to 4.6, these equations fitted the test data reasonably well. These figures also show the coefficients of the SWCCs for the base materials tested.

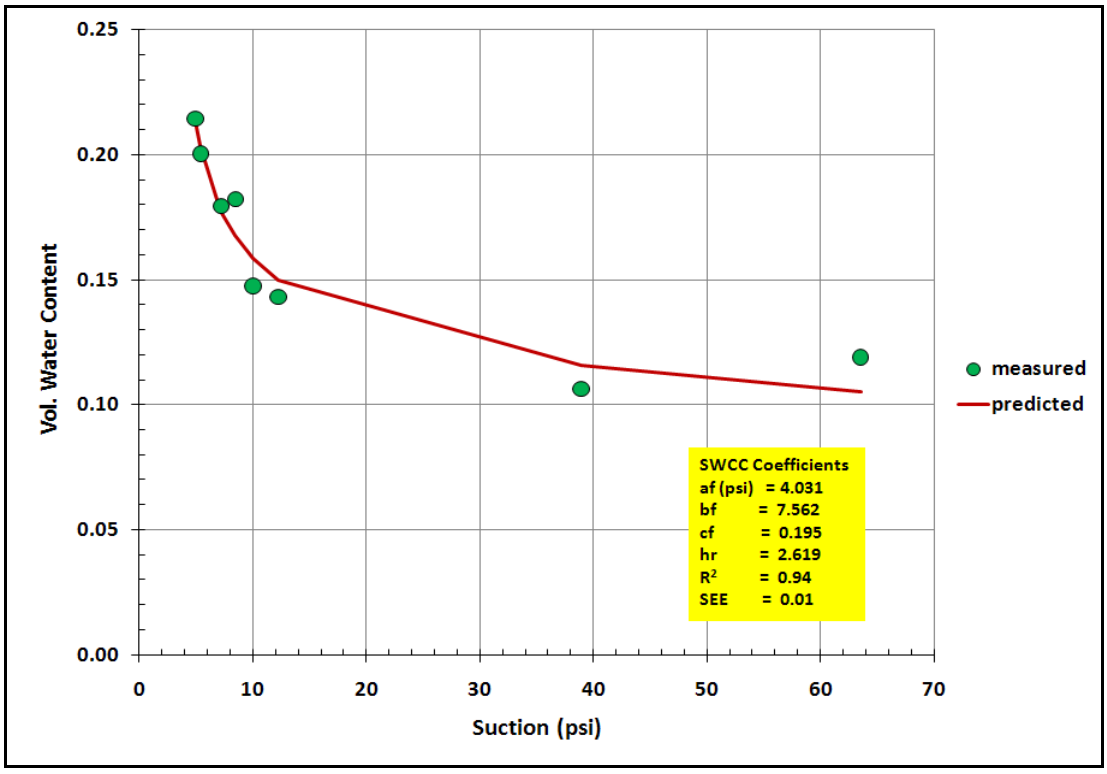

Figure 4.1. SWCC of Base Material from Source Pit 03-037.

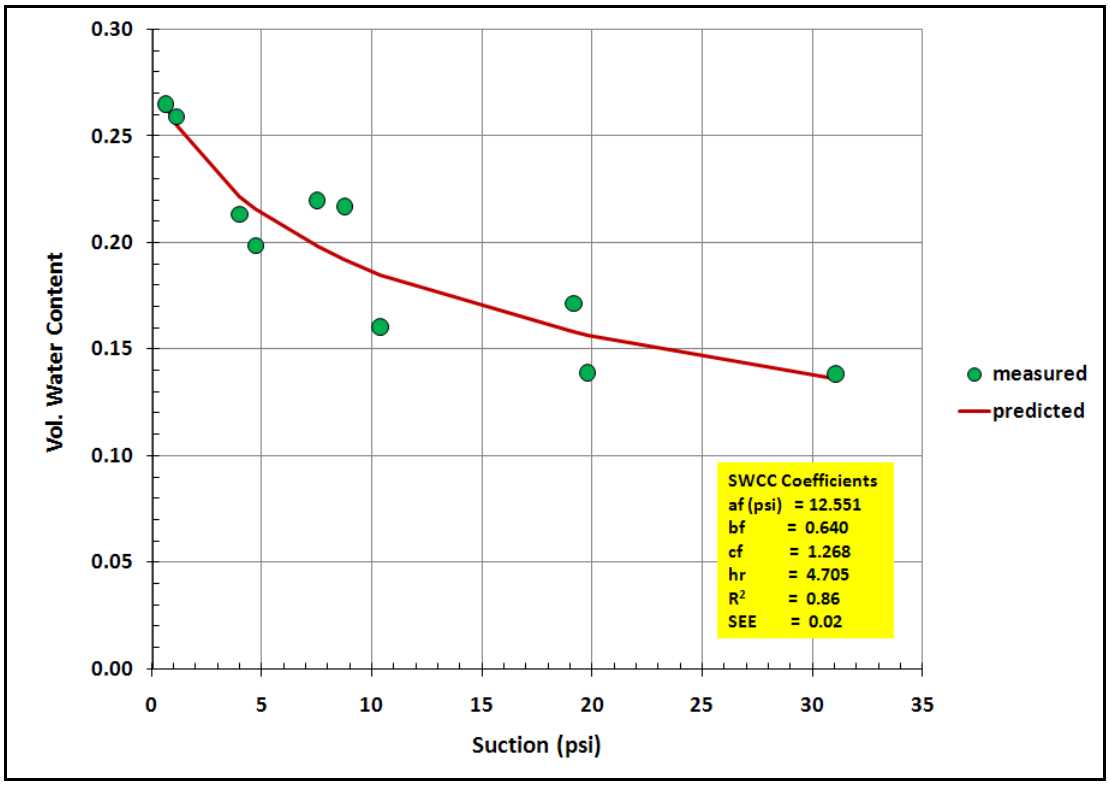

Figure 4.2. SWCC of Base Material from Source Pit 26-098.

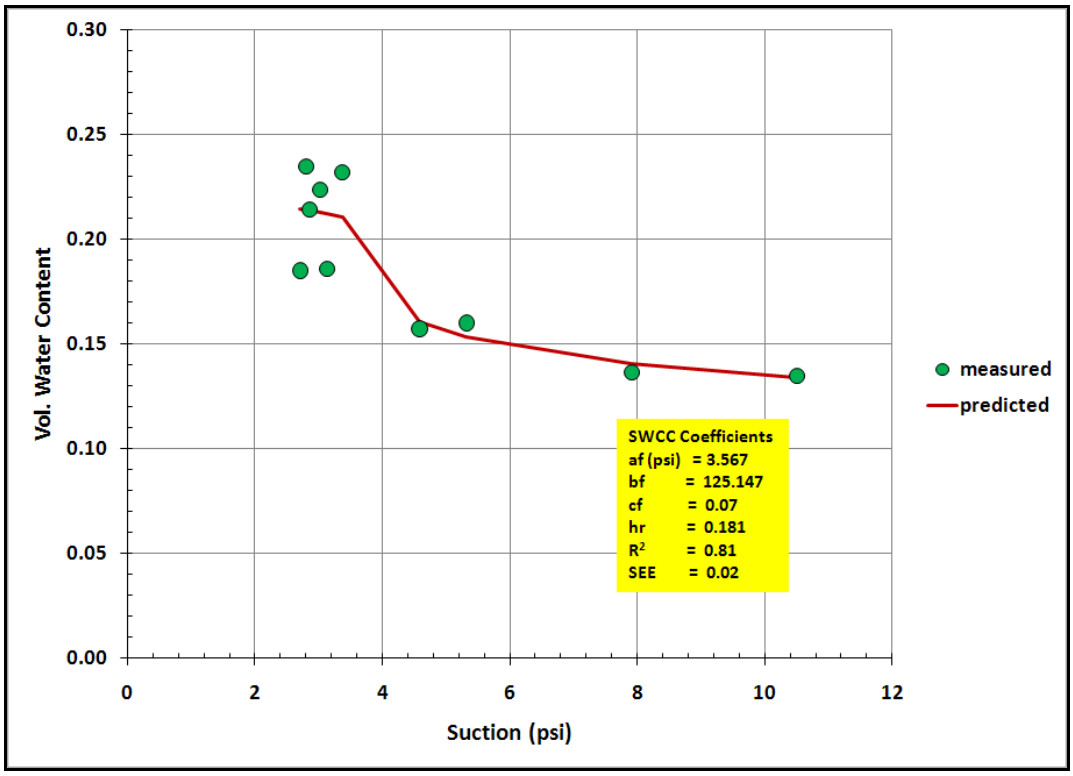

Figure 4.3. SWCC of Base Material from Source Pit 36-527.

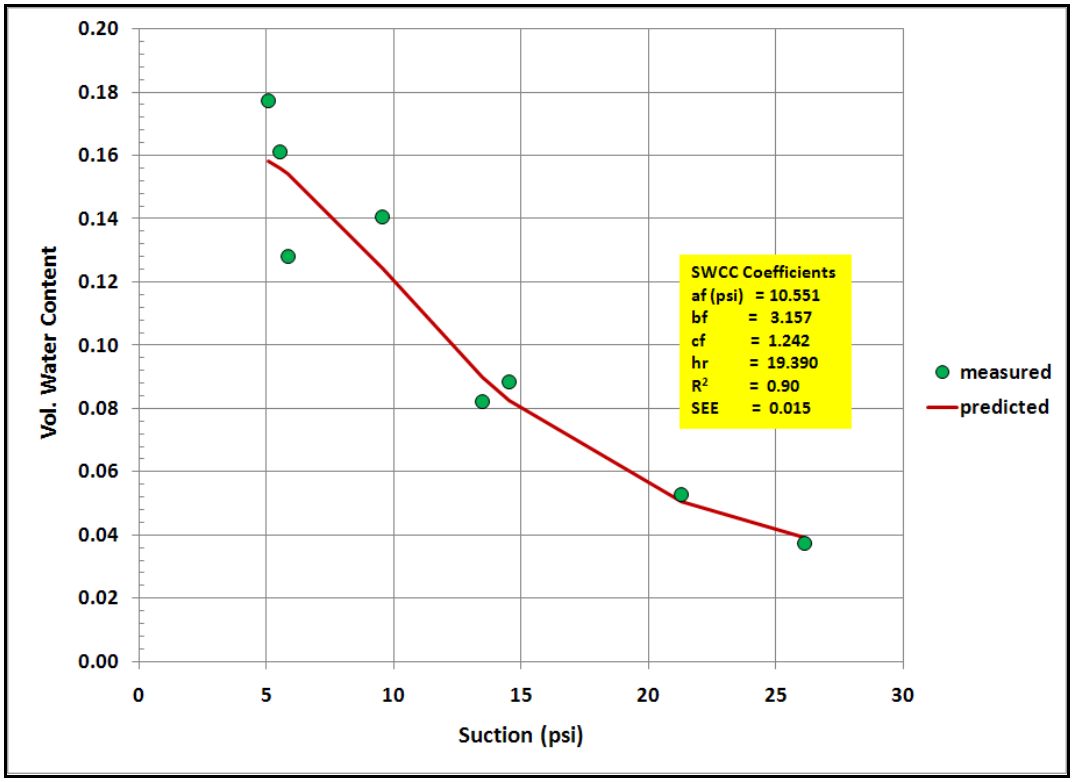

Figure 4.4. SWCC of Base Material from Source Pit 87-089.

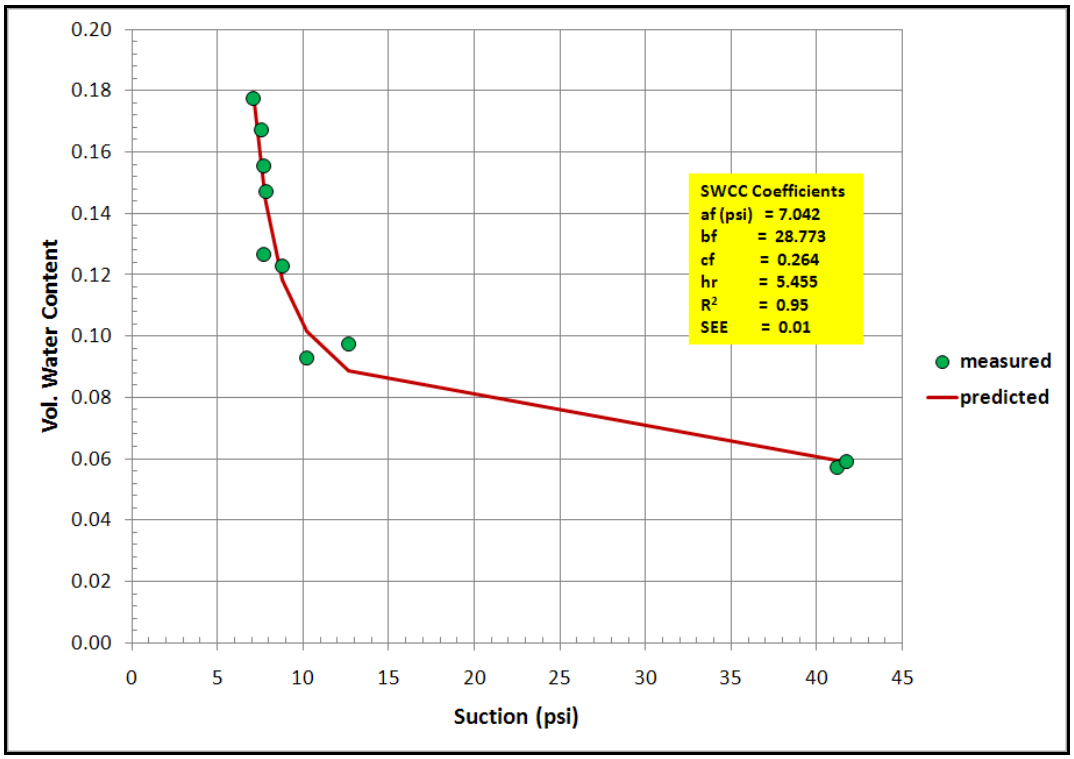

Figure 4.5. SWCC of Base Material from Source Pit 94-209.

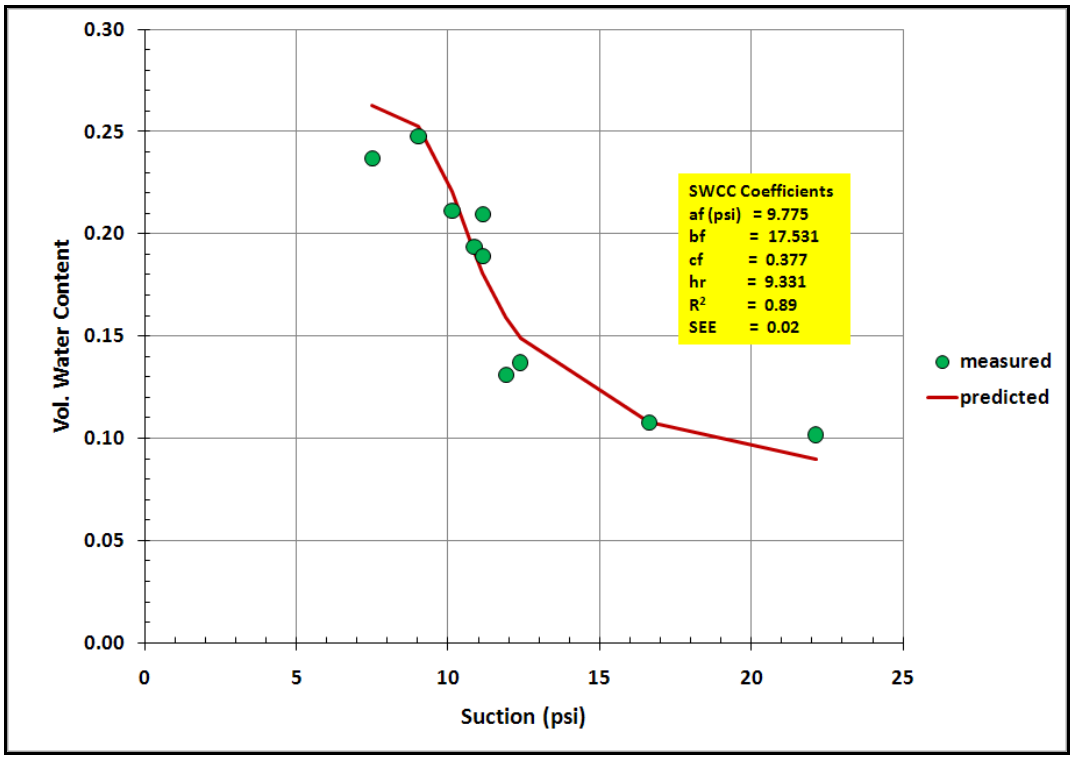

Figure 4.6. SWCC of Base Material from Source Pit 38-627.

Oh and Fernando (2008) conducted soil suction tests on base, mechanically stabilized subgrade, and embankment soils sampled from selected M-E PDG calibration sections. They established the soil suction coefficients of embankment soil for each county based on examination of the test results with published data as presented in Table 4.2. Researchers used the available data (presented in Appendix C) from the earlier M-E PDG project for characterizing resilient modulus properties in this study. For mechanically stabilized subgrade, researchers used the soil suction coefficients of embankment soil, or the coefficients determined from soil suction tests on subgrade soil samples from a neighboring test section (for example, subgrade suction coefficients for section 26005 were used for section 26060 in Alachua County) in cases where the subgrade soil suction coefficients were not available. For these cases, researchers considered the similarity of the SWCCs between the two materials as illustrated in Figures 4.7 and 4.8.

Table 4.2. Soil Suction Coefficients for Embankment Soils (after Oh and Fernando, 2008).

County Name	Soil Suction Coefficients			
	a_f (psi)	b_f	c_f	h_r (psi)
Alachua	2.584	0.989	1.224	100.049
Baker	1.715	0.855	2.187	100.049
Bay	6.013	0.542	5.318	100.078
Bradford	2.025	1.515	0.640	100.052
Brevard	4.807	0.414	3.551	100.716
Broward	1.214	0.827	2.857	99.424
Calhoun	0.827	1.267	0.793	99.990
Charlotte	2.857	0.790	1.517	99.427
Citrus	1.378	0.733	3.342	100.765
Clay	1.694	0.846	2.958	100.050
Collier	1.083	0.867	2.374	99.427
Columbia	2.163	0.861	2.290	100.050
Dade	3.359	1.264	0.636	99.415
De Soto	1.730	0.840	2.949	99.424
Dixie	1.565	0.871	2.812	100.050
Duval	1.581	0.905	2.806	100.050
Escambia	7.132	1.608	0.354	99.989
Flagler	3.999	0.624	5.304	100.716
Franklin	6.618	0.629	6.397	99.986
Gadsden	6.013	0.542	5.318	100.078
Gilchrist	1.563	0.871	2.812	100.050

Table 4.2. Soil Suction Coefficients for Embankment Soils (continued).

County Name	Soil Suction Coefficients			
	a_f (psi)	b_f	c_f	h_r (psi)
Glades	1.426	0.768	3.161	99.424
Gulf	7.332	2.451	0.607	99.988
Hamilton	6.708	0.802	1.570	100.035
Hardee	1.423	0.769	3.161	99.424
Hendry	1.912	1.073	1.197	99.425
Hernando	1.303	0.809	3.400	100.765
Highlands	0.865	0.941	2.233	99.425
Hillsborough	1.377	0.730	3.327	100.765
Holmes	10.447	1.979	0.364	99.941
Indian River	2.381	0.681	4.168	99.414
Jackson	5.888	0.646	5.812	99.999
Jefferson	7.327	1.903	0.357	99.424
Lafayette	5.102	0.668	4.453	100.033
Lake	3.999	0.625	5.304	100.716
Lee	1.211	0.822	2.835	99.424
Leon	8.010	2.344	0.288	99.634
Levy	4.783	0.687	5.191	100.033
Liberty	6.618	0.629	6.397	99.986
Madison	6.016	0.495	2.610	100.034
Manatee	1.423	0.769	3.161	99.424
Marion	3.997	0.597	5.242	100.763
Martin	3.997	0.597	5.242	100.763
Monroe	12.862	18.823	1.500	100.040
Nassau	3.997	0.597	5.242	100.763
Okaloosa	6.013	0.542	5.318	100.078
Okeechobee	1.206	0.829	2.843	99.424
Orange	3.998	0.613	5.240	100.763
Osceola	1.674	0.724	3.414	100.765
Palm Beach	2.381	0.681	4.168	99.414
Pasco	1.381	0.728	3.323	100.766
Pinellas	1.378	0.728	3.325	100.765
Polk	6.013	0.542	5.318	100.078
Putnam	4.996	0.674	5.176	100.033
St. Johns	4.863	0.674	5.100	100.033
St. Lucie	5.829	1.560	0.714	100.717
Santa Rosa	7.332	2.451	0.607	99.988
Sarasota	1.149	0.926	2.902	99.424
Seminole	1.655	0.734	3.426	100.765
Sumter	1.405	0.832	3.330	100.765
Suwannee	1.316	0.722	1.419	100.116
Taylor	1.405	1.042	1.602	100.116
Union	7.946	1.845	0.510	100.082
Volusia	1.549	0.594	3.192	100.765
Wakulla	5.888	0.646	5.812	99.999
Walton	6.013	0.542	5.318	100.078
Washington	5.888	0.646	5.812	99.999

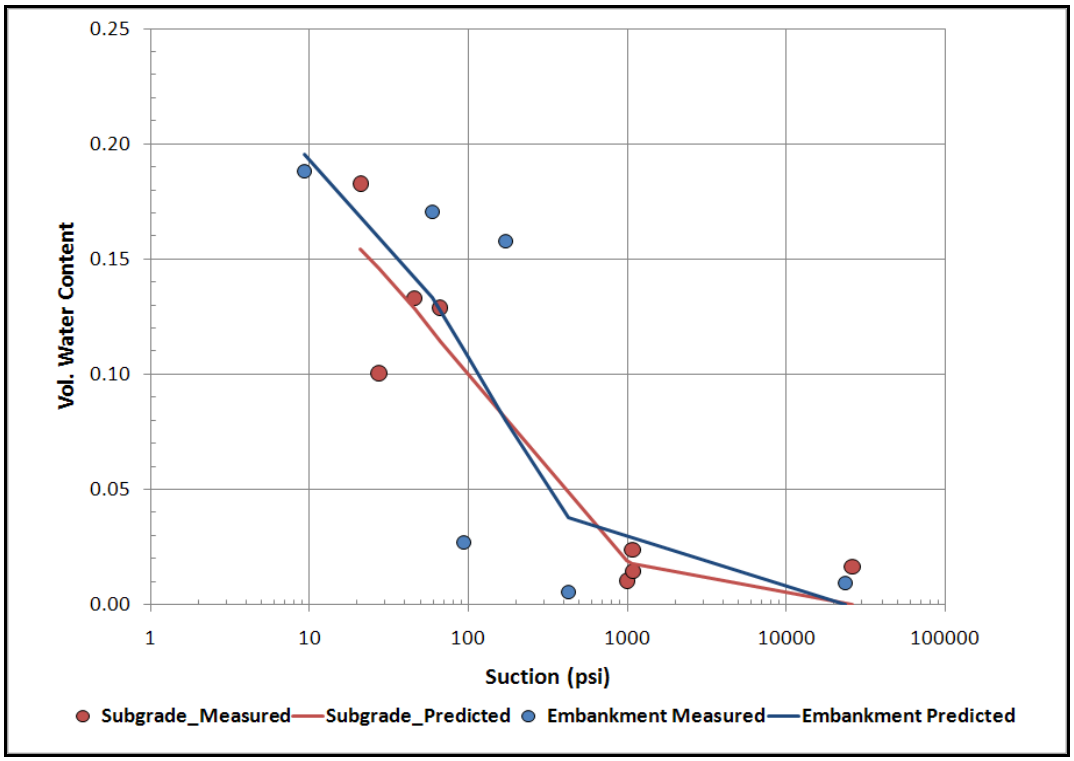

Figure 4.7. SWCCs of Subgrade and Embankment on Section 86190000.

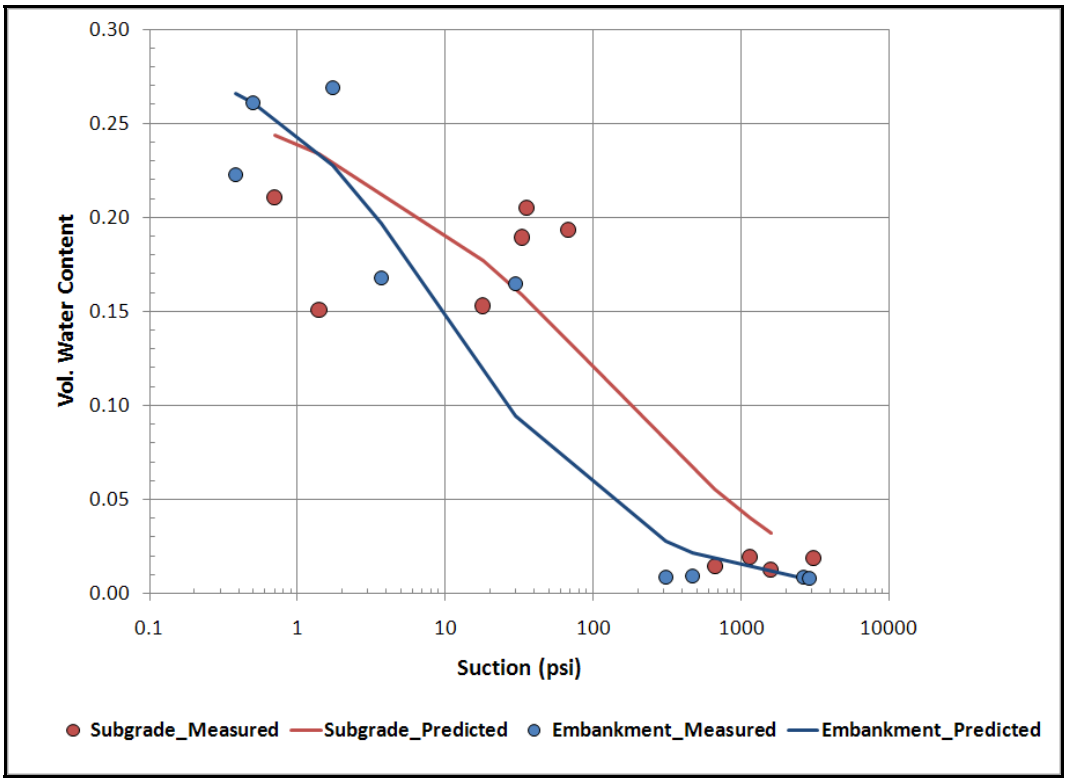

Figure 4.8. SWCCs of Subgrade and Embankment on Section 28040000.

CHARACTERIZING RESILIENT MODULUS FROM TEST DATA

Using the laboratory test data on resilient modulus and soil suction, researchers investigated the relationship between resilient modulus, stress state and moisture content. From reviewing the resilient modulus model incorporated into the M-E PDG, researchers found the following equation from NCHRP Project 1-28A, "Harmonized Test Methods for Laboratory Determination of Resilient Modulus for Flexible Pavement Design".

$$M_R = k_1 P_a \left(\frac{\theta - 3k_4}{P_a} \right)^{k_2} \left(\frac{\tau_{oct}}{P_a} + 1 \right)^{k_3} \tag{4.2}$$

The above equation is slightly different from equation (4.1) in that the coefficient k_4 was included to take into account the effect of moisture content variation on the bulk stress term. Researchers considered this equation to model the effect of moisture content on the resilient modulus. During this investigation, researchers also reviewed the work of Lamborn (1986) who proposed a micromechanical approach to model partially saturated soils. His approach modeled these materials as consisting of two phases, with solids represented as spherical particles in contact with each other, and an air-water mixture surrounding the particles. From micromechanics, Lamborn determined the following relationship between the mean principal stress acting on the system and the Helmholtz free energy per unit initial volume of the two phases.

$$\sigma_m = C_s \frac{\partial \overline{F_s}}{\partial \overline{\varepsilon_{kk}}} + C_w \frac{\partial \overline{F_w}}{\partial \overline{\varepsilon_{kk}}} \tag{4.3}$$

where σ_m = mean principal stress (= θ/3); C_s, C_w = initial volume fractions for solid and water, respectively, F = Helmholtz free energy, and ε_{kk} = volumetric strain. The overbars in equation (4.3) denote average values for the corresponding quantities, and the subscripts *s* and *w* represent the solid and water phases, respectively.

From this equation, Chandra et al. (1989) determined the following relationship between the change in mean principal stress σ_m and the change in soil suction, ΔS:

$$\Delta \sigma_m = -\Delta S V_w \tag{4.4}$$

where V_w is the volumetric water content. Based on the above equation, the effect of moisture content on soil structure integrity is conceptually illustrated in Figure 4.9. This

figure shows that soil moisture exerts surface tension forces that hold surrounding particles together. The amount of available soil suction is related to the moisture content of the material according to its soil-water characteristic curve. The higher the soil suction, the greater the soil cohesion and stiffness.

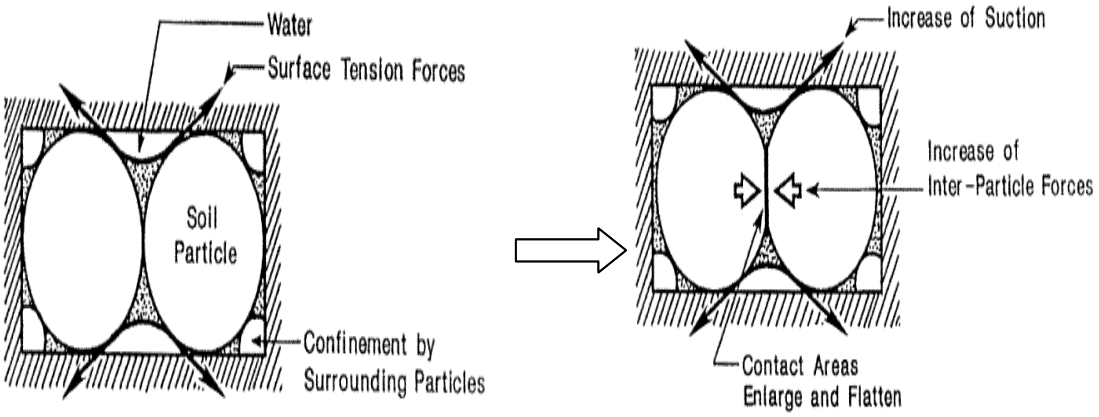

Figure 4.9. Illustration of Suction Effects on Soil Particles (after Texas Transportation Researcher, 1989).

Given the relationship between mean principal stress and soil suction, researchers propose a modified form of the resilient modulus relationship given in equation (4.2). Since the mean principal stress is one third of the bulk stress, the change in bulk stress due to soil suction can be determined from equation (4.4). This additional confinement imparted by soil suction is then added to the bulk stress associated with surface loads and gravimetric stresses to get the following proposed model that relates resilient modulus to the stress state and the moisture content:

$$M_R = k_1 P_a \left(\frac{\theta + 3k_4 SV_w}{P_a} \right)^{k_2} \left(\frac{\tau_{oct}}{P_a} + 1 \right)^{k_3} \qquad (4.5)$$

Equation (4.5) permits one to estimate the resilient modulus at any specific field moisture content using the soil-water characteristic curve for the given material. Researchers determined the coefficients of the above equation by fitting the resilient modulus test data at optimum and field moisture content to the stress states used in the laboratory tests and the soil suction values corresponding to optimum and field moisture contents. Figure 4.10 illustrates the calculations done to characterize the resilient modulus of the base material on Site 26060000. In general, researchers observed that

equation (4.5) explains the resilient modulus data reasonably well as indicated by the goodness-of-fit of the predictions. Data for the materials found on other sections are presented in Appendix D.

CHARACTERIZATION OF AC PROPERTIES

Dynamic modulus tests, extractions, and dynamic shear rheometer (DSR) tests were conducted on AC cores sampled from the test sections. DM tests were carried out on cores that meet the minimum height requirement (6 inches) under different ranges of temperature and load frequency. Table 4.3 presents data from DM tests conducted on cores from section 93310000. As expected, higher frequency and lower temperature yields higher dynamic modulus. Given the test data, researchers generated the master curve at a reference temperature corresponding to the mid-depth AC temperature estimated from the measured infrared surface and air temperatures at a given station. Figure 4.11 illustrates master curves determined from DM tests on cores obtained from section 93310000. The master curves are observed to be comparable between the AC cores tested reflecting the uniformity in the hot-mix material placed on this section. Data from extractions, DSR and dynamic modulus tests on AC cores sampled from the test sections are presented in Appendix E of this report.

Table 4.3. DM Test Data (in ksi) on Section 93310000.

Section	Temp (°F)	Frequency (Hz)			
		0.1	1	10	25
93310-2A	39.9	923.1	1294.6	1682.7	1857.1
	70.0	273.2	513.0	840.9	984.0
	99.1	52.0	129.7	294.9	390.4
	129.6	19.0	46.2	83.2	126.3
93310-3A	39.9	902.5	1269.5	1665.7	1824.2
	70.0	252.6	488.2	812.6	964.3
	99.1	54.7	132.1	286.9	380.3
	129.6	14.8	40.1	78.2	114.0
93310-2B	39.9	747.9	1076.4	1450.2	1608.1
	70.0	197.8	382.7	656.3	785.4
	99.1	41.6	106.3	235.1	312.4
	129.6	16.8	36.6	67.4	101.1
93310-3B	39.9	831.2	1189.6	1581.0	1755.2
	70.0	201.2	403.0	701.4	840.5
	99.1	38.0	98.0	222.2	301.4
	129.6	14.7	33.6	62.0	91.5

K1	283.47
K2	1.55
K3	-1.05
K4	7.69

$$M_R = K_1 P_a \left(\frac{\theta + 3K_4 SV_W}{P_a} \right)^{K_2} \left(\frac{\tau_{OCT}}{P_a} + 1 \right)^{K_3}$$

	Axial stress	Test sequence	Confining pressure (psi)	Bulk stress (psi)	M_R_Tested (psi)	Oct. shear stress (psi)	Soil suction (psi)	Vol. water content	M_R_Pred. (psi)	Error
OPTIMUM	5.6	1.0	3.0	11.6	15414.8	1.2	3.60	0.23	11862.1	12621431.2
	8.2	2.0	3.0	14.0	15288.1	2.5	3.60	0.23	12316.7	8829104.2
	11.0	3.0	3.0	16.7	16238.2	3.8	3.60	0.23	12850.3	11477784.0
	9.5	4.0	5.0	19.4	19639.2	2.1	3.60	0.23	15910.7	13901882.6
	14.2	5.0	5.0	23.8	20434.7	4.3	3.60	0.23	16509.3	15408846.0
	19.0	6.0	5.0	28.4	21125.1	6.6	3.60	0.23	17211.5	15316585.0
	19.2	7.0	10.0	39.0	28657.5	4.3	3.60	0.23	26517.2	4580848.8
	28.8	8.0	10.0	48.2	29863.5	8.9	3.60	0.23	26606.5	10608037.5
	38.2	9.0	10.0	57.4	30799.3	13.3	3.60	0.23	27073.6	13881339.8
	24.2	10.0	15.0	54.1	34379.1	4.3	3.60	0.23	38011.0	13190865.1
	28.9	11.0	15.0	58.5	34722.1	6.5	3.60	0.23	37112.9	5716063.1
	43.2	12.0	15.0	72.3	37264.9	13.3	3.60	0.23	35738.9	2328856.3
	33.9	13.0	20.0	73.6	40815.6	6.5	3.60	0.23	48901.9	65386876.2
	38.6	14.0	20.0	78.2	41961.2	8.7	3.60	0.23	47483.7	30497381.6
	57.4	15.0	20.0	96.3	45137.7	17.6	3.60	0.23	44109.8	1056536.7
FIELD	30.0	1.0	20.0	70.0	69881.2	4.7	6.81	0.20	62445.6	55287076.9
	40.0	2.0	20.0	80.0	61812.3	9.5	6.81	0.20	57385.7	19595157.2
	50.1	3.0	20.0	90.1	53546.3	14.2	6.81	0.20	54281.5	540495.2
	25.1	4.0	15.0	55.1	48574.4	4.8	6.81	0.20	48755.2	32663.5
	35.1	5.0	15.0	65.1	46077.2	9.5	6.81	0.20	45894.9	33243.7
	45.1	6.0	15.0	75.1	44123.6	14.2	6.81	0.20	44280.6	24650.4
	14.7	7.0	10.0	34.7	40424.4	2.2	6.81	0.20	37342.2	9500155.0
	20.1	8.0	10.0	40.1	34513.3	4.8	6.81	0.20	36336.2	3323009.9
	30.2	9.0	10.0	50.2	34763.9	9.5	6.81	0.20	35358.1	353078.6
	40.2	10.0	10.0	60.2	33795.9	14.2	6.81	0.20	35033.9	1532617.0
	9.9	11.0	5.0	19.9	22986.9	2.3	6.81	0.20	25125.1	4572222.6
	15.2	12.0	5.0	25.2	21026.0	4.8	6.81	0.20	25283.6	18127081.9
	20.2	13.0	5.0	30.2	22346.5	7.2	6.81	0.20	25534.0	10159656.0
	7.9	14.0	3.0	13.9	17825.3	2.3	6.81	0.20	20747.4	8538632.2
	9.9	15.0	3.0	15.9	17756.6	3.3	6.81	0.20	20945.6	10170177.1
	11.9	16.0	3.0	17.9	18365.8	4.2	6.81	0.20	21145.8	7728415.2
									SSE	374320770.5
									SEE	3474.89

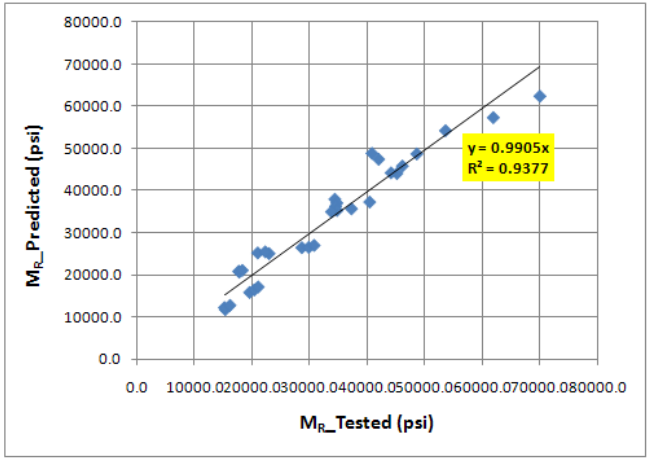

Figure 4.10. Resilient Modulus Properties of Base Material on Section 26060000.

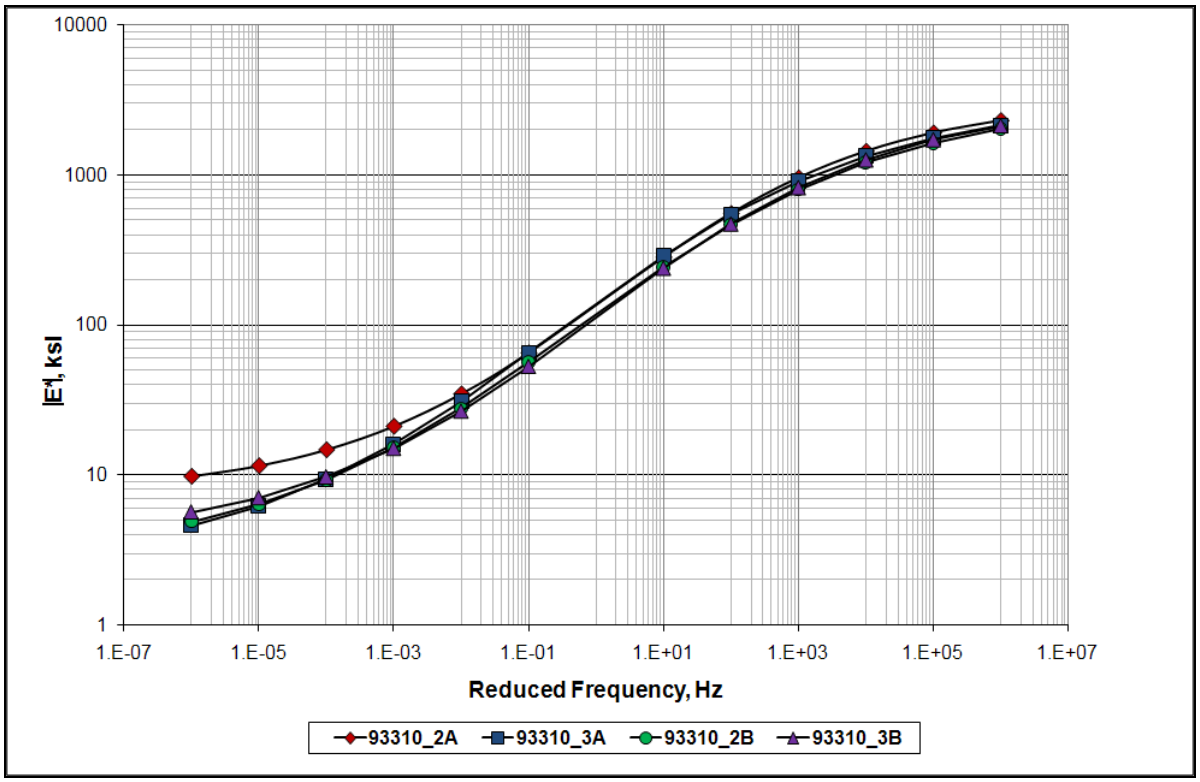

Figure 4.11. DM Master Curves on Section 93310000 AC Cores.

Extractions provided mix volumetric and gradation properties that are needed to predict the dynamic modulus of asphalt mixtures using the M-E PDG prediction equation. In addition to these properties, DSR tests were performed on the extracted binder to characterize the viscosity-temperature relationship for dynamic modulus prediction. To establish the DSR test temperatures, researchers used FDOT's temperature correction procedure to estimate pavement temperatures at the different sites given the infrared surface and air temperatures during the time of testing. Tables 4.4 and 4.5 show, respectively, the estimated pavement temperatures at the mid-depth of the asphalt concrete layer and the recommended DSR test temperatures. Agreement was reached with SMO on using the temperatures shown in Table 4.5 for the DSR testing. Table 4.6 presents data from DSR tests and extractions conducted on AC samples taken on section 16003001 in Polk County. Given the test data, researchers calculated the temperature-viscosity coefficients (A-VTS) using the following equations:

$$\eta = \frac{G^*}{10}\left(\frac{1}{\sin\delta}\right)^{4.8628} \qquad (4.6)$$

$$\log\log\eta = A + VTS\log T_R \quad (4.7)$$

Where G^* is binder complex shear modulus in Pa, δ is binder phase angle in degrees, η is viscosity in cP, T_R is temperature in Rankine, and A and VTS are regression coefficients. DSR test data for all sections are tabulated in Appendix E.

Table 4.4. Estimated Pavement Temperatures.

Section	Surf. Temp., °F	Time	Depth, in	Prev. Day's Avg. Air Temp., °F	Pavement Temp., °F
12005-1A	87	13:53	0.8	65.5	82.9
2A	87	13:54	0.8	65.5	82.9
3A	87	13:55	0.8	65.5	82.9
4A	87	13:56	0.8	65.5	83.0
12005-1B	88	14:00	2.3	65.5	81.1
2B	89	14:00	2.3	65.5	81.7
3B	88	14:01	2.3	65.5	81.1
4B	89	14:02	2.1	65.5	81.9
16020-1A	111	13:43	2.3	65.5	96.1
2A	111	13:43	2.3	65.5	96.1
3A	110	13:44	2.3	65.5	95.4
4A	109	13:45	2.3	65.5	94.6
16020-1B	111	13:50	2.5	65.5	95.5
2B	113	13:50	2.5	65.5	96.8
3B	114	13:51	2.3	65.5	98.3
4B	113	13:52	2.3	65.5	97.5
26060-1A	59	9:25	2.0	52	55.3
2A	60	9:27	2.0	52	56.0
3A	60	9:29	1.6	52	56.3
4A	59	9:30	1.6	52	55.7
26060-1B	62	9:35	2.2	52	57.1
2B	64	9:38	2.1	52	58.5
3B	64	9:39	1.7	52	59.0
4B	65	9:40	1.5	52	59.9
71020-1A	85	10:58	3.0	56	71.6
2A	84	10:58	3.0	56	71.0
3A	82	10:59	3.0	56	69.9
4A	83	11:00	3.0	56	70.5

Table 4.4. Estimated Pavement Temperatures (continued).

Section	Surf. Temp., °F	Time	Depth, in	Prev. Day's Avg. Air Temp., °F	Pavement Temp., °F
71020-1B	84	11:04	3.0	56	71.1
2B	83	11:05	3.0	56	70.5
3B	81	11:06	3.0	56	69.4
4B	83	11:07	3.0	56	70.5
54020-1A	64	8:53	2.5	52	58.0
2A	64	8:54	2.4	52	58.1
3A	65	8:55	2.3	52	58.8
4A	65	8:56	2.5	52	58.6
54020-1B	65	9:00	2.4	52	58.8
2B	65	9:01	2.5	52	58.6
3B	66	9:02	2.3	52	59.5
4B	66	9:03	2.5	52	59.2
50020-1A	68	12:17	3.5	48	58.8
2A	68	12:18	2.5	48	60.1
3A	68	12:19	2.4	48	60.4
4A	68	12:19	2.3	48	60.6
50020-1B	70	12:23	3.0	48	60.7
2B	70	12:25	2.5	48	61.5
3B	70	12:27	2.3	48	62.0
4B	70	12:29	2.3	48	62.0
89010-1A	86	8:33	1.5	78	80.0
2A	82	8:34	1.6	78	77.3
3A	80	8:35	1.5	78	75.8
4A	82	8:35	1.4	78	77.1
89010-1B	83	8:39	1.5	78	77.9
2B	82	8:40	1.6	78	77.3
3B	80	8:41	1.5	78	75.8
4B	82	8:42	1.5	78	77.2
77002-1A	96	9:48	2.6	82	87.7
2A	96	9:49	2.8	82	87.7
3A	95	9:51	3.0	82	87.1
4A	96	9:53	3.0	82	87.7
77002-1B	96	9:56	2.8	82	87.7
2B	97	9:57	2.9	82	88.3
3B	96	9:58	3.0	82	87.7
4B	96	9:59	3.0	82	87.7
92060-1A	94	9:05	4.1	78	84.5
2A	90	9:06	4.0	78	82.5

Table 4.4. Estimated Pavement Temperatures (continued).

Section	Surf. Temp., °F	Time	Depth, in	Prev. Day's Avg. Air Temp., °F	Pavement Temp., °F
3A	88	9:07	4.0	78	81.5
4A	90	9:09	4.0	78	82.5
92060-1B	92	9:12	4.3	78	83.5
2B	91	9:13	4.0	78	83.0
3B	90	9:13	4.3	78	82.5
4B	91	9:14	4.0	78	83.0
87120-1A	94	9:54	1.9	76	84.9
2A	90	9:55	1.8	76	82.4
3A	88	9:56	2.0	76	81.0
4A	90	9:57	2.0	76	82.3
87120-1B	92	9:48	2.0	76	83.5
2B	91	9:49	1.8	76	83.0
3B	90	9:50	1.8	76	82.3
4B	91	9:51	2.0	76	82.9
16250-1A	97	15:15	6.5	73	89.4
2A	96	15:16	7	73	88.9
3A	94	15:17	7.75	73	87.9
4A	97	15:17	6	73	89.6
16250-1B	95	15:21	3	73	89.6
2B	95	15:22	3.25	73	89.6
3B	93	15:23	3.375	73	88.3
4B	96	15:23	3.125	73	90.3
16003-1A	80	10:27	2	72.5	74.9
2A	79	10:28	2.15	72.5	74.3
3A	79	10:29	2.25	72.5	74.3
4A	79	10:29	2.25	72.5	74.3
16003-1B	80	10:34	1.875	72.5	75.0
2B	81	10:35	2.25	72.5	75.6
3B	80	10:36	2.125	72.5	75.0
4B	81	10:37	2.125	72.5	75.6
26005-1A	108	13:40	2.4	50	88.4
2A	98	13:41	2.45	50	81.7
3A	109	13:42	2.5	50	88.7
4A	110	13:43	2.4	50	89.8
26005-1B	108	13:47	2.35	50	88.8
2B	88	13:48	2.45	50	75.3
3B	107	13:49	2.45	50	87.8
4B	105	13:50	2.45	50	86.5

Table 4.4. Estimated Pavement Temperatures (continued).

Section	Surf. Temp., °F	Time	Depth, in	Prev. Day's Avg. Air Temp., °F	Pavement Temp., °F
28040-1A	75	10:16	2.1	43	62.9
2A	75	10:17	1.9	43	63.6
3A	75	10:18	1.8	43	64.0
4A	75	10:19	1.8	43	64.0
28040-1B	77	10:24	1.65	43	66.0
2B	77	10:25	1.5	43	66.7
3B	77	10:26	1.85	43	65.2
4B	77	10:27	1.75	43	65.6
50010-1A	53	9:06	5.75	48	49.0
2A	53	9:07	7	48	48.8
3A	53	9:08	7.25	48	48.8
4A	53	9:10	7	48	48.8
50010-1B	54	9:14	2.75	48	50.5
2B	54	9:15	2.75	48	50.5
3B	54	9:16	2.9	48	50.4
4B	54	9:17	3	48	50.4
58060-1A	52	10:47	3	59	53.7
2A	52	10:48	3	59	53.7
3A	52	10:49	3	59	53.7
4A	52	10:49	3	59	53.7
58060-1B	53	10:54	3	59	54.3
2B	53	10:55	3	59	54.3
3B	53	10:56	3	59	54.3
4B	53	10:57	3	59	54.3
93100-1A	96	9:21	1	78	87.6
2A	95	9:21	1.3	78	86.5
3A	97	9:25	1.25	78	88.0
4A	99	9:26	1.25	78	89.5
93100-1B	97	9:30	1.25	78	88.0
2B	97	9:31	1.25	78	88.0
3B	98	9:32	1.25	78	88.8
4B	99	9:34	1.25	78	89.5
93310-1A	109	14:03	4	82	99.2
2A	110	14:04	3.75	82	99.9
3A	110	14:04	4.125	82	99.7
4A	110	14:05	4	82	99.8
93310-1B	108	14:10	4	82	98.9
2B	107	14:11	3.875	82	98.4

Table 4.4. Estimated Pavement Temperatures (continued).

Section	Surf. Temp., °F	Time	Depth, in	Prev. Day's Avg. Air Temp., °F	Pavement Temp., °F
3B	107	14:12	4	82	98.3
4B	108	14:12	4	82	98.9
86190-1A	111	10:16	2	83	98.0
2A	111	10:17	2	83	98.0
3A	109	10:19	2	83	96.7
4A	110	10:19	2	83	97.4
86190-1B	111	10:24	2.125	83	97.9
2B	111	10:25	2	83	98.1
3B	115	10:26	2	83	100.7
4B	115	10:26	2	83	100.7
77040-1A	132	14:20	1.875	80	117.1
2A	135	14:21	3.75	80	114.0
3A	139	14:22	2	80	121.7
4A	137	14:23	2	80	120.3
77040-1B	134	14:27	2	80	118.3
2B	135	14:27	4.375	80	113.1
3B	138	14:29	4.75	80	114.1
4B	138	14:30	2	80	121.2
79270-1A	93	9:15	1.25	78	85.1
2A	94	9:16	1.25	78	85.8
3A	93	9:17	1.25	78	85.1
4A	93	9:18	1.25	78	85.1
79270-1B	94	9:22	1.25	78	85.8
2B	94	9:23	1.25	78	85.8
3B	93	9:24	1.25	78	85.1
4B	94	9:24	1.25	78	85.8
87060-1A	96	10:31	4	74	84.0
2A	97	10:32	4	74	84.5
3A	97	10:33	4	74	84.6
4A	97	10:34	4	74	84.6
87060-1B	97	10:37	4	74	84.6
2B	99	10:38	4	74	85.6
3B	100	10:38	4	74	86.2
4B	99	10:39	4	74	85.6
90060-1A	113	12:53	2	77	100.2
2A	117	12:54	2	77	103.0
3A	114	12:55	2	77	101.0
4A	109	12:55	2	77	97.6

Table 4.4. Estimated Pavement Temperatures (continued).

Section	Surf. Temp., °F	Time	Depth, in	Prev. Day's Avg. Air Temp., °F	Pavement Temp., °F
90060-1B	114	12:59	2	77	101.1
2B	117	13:00	2	77	103.1
3B	116	13:01	2	77	102.5
4B	112	13:02	2	77	99.8
10060-1A	113	13:25	1.875	69	99.2
2A	113	13:26	1.75	69	99.7
3A	113	13:27	2	69	98.8
4A	113	13:27	2	69	98.8
10060-1B	113	13:31	2	69	99.0
2B	114	13:32	1.75	69	100.6
3B	114	13:33	1.75	69	100.6
4B	114	13:34	2	69	99.7
10160-1A	71	8:44	3.25	66	67.1
2A	68	8:45	4.5	66	65.7
3A	65	8:46	2.5	66	63.4
4A	64	8:46	2.75	66	63.0
10160-1B	72	8:52	3	66	67.6
2B	70	8:53	2.75	66	66.5
3B	67	8:54	2.75	66	64.7
4B	67	8:54	2.625	66	64.7

Table 4.5. Recommended DSR Test Temperatures.

District	County	Project No.	Highway	DSR Temperature (deg. F)
1	Polk	16020	US 17	70, 80, 90, 100, 110, 120, 130
1	Polk	16250	SR 37	70, 80, 90, 100, 110, 120, 130
1	Polk	16003	SR 563	70, 80, 90, 100, 110, 120, 130
1	Lee	12005	CR 884	70, 80, 90, 100, 110, 120, 130
2	Alachua	26005	SR 222	70, 80, 90, 100, 110, 120, 130
2	Alachua	26060	US 301	50, 60, 70, 80, 90, 100, 110
2	Bradford	28040	SR 18	50, 60, 70, 80, 90, 100, 110
2	Clay	71020	US 17	70, 80, 90, 100, 110, 120, 130
3	Gadsden	50010	RS 90	50, 60, 70, 80, 90, 100, 110
3	Gadsden	50020	US 27	50, 60, 70, 80, 90, 100, 110
3	Jefferson	54020	US 27	50, 60, 70, 80, 90, 100, 110
3	Santa Rosa	58060	SR 89	50, 60, 70, 80, 90, 100, 110
4	Palm Beach	93100	US 27	70, 80, 90, 100, 110, 120, 130
4	Palm Beach	93310	SR 710	70, 80, 90, 100, 110, 120, 130
4	Broward	86190	SR 823	70, 80, 90, 100, 110, 120, 130
4	Martin	89010	US 1	70, 80, 90, 100, 110, 120, 130
5	Seminole	77002	SR 414	70, 80, 90, 100, 110, 120, 130
5	Seminole	77040	SR 46	70, 80, 90, 100, 110, 120, 130
5	Volusia	79270	SR 483	70, 80, 90, 100, 110, 120, 130
5	Osceola	92060	US 441	70, 80, 90, 100, 110, 120, 130
6	Dade	87060	A1A	70, 80, 90, 100, 110, 120, 130
6	Dade	87120	US 41	70, 80, 90, 100, 110, 120, 130
6	Monroe	90060	US 1	70, 80, 90, 100, 110, 120, 130
7	Hillsborough	10060	US 41	70, 80, 90, 100, 110, 120, 130
7	Hillsborough	10160	SR 580	50, 60, 70, 80, 90, 100, 110

Table 4.6. Properties Determined from Extractions and DSR Testing on Core Samples from Section 16003001.

Temp. (°F)	Lift 1 - Core A		Lift 1 - Core B		Lift 2 - Core A		Lift 2 - Core B		Lift 3 - Core A		Lift 3 - Core B	
	Complex Modulus G* (Pa)	Phase Angle δ (°)	Complex Modulus G* (Pa)	Phase Angle δ (°)	Complex Modulus G* (Pa)	Phase Angle δ (°)	Complex Modulus G* (Pa)	Phase Angle δ (°)	Complex Modulus G* (Pa)	Phase Angle δ (°)	Complex Modulus G* (Pa)	Phase Angle δ (°)
70	7086000	48	7414000	47.5	4579000	45.43	6459000	39.44	5365000	45.44	9077000	41.87
80	3277000	53.34	3400000	52.77	2306000	49.24	3791000	42.88	2761000	48.88	4646000	46.27
90	1408000	57.94	1473000	57.29	1107000	52.8	2010000	46.37	1299000	52.76	2287000	50.43
100	578496	61.63	613603	61.09	507999	56.21	977883	50.08	583647	56.58	1051000	54.38
110	243436	64.26	260948	63.79	228287	59.44	477923	53.37	269170	59.95	494440	57.85
120	105585	66.18	109931	66.1	91742	64.03	175268	57.89	86745	63.86	169299	62.18
130	48590	67.02	50021	67.03	42239	66.72	83329	60.12	42023	66.59	81434	65
A-VTS	9.24	-3.03	9.28	-3.05	9.16	-3.00	8.76	-2.85	9.42	-3.10	9.20	-3.01

	Gradation				Air Void %	Vol. binder Content (%)	Average Thickness (in)
Core A	Retain 3/4"	Retain 3/8"	Retain #4	#200P			
Lift 1	0	7.6	34.7	3.6	4.8	11.86	1.5
Lift 2	0	12.3	29.6	10.4	2.6	14.32	1.2
Lift 3	0	11.1	37.8	6.4	7.4	12.2	1.5
	Gradation				Air Void %	Vol. binder Content (%)	Average Thickness (in)
Core B	Retain 3/4"	Retain 3/8"	Retain #4	#200P			
Lift 1	0	7	33.7	3.7	5.2	12.2	1.4
Lift 2	0	10.4	30.2	10.7	3.9	14.32	1.1
Lift 3	0	8.5	31.2	6.5	7.4	12.98	1.7

CHAPTER V. DEVELOPMENT OF CORRECTION FACTORS

This project aims to recommend correction factors for determining equivalent laboratory modulus values given the corresponding base, stabilized subgrade and embankment moduli obtained from in-situ pavement testing, such as with the FWD. These factors are needed to establish candidate overlay designs on flexible pavement rehabilitation projects using the M-E PDG program. In this chapter, researchers present the methodology used to evaluate CFs based on the data from laboratory and field tests presented in earlier chapters. Researchers also performed a sensitivity analysis to gauge the impact of the proposed correction factors on asphalt concrete overlay designs based on the M-E PDG.

DETERMINING CORRECTION FACTORS

Comparing resilient modulus determined from laboratory and field tests calls for determining the state of stress since the resilient modulus of unbound pavement materials varies with the stress state. To determine correction factors, researchers determined the resilient modulus from laboratory test data based on the predicted stress state for the given pavement section and FWD load level. Researchers used the following procedure to calculate resilient modulus values and CFs:

- Compute vertical and horizontal stresses at different pavement depths along the vertical axis of the FWD load plate as illustrated in Figure 5.1. Do these calculations using the multi-layer elastic program BISAR (De Jong et al., 1973) with the FWD backcalculated layer moduli and the corresponding layer thicknesses for each test station on a given project (See Table 3.1). The evaluation points were selected based on a review of the literature (Ping et al., 2000, and Khazanovich et al., 2006).
- Compute the gravimetric stresses at a given depth using the following equations:

$$\sigma_{vw} = \sum_{i=1}^{n} \gamma_i * h_i \qquad (5.1)$$

$$\sigma_{hw} = k_0 * \sigma_{vw} \qquad (5.2)$$

where,

σ_{vw} = vertical stress associated with the weight of the soil mass (psi),

σ_{hw} = horizontal stress due to the weight of soil (psi),

k_0 = coefficient of earth pressure at rest (assumed to be 0.5),

γ_i = material unit weight (pci), and

h_i = depth of stress evaluation.

Figure 5.2 illustrates an example calculation of gravimetric stresses.

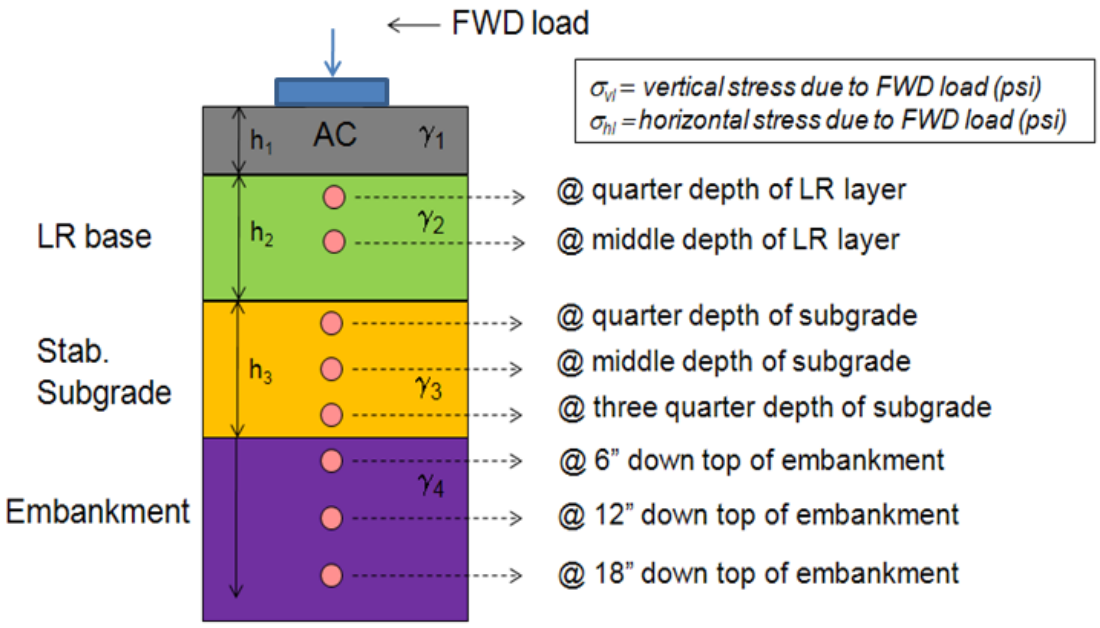

Figure 5.1. Calculation of In-Situ Load Associated Stresses.

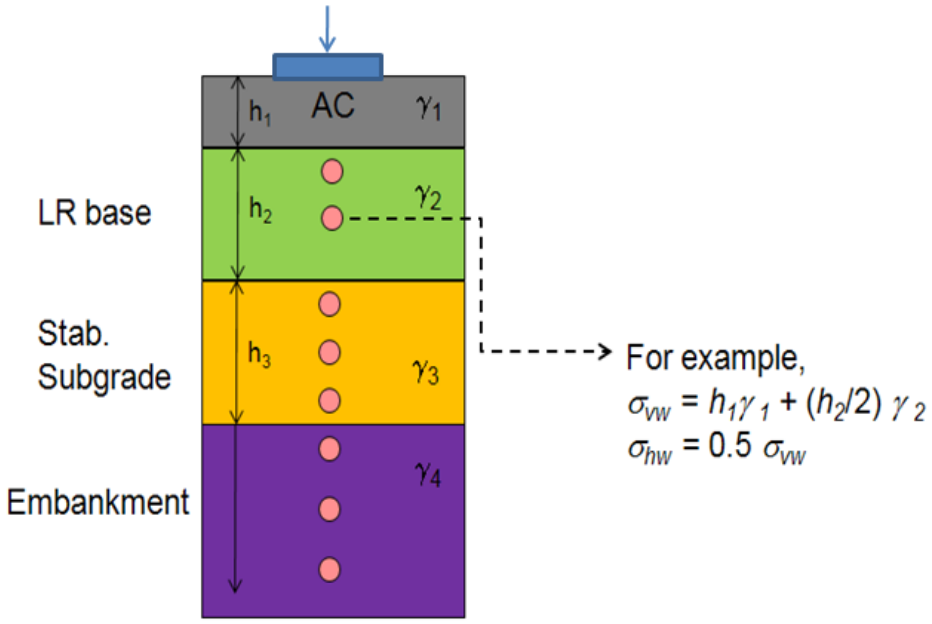

Figure 5.2. Calculation of Gravimetric Stresses.

- Compute the total vertical and horizontal stresses by adding the gravimetric stresses with the load-associated stresses as illustrated in Figure 5.3. Using the total stresses, calculate bulk and octahedral shear stresses.

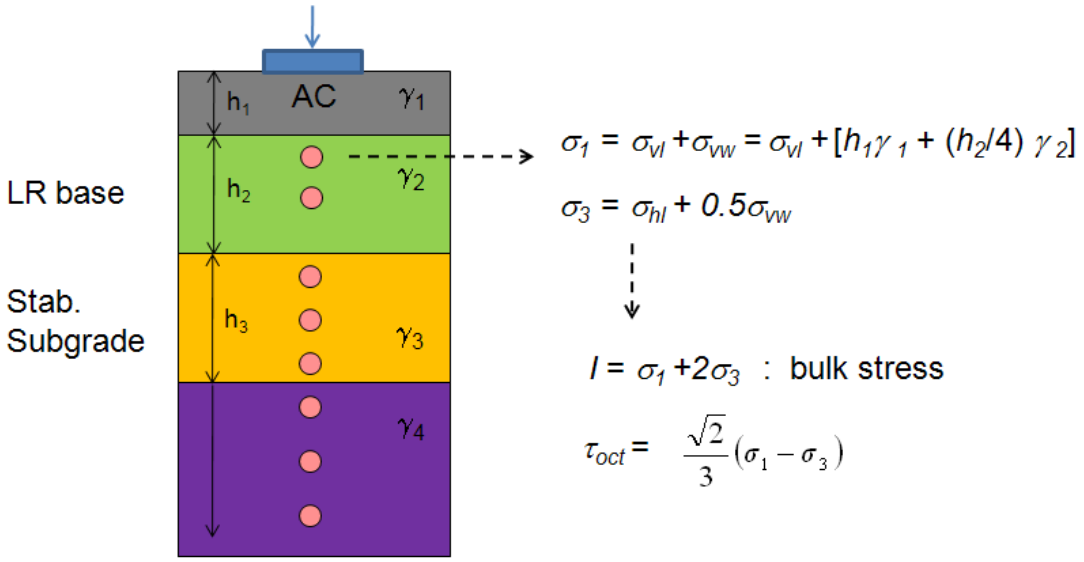

Figure 5.3. Calculation of Total Stresses.

- Compute the resilient modulus corresponding to the field moisture content at the evaluation depth using equation (4.5).
- Calculate the CF by taking the ratio of the resilient modulus and the corresponding FWD backcalculated modulus, which researchers determined using the MODULUS program.

Prior to assessing the CFs, researchers reviewed the stress states evaluated from the above procedure to establish the range of bulk and octahedral shear stresses over which the calculated resilient modulus values will vary. In reviewing the calculated stresses, researchers considered the following recommendations from NCHRP Project 1-28A on the stress states to be used for determining laboratory resilient modulus values:

- For base and subbase materials, use 5 psi confining pressure (σ_3) and 15 psi cyclic stress (σ_d) with 1 psi contact stress (σ_c). This contact stress is applied to the specimen during testing to maintain a positive contact between the loading ram and the specimen top cap. The contact load includes the weight of the top cap and the static load applied by the loading ram.
- For subgrade soils, use 2 psi confining pressure and 6 psi cyclic stress with 0.4 psi contact stress.

Using the above stress levels, researchers computed the corresponding bulk and octahedral shear stresses as follows:

- Base and subbase materials:

  $\theta = \sigma_1 + \sigma_2 + \sigma_3 = \sigma_1 + 2\sigma_3 = \sigma_d + \sigma_c + 3\sigma_3 =$ 31 psi, (since $\sigma_2 = \sigma_3$)

  $\tau_{oct} = (1/3)\,[(\sigma_1-\sigma_2)^2 + (\sigma_2-\sigma_3)^2 + (\sigma_3-\sigma_1)^2]^{0.5} = (1/3)\,[2(\sigma_d + \sigma_c)^2]^{0.5} =$ 7.5 psi.
- Subgrade soils:

  $\theta = \sigma_1 + \sigma_2 + \sigma_3 = \sigma_1 + 2\sigma_3 = \sigma_d + \sigma_c + 3\sigma_3 =$ 12.4 psi,

  $\tau_{oct} = (1/3)\,[(\sigma_1-\sigma_2)^2 + (\sigma_2-\sigma_3)^2 + (\sigma_3-\sigma_1)^2]^{0.5} = (1/3)\,[2(\sigma_d + \sigma_c)^2]^{0.5} =$ 3 psi.

Figures 5.4 to 5.6 show the range of bulk and octahedral shear stresses calculated for each material. In all figures, the top and bottom arrows indicate, respectively, the averages of maximum and minimum values for the given group of test sites, while the circular markers represent overall mean values. The horizontal lines denote the stress levels based on the NCRHP Project 1-28A recommendations.

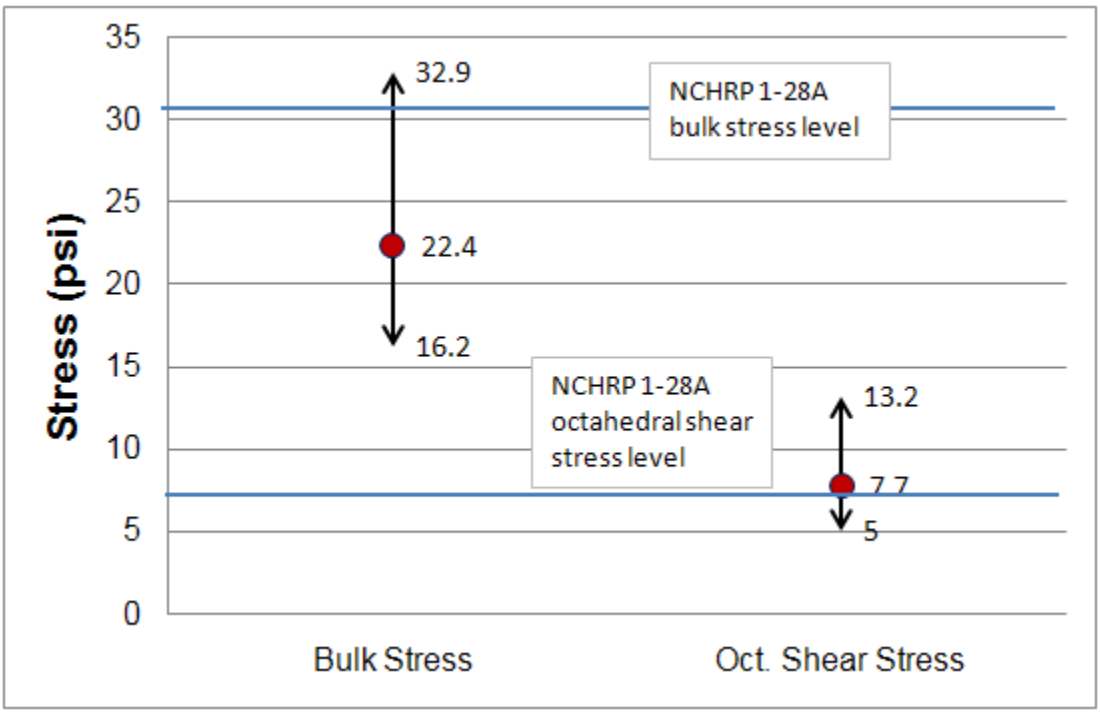

Figure 5.4. Computed Stress Ranges for Base Layer.

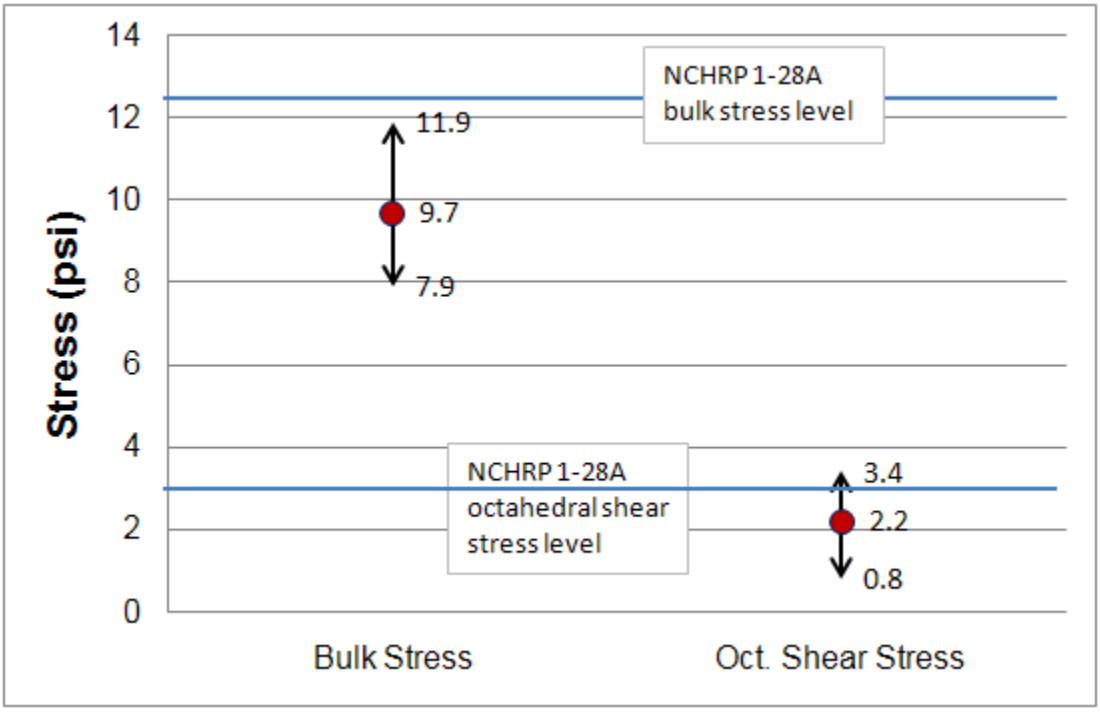

Figure 5.5. Computed Stress Ranges for Subgrade Layer.

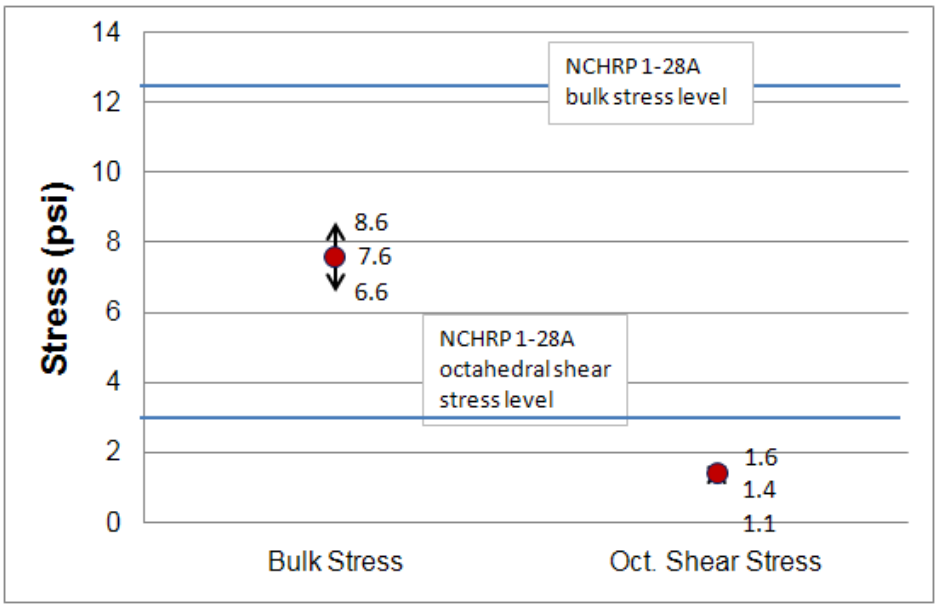

Figure 5.6. Computed Stress Ranges for Embankment Layer.

Based on the comparisons presented in the previous charts, researchers are of the opinion that the proposed stress levels from NCHRP Project 1-28A appear to be applicable for the Florida base and stabilized subgrade layers found on our test sites. For embankment soils, the proposed NCHRP stress levels somewhat overestimate the calculated stress values on our test sites particularly with respect to the bulk stress. Given that these calculated bulk stresses are based on FWD test data collected on this project, researchers consider these calculated stress values for embankment materials to be representative of Florida pavements.

From the evaluation of stress states, researchers made a decision to assess the CF for the following conditions: (a) based on in-situ stress calculation due to FWD load and (b) based on NCHRP 1-28A stress recommendations. Table 5.1 illustrates the procedure to determine the CFs based on the procedure presented previously. It should be noted that CFs were obtained based on FWD data taken along the outer wheel path. This approach was taken in consultation with the project manager who noted that typical pavement designs are based on the outer wheel path condition, which is influenced by traffic and the environment. Researchers generated charts showing the relationships between FWD backcalculated layer moduli and CFs evaluated at the different positions considered in the analysis.

Table 5.1. Calculation of CFs at Section 89010000-1A.

Section 89010-1A	FWD Backcalculated Moduli (ksi)			Unit weight (pci)	Moisture & Suction					Correction Factor (CF) In-situ CF = (In-situ M_R)/FWD M_R NCHRP CF = (NCHRP M_R)/FWD M_R		
	Layer	M_R_FWD	Thick (in)		Layer	W_{field} (%)	γ_d (pcf)	V_w	S (psi)			
	AC	1164.20	3.00	0.08	Base	6.35	120.0	0.12	9.4			
	Base	67.20	10.0	0.07	Stab. subg.	7.50	116.0	0.14	32.9			
	Stab. subg.	55.00	16.0	0.06	Embank.	8.00	106.0	0.14	6.9			
	Embankment	35.70		0.06	Calculated Total Stresses (psi)				In-situ M_R[4]	NCHRP M_R[5]	In-situ CF	NCHRP CF
Location	Depth (in)	R_STRE[1]	Z_STRE[1]	Gravi. [2]	Sigma_V[3]	Sigma_H[3]	θ	τ_{oct}				
b 1/4	5.5	1.00	31.56	0.41	31.97	1.20	34.38	14.50	27015.27	33165.05	0.40	0.49
b 1/2	8	-0.75	22.68	0.58	23.26	-0.47	22.33	11.18	23130.56	33165.05	0.34	0.49
s 1/4	17	-0.62	8.38	1.18	9.57	-0.03	9.51	4.52	18289.54	21376.98	0.33	0.39
s 1/2	21	-0.75	5.88	1.44	7.31	-0.04	7.24	3.46	15660.47	21376.98	0.28	0.39
s 3/4	25.00	-0.97	4.25	1.69	5.94	-0.12	5.70	2.86	13493.24	21376.98	0.25	0.39
e +6	35.00	-0.19	2.33	2.32	4.65	0.97	6.58	1.73	11641.09	16185.72	0.33	0.45
e +12	41.00	-0.14	1.76	2.70	4.45	1.21	6.87	1.53	11941.25	16185.72	0.33	0.45
e +18	47.00	-0.11	1.38	3.07	4.45	1.43	7.30	1.42	12374.75	16185.72	0.35	0.45

(1) FWD load-associated vertical and horizontal stresses calculated using the multi-layer elastic program BISAR with the FWD backcalculated layer moduli and the corresponding layer thicknesses at each corresponding depth (as shown in Figure 5.1)

(2) Gravimetric stress calculated using equations (5.1) and (5.2).

(3) Total vertical and horizontal stresses by adding the gravimetric stresses with the load-associated stresses.

(4) Resilient modulus computed using equation (4.5) corresponding to the field moisture content at the evaluation depth based on calculated bulk and octahedral shear stresses.

(5) Resilient modulus computed using equation (4.5) corresponding to the field moisture content at the evaluation depth based on NCHRP 1-28A stress recommendations.

Figures 5.7 to 5.10 show relationships between FWD backcalculated base modulus and the correction factor. The generated curves appear to fit the data reasonably well as indicated by the goodness-of-fit statistics shown in the charts. The charts exhibit a general trend that the correction factor decreases as the FWD backcalculated modulus increases. Figure 5.7 indicates that the CFs determined at the quarter depths tend to be slightly higher than the corresponding values calculated at the mid-depth of the base layer. This observation is attributed to the greater bulk stress induced at the upper (quarter depth) location, thereby increasing the resilient modulus and the calculated correction factor within the same material as may be observed in Table 5.1. Researchers conducted statistical tests of significance of the differences between correction factors at the two different depths. Although this analysis showed that the differences between the correction factors calculated at quarter- and mid-depths are statistically significant, the magnitudes of the differences within the 95 percent confidence interval are not significant enough as to cause differences in resilient moduli that result in significantly different overlay designs based on the M-E PDG. Thus, researchers combined the two sets of CFs and fitted the power law model to the combined dataset as shown in Figure 5.8.

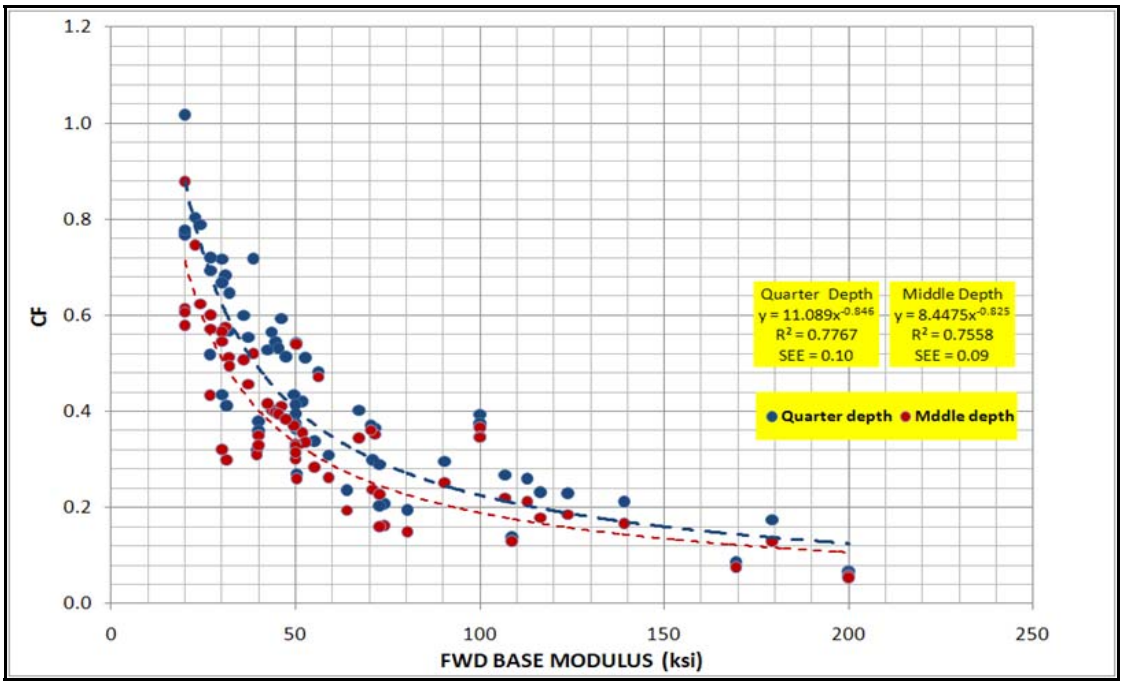

Figure 5.7. CFs for Limerock Base using Calculated Stresses at Different Depths due to FWD Load.

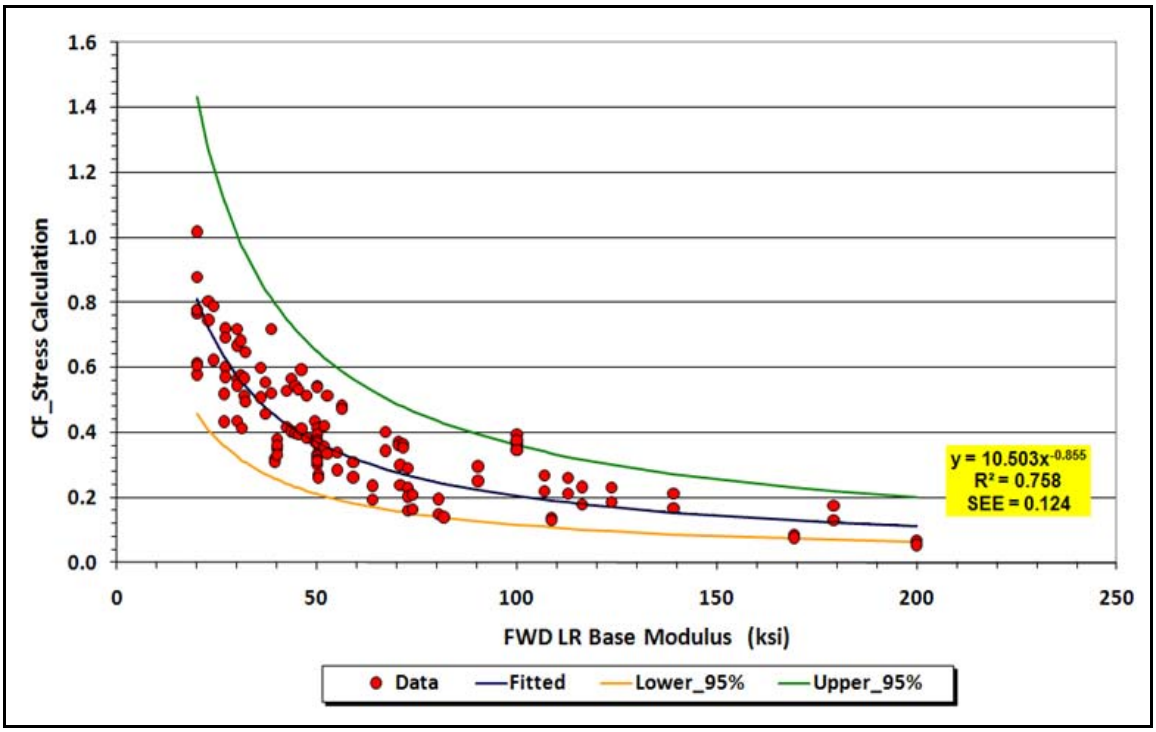

Figure 5.8. Relationship between CFs and Backcalculated Modulus for Limerock Base using Combined Dataset at Quarter- and Mid-Depth Positions.

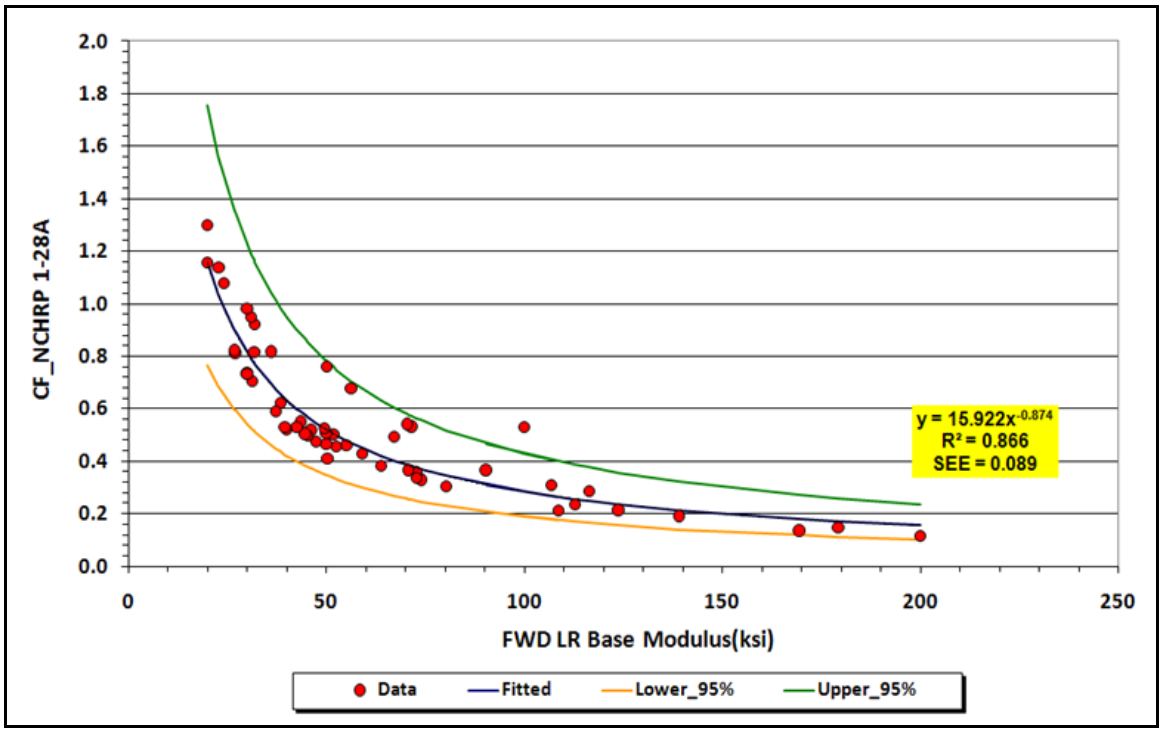

Figure 5.9. CFs for Limerock Base Determined using NCHRP 1-28A Recommended Stresses.

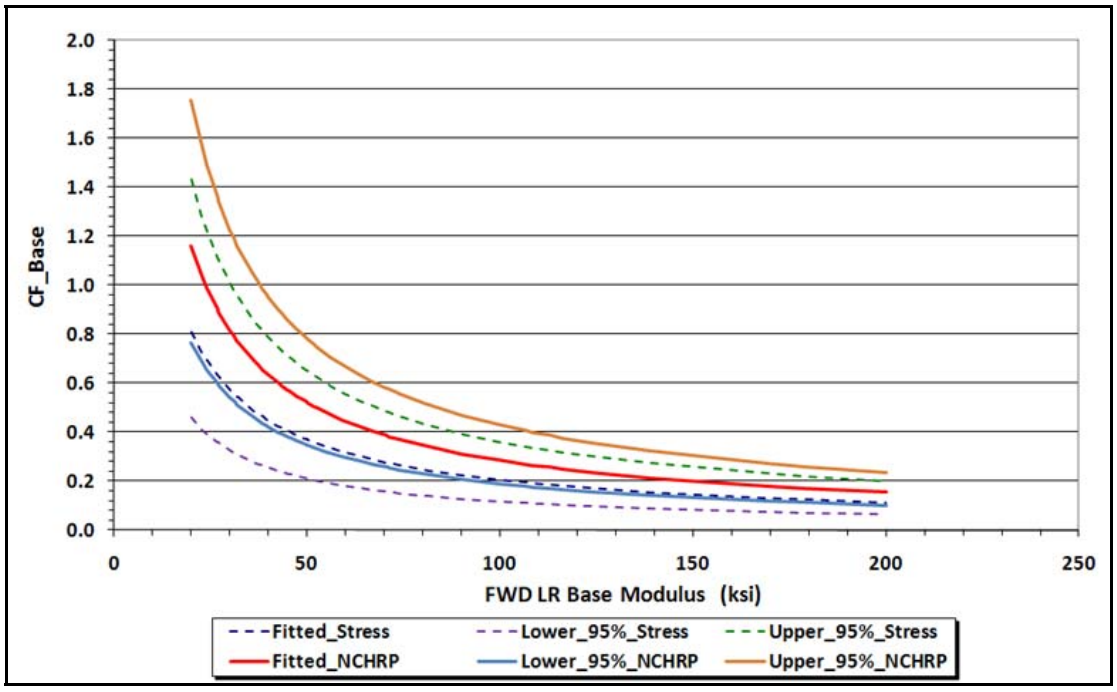

Figure 5.10. Comparison of CFs for Limerock Base Determined using NCHRP 1-28A Recommended Stresses and Calculated Stresses due to FWD Load.

To consider the variability of the calculated CFs, researchers determined the 95 percent confidence interval bands for the fitted curves based on calculated stresses due to the FWD load and the NCHRP 1-28A recommended stress levels. While the power law fit appears statistically reasonable, the calculated CFs are also observed to vary for a given FWD backcalculated modulus. Figures 5.8 and 5.9 show, respectively, the 95 percent confidence interval bands based on FWD load induced calculated stresses and NCHRP 1-28A recommended stress levels.

Figure 5.9 shows a statistically better fit when NCHRP recommended stresses are used to compute the correction factors compared to the case where FWD load induced stresses are used in the calculations. This result is somewhat to be expected since the CFs shown in Figure 5.9 are determined based on resilient moduli computed at a fixed stress state, i.e., 31 psi bulk stress and 7.5 psi octahedral shear stress. In contrast, the CFs plotted in Figure 5.8 are based on resilient moduli that vary with the depth at which stresses are computed and the given pavement structure.

Figure 5.10 compares CFs for base material determined from the two methods. The fitted curve for CFs based on NCHRP 1-28A recommended stress levels is observed

to be higher compared to the fitted curve for CFs computed from FWD load induced stresses. This finding is consistent with the results shown in Figure 5.4, which shows that the NCHRP recommended bulk stress closely corresponds to the upper limit of the calculated bulk stresses based on the FWD load and pavement structures tested. The average of the calculated FWD load induced bulk stresses is 22.4 psi compared to the recommended bulk stress of 31 psi from NCHRP 1-28A. For granular base materials, the resilient modulus model will predict a higher resilient modulus with a higher bulk stress.

With respect to the octahedral shear stress, Figure 5.4 shows that the average of the calculated FWD load induced stresses is 7.7 psi, which is close to the NCHRP 1-28A recommended octahedral shear stress of 7.5 psi. However, the upper limit of 13.2 psi in the calculated octahedral shear stresses due to the FWD load is significantly higher than the NCHRP 1-28A recommended stress level of 7.5 psi. Based on the laboratory resilient modulus data on base materials, a lower resilient modulus is determined with a higher octahedral shear stress.

Thus, the fitted curves shown in Figure 5.10 are consistent with the stress comparisons given in Figure 5.4. Figure 5.10 also shows that the lower bound of the 95 percent confidence interval of CFs based on NCHRP stress level calculations lines up closely with the fitted line of calculated CFs based on FWD load induced stresses. This observation again reflects the higher CFs based on the NCHRP recommended stress levels.

Researchers proceeded to generate the charts for subgrade and embankment materials that are shown in Figures 5.11 to 5.18. Figure 5.11 exhibits a similar trend noted previously in the calculated CFs for limerock base. Specifically, the quarter-depth location (closest to the top of the stabilized subgrade) yields slightly higher CFs due to the larger bulk stresses computed at that position under the FWD load. However, researchers found that the differences in the calculated CFs between the three evaluation positions are not significant enough as to result in significantly different overlay designs based on the M-E PDG. This finding reflects the relative insensitivity of the alligator cracking predictions to changes in the stabilized subgrade resilient modulus. Thus, researchers combined the calculated CFs at the three depths to get the fitted curve shown in Figure 5.12.

Using the NCHRP recommended stress levels, a slightly better fit to the calculated CFs was achieved (Figure 5.13) compared to the fitted curve based on calculated FWD load induced stresses (Figure 5.12). A similar observation was made earlier between the calculated CFs for limerock base from the two methods. In addition, Figure 5.14 indicates that the calculated CFs based on NCHRP recommended stress levels are higher than the calculated CFs based on FWD load induced stresses. A similar observation was made earlier from comparisons of the calculated CFs for limerock base between the two methods. Figure 5.14 also shows that the fitted curve based on calculated FWD load induced stresses lies between the fitted curve based on NCHRP recommended stress levels and the lower bound of the 95 percent confidence interval based on these stress levels.

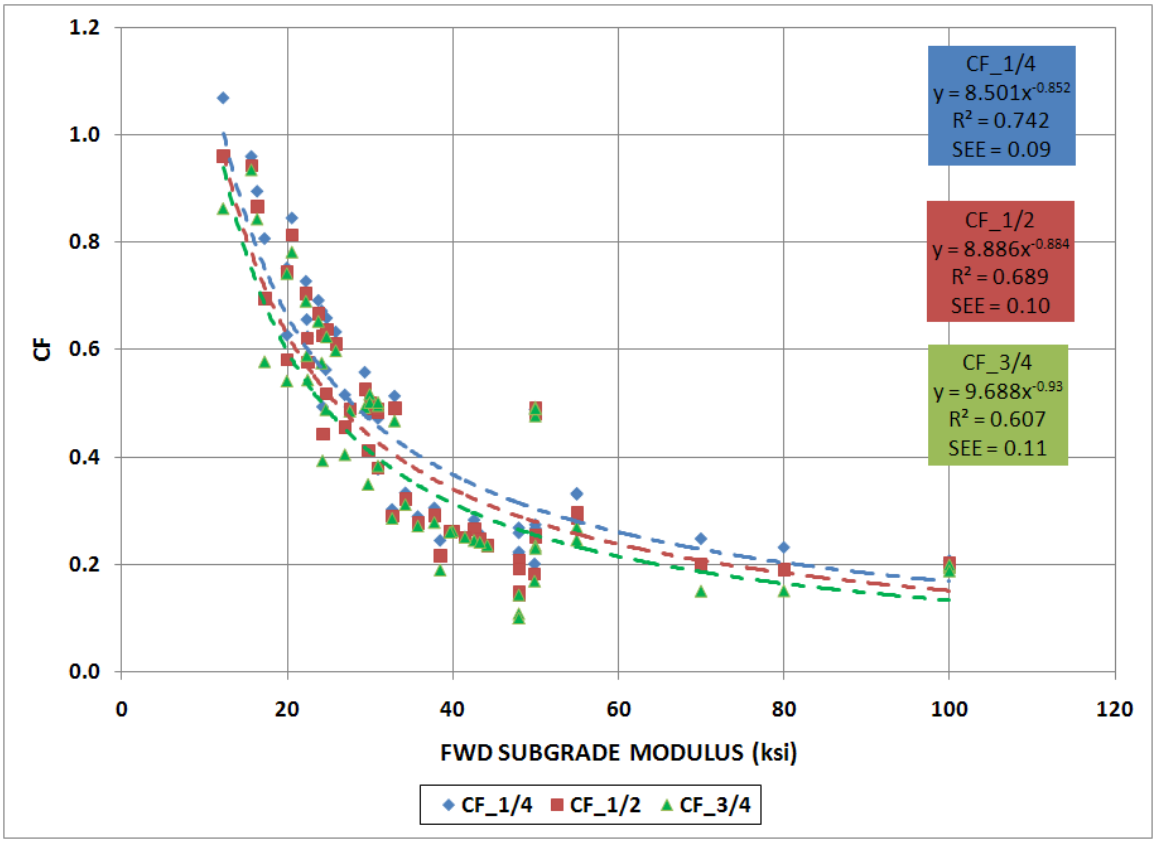

Figure 5.11. CFs for Stabilized Subgrade using Calculated Stresses at Different Depths due to FWD Load.

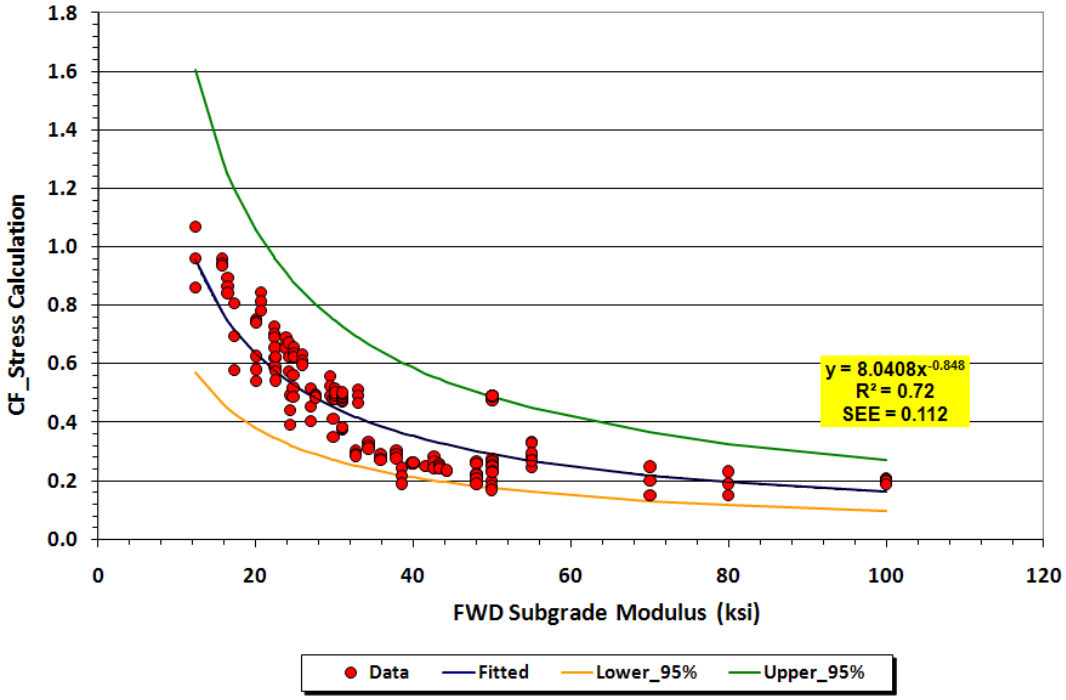

Figure 5.12. Relationship between CFs and Backcalculated Modulus for Stabilized Subgrade using Combined Dataset for all Three Positions.

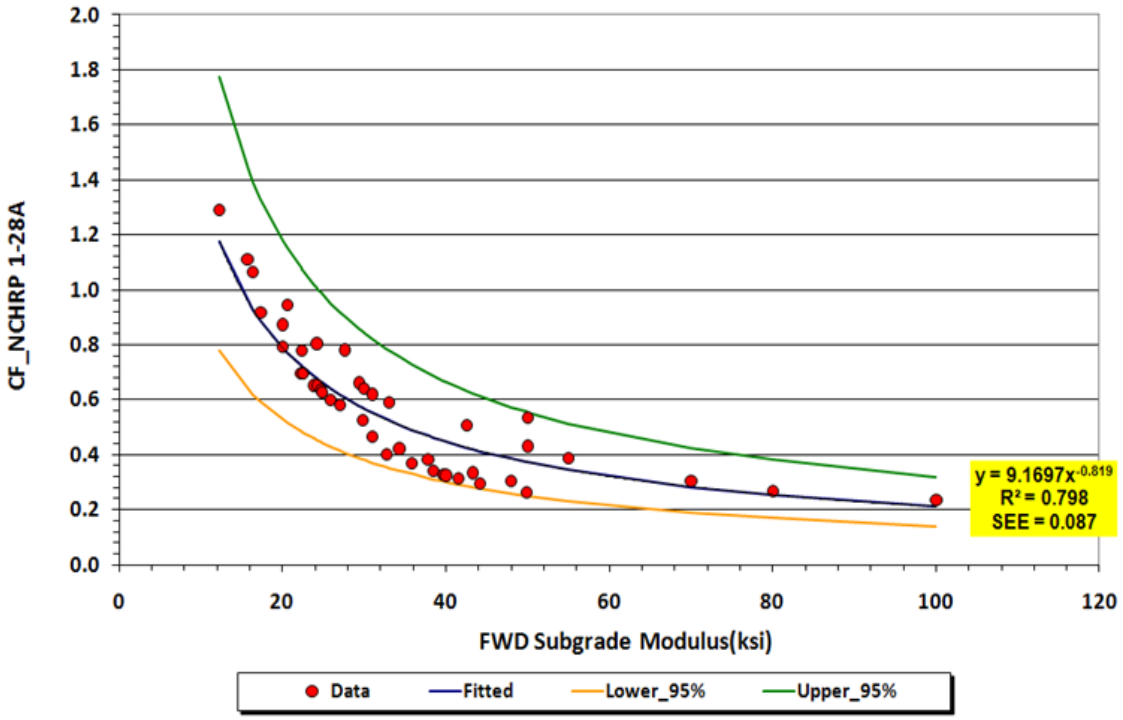

Figure 5.13. CFs for Stabilized Subgrade Determined using NCHRP 1-28A Recommended Stresses.

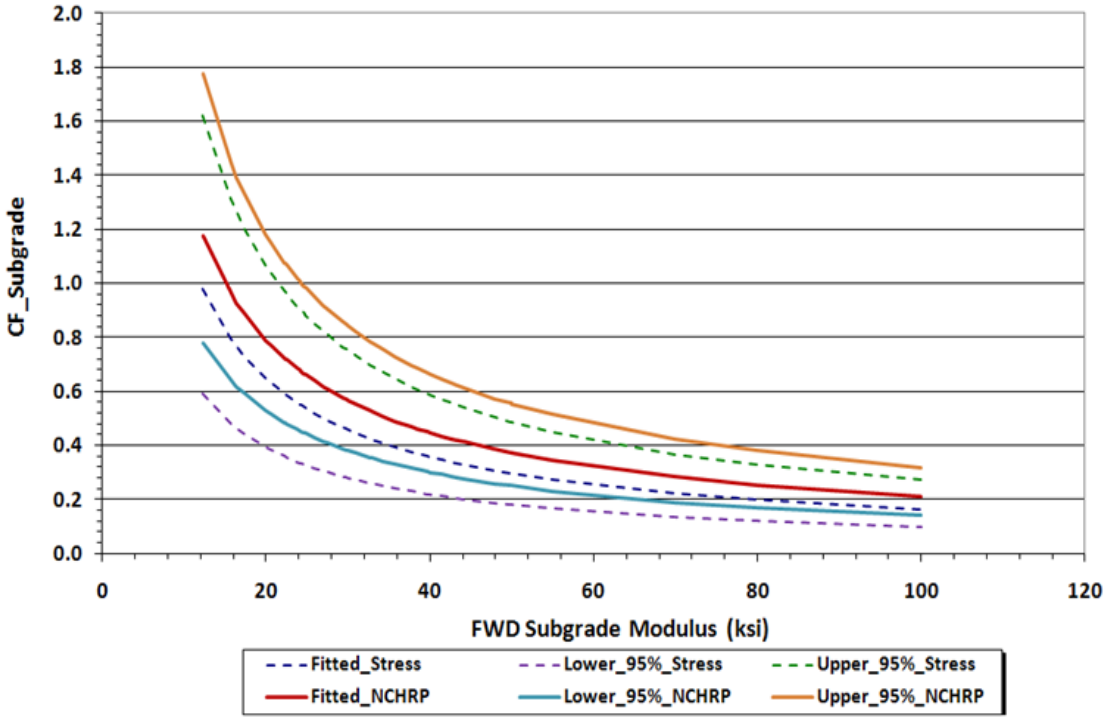

Figure 5.14. Comparison of CFs for Stabilized Subgrade Determined using NCHRP 1-28A Recommended Stresses and Calculated Stresses due to FWD Load.

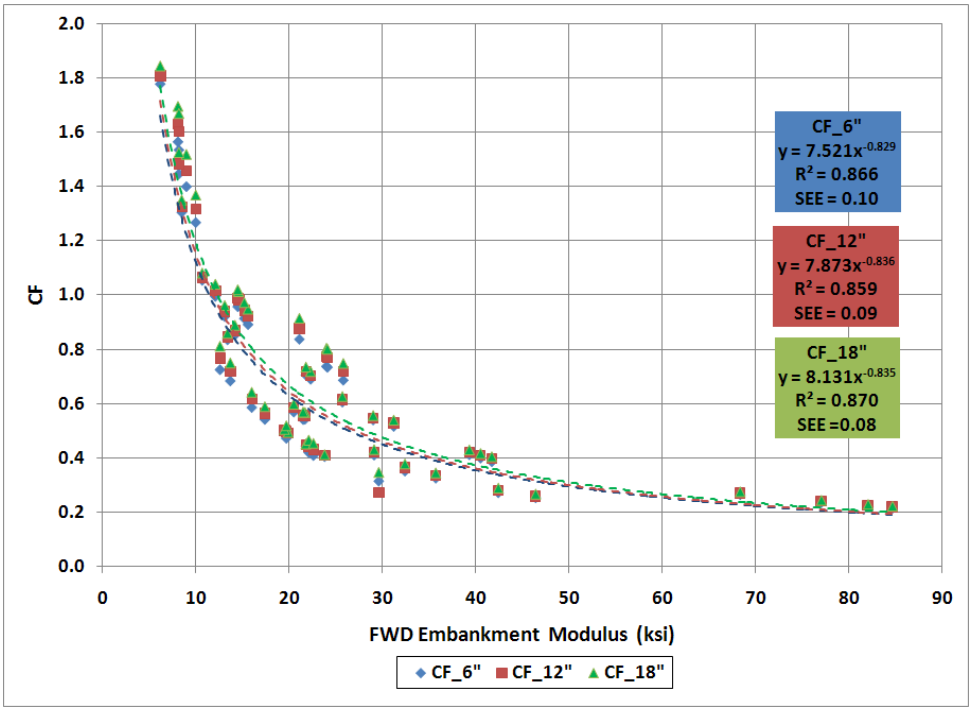

Figure 5.15. CFs for Embankment using Calculated Stresses at Different Depths due to FWD Load.

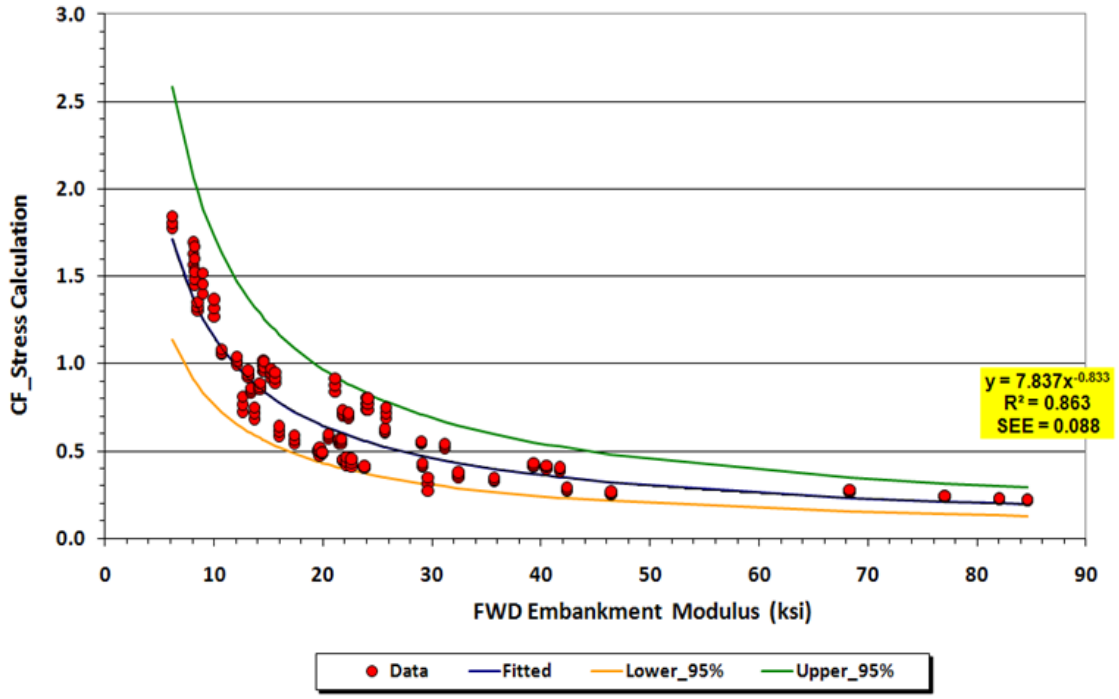

Figure 5.16. Relationship between CFs and Backcalculated Modulus for Embankment using Combined Dataset of CFs at Different Depths.

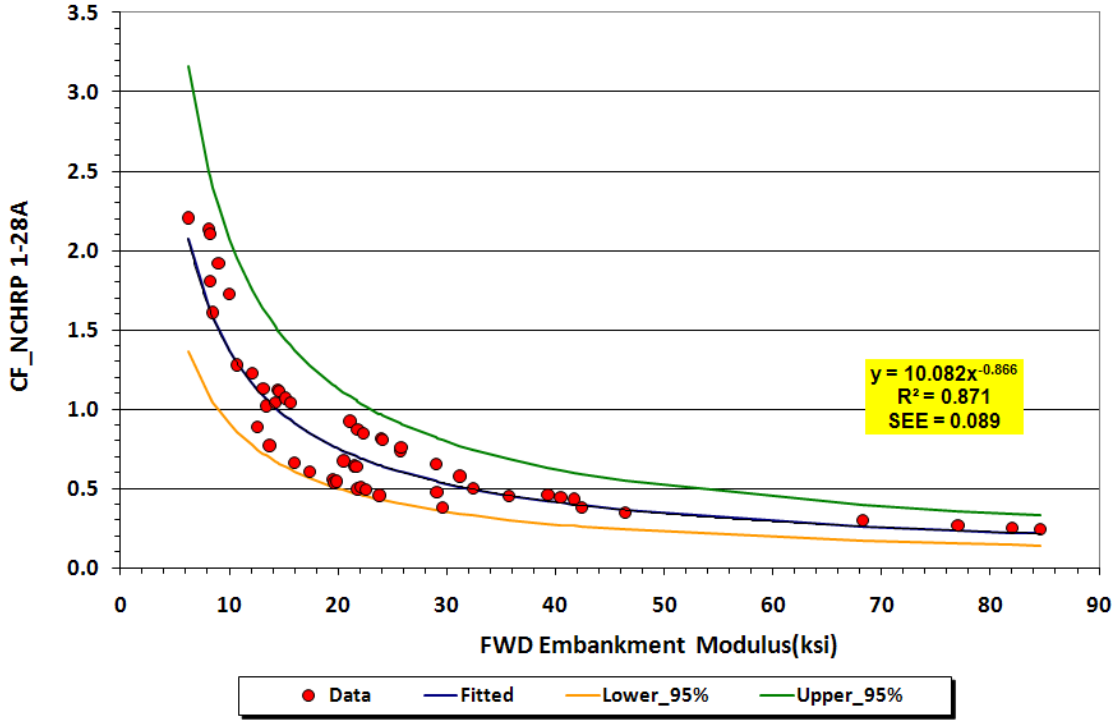

Figure 5.17. CFs for Embankment Determined using NCHRP 1-28A Recommended Stresses.

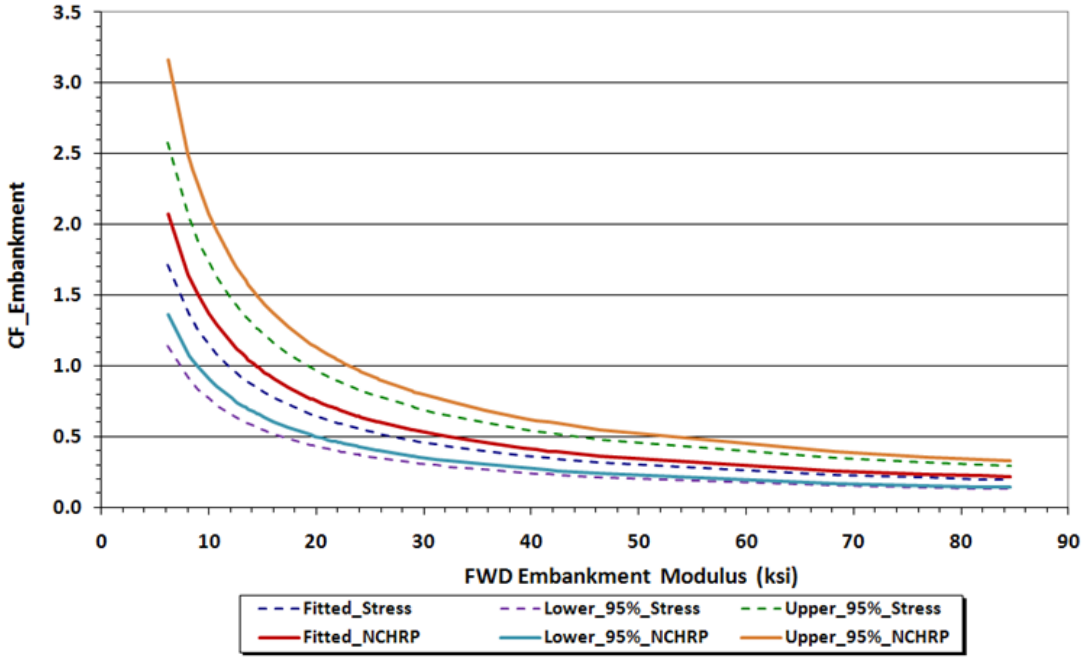

Figure 5.18. Comparison of CFs for Embankment Determined using NCHRP 1-28A Recommended Stresses and Calculated Stresses due to FWD Load.

Figure 5.15 shows close agreement between the fitted curves to the calculated CFs at different depths within the embankment. While statistical tests indicated that the differences between the correction factors are statistically significant, the effect of these differences in terms of required overlay thickness was observed to be minimal. Thus, researchers pooled the calculated CFs at the three depths and generated the fitted curve shown in Figure 5.16 for embankment soil.

Figure 5.17 shows the fitted curve to the calculated CFs based on NCHRP 1-28A recommended stress levels while Figure 5.18 compares the fitted curves to the calculated CFs between the two methods. Figure 5.18 presents a similar trend previously noted in the results obtained for the base and stabilized subgrade. For the embankment materials, the calculated CFs based on NCHRP recommended stress levels were also found to be higher than the calculated CFs based on FWD load induced stresses.

Researchers summarized all the equations needed for obtaining the CFs to determine equivalent laboratory resilient modulus in Table 5.2. In addition, researchers prepared Tables 5.3 to 5.5 to show correction factors determined from these equations that could be included in a pavement design manual.

Table 5.2. Summary of Fitted Equations for CFs.

Material	Curve	FWD load induced stresses	Equation Number	NCHRP recommended stress	Equation Number
LR Base	Lower Bound	$5.997x^{-0.856*}$	(5.3)	$10.653x^{-0.876}$	(5.12)
	Fitted	$10.503x^{-0.855}$	(5.4)	$15.922x^{-0.874}$	(5.13)
	Upper Bound	$18.392x^{-0.854}$	(5.5)	$23.796x^{-0.872}$	(5.14)
Subgrade	Lower Bound	$4.830x^{-0.848}$	(5.6)	$6.192x^{-0.820}$	(5.15)
	Fitted	$8.041x^{-0.848}$	(5.7)	$9.170x^{-0.819}$	(5.16)
	Upper Bound	$13.387x^{-0.848}$	(5.8)	$13.579x^{-0.817}$	(5.17)
Embankment	Lower Bound	$5.224x^{-0.833}$	(5.9)	$6.728x-^{0.868}$	(5.18)
	Fitted	$7.837x^{-0.833}$	(5.10)	$10.082x^{-0.866}$	(5.19)
	Upper Bound	$11.758x^{-0.833}$	(5.11)	$15.106x^{-0.864}$	(5.20)

*x is backcalculated in-situ modulus.

Table 5.3. CFs Determined from Equations for LR Base Material.

LR Base	CFs_FWD Load Induced Stresses			CFs_NCHRP Recommended Stresses		
FWD Modulus (ksi)	Lower Bound	Fitted	Upper Bound	Lower Bound	Fitted	Upper Bound
20	0.46	0.81	1.42	0.77	1.16	1.75
25	0.38	0.67	1.18	0.64	0.96	1.44
30	0.33	0.57	1.01	0.54	0.81	1.23
35	0.29	0.50	0.88	0.47	0.71	1.07
40	0.26	0.45	0.79	0.42	0.63	0.95
45	0.23	0.41	0.71	0.38	0.57	0.86
50	0.21	0.37	0.65	0.35	0.52	0.79
55	0.19	0.34	0.60	0.32	0.48	0.72
60	0.18	0.32	0.56	0.29	0.44	0.67
65	0.17	0.30	0.52	0.28	0.41	0.62
70	0.16	0.28	0.49	0.26	0.39	0.59
75	0.15	0.26	0.46	0.24	0.37	0.55
80	0.14	0.25	0.44	0.23	0.35	0.52
85	0.13	0.24	0.41	0.22	0.33	0.49
90	0.13	0.22	0.39	0.21	0.31	0.47
95	0.12	0.21	0.38	0.20	0.30	0.45
100	0.12	0.20	0.36	0.19	0.28	0.43
105	0.11	0.20	0.35	0.18	0.27	0.41
110	0.11	0.19	0.33	0.17	0.26	0.39
115	0.10	0.18	0.32	0.17	0.25	0.38

Table 5.3. CFs Determined from Equations for LR Base Material (continued).

LR Base	CFs_FWD Load Induced Stresses			CFs_NCHRP Recommended Stresses		
FWD Modulus (ksi)	Lower Bound	Fitted	Upper Bound	Lower Bound	Fitted	Upper Bound
120	0.10	0.18	0.31	0.16	0.24	0.37
125	0.10	0.17	0.30	0.16	0.23	0.35
130	0.09	0.16	0.29	0.15	0.23	0.34
135	0.09	0.16	0.28	0.14	0.22	0.33
140	0.09	0.15	0.27	0.14	0.21	0.32
145	0.08	0.15	0.26	0.14	0.21	0.31
150	0.08	0.14	0.25	0.13	0.20	0.30
155	0.08	0.14	0.25	0.13	0.19	0.29
160	0.08	0.14	0.24	0.12	0.19	0.28
165	0.08	0.13	0.23	0.12	0.18	0.28
170	0.07	0.13	0.23	0.12	0.18	0.27
175	0.07	0.13	0.22	0.12	0.17	0.26
180	0.07	0.12	0.22	0.11	0.17	0.26
185	0.07	0.12	0.21	0.11	0.17	0.25
190	0.07	0.12	0.21	0.11	0.16	0.25
195	0.07	0.12	0.20	0.11	0.16	0.24
200	0.06	0.11	0.20	0.10	0.16	0.23

Table 5.4. CFs Determined from Equations for Subgrade Material.

Subgrade	CFs_FWD Load Induced Stresses			CFs_NCHRP Recommended Stresses		
FWD Modulus (ksi)	Lower Bound	Fitted	Upper Bound	Lower Bound	Fitted	Upper Bound
10	0.69	1.14	1.90	0.94	1.39	2.07
15	0.49	0.81	1.35	0.67	1.00	1.49
20	0.38	0.63	1.06	0.53	0.79	1.17
25	0.32	0.52	0.87	0.44	0.66	0.98
30	0.27	0.45	0.75	0.38	0.57	0.84
35	0.24	0.39	0.66	0.34	0.50	0.74
40	0.21	0.35	0.59	0.30	0.45	0.67
45	0.19	0.32	0.53	0.27	0.41	0.61
50	0.18	0.29	0.49	0.25	0.37	0.56
55	0.16	0.27	0.45	0.23	0.34	0.51
60	0.15	0.25	0.42	0.22	0.32	0.48

Table 5.4. CFs Determined from Equations for Subgrade Material (continued).

Subgrade	CFs_FWD Load Induced Stresses			CFs_NCHRP Recommended Stresses		
FWD Modulus (ksi)	Lower Bound	Fitted	Upper Bound	Lower Bound	Fitted	Upper Bound
65	0.14	0.23	0.39	0.20	0.30	0.45
70	0.13	0.22	0.36	0.19	0.28	0.42
75	0.12	0.21	0.34	0.18	0.27	0.40
80	0.12	0.20	0.33	0.17	0.25	0.38
85	0.11	0.19	0.31	0.16	0.24	0.36
90	0.11	0.18	0.29	0.15	0.23	0.34
95	0.10	0.17	0.28	0.15	0.22	0.33
100	0.10	0.16	0.27	0.14	0.21	0.32

Table 5.5. CFs Determined from Equations for Embankment Material.

Embankment	CFs_FWD Load Induced Stresses			CFs_NCHRP Recommended Stresses		
FWD Modulus (ksi)	Lower Bound	Fitted	Upper Bound	Lower Bound	Fitted	Upper Bound
5	1.37	2.05	3.08	1.66	2.50	3.76
10	0.77	1.15	1.73	0.91	1.37	2.07
15	0.55	0.82	1.23	0.64	0.97	1.46
20	0.43	0.65	0.97	0.50	0.75	1.14
25	0.36	0.54	0.81	0.41	0.62	0.94
30	0.31	0.46	0.69	0.35	0.53	0.80
35	0.27	0.41	0.61	0.31	0.46	0.70
40	0.24	0.36	0.54	0.27	0.41	0.62
45	0.22	0.33	0.49	0.25	0.37	0.56
50	0.20	0.30	0.45	0.23	0.34	0.51
55	0.19	0.28	0.42	0.21	0.31	0.47
60	0.17	0.26	0.39	0.19	0.29	0.44
65	0.16	0.24	0.36	0.18	0.27	0.41
70	0.15	0.23	0.34	0.17	0.25	0.38
75	0.14	0.21	0.32	0.16	0.24	0.36
80	0.14	0.20	0.31	0.15	0.23	0.34
85	0.13	0.19	0.29	0.14	0.22	0.33
90	0.12	0.18	0.28	0.14	0.20	0.31

SENSITIVITY ANALYSIS

Researchers conducted a sensitivity analysis to evaluate the potential impact of the calculated CFs on AC overlay designs using the M-E PDG program. For this analysis, researchers considered a typical flexible pavement structure consisting of a 4-inch AC surface over 8 inches of limerock base, 12 inches of mechanically stabilized subgrade, and A-2-4 embankment. All M-E PDG runs were executed with a reliability level of 95 percent, average annual daily truck traffic of 3000 (equivalent to 15.5 million cumulative trucks over a 20-year design period), and a performance criterion of 35 percent on alligator cracking. The project was assumed to be located in the Miami area with the ground water table located at 5-ft depth.

For the sensitivity analysis, researchers selected three levels of the correction factor based on the upper and lower bounds of the 95 percent confidence interval and the mean value from the fitted curve. Researchers used the calculated CFs based on the NCHRP recommended stress levels for this analysis. The initial analysis varied the CFs one at a time for each layer. For this analysis, researchers assumed reference backcalculated moduli of 50, 30 and 20 ksi, respectively, for the base, stabilized subgrade and embankment materials. Researchers then varied the resilient modulus of each layer, one at a time, according to the selected CFs for that layer. For each CF, researchers ran the M-E PDG program iteratively to determine the thickness of overlay required to satisfy the given performance criterion of 35 percent alligator cracking over the specified 20-year design period. Tables 5.6 to 5.8 present the results from this sensitivity analysis.

The results summarized in these tables indicate that the required overlay thickness is most sensitive to the variation of CFs for the base material at the assumed reference backcalculated modulus of 50 ksi. For this case, there is a 1-inch difference in required overlay thickness between CFs corresponding to the lower and upper bounds of the 95 percent confidence interval. However, if the overlay thickness based on the fitted curve (corresponding to the mean CF) is used as the reference, the difference is half an inch in either direction. The sensitivity was found to be less for the stabilized subgrade where a maximum difference of 0.5-inch was obtained. For the embankment material, the results show no differences in the required overlay thickness for the range of correction factors considered in the analysis. However, it should be noted that all analyses done herein are

based on alligator cracking. The sensitivity of predicted pavement performance and overlay thickness design to the correction factors will vary if other distresses, such as rutting and longitudinal cracking, are used as performance criteria. At the time of this report, version 1.1 of the M-E PDG program did not yet have the rutting and longitudinal cracking models from NCHRP 9-30A and NCHRP 1-42A. Researchers recommend that the Florida DOT re-evaluate the sensitivity of the overlay thickness design to the corrections factors when a later version of the M-E PDG program is released that incorporates the models developed from these NCHRP projects.

Table 5.6. Sensitivity of Overlay Thickness to the CF for Base Material.

FWD Base Modulus (ksi)	CF Level	CF*	Equivalent Lab. Modulus (ksi)	Overlay Thickness (in)
50	Lower bound	0.35	17.5	2.0
	Fitted	0.52	26.1	1.5
	Upper bound	0.79	39.0	1.0

*Used equations (5.12) to (5.14) from in Table 5.2.

Table 5.7. Sensitivity of Overlay Thickness to the CF for Stabilized Subgrade.

FWD Subgrade Modulus (ksi)	CF Level	CF*	Equivalent Lab. Modulus (ksi)	Overlay Thickness (in)
30	Lower bound	0.38	11.4	1.5
	Fitted	0.57	17.0	1.5
	Upper bound	0.84	25.3	1.0

*Used equations (5.15) to (5.17) in Table 5.2.

Table 5.8. Sensitivity of Overlay Thickness to the CF for Embankment Material.

FWD Embankment Modulus (ksi)	CF Level	CF*	Equivalent Lab. Modulus (ksi)	Overlay Thickness (in)
20	Lower bound	0.50	10.0	1.0
	Fitted	0.75	15.1	1.0
	Upper bound	1.14	22.7	1.0

*Used equations (5.18) to (5.20) in Table 5.2.

Researchers also conducted a sensitivity analysis where the base, stabilized subgrade and embankment moduli were varied simultaneously from the respective reference backcalculated values according to the given level of the correction factors as shown in Table 5.9. The results revealed a maximum difference of 1.5 inches in required overlay thickness when the correction factors for the underlying layers are varied from the lower bound to the upper bound values.

Table 5.9. Sensitivity of Overlay Thickness when Underlying Layer Moduli are Varied Simultaneously.

Layer	FWD (ksi)	Lower Bound (ksi)[a]	Fitted_NCHRP (ksi)[b]	Upper Bound (ksi)[c]	Fitted_FWD (ksi)[d]
Base	50	17.5	26.5	38.0	18.5
Subgrade	30	11.7	15.9	25.2	13.5
Embankment	20	10.8	13.4	22.6	12.9
Overlay Thickness (in)		2.0	1.5	0.5	1.75

[a]Used equations (5.12), (5.15), and (5.18) in Table 5.2.
[b]Used equations (5.13), (5.16), and (5.19) in Table 5.2.
[c]Used equations (5.14), (5.17), and (5.20) in Table 5.2.
[d]Used equations (5.4), (5.7), and (5.10) in Table 5.2.

From the preceding evaluation of correction factors, researchers recommend that the fitted curves based on calculated FWD load induced stresses be considered for converting FWD backcalculated modulus to the equivalent laboratory resilient modulus

for asphalt concrete overlay design based on the M-E PDG. Employing these fitted curves is expected to provide overlay thickness designs that are between the thickness designs based on the lower bound and fitted CFs obtained using NCHRP recommended stress levels. Using the fitted curve to the calculated CFs based on FWD load induced stresses is also in line with the recommended use of average input values for performance predictions using the M-E PDG program.

CHAPTER VI. INVESTIGATING APPLICATION OF PSPA FOR PAVEMENT EVALUATION

This chapter documents efforts made during this project to investigate the applicability of the PSPA for in-situ assessment of asphalt concrete layer modulus. Compared to the FWD, the PSPA provides a direct measurement of seismic modulus at a higher load frequency relative to the frequencies associated with typical truck traffic. Thus, the seismic modulus determined from PSPA tests needs to be corrected to the load frequencies typically used for pavement design.

Researchers compared AC moduli determined from laboratory dynamic modulus tests with corresponding values determined from FWD and PSPA measurements. A methodology was also investigated to obtain a composite modulus from mixture properties determined from laboratory tests of individual AC lifts for the purpose of comparing the composite modulus with corresponding values determined from field tests with the FWD and the PSPA. This evaluation is particularly relevant on projects where the asphalt cores are not thick enough to run laboratory dynamic modulus tests according to AASHTO TP-62.

CORRELATION BETWEEN LABORATORY DYNAMIC MODULUS AND FIELD MODULUS

The State Materials Office conducted dynamic modulus tests on 24 asphalt concrete cores from different test sections. Researchers used the data from these tests to generate master curves for comparisons with FWD and PSPA moduli. The DM test data for the cores tested are presented in Appendix E, while the FWD backcalculated and PSPA moduli were given earlier in Tables 3.1 and 3.2, respectively. To compare the asphalt concrete moduli determined from FWD and PSPA tests, researchers used the following procedure to account for temperature and frequency effects:

- Step 1: Determine load frequency using FWD time-history data.
- Step 2: Using the DM data, generate the master curve corresponding to the FWD test temperature and determine the lab modulus at the corresponding frequency.
- Step 3: Correct the PSPA seismic modulus using the master curve at corresponding load frequency.

For step 1, researchers analyzed the FWD load-history data to determine the loading time for each test station. Table 6.1 presents the computed test frequencies from this step. This table shows that the estimated FWD test frequencies ranged from 14.2 to 20 Hz. Figure 6.1 illustrates how the load frequency was determined from the FWD time-history data. As shown, researchers used the equation determined by Lytton et al. (1990) to calculate the frequency from the FWD loading time.

Table 6.1. FWD Load Frequencies (Hz) Determined from Time-History Data.

FWD Station		-45	-30	-15	15	30	45
16020 US 17	Center	16.1	16.4	16.3	16.1	15.3	16.4
	OWP	16.6	15.8	15.9	14.5	14.2	16.5
16250 SR 37	Center	16.9	17.3	17.5	15.4	16.8	16.3
	OWP	17.3	15.5	17.2	17.8	17.6	17.3
16003001 SR 563	Center	17.6	17.8	17.2	18.3	18.1	16.5
	OWP	18.6	17.9	16.6	17.9	18.3	15.6
12005 SR 884	Center	17.4	17.2	17.5	17.2	17.4	17.2
	OWP	16.3	17.4	17.0	17.0	16.7	17.1
26005 SR 222	Center	16.6	16.6	15.9	16.8	16.4	16.6
	OWP	17.0	16.7	16.8	16.8	15.8	17.0
26060 US 301	Center	17.8	18.7	18.8	18.6	18.9	16.2
	OWP	19.4	19.2	19.3	18.5	18.2	18.4
28040 SR 18	Center	16.7	18.5	18.7	18.2	17.2	18.5
	OWP	18.3	18.7	18.6	18.6	18.4	18.2
71020 US 17	Center	17.6	17.8	16.7	16.0	16.4	17.0
	OWP	17.6	15.7	17.5	17.1	16.9	16.9
50010 US 90	Center	18.6	19.4	16.5	16.3	19.0	16.5
	OWP	20.0	17.6	20.0	18.9	17.9	19.4
50020 US 27	Center	17.8	18.1	18.0	17.8	17.5	17.2
	OWP	17.4	18.1	17.9	18.1	18.0	16.1
54020 US 27	Center	18.0	18.1	18.5	18.0	18.1	18.0
	OWP	18.5	18.4	18.7	18.2	18.5	18.6
58060 SR 89	Center	18.9	19.6	19.0	19.0	19.3	16.1
	OWP	19.5	19.2	19.2	18.2	18.9	19.3
93100 US 27	Center	17.0	17.5	17.3	17.2	16.5	17.3
	OWP	16.7	17.4	17.2	17.4	17.0	17.6
93310 SR 710	Center	16.7	15.9	16.7	16.4	16.9	16.4
	OWP	15.7	16.6	16.1	15.1	16.2	16.4
86190 SR 823	Center	15.4	14.8	17.0	14.8	16.0	15.6
	OWP	17.3	15.7	16.8	16.9	15.7	15.5

Table 6.1. FWD Load Frequencies (Hz) Determined from Time-History Data (continued).

FWD Station		-45	-30	-15	15	30	45
89010 US 1	Center	17.3	17.2	17.3	16.2	17.1	17.3
	OWP	15.8	17.2	17.2	17.5	17.4	17.1
77002 SR 414	Center	17.2	17.2	17.2	17.1	17.0	17.2
	OWP	17.4	17.0	17.1	16.8	17.5	17.2
77040 SR 46	Center	16.9	16.8	16.5	17.1	16.8	16.9
	OWP	16.9	16.8	17.0	16.6	16.3	15.3
79270 SR 483	Center	17.4	17.5	17.3	16.9	17.2	16.5
	OWP	16.0	17.5	15.0	17.5	17.2	15.9
92060 US 441	Center	16.8	16.1	16.6	17.2	17.2	14.9
	OWP	17.5	17.6	17.0	15.4	17.1	16.0
87060 A1A	Center	16.2	16.4	15.0	16.2	16.6	16.5
	OWP	16.3	15.2	16.8	16.2	16.4	16.4
87120 US 41	Center	14.9	17.5	17.5	15.6	14.9	17.2
	OWP	17.5	16.9	17.2	15.6	14.8	16.9
90060 US 1	Center	16.3	14.9	17.1	15.1	17.1	16.1
	OWP	17.1	17.0	16.8	16.6	17.1	15.0
10060 US 41	Center	14.6	16.9	15.9	16.7	16.3	16.9
	OWP	15.8	16.4	15.3	14.9	16.5	16.5
10160 SR 580	Center	18.8	18.8	18.7	18.7	18.3	18.7
	OWP	19.0	19.2	18.9	18.2	18.7	18.7

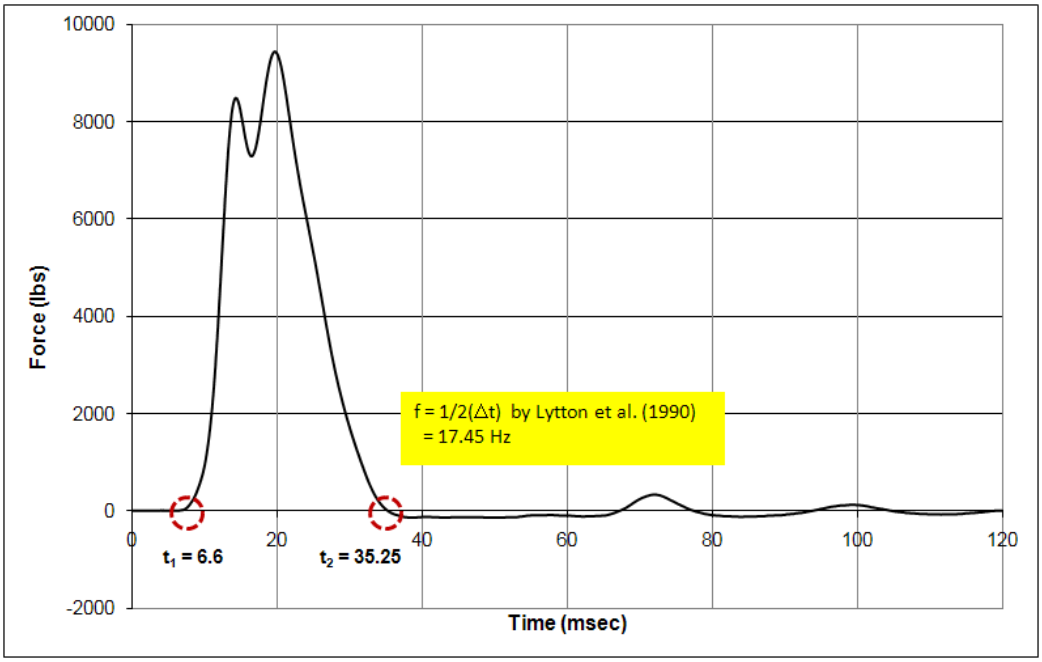

Figure 6.1. Illustration of Method for Determining FWD Load Frequency.

With respect to the load frequency of the PSPA, researchers used a representative value of 10 kHz based on a review of the literature (Saeed and Hall, 2002, and Celaya and Nazarian, 2006).

In step 2, researchers used the laboratory DM data to generate the master curve corresponding to the pavement temperature at the time of the FWD and PSPA tests. From this curve, the laboratory DM corresponding to the FWD load frequency was obtained. In the third step, the master curve was used to correct the PSPA modulus to the corresponding FWD load frequency. No temperature correction was necessary since the PSPA tests were conducted at close to the same time as the FWD tests. Thus, the PSPA and FWD test temperatures were close to the same if not equal. Researchers then adjusted the seismic AC moduli from the PSPA to the corresponding FWD load frequency. Figure 6.2 illustrates how researchers did the frequency correction on the PSPA modulus using the master curve. In the example shown, the PSPA modulus was corrected by dividing the actual measured PSPA modulus by the ratio of the laboratory DM at 10 kHz to the DM corresponding to the FWD load frequency (17.5 Hz).

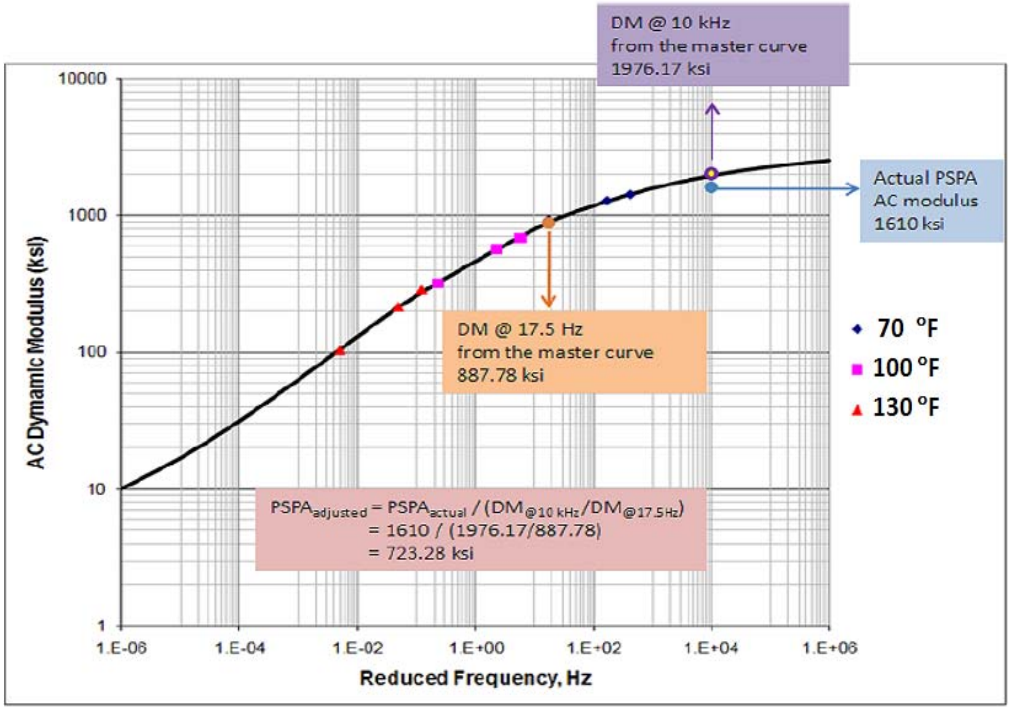

Figure 6.2. PSPA Modulus Correction Procedure.

Figure 6.3 compares the FWD backcalculated AC moduli to the laboratory dynamic moduli determined at the corresponding FWD test frequencies. The data exhibit a significant linear relationship between the laboratory and backcalculated asphalt concrete moduli. Consequently, researchers fitted the following simple linear equation to the data:

$$E_{FWD} = \beta_0 + \beta_1 E_{DM} \qquad (6.1)$$

where E_{FWD} is the backcalculated AC modulus in ksi, E_{DM} is the corresponding AC laboratory dynamic modulus, and β_0 and β_1 are model coefficients determined by regression analysis. The regression analysis showed that β_0 is not statistically significant at the 95 percent confidence level. Thus, equation (6.1) was refitted to the data setting β_0 to zero resulting in the following relationship:

$$E_{FWD} = 0.882 E_{DM} \qquad (6.2)$$

The SEE of the above equation is 238 ksi. Note that the β_1 coefficient is close to unity, indicating the good correlation between the AC moduli from DM and FWD tests at corresponding FWD load frequencies and test temperatures.

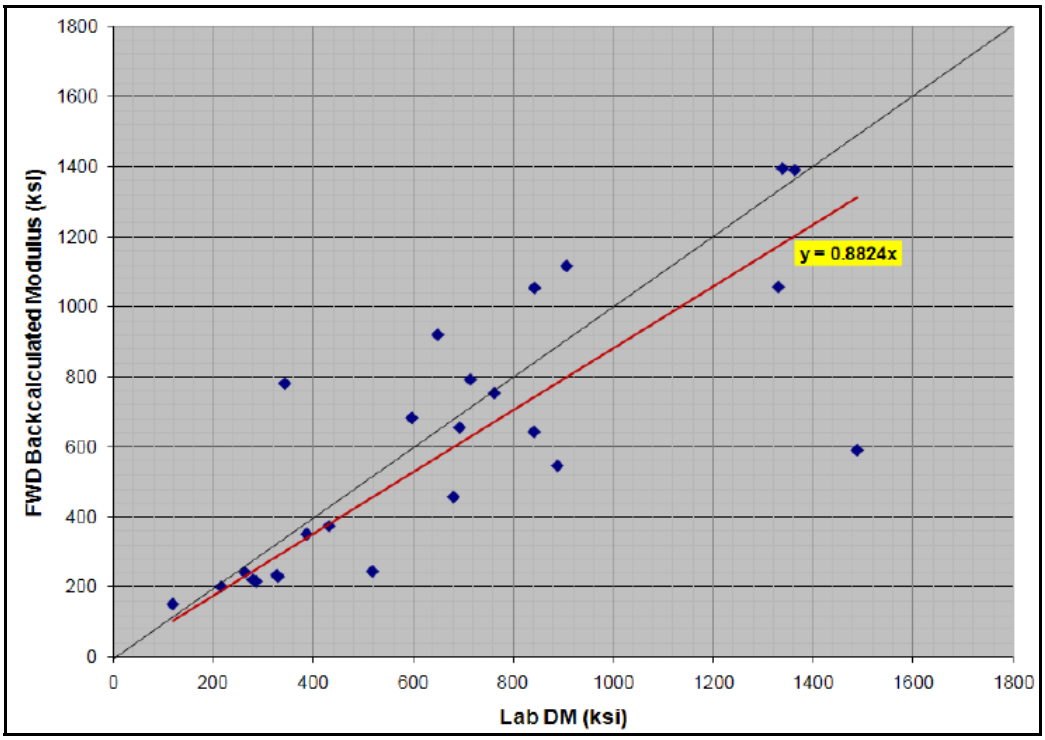

Figure 6.3. Comparisons of AC Moduli from DM and FWD Tests.

Figure 6.4 compares the AC moduli obtained from laboratory DM and PSPA tests after correcting the PSPA seismic modulus following the procedure presented earlier. Similar to Figure 6.3, the data exhibit a significant linear relationship between the two sets of moduli. Consequently, the following simple linear equation was fitted to the data:

$$E_{PSPA} = \beta_0 + \beta_1 E_{DM} \quad (6.3)$$

where E_{PSPA} is the AC modulus in ksi based on the PSPA after frequency correction. The regression analysis showed that β_0 was also not statistically significant at the 95 percent confidence level. Thus, a regression through the origin was performed and the relationship given in Equation 6.4 was obtained:

$$E_{PSPA} = 0.978\ E_{DM} \quad (6.4)$$

The standard error of the estimate (SEE) of the above equation is 222 ksi.

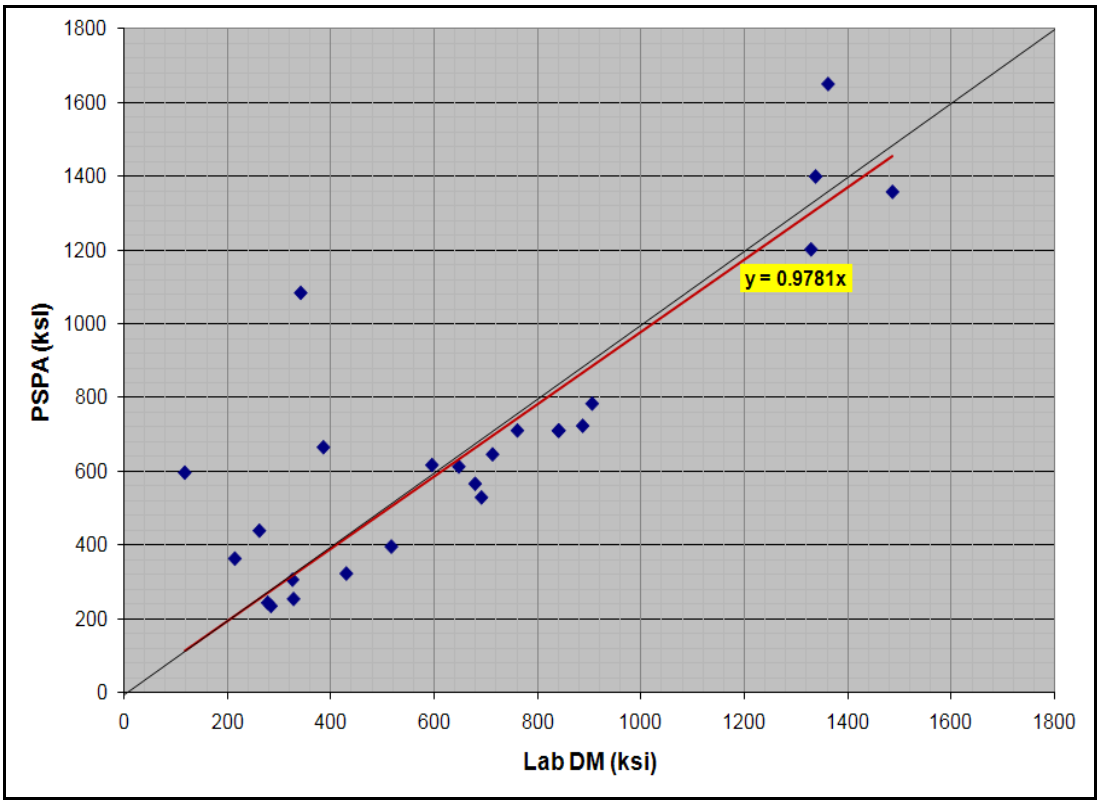

Figure 6.4. Comparison of AC Moduli from DM and PSPA Tests.

Researchers also compared the FWD backcalculated modulus with the frequency corrected PSPA modulus. Figure 6.5 shows this comparison. The data also reveal a significant linear relationship. From the regression analysis, the intercept coefficient was

not found to be statistically significant at the 95 percent confidence level. Consequently, researchers conducted a linear regression analysis with β_0 set to zero, and obtained the following relationship:

$$E_{FWD} = 0.868\ E_{PSPA} \quad (6.5)$$

The standard error of the estimate (SEE) of the above equation is 234 ksi. Again, note that the β_1 coefficient is close to unity, reflecting the good correspondence between the AC moduli from the FWD and PSPA at corresponding load frequencies and temperatures.

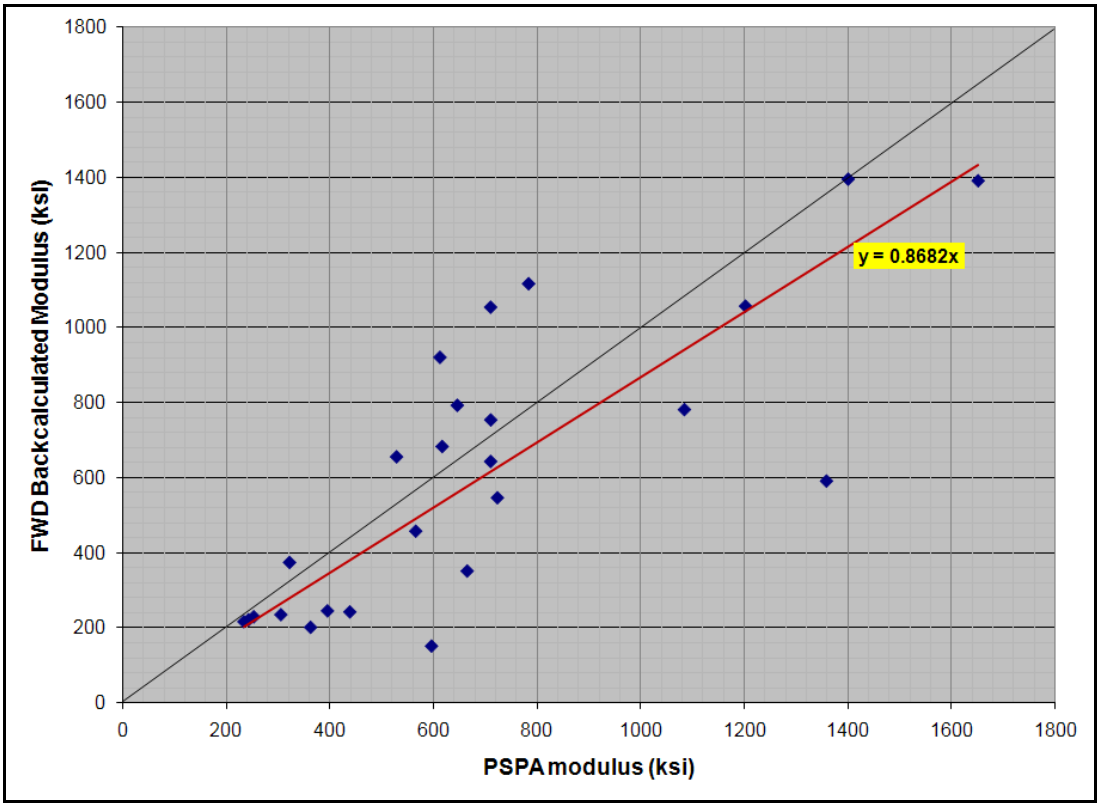

Figure 6.5. Comparison of AC Moduli from FWD and PSPA Tests.

PROCEDURE FOR DETERMINING COMPOSITE AC MODULUS

In practice, it is not uncommon to have AC cores less than 6 inches with multiple lifts. For this case, it is not feasible to perform the DM test on the entire core to establish the master curve. More than likely, extractions and DSR tests would have to be done on individual lifts to determine the master curve for each lift using the dynamic modulus prediction equation in the M-E PDG. Since the FWD and PSPA provide estimates of the modulus for the entire asphalt bound material, one cannot directly compare these

estimates with moduli determined from laboratory test data on individual lifts. Thus, an effort was made in this project to investigate a methodology for determining a composite AC modulus from test data on individual lifts in order to compare with FWD and PSPA moduli, and also to correct the PSPA seismic modulus determined from field tests.

To come up with a procedure for combining individual master curves, PSPA adjusted moduli using DM test data were compared with the corresponding values determined from the master curve of each individual lift that researchers generated from the DSR and volumetric test data. For this comparison, researchers used data obtained from DM, DSR, and volumetric tests conducted on 14 cores taken from three of the sections tested, specifically, sections 92060000, 93100000, and 87060000. DSR and volumetric test data on these sections are given in Appendix E of this report. Researchers employed the following procedure to correct the PSPA moduli from field tests using the DSR and volumetric test data on each lift:

- Determine the master curve of each lift using the M-E PDG dynamic modulus prediction equation as illustrated in Figure 6.6. Ping and Xiao (2007) verified the applicability of this equation to Florida mixtures in an earlier project conducted for the Florida DOT. Based on their findings, researchers deemed it appropriate to use the M-E PDG dynamic modulus prediction equation to determine the master curves for the AC samples tested in the laboratory.

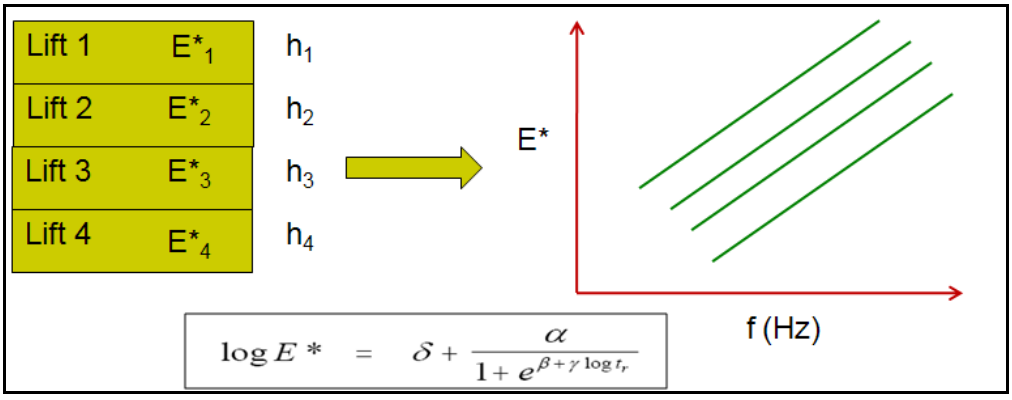

Figure 6.6. Step 1 of Procedure to Correct PSPA Moduli using DSR and Volumetric Test Data.

- Using the master curve for each lift, determine the FWD and PSPA moduli at the corresponding FWD and PSPA test frequencies as illustrated in Figure 6.7.

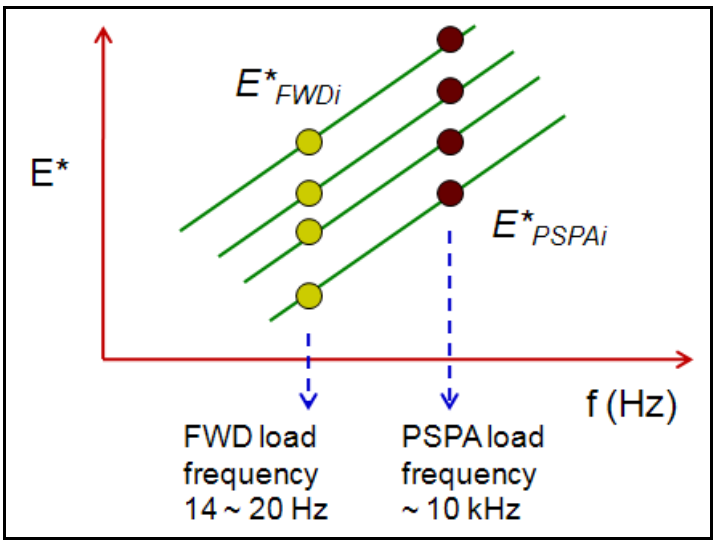

Figure 6.7. Step 2 of Procedure to Correct PSPA Moduli using DSR and Volumetric Test Data.

- Determine composite FWD and PSPA moduli using an equation originally proposed by Odemark in 1949 as an empirical method for transforming multilayer, linearly elastic systems into an equivalent single layer (Odemark, 1949). On the basis of his method, researchers computed composite FWD and PSPA moduli as follows:

$$E^*_{FWD\_Comp.} = \sum_{i=1}^{n} E^i_{FWDi} h_i^3 / \sum_{i=1}^{n} h_i^3 \quad (6.6)$$

$$E^*_{PSPA\_Comp.} = \sum_{i=1}^{n} E^i_{PSPAi} h_i^3 / \sum_{i=1}^{n} h_i^3 \quad (6.7)$$

where h_i is the thickness of lift i.

- Determine the PSPA corrected modulus using equation (6.8).

$$E^*_{PSPA\_Corrected} = E^*_{PSPA\_Measured} * \frac{E^*_{FWD\_Comp.}}{E^*_{PSPA\_Comp.}} \quad (6.8)$$

Figure 6.8 compares the corrected PSPA modulus using the above procedure, with the corresponding PSPA modulus after adjusting its value to the FWD test frequency using the master curve generated from DM test data. Although the number of

data points for this comparison is rather limited, the trend line shows a statistically reasonable agreement in adjusted PSPA modulus determined from the proposed approach when compared to the adjusted PSPA modulus based on DM test data that is regarded as the reference.

Based on this limited verification, other test sections were evaluated where only DSR and volumetric test data are available (since the cores from these sections were not thick enough to run the DM test). Figure 6.9 shows the comparison of adjusted PSPA modulus with the corresponding FWD backcalculated asphalt concrete moduli. In this comparison, the PSPA modulus was adjusted to the corresponding temperature and load frequency of the FWD test. While there are several points that are noticeably farther from the line of equality, researchers are of the opinion that the results presented seem promising enough to merit further investigation in a follow-up project where additional DM, DSR and volumetric test data can be collected and used to assess the applicability of the proposed method for correcting the PSPA modulus, particularly for tests done on pavements with thin (< 3-inch) AC surface layers.

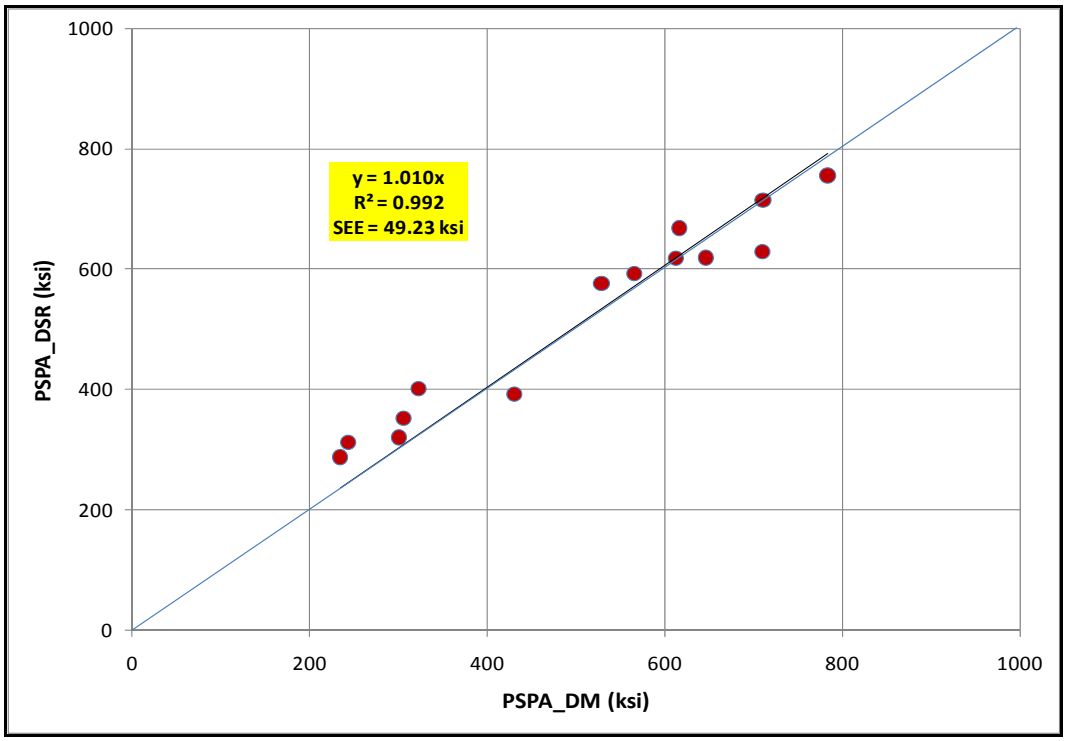

Figure 6.8. Comparison of Corrected PSPA Modulus Values.

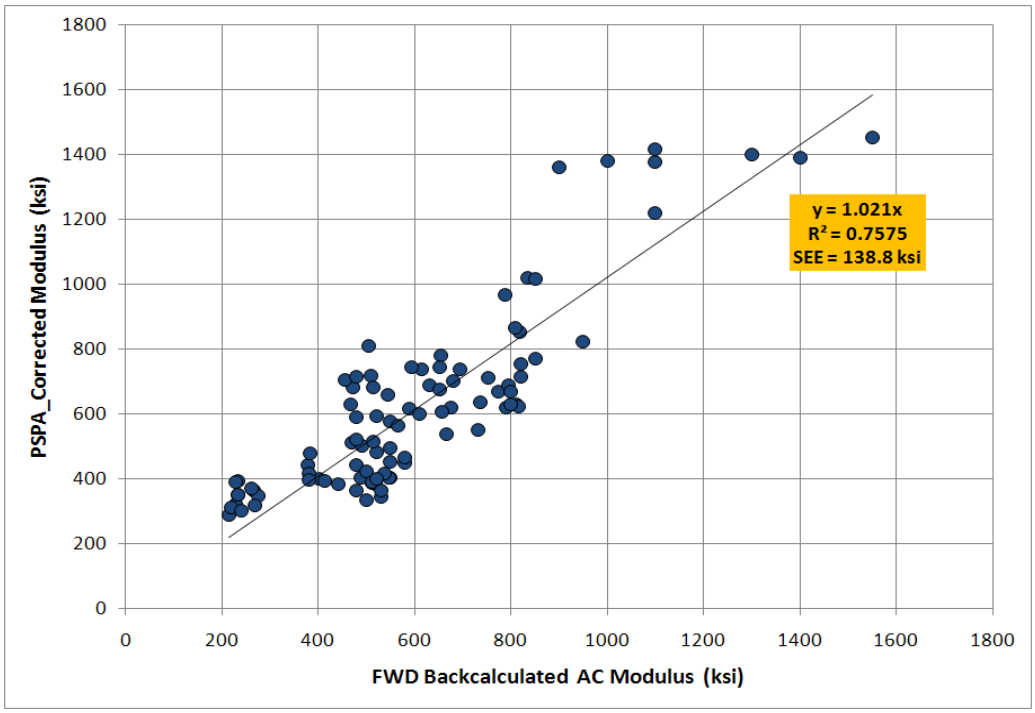

Figure 6.9. Comparisons FWD Backcalculated AC Moduli and Corresponding Corrected PSPA Moduli.

To provide an approximate but simpler method of correcting the PSPA modulus determined from field testing, researchers evaluated the relationship between the measured PSPA moduli and the corresponding moduli after correction based on the following equation:

$$E^*_{PSPA\_corrected} = \frac{E^*_{PSPA\_measured}}{aT + b} \tag{6.9}$$

where T is the pavement temperature (°F) at mid-depth of the asphalt concrete layer and a and b are regression constants. Researchers used the Microsoft Excel solver function to find the regression constants that provide the least sum of squared errors (SSE) between predicted and corrected PSPA modulus values. From this analysis, a and b were determined to be 0.0293 and 0.0702, respectively. Figure 6.10 shows that the relationship obtained gives fairly good predictions. Researchers note that the pavement temperatures used in determining equation (6.9) range from 54 to 103 °F. Researchers provide this equation as an alternative method for correcting PSPA modulus when DSR and volumetric test data are not readily available.

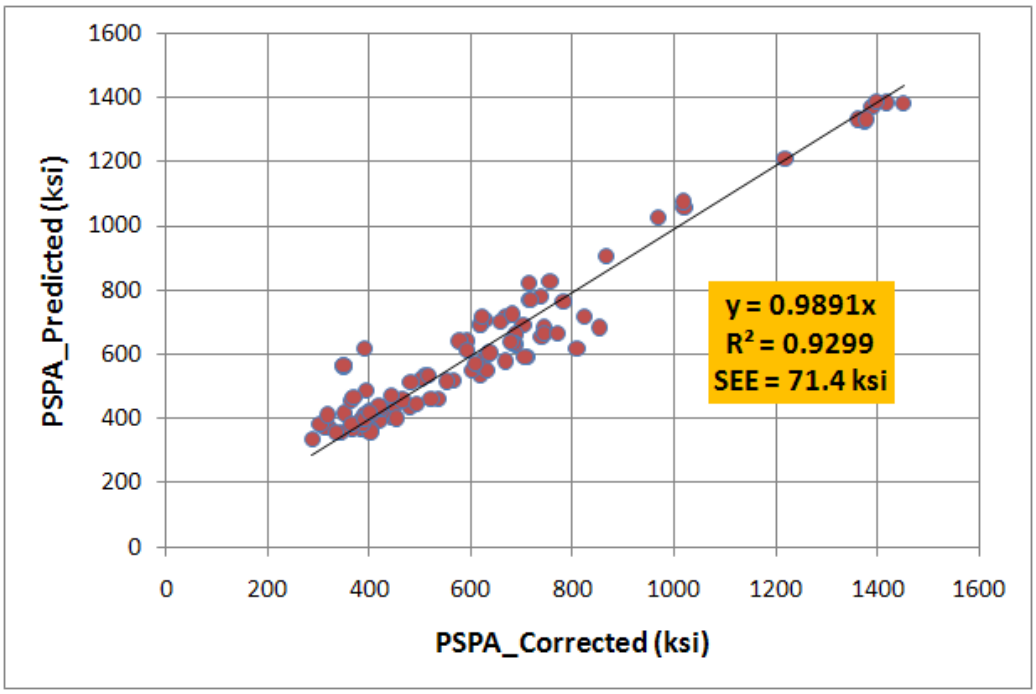

Figure 6.10. Comparison of Corrected PSPA Moduli Based on Laboratory Test Data with corresponding Corrections based on Equation (6.9).

CHAPTER VII. PROJECT SUMMARY AND RECOMMENDATIONS

The primary objectives of this project were (a) to recommend correction factors for determining equivalent laboratory modulus values given the corresponding base, subgrade, and embankment moduli from in-situ pavement testing, and (b) to evaluate nondestructive tests with the FWD and the portable seismic pavement analyzer to recommend a procedure for characterizing existing pavement condition for flexible pavement overlay design based on the M-E PDG. To accomplish these objectives, researchers executed a comprehensive work plan that included the following tasks:

- Reviewed available data and findings from earlier projects conducted by FSU and TTI to compile information that can be used to accomplish the study objectives;
- Developed field and laboratory test plans to collect additional data to fill gaps in the available information as identified from the literature review. Chapter II of this report documents the test program, which researchers and FDOT personnel jointly developed and executed in this project.
- Conducted field and laboratory tests to characterize material properties of in-service pavement sections. Field tests included FWD, PSPA, DCP, and material sampling of AC cores and underlying materials to measure the field moisture contents at the time of tests. Laboratory tests included resilient modulus, dynamic modulus, DSR, soil suction and extractions to characterize properties of asphalt concrete mixtures and underlying materials for evaluating correction factors and investigating the applicability of the PSPA for in-situ assessment of asphalt concrete layer modulus.
- Analyzed test data to determine correction factors and establish the relationships between these factors and FWD backcalculated moduli. In this evaluation, researchers determined correction factors using stress-compatible resilient moduli corresponding to calculated FWD load induced stresses and gravimetric stresses. Given the stress-compatible resilient modulus, the correction factor was calculated by dividing this value by the corresponding FWD backcalculated modulus. Researchers also used the NCHRP 1-28A

recommended stress levels to calculate correction factors given that these recommended stresses generally cover the range of calculated bulk and octahedral shear stresses due to FWD and gravimetric loads.

- Conducted a sensitivity analysis to examine the impact of proposed CFs on design of asphalt concrete overlays using the M-E PDG program.
- Investigated a procedure for frequency correction of asphalt concrete modulus determined from the PSPA.

Based on the research conducted, the following findings are noted:

- Using the *MODULUS 6.1* program, researchers conducted backcalculations of pavement layer moduli using the FWD data collected on in-service pavement sections tested during this project. For these backcalculations, researchers aimed to be within an average absolute error per sensor of 5 percent. For the majority of cases, this criterion was met, with an overall average absolute error per sensor of about 3 percent across all test stations. Comparisons of measured and predicted deflections presented in Appendix A showed excellent correlations between measured and predicted values on all test sections with standard errors of estimate (SEE) below 0.5 mils.
- PSPA seismic moduli showed a slightly higher coefficient of variation than those reported by Celaya and Nazarian (2006). The coefficient of variation of the PSPA seismic modulus ranged from 1.4 to 25.4 percent, with an overall average COV of 9.7 percent. Celaya and Nazarian (2006) reported that the variability of PSPA is less than 3 percent when repeat measurements are made without moving the device and around 7 percent when the device is moved within a small area. Researchers recognized during field testing that special caution needs to be taken when using the PSPA on open-graded surfaces. In analyzing the PSPA data, researchers used the average PSPA modulus per station to compare with the corresponding FWD modulus and dynamic AC modulus from laboratory tests.
- Researchers analyzed the DCP data to estimate in-situ moduli of underlying layers using a correlation equation incorporated into the M-E PDG program. From this analysis, researchers found that the base modulus determined from

DCP measurements ranged from 30 to 70 ksi. The subgrade modulus varied from 20 to 50 ksi while the embankment modulus ranged from 15 to 35 ksi.

- As noted earlier, researchers collected underlying material samples to determine field moisture contents. These measurements were conducted so that comparisons between laboratory and FWD backcalculated moduli can be made based on the in-situ moisture condition at the time of the FWD test. From these measurements, researchers found that the base layer moisture content varied from 5.4 to 15 percent. District 6 base materials generally had lower moisture contents than other areas. Most ground water table depths were found to be within 10 feet except for District 3 sections and test sections located in Alachua County in District 2.
- For characterizing the resilient modulus, researchers proposed the model given in equation (4.5) that accounts for the effect of soil moisture based on the material's soil water characteristic curve. Researchers fitted the resilient modulus and soil suction data to the proposed resilient modulus model, and found that the model fitted the test data reasonably well as indicated by the goodness-of-fit of the model predictions.
- Researchers generated charts showing the relationships between calculated correction factors for base, stabilized subgrade and embankment materials and the corresponding FWD backcalculated modulus. To quantify these relationships, researchers fitted a power law model to the data and found that the model gave a reasonable fit to the data as indicated by the goodness-of-fit statistics from the regression analysis. Researchers also determined the 95 percent confidence interval bands of the fitted curves to account for the variability in calculated CFs.
- For a given material, researchers calculated correction factors at selected depths within the layer. For the base and stabilized subgrade, researchers found the CFs to be slightly higher at locations closest to the top of the layer compared to the calculated CFs at the lower depths. This observation is specific to CFs based on calculated FWD load induced stresses. The higher CF is mainly attributed to the higher calculated bulk stress under the FWD

load at the upper depths resulting in a higher resilient modulus. In contrast to the base and stabilized subgrade, the calculated CFs for the embankment tends to increase with depth due to the higher calculated gravimetric stresses within this layer and the diminished influence of the surface load and the associated stresses.

- Comparison of CFs determined from the two approaches used in this project show the fitted CF curves based on NCHRP 1-28A recommended stresses to be generally higher than those calculated based on FWD load induced stresses. Researchers note that the NCHRP recommended bulk stress is close to the upper limit of the calculated bulk stresses based on the FWD load. A higher bulk stress would give a higher resilient modulus resulting in a higher correction factor. Researchers also found that the fitted CF curve based on calculated FWD load induced stresses generally lies between the fitted CF curve based on NCHRP recommended stresses and the lower bound of the 95 percent confidence interval for these CFs.
- Researchers conducted a sensitivity analysis to evaluate the potential impact of the calculated CFs on overlay designs using the M-E PDG program. The results from this analysis indicate that the required overlay thickness is most sensitive to the variation of CFs for the base material where a 1-inch difference in required overlay thickness was determined between CFs corresponding to the lower and upper bounds of the 95 percent confidence interval for the fitted CF curve. However, if the overlay thickness based on the fitted curve (corresponding to the mean CF) is used as the reference, the difference is half an inch in either direction. The sensitivity was found to be less for the stabilized subgrade where a maximum difference of 0.5-inch was obtained. For the embankment material, the results show no differences in the required overlay thickness for the range of correction factors considered in the analysis. The sensitivity analysis also showed a maximum difference of 1.5 inches in required overlay thickness when the correction factors for base, stabilized subgrade and embankment were simultaneously varied from the respective lower bound values to the corresponding upper bound values.

- Researchers compared AC moduli determined from laboratory dynamic modulus tests with corresponding values determined from FWD and PSPA measurements. From these comparisons, researchers found a significant linear relationship between the FWD backcalculated AC moduli and laboratory dynamic moduli determined at corresponding FWD test frequencies. A significant linear relationship was also observed between laboratory dynamic moduli and frequency corrected PSPA AC moduli.
- To correct PSPA AC modulus, researchers investigated a procedure to determine a composite modulus based on properties of individual lifts using Odemark's equation. For this investigation, researchers used data obtained from DM, DSR, and volumetric tests conducted on 14 cores taken from three of the field sections tested. Using data from DSR tests and extractions done on individual lifts, researchers performed frequency corrections of PSPA moduli using Odemark's equation as explained in Chapter VI of this report. Researchers then compared the corrected PSPA moduli from this analysis with the corrected moduli based on data from laboratory dynamic modulus tests. Although the number of data points for this comparison is rather limited, the trend line shows a statistically reasonable agreement in adjusted PSPA modulus determined from the proposed approach when compared to the adjusted PSPA modulus based on DM test data that is regarded as the reference.
- To provide an approximate but simpler method of correcting the PSPA modulus determined from field testing, researchers also evaluated the relationship between the measured PSPA moduli and the corresponding moduli after correction. In this regard, researchers fitted the PSPA test data to equation (6.9) to determine the model coefficients. The resulting equation was found to provide fairly good predictions of corrected PSPA moduli over the range of pavement temperatures at which PSPA tests were conducted. Researchers provide this equation as an alternative method for correcting PSPA modulus when DSR and volumetric test data are not readily available.

Given the above findings, researchers offer the following recommendations with respect to implementing the M-E PDG program for thickness design of flexible pavement overlays:

- From the evaluation of correction factors, researchers recommend that the fitted curves based on calculated FWD load induced stresses be considered for converting FWD backcalculated modulus to the equivalent laboratory resilient modulus for asphalt concrete overlay design based on the M-E PDG. Employing these fitted curves is expected to provide overlay thickness designs that are between the thickness designs based on the lower bound and fitted CFs obtained using NCHRP recommended stress levels. Using the fitted curve to the calculated CFs based on FWD load induced stresses is consistent with the recommended use of average input values for performance predictions with the M-E PDG program.
- The Florida DOT presently uses the FWD to estimate the embankment modulus. Researchers recommend that the Department consider expanding the application of the FWD for nondestructive assessment of pavement layer moduli by backcalculation. In this project, researchers used the MODULUS program to backcalculate pavement layer moduli from measured FWD deflections. In general, the predicted deflection basins from backcalculations done in this project using MODULUS provided a reasonable match with the measured basins for flexible pavement sections that covered the range of materials found in Florida. Based on this experience, researchers recommend that the Department consider using the MODULUS program for backcalculating pavement layer moduli from FWD deflections.
- Recognizing that ground penetrating radar, DCP and PSPA can support FWD data interpretation, researchers recommend that the Department adopt an integrated approach of collectively utilizing these pavement evaluation tools to provide supporting information needed for thickness design of flexible pavement overlays using the M-E PDG.

REFERENCES

Applied Research Associates. *Guide for Mechanistic-Empirical Design of New and Rehabilitated Pavement Structures*. Final Report, National Cooperative Highway Research Program Project 1-37A, Transportation Research Board, Washington, D.C., 2004.

Bulut, R., R. L. Lytton, and W. K. Wray. *Soil Suction Measurements by Filter Paper*. Expansive Clay Soils and Vegetative Influence on Shallow Foundations, ASCE Geotechnical Special Publication No. 115 (eds. C. Vipulanandan, M. B. Addison, and M. Hasen), American Society of Civil Engineers, Reston, Va., 2001, pp. 243-261.

Celaya, M., and S. Nazarian. *Seismic Testing to Determine Quality of Hot-Mix Asphalt*. Journal of the Transportation Research Board, No. 1946, Transportation Research Board (TRB) of the National Academics, Washington, D.C., 2006, pp. 113-122.

Chandra, D., K. M. Chua and R. L. Lytton. *Effects of Temperature and Moisture on Load Response of Granular Base Material in Thin Pavements*. Transportation Research Record No.1252, National Research Council, Washington, D.C., 1989, pp 33-41.

De Jong, D. L., M. G. F. Peutz, and A. R. Korswagen. *Computer Program BISAR*. External Report, Koninklijke/Shell-Laboratorium, The Netherlands, 1973.

Fredlund, D. G., and A. Xing. *Equations for the Soil-Water Characteristic Curve*. Canadian Geotechnical Journal, Vol. 31, No. 4, 1994, pp. 521-532.

Khazanovich, L., C. Celauro, B. Chadbourn, and J. Zollars. *Evaluation of Subgrade Resilient Modulus Predictive Model for Use in Mechanistic-Empirical Pavement Design Guide*. Journal of the Transportation Research Board, No. 1947, Transportation Research Board (TRB) of the National Academics, Washington, D.C., 2006, pp. 155-166.

Lamborn, M. *A Micromechanical Approach to Modeling Partly Saturated Soils*. Master's Thesis, Texas A&M University, College Station, Tex., 1986.

Lytton, R. L., F. P. Germann, Y. J. Chou, and S. M. Stoffels. *Determining Asphaltic Concrete Pavement Structural Properties by Nondestructive Testing*. National Cooperative Highway Research Program (NCHRP) Report 327, Transportation Research Board, Washington D.C., 1990.

NCHRP Project 1-28A Research Results Digest Number 285. *Laboratory Determination of Resilient Modulus for Flexible Pavement Design*. Transportation Research Board (TRB) of the National Academics, Washington, D.C., 2004.

Odemark, N. *Investigation as to the Elastic Properties of Soils and Design of Pavements According to the Theory of Elasticity*. Statens Vaginstitute, meddelande 77, Stockholm, Sweden, 1949.

Oh, J. H., and E. G. Fernando. *Development of Thickness Design Tables Based on the M-E PDG*. Research Report No. BDH10-1, Texas Transportation Institute, The Texas A&M University System, College Station, Tex., 2008.

Ping, W. V., Y. Wang, and Z. Yang. *Field and Laboratory Evaluation of Resilient Modulus Measurements of Florida Pavement Soils*. Research Report No. FL/DOT/RMC/0636(F) -4538, FAMU-FSU College of Engineering, Tallahassee, Fla., 2000.

Ping, W. V., and Y. Xiao. Evaluation of the Dynamic Complex Modulus Test and Indirect Diametral Test for Implementing the AASHTO 2002 Design Guide for Pavement Structures in Florida. Research Report No. FL/DOT/RMC/BC-352-12, FAMU-FSU College of Engineering, Tallahassee, Fla., 2007.

Saeed, A., and J. W. Hall. *Comparison of Non-Destructive Testing Devices to Determine In Situ Properties of Asphalt Concrete Pavement Layers*. Pavement Evaluation 2002 Conference, Roanoke, Va, 2002.

Scullion, T., and W. Liu. *MODULUS 6.0 for Windows: User's Manual*. Research Report 0-1869-2, Texas Transportation Institute, College Station, Tex., 2001.

Steyn, W. J. and E. Sadzik. *Application of the Portable Pavement Seismic Analyzer (PSPA) for Pavement Analysis*. Proceedings of the 26th Southern African Transport Conference (SATC 2007), Pretoria, South Africa, July 2007, pp. 294-304.

Texas Transportation Researcher. *Models Developed to Predict Climatic Effects on Low-Volume Roads*. Vol. 25, No. 4, Texas Transportation Institute, Texas A&M University System, College Station, Tex., 1989, pp 5-6.

APPENDIX A

PLOTS OF MEASURED AND PREDICTED FWD DEFLECTIONS

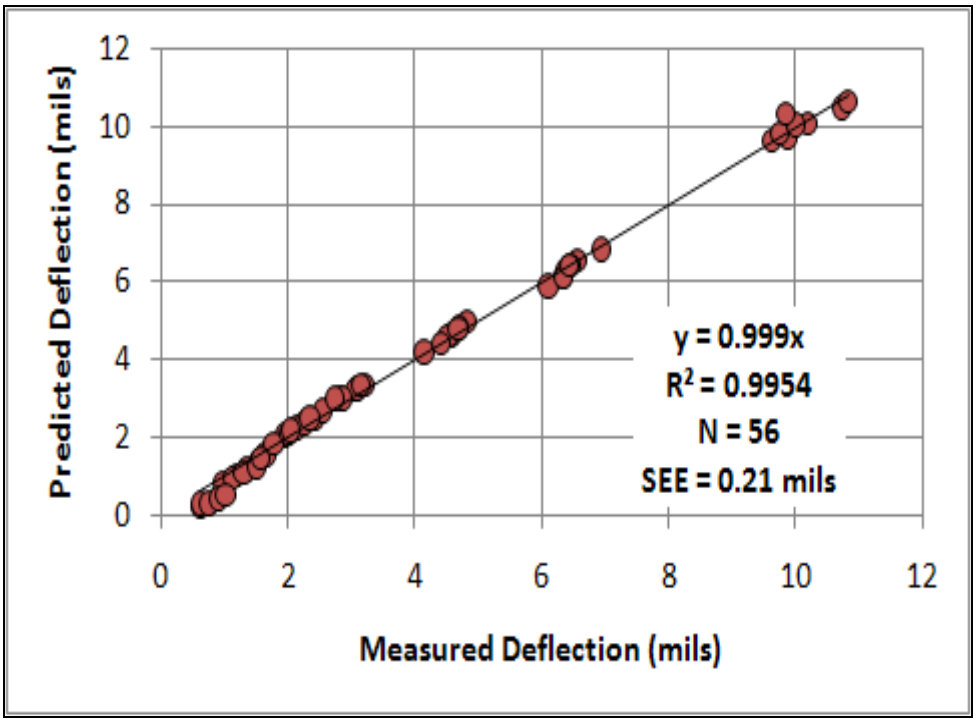

Figure A1. Comparison of Measured and Predicted FWD Deflections on Section 16020000.

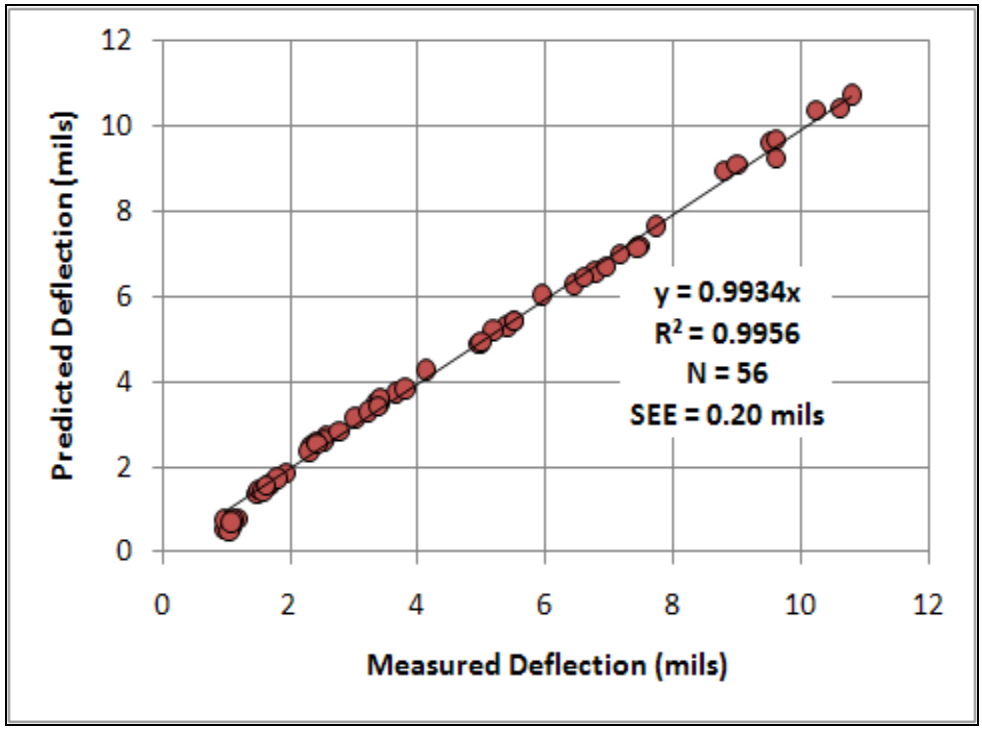

Figure A2. Comparison of Measured and Predicted FWD Deflections on Section 16003001.

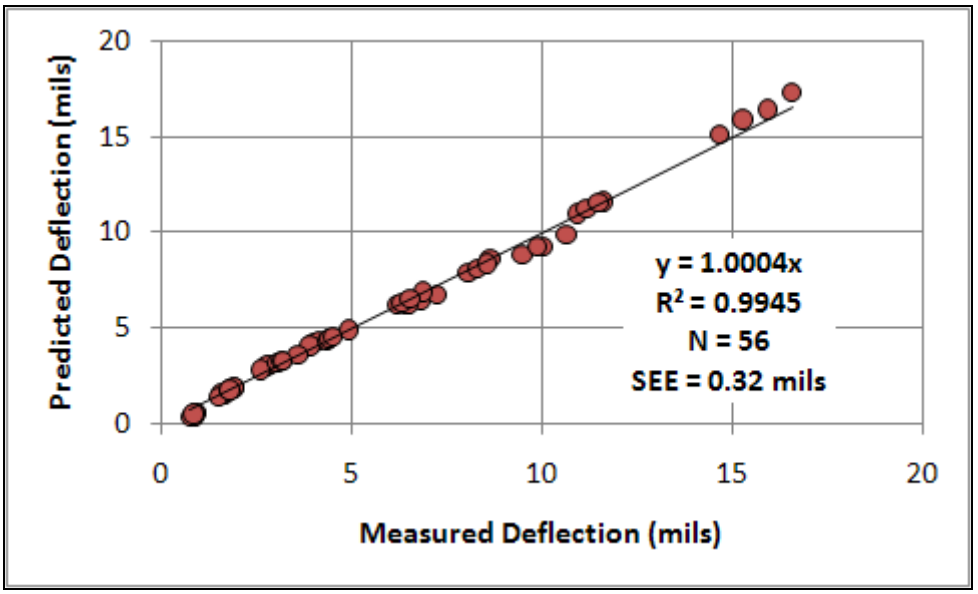

Figure A3. Comparison of Measured and Predicted FWD Deflections on Section 12005000.

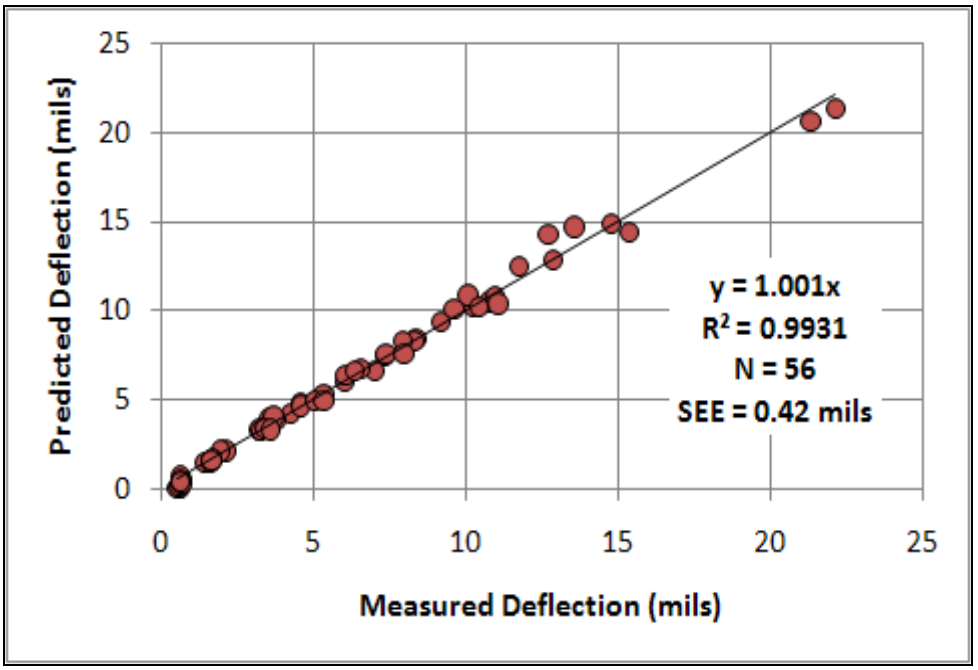

Figure A4. Comparison of Measured and Predicted FWD Deflections on Section 26060000.

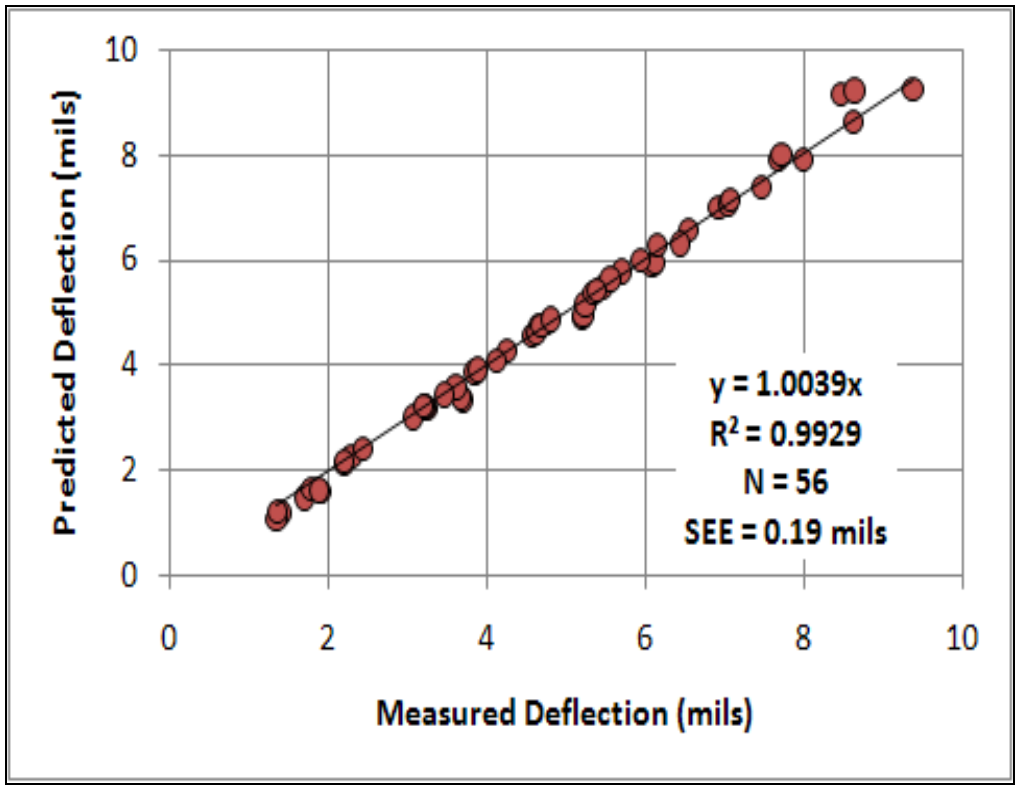

Figure A5. Comparison of Measured and Predicted FWD Deflections on Section 71020000.

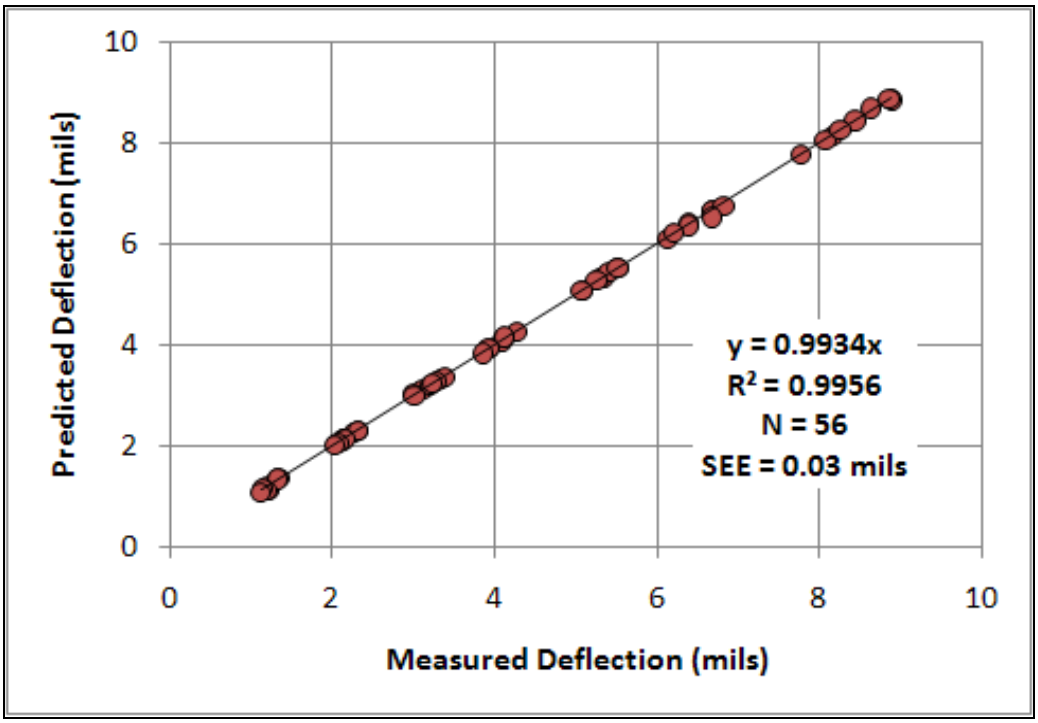

Figure A6. Comparison of Measured and Predicted FWD Deflections on Section 260050000.

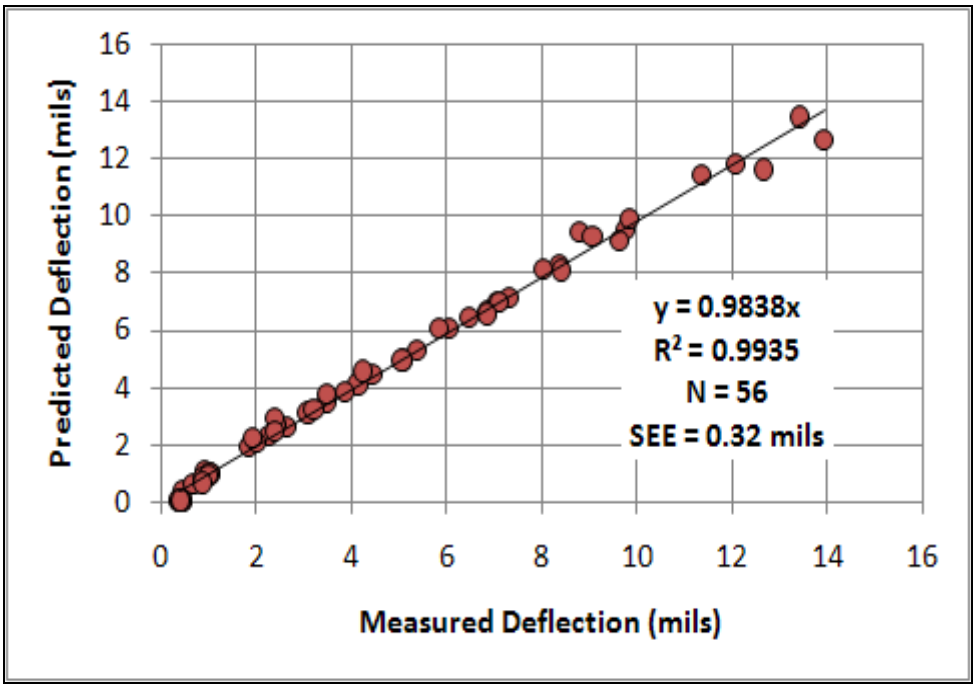

Figure A7. Comparison of Measured and Predicted FWD Deflections on Section 54020000.

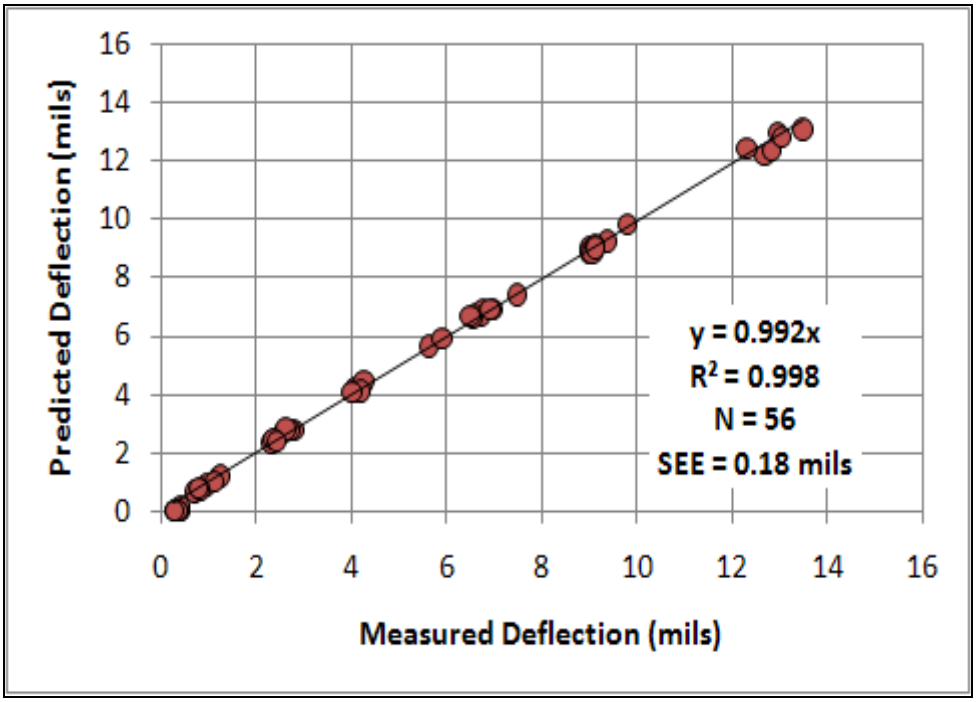

Figure A8. Comparison of Measured and Predicted FWD Deflections on Section 50020000.

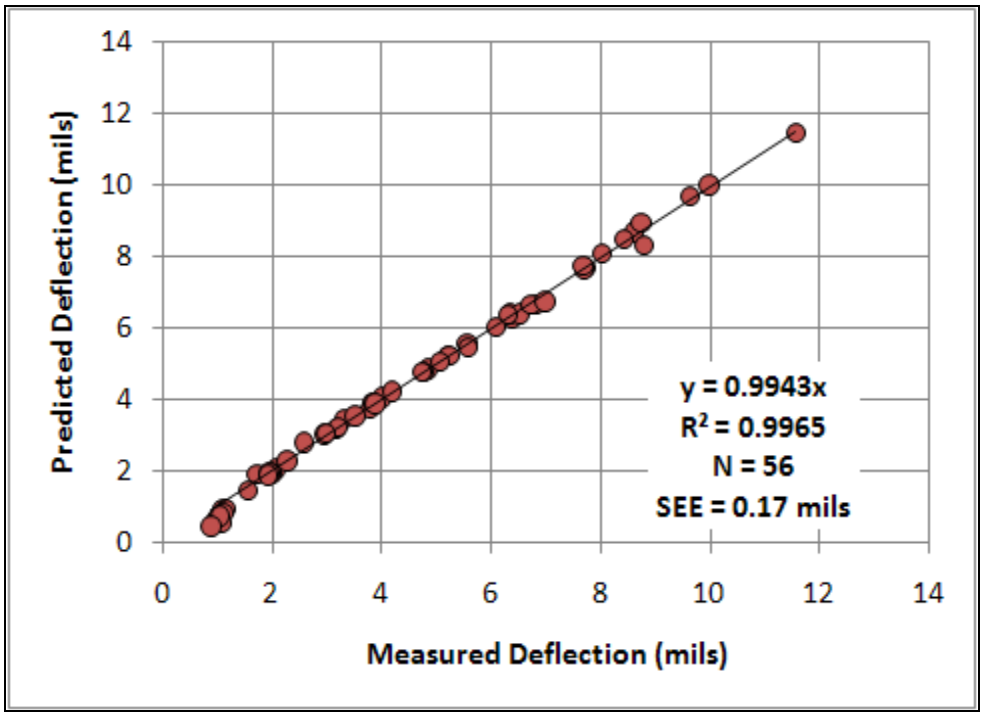

Figure A9. Comparison of Measured and Predicted FWD Deflections on Section 58060000.

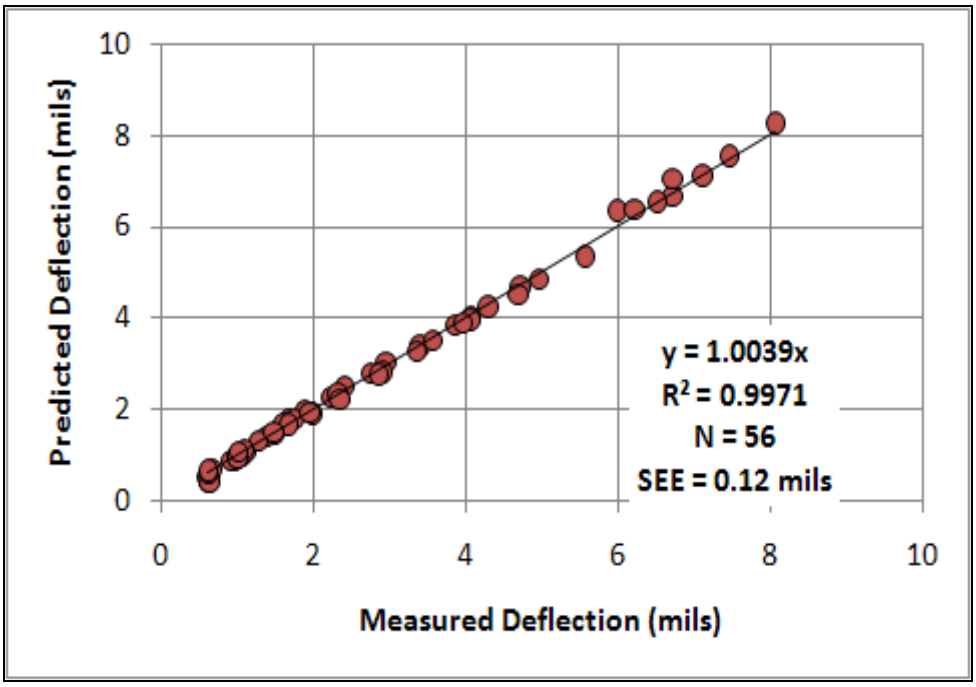

Figure A10. Comparison of Measured and Predicted FWD Deflections on Section 89010000.

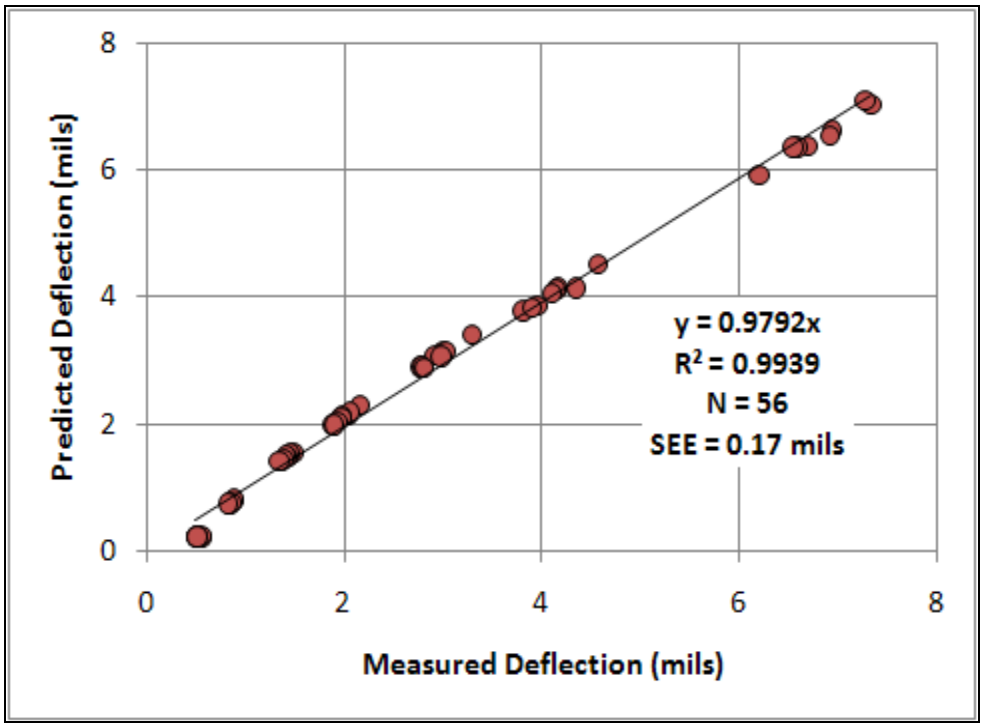

Figure A11. Comparison of Measured and Predicted FWD Deflections on Section 93310000.

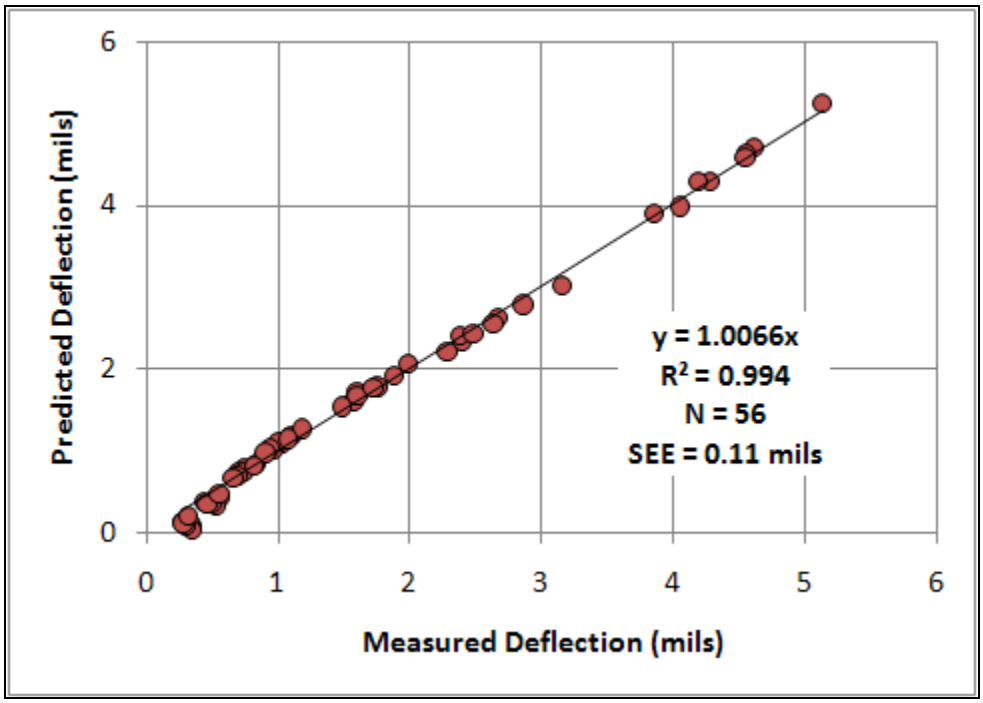

Figure A12. Comparison of Measured and Predicted FWD Deflections on Section 86190000.

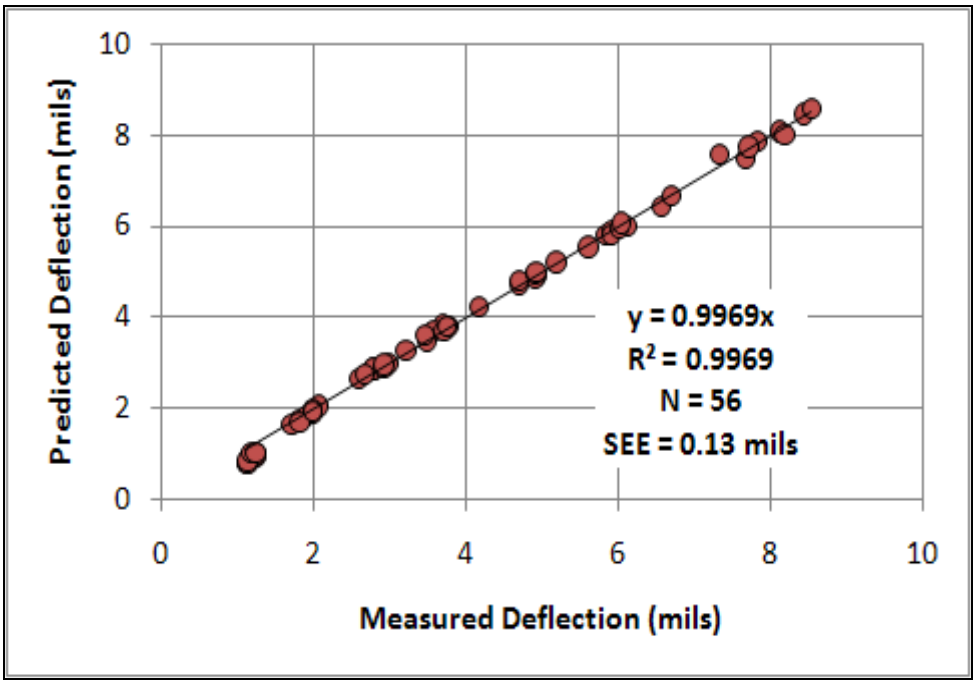

Figure A13. Comparison of Measured and Predicted FWD Deflections on Section 77002000.

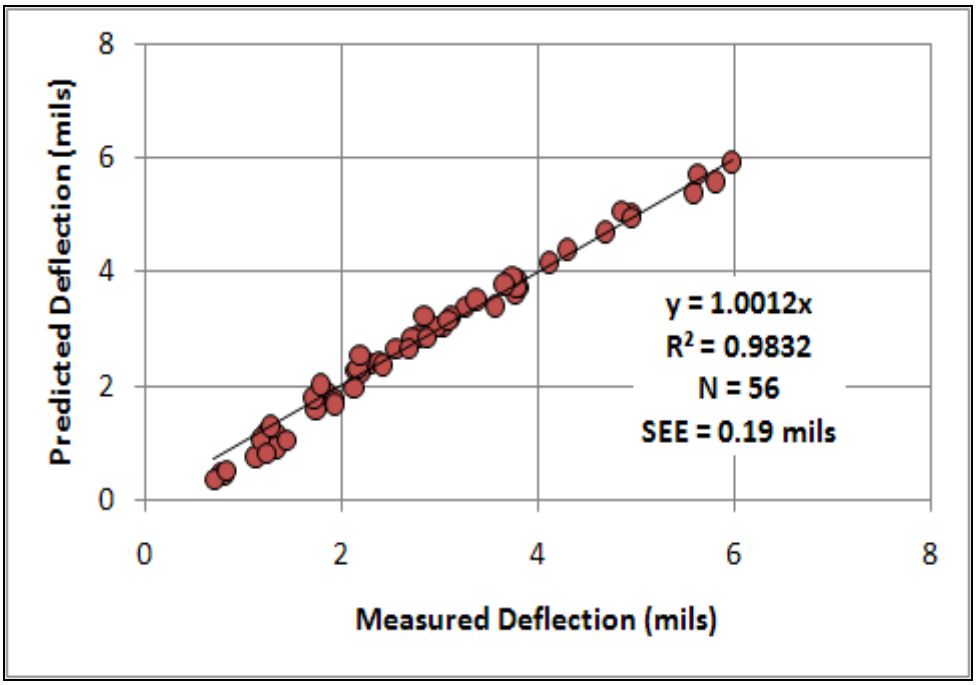

Figure A14. Comparison of Measured and Predicted FWD Deflections on Section 92060000.

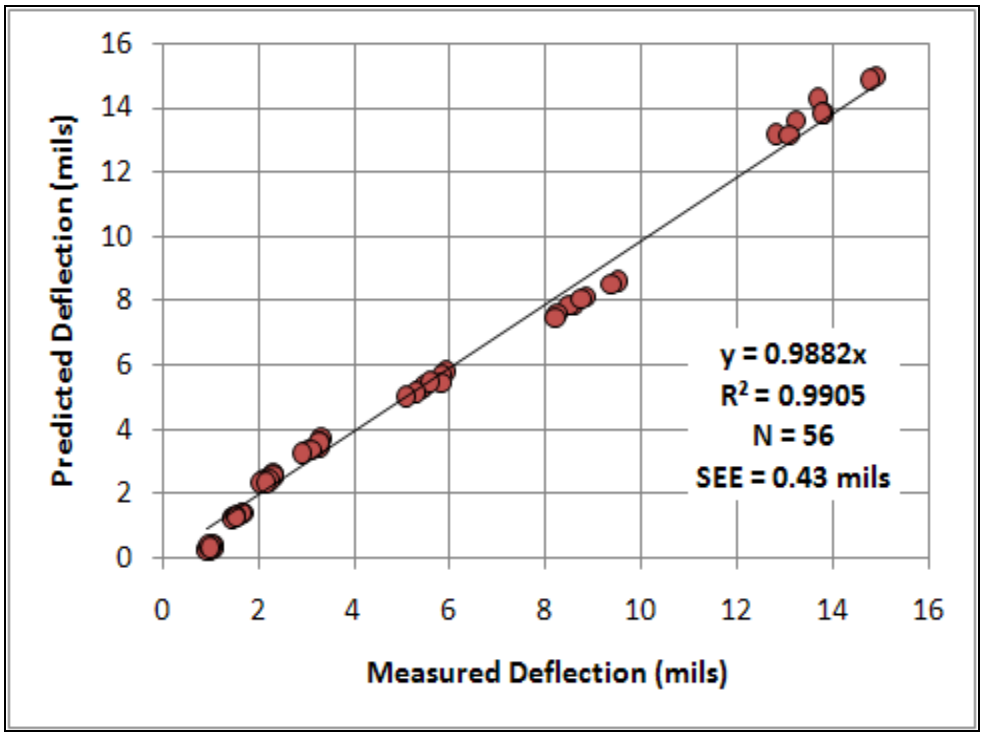

Figure A15. Comparison of Measured and Predicted FWD Deflections on Section 79270000.

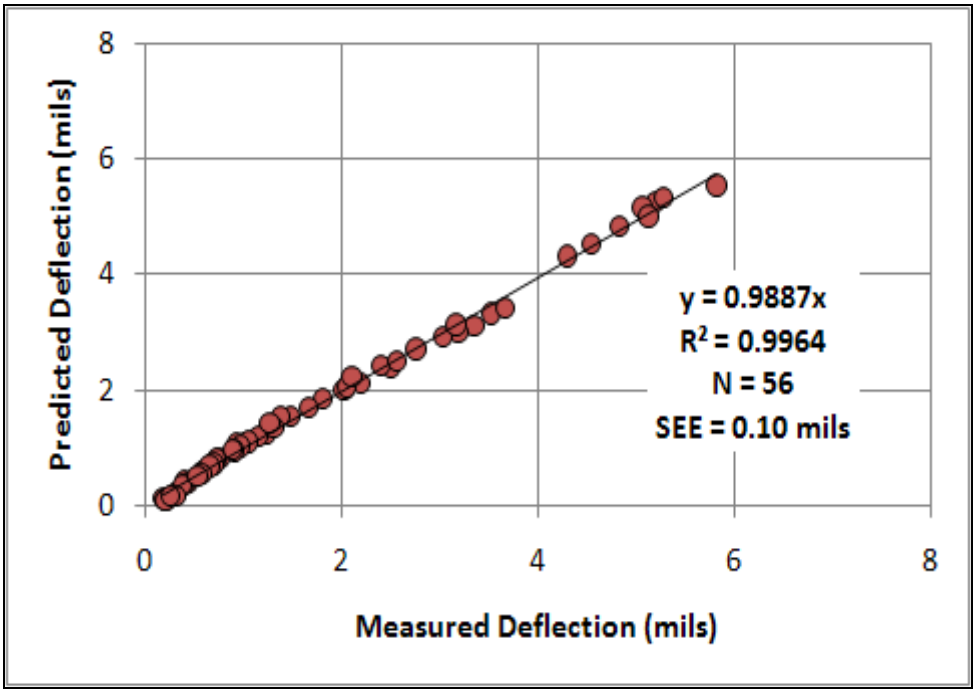

Figure A16. Comparison of Measured and Predicted FWD Deflections on Section 87120000.

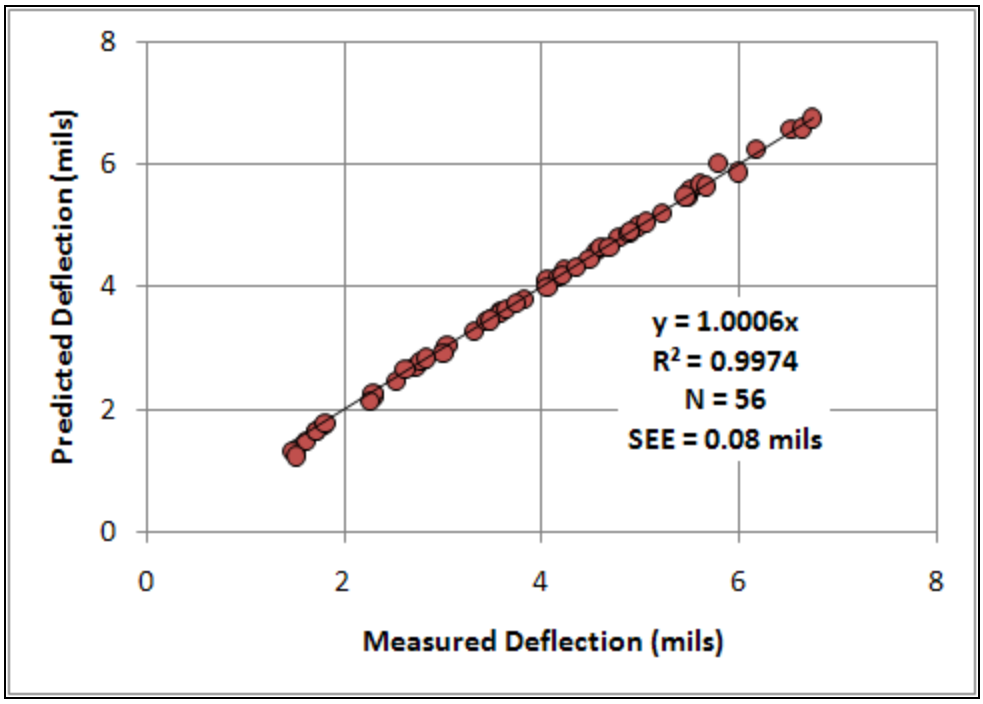

Figure A17. Comparison of Measured and Predicted FWD Deflections on Section 8706000.

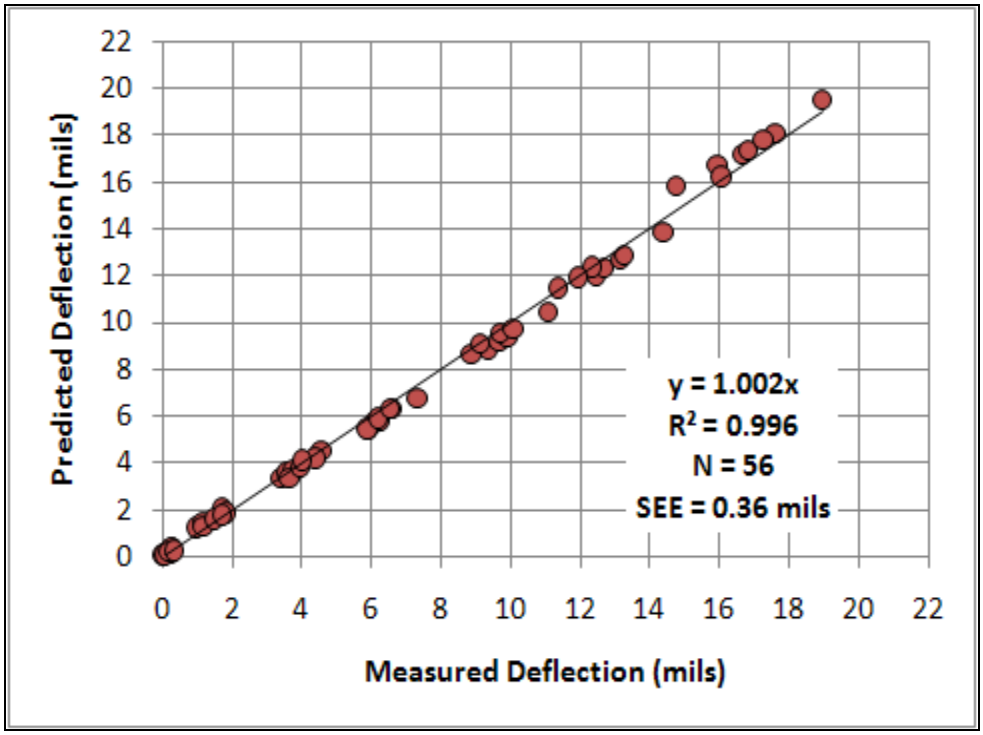

Figure A18. Comparison of Measured and Predicted FWD Deflections on Section 90060000.

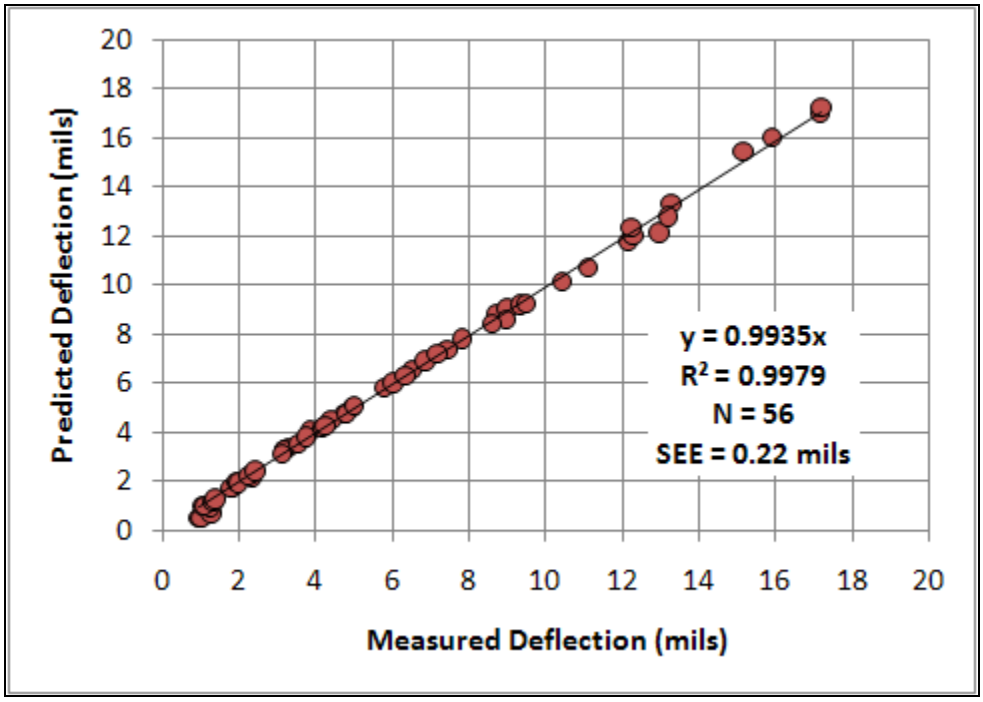

Figure A19. Comparison of Measured and Predicted FWD Deflections on Section 10060000.

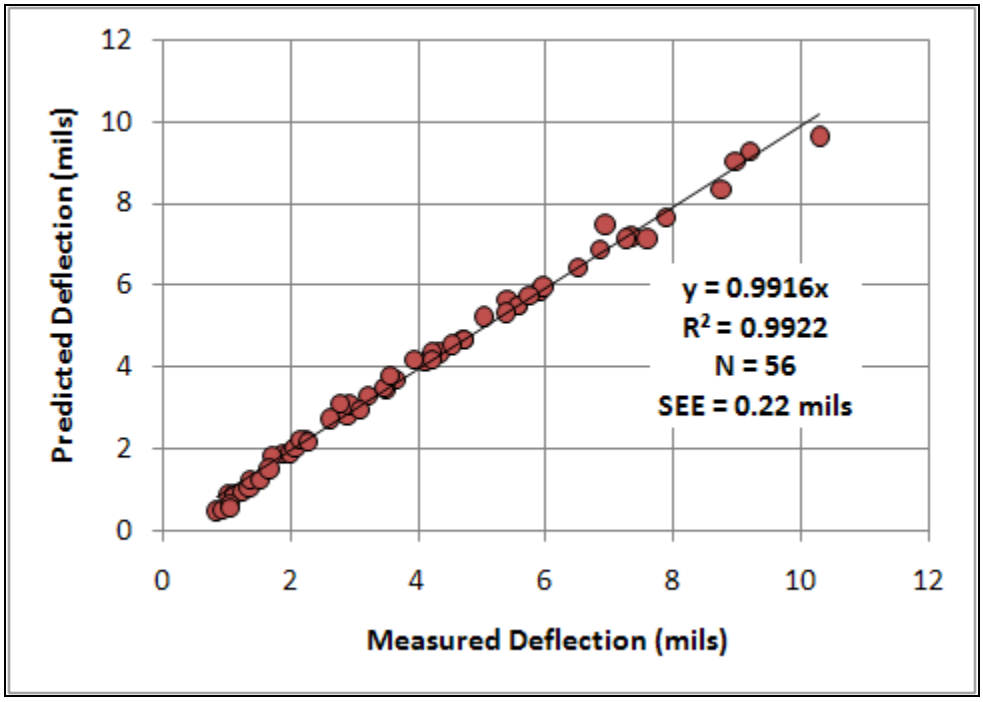

Figure A20. Comparison of Measured and Predicted FWD Deflections on Section 101600000.

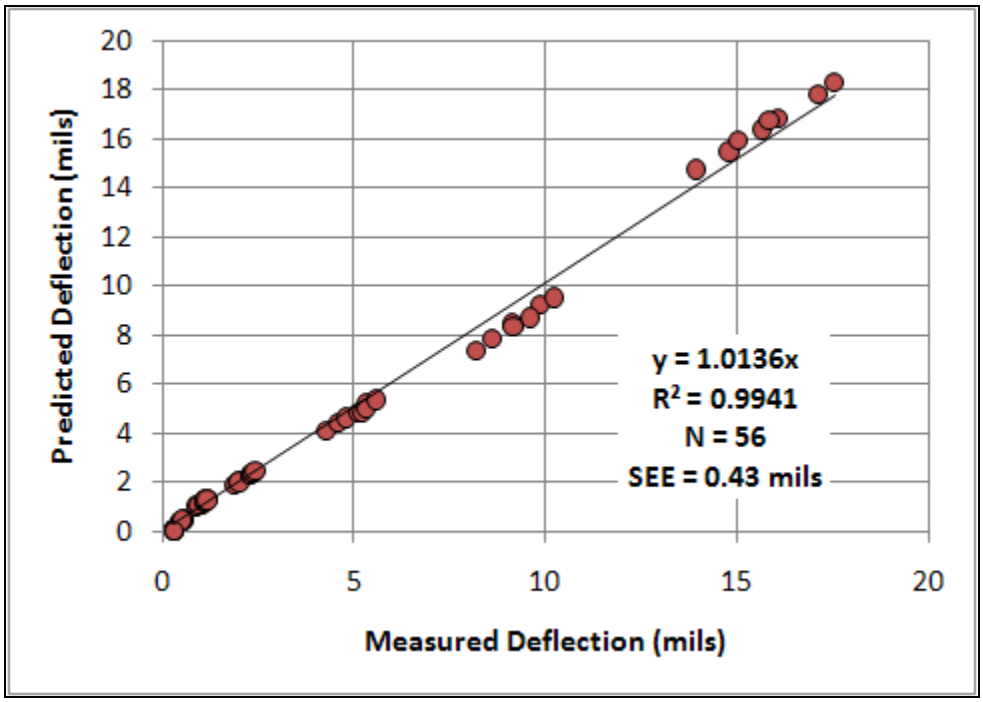

Figure A21. Comparison of Measured and Predicted FWD Deflections on Section 93100000.

APPENDIX B

DCP DATA ANALYSIS RESULTS

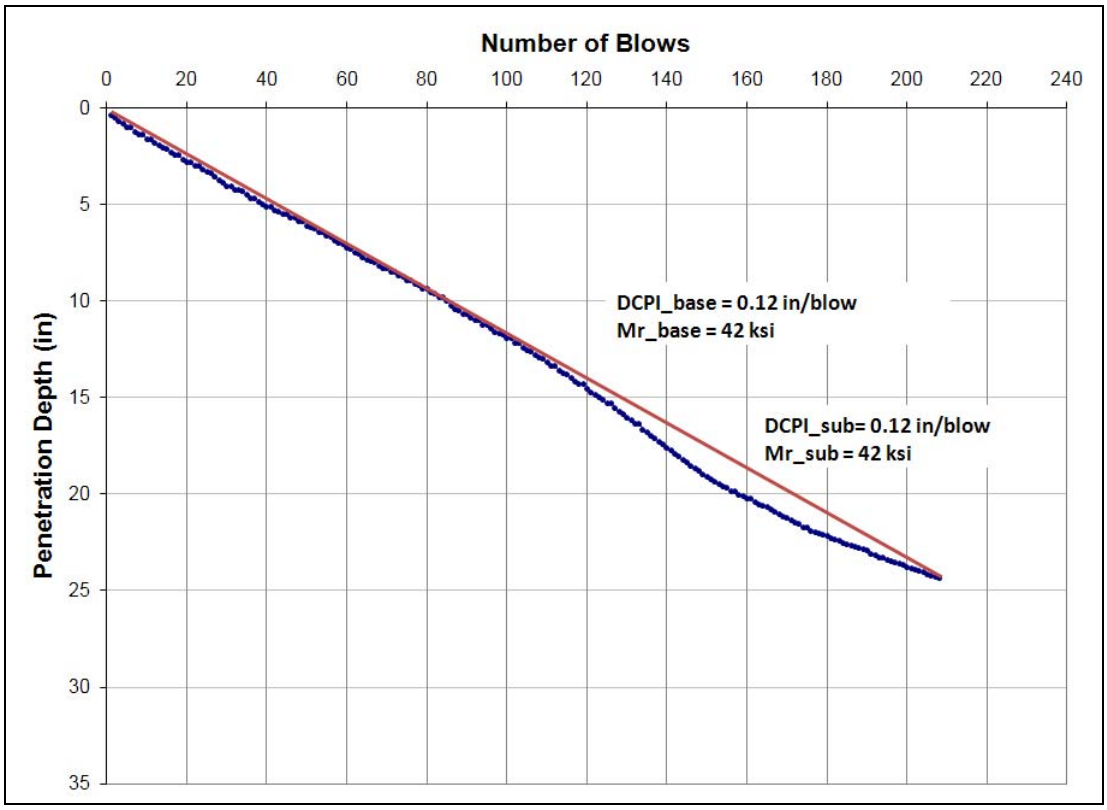

Figure B1. DCP Data Analysis on Section 16020000-2A.

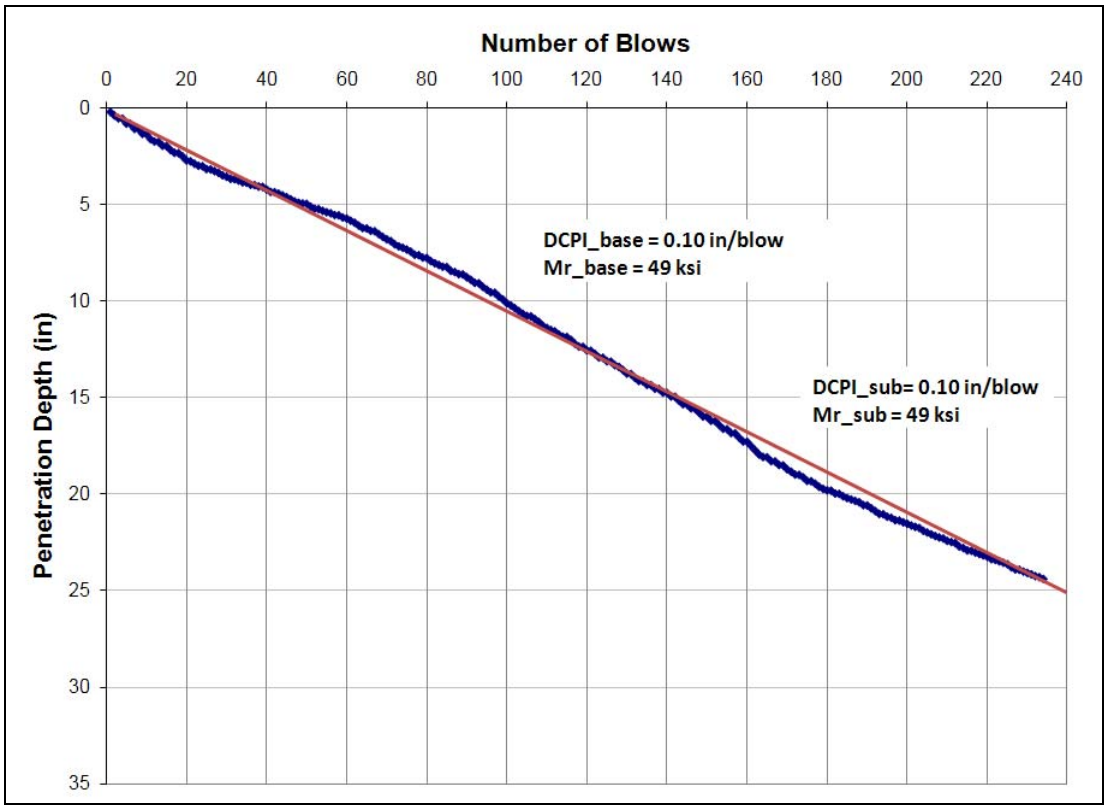

Figure B2. DCP Data Analysis on Section 16020000-3A.

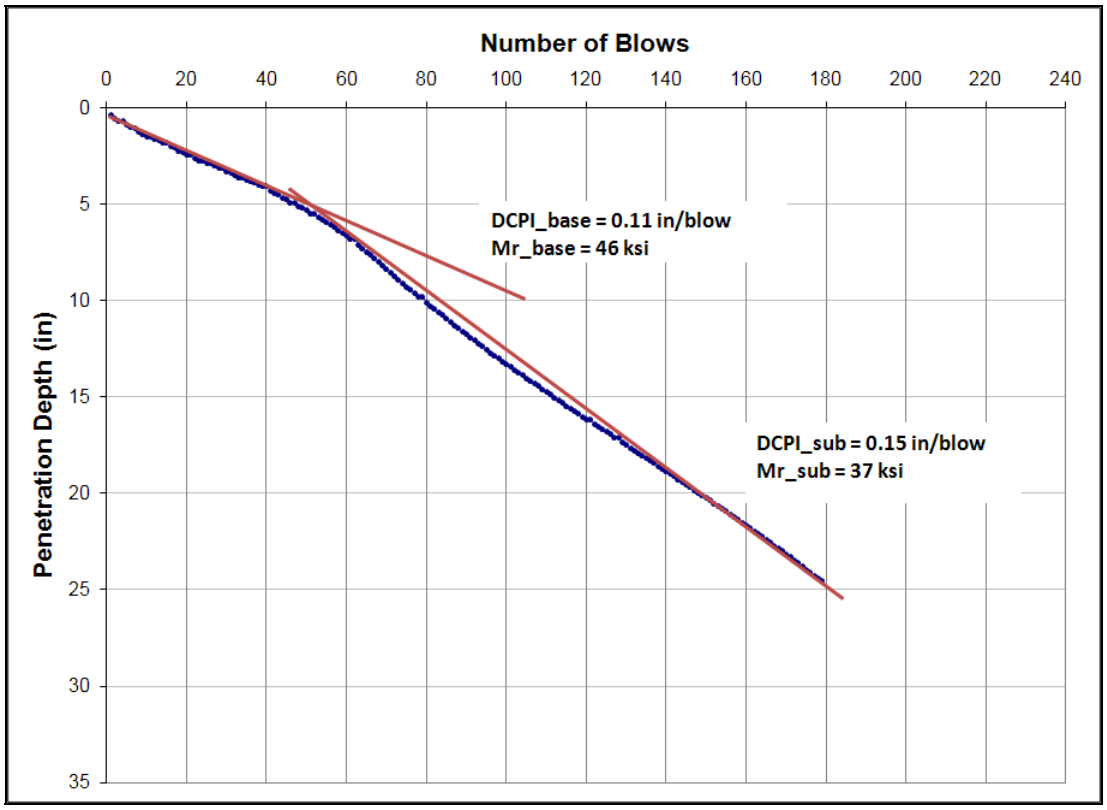

Figure B3. DCP Data Analysis on Section 16003000-2A.

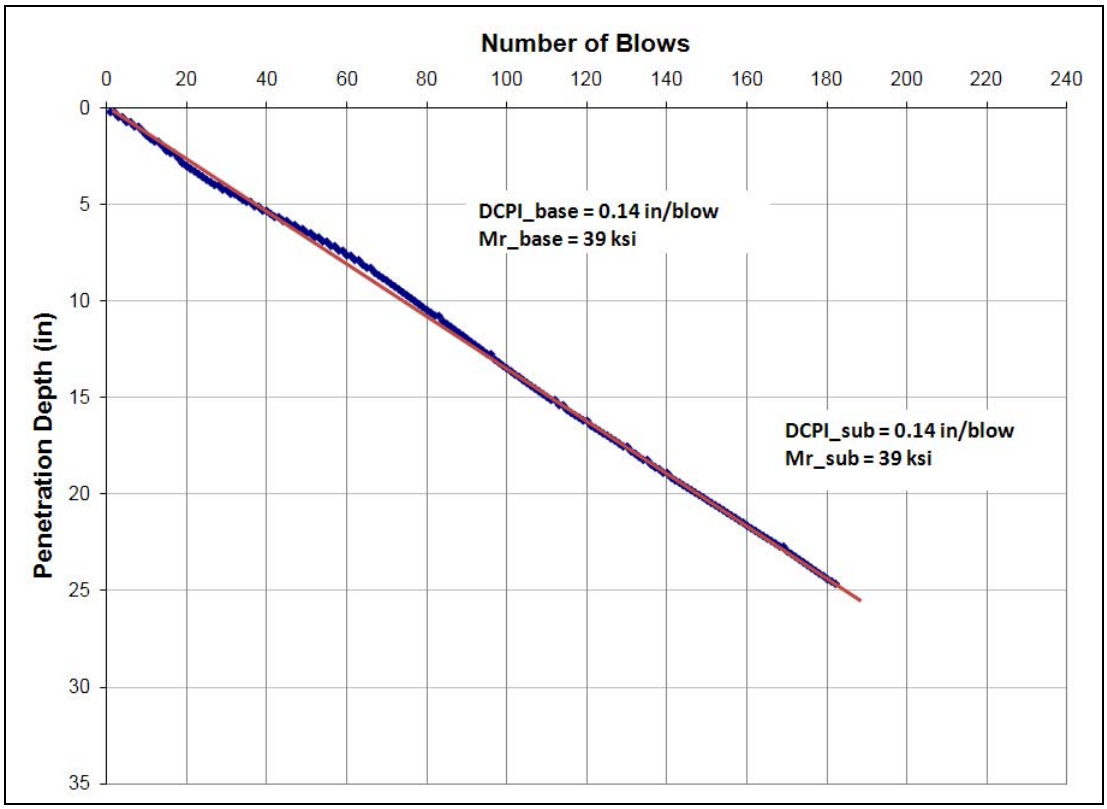

Figure B4. DCP Data Analysis on Section 16003000-3A.

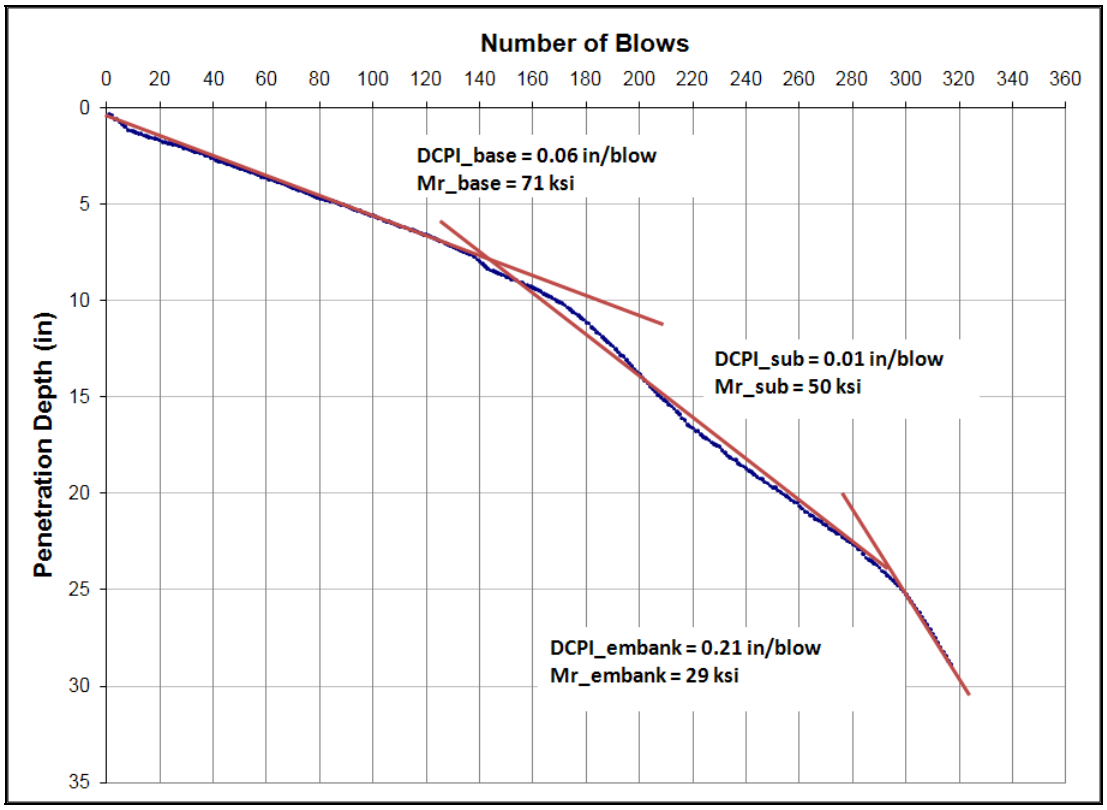

Figure B5. DCP Data Analysis on Section 12005000-2A.

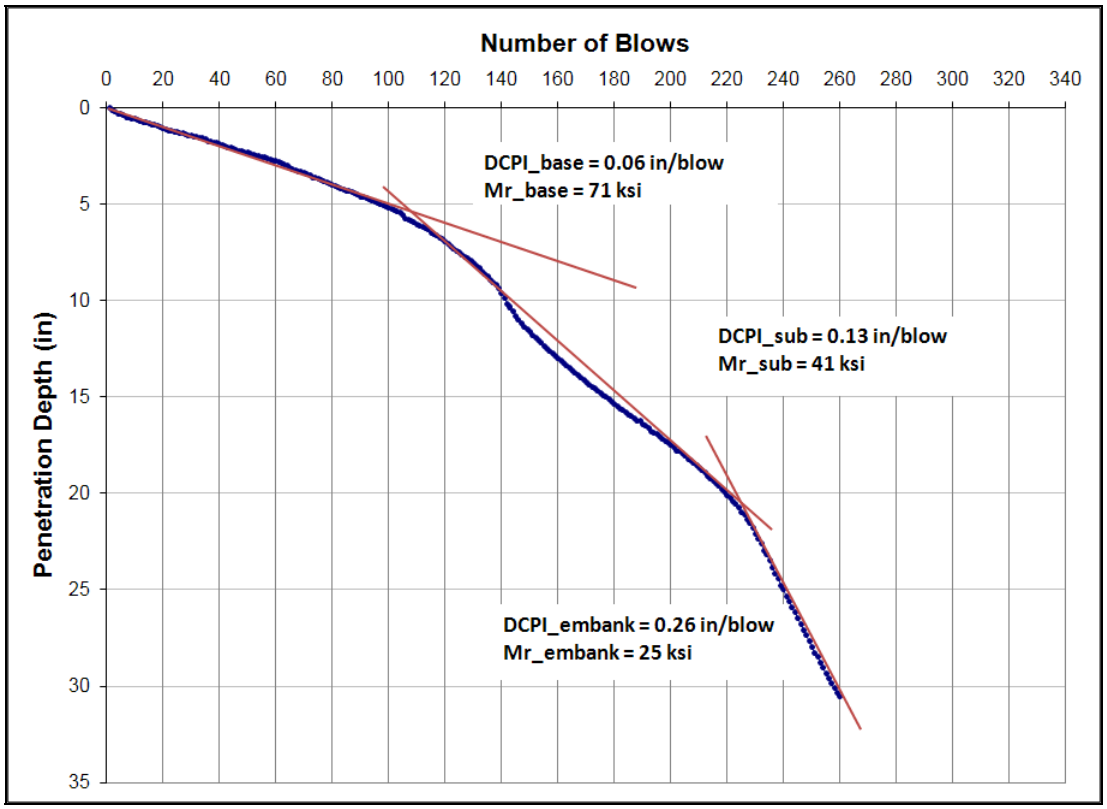

Figure B6. DCP Data Analysis on Section 12005000-3A.

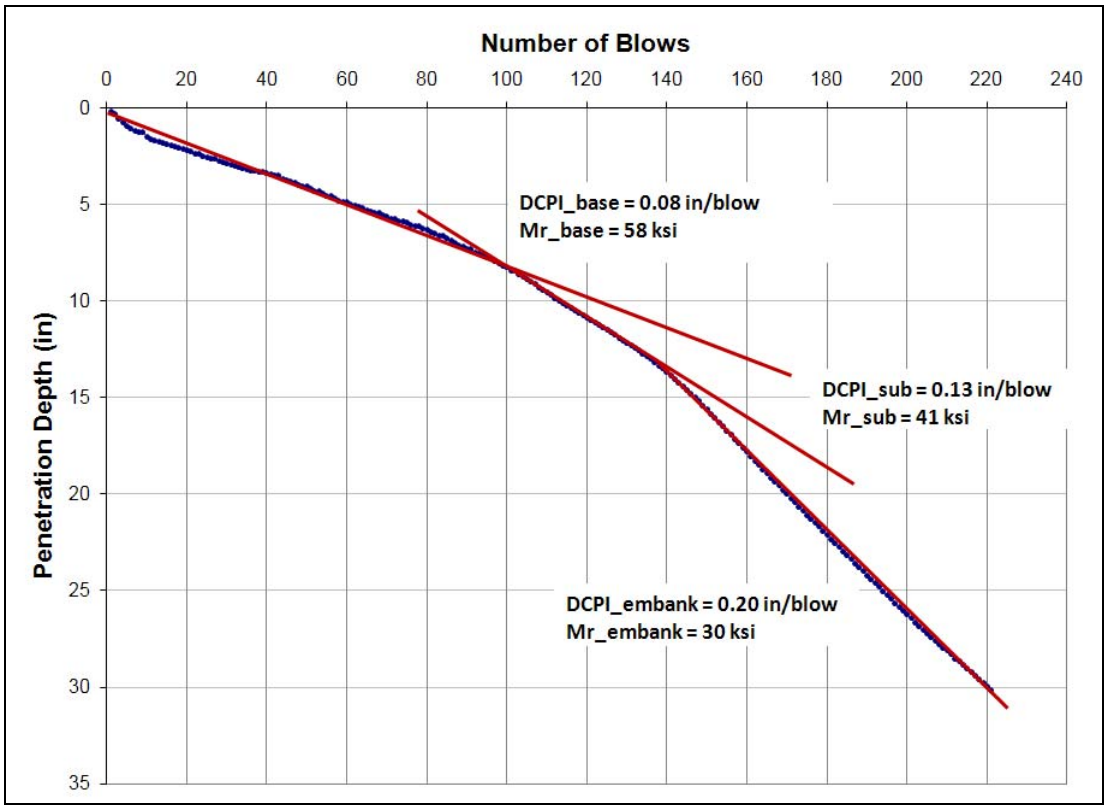

Figure B7. DCP Data Analysis on Section 26060000-2A.

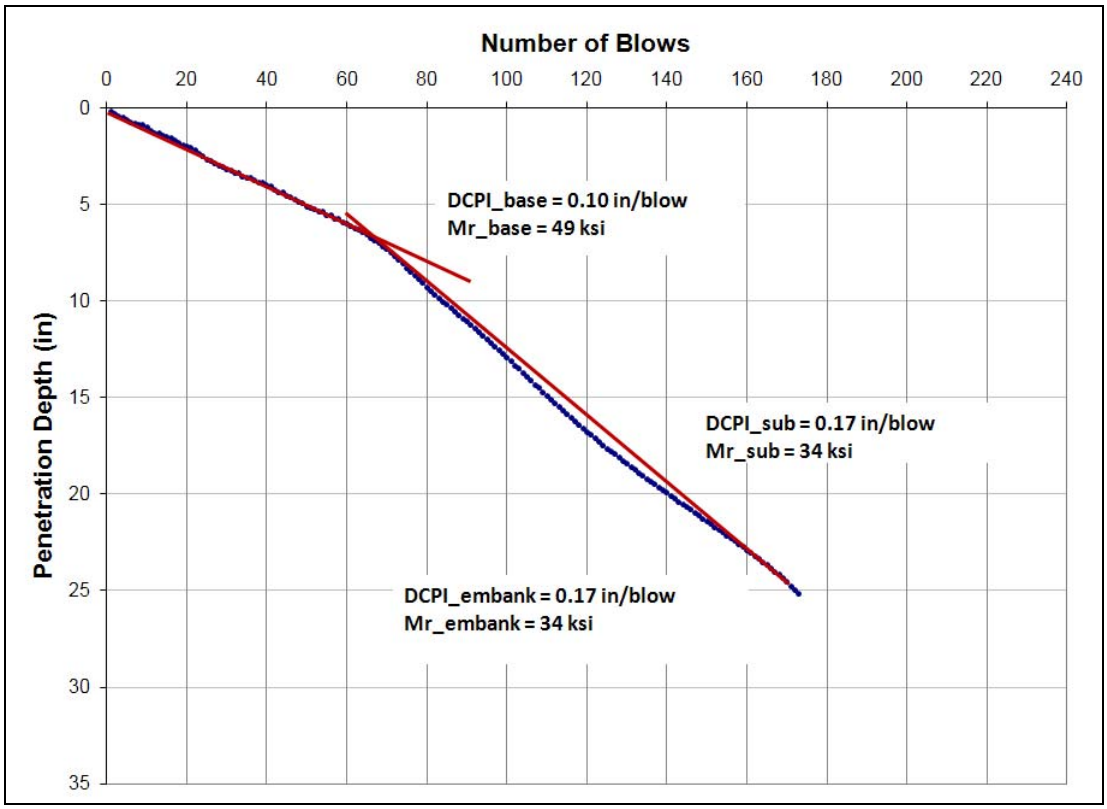

Figure B8. DCP Data Analysis on Section 26060000-3A.

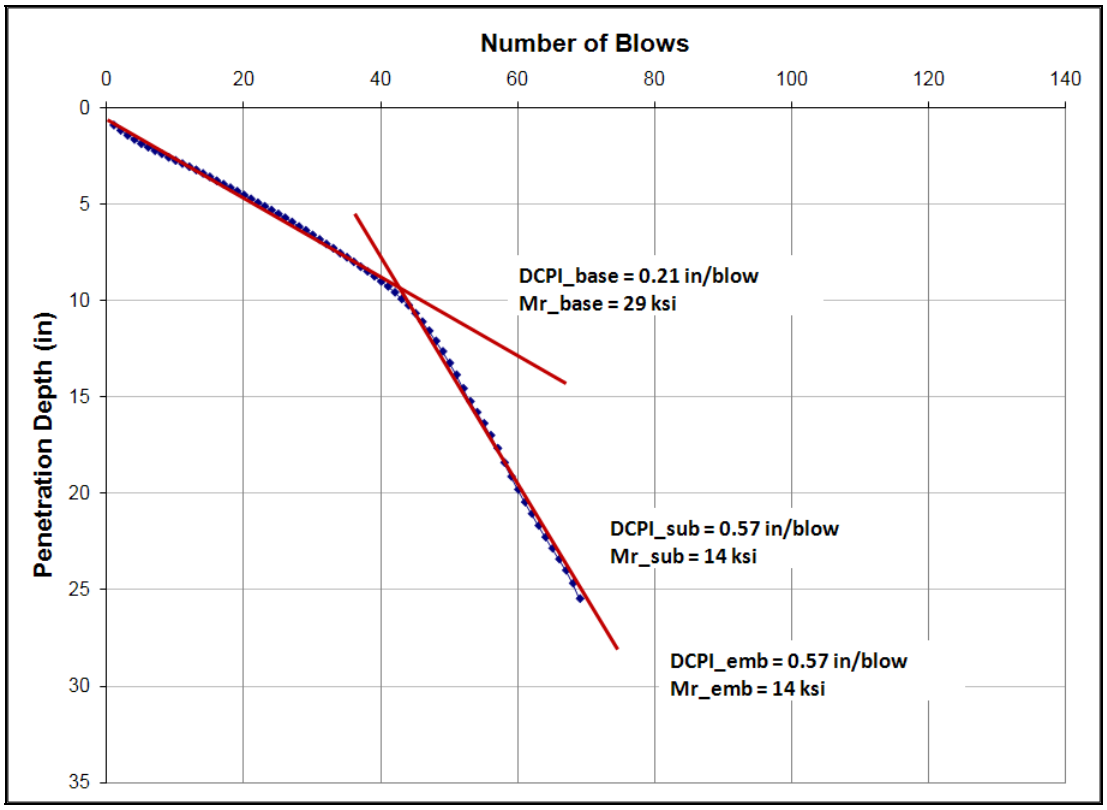

Figure B9. DCP Data Analysis on Section 71020000-2A.

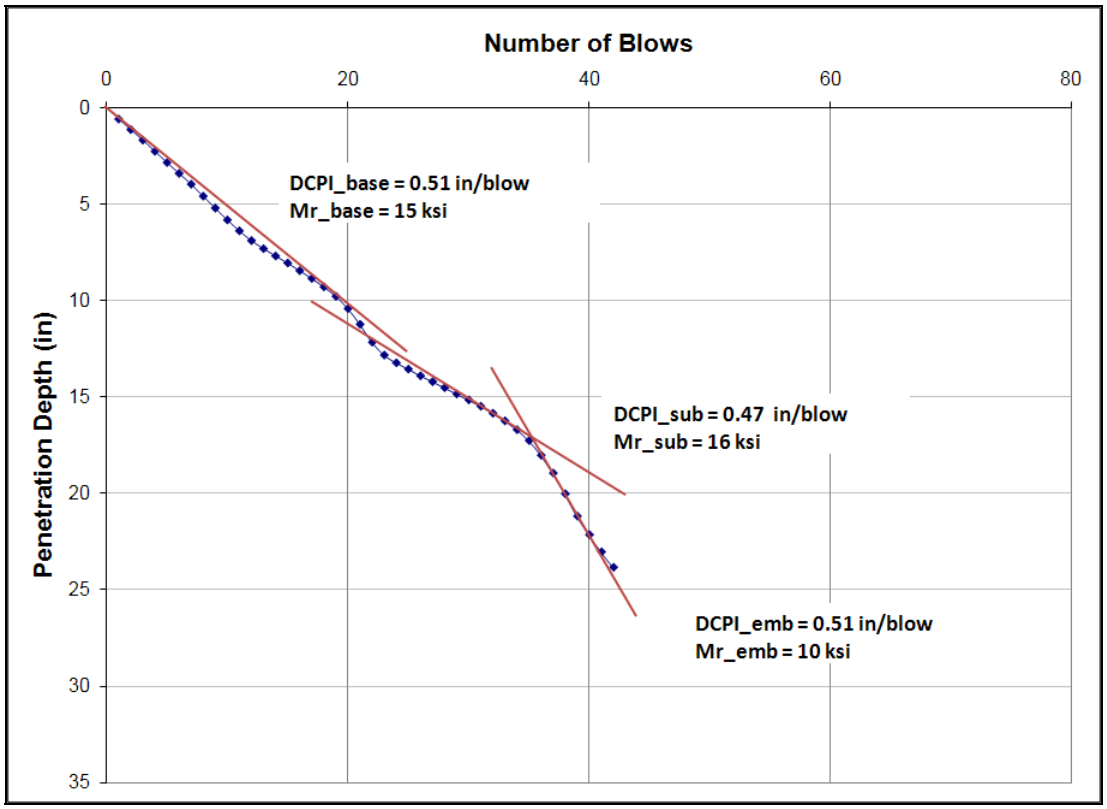

Figure B10. DCP Data Analysis on Section 71020000-3A.

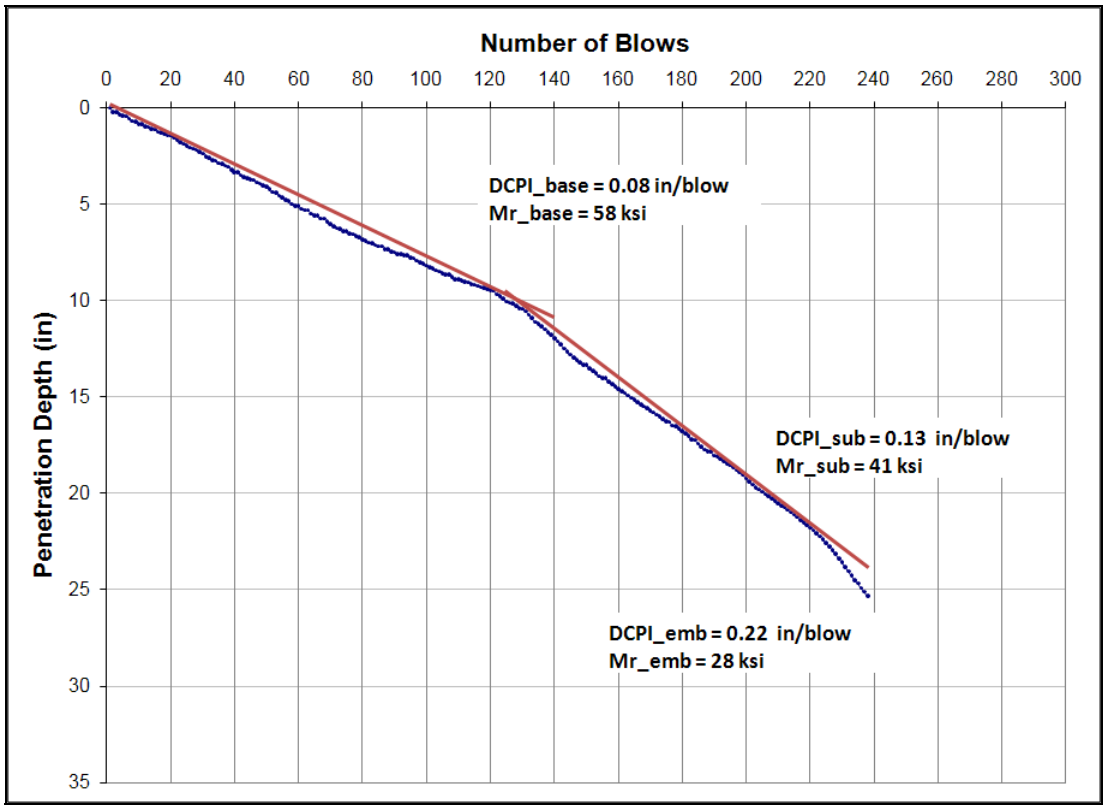

Figure B11. DCP Data Analysis on Section 26005000-2A.

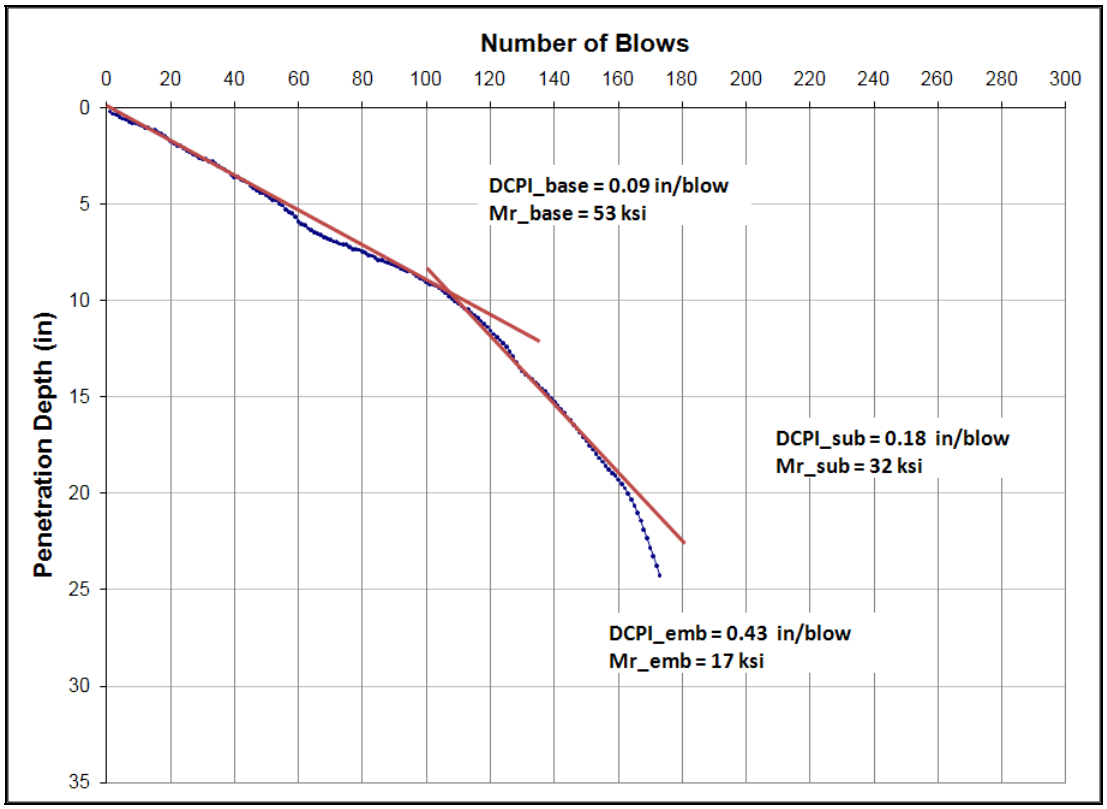

Figure B12. DCP Data Analysis on Section 26005000-3A.

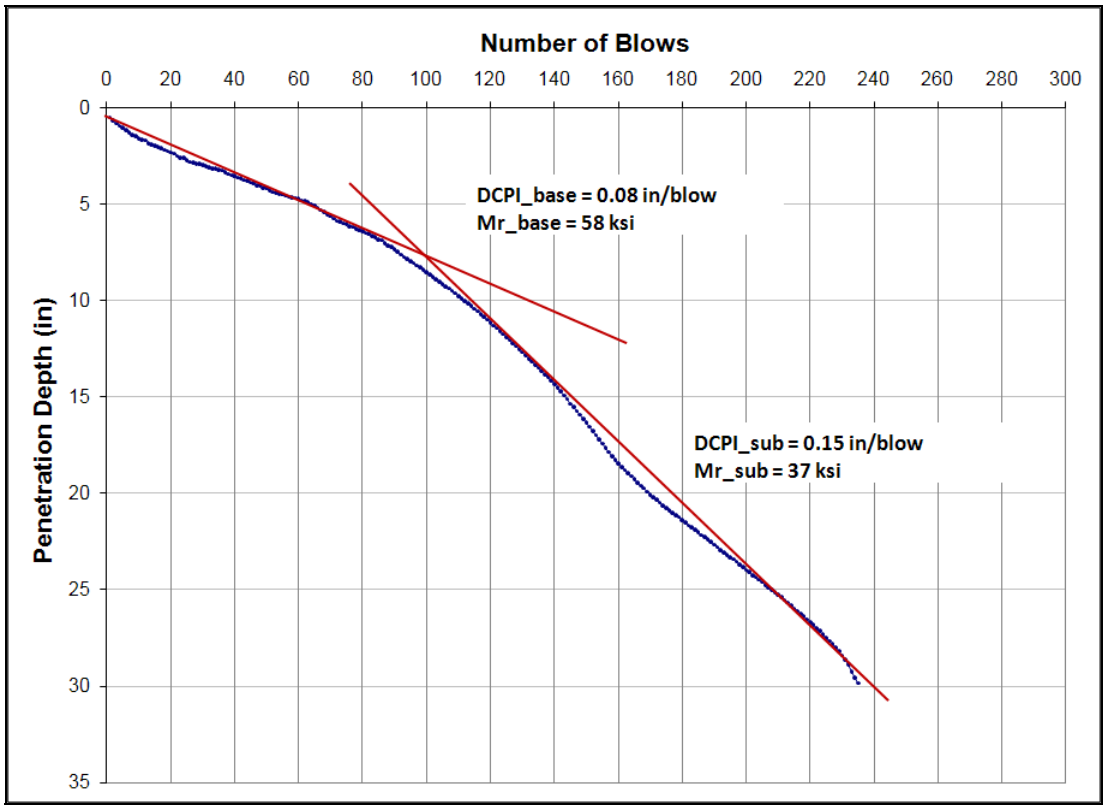

Figure B13. DCP Data Analysis on Section 50020000-2A.

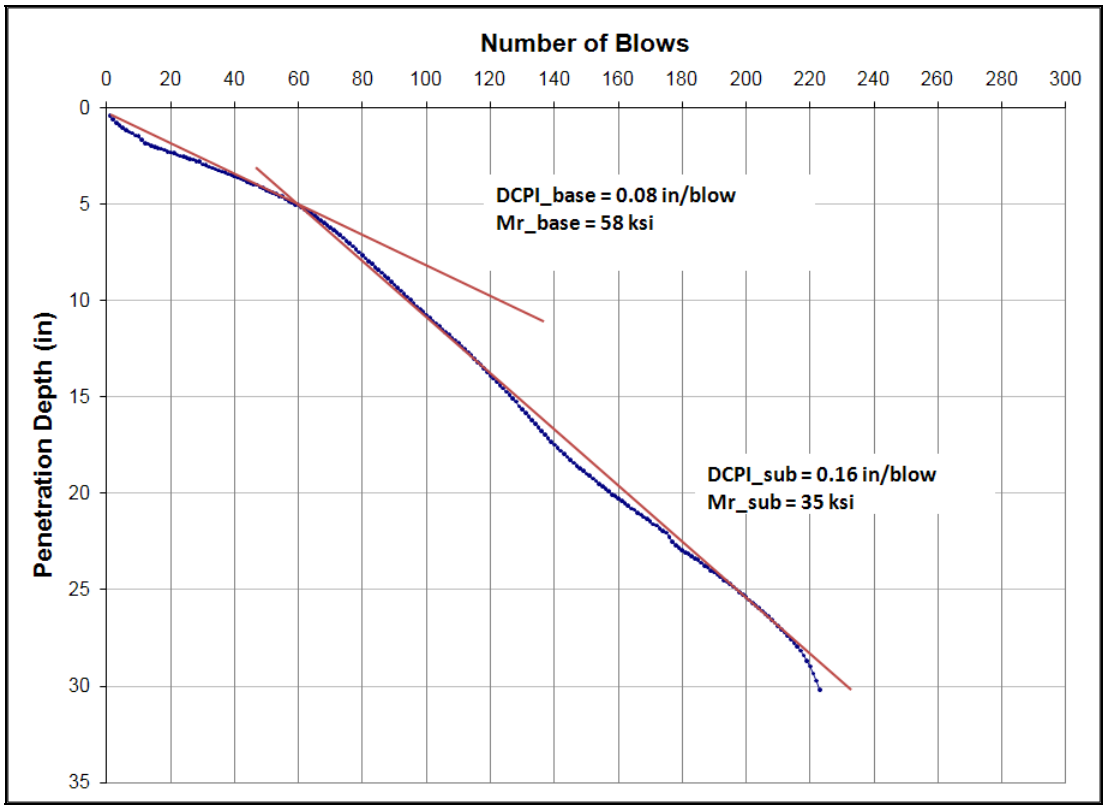

Figure B14. DCP Data Analysis on Section 50020000-3A.

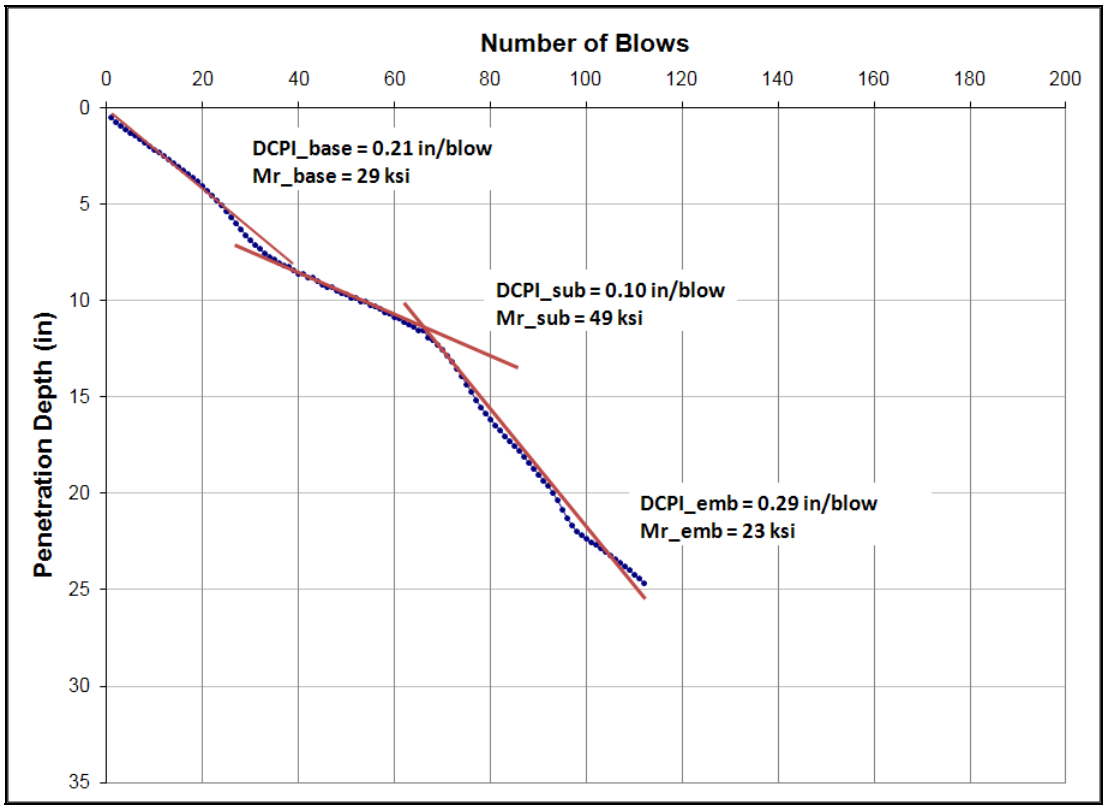

Figure B15. DCP Data Analysis on Section 58060000-2A.

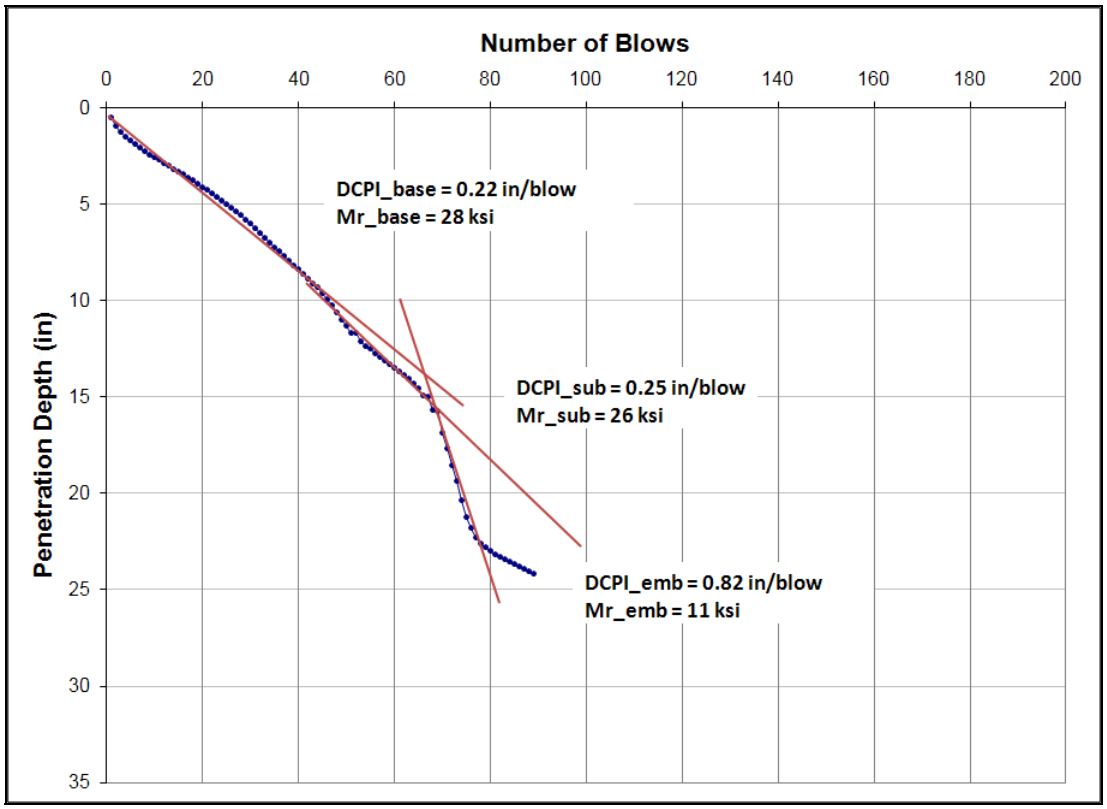

Figure B16. DCP Data Analysis on Section 58060000-3A.

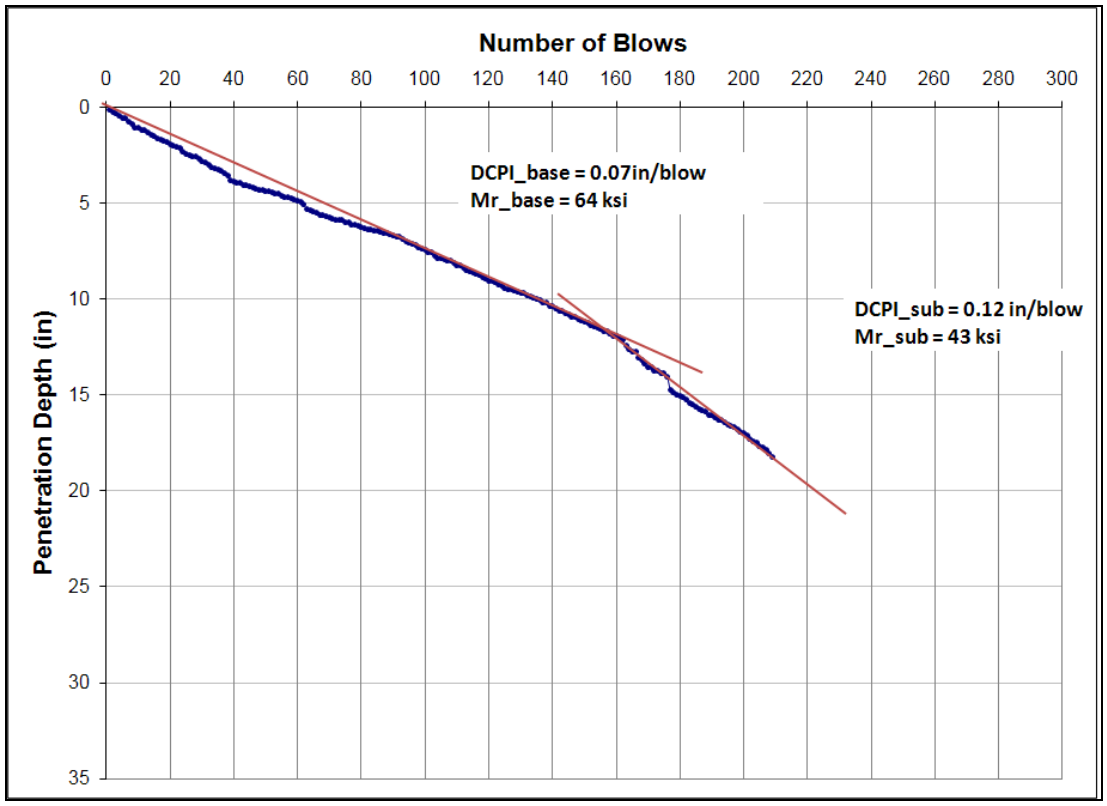

Figure B17. DCP Data Analysis on Section 89010000-2A.

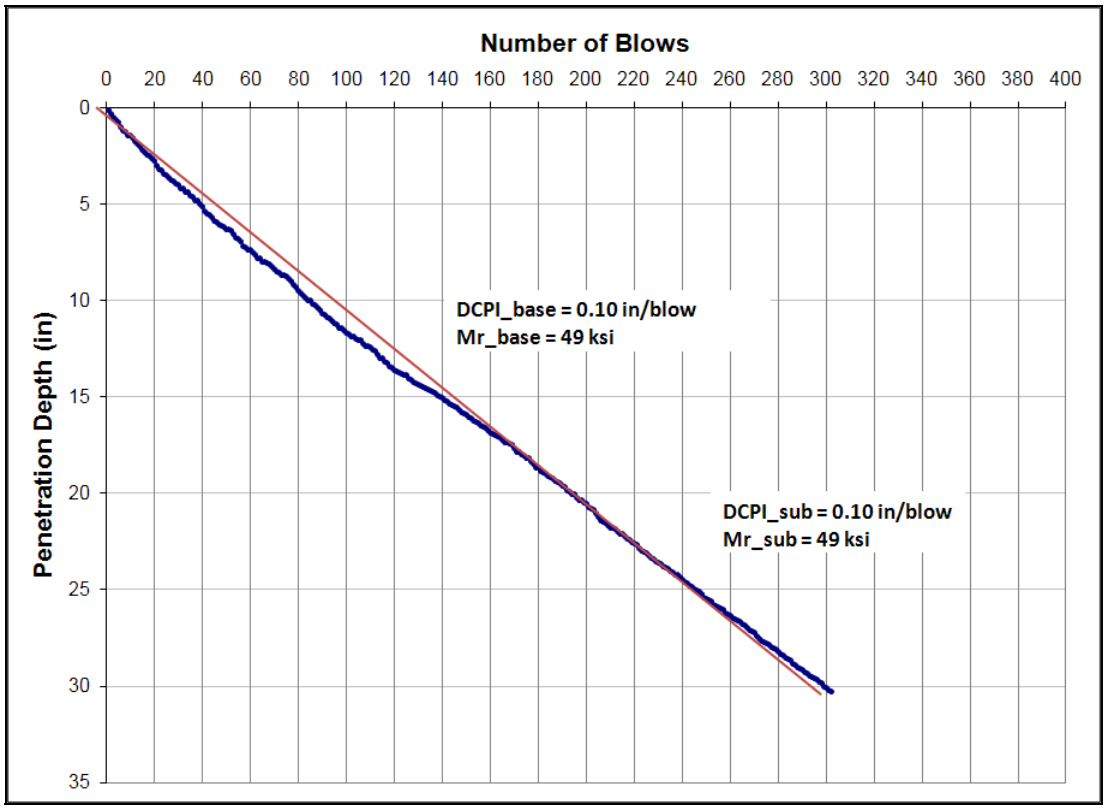

Figure B18. DCP Data Analysis on Section 89010000-3A.

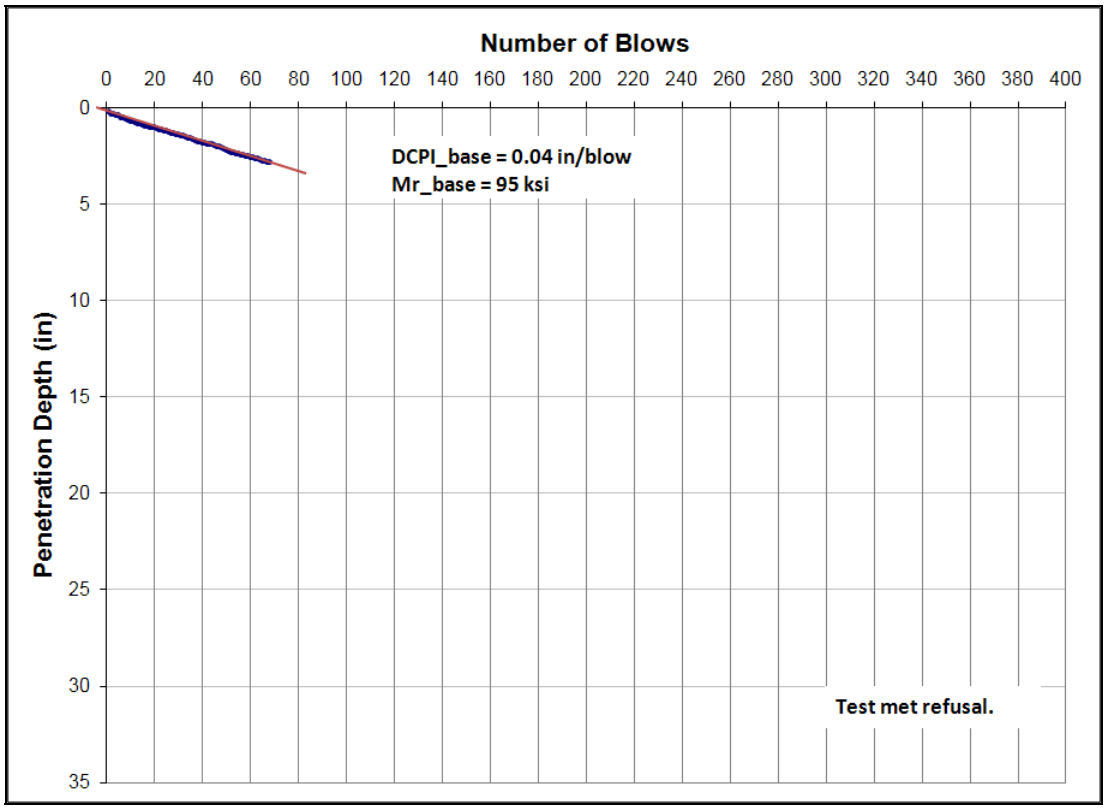

Figure B19. DCP Data Analysis on Section 93310000-2A.

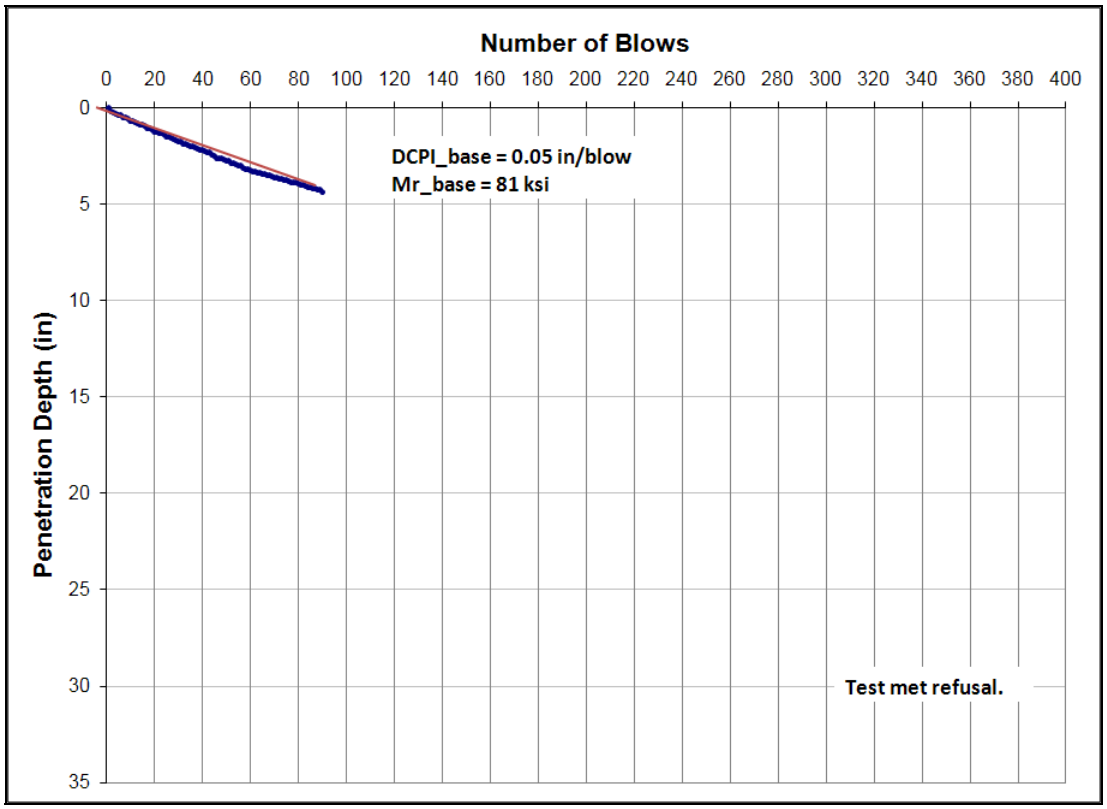

Figure B20. DCP Data Analysis on Section 93310000-3A.

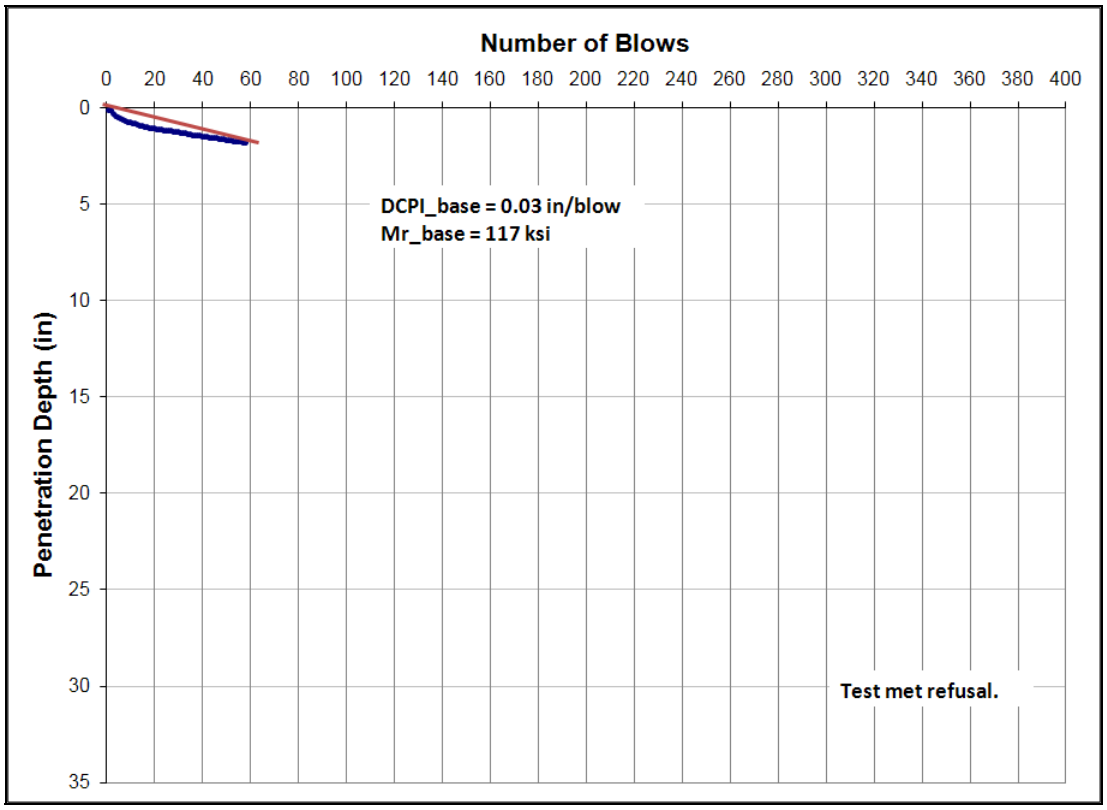

Figure B21. DCP Data Analysis on Section 86190000-2A.

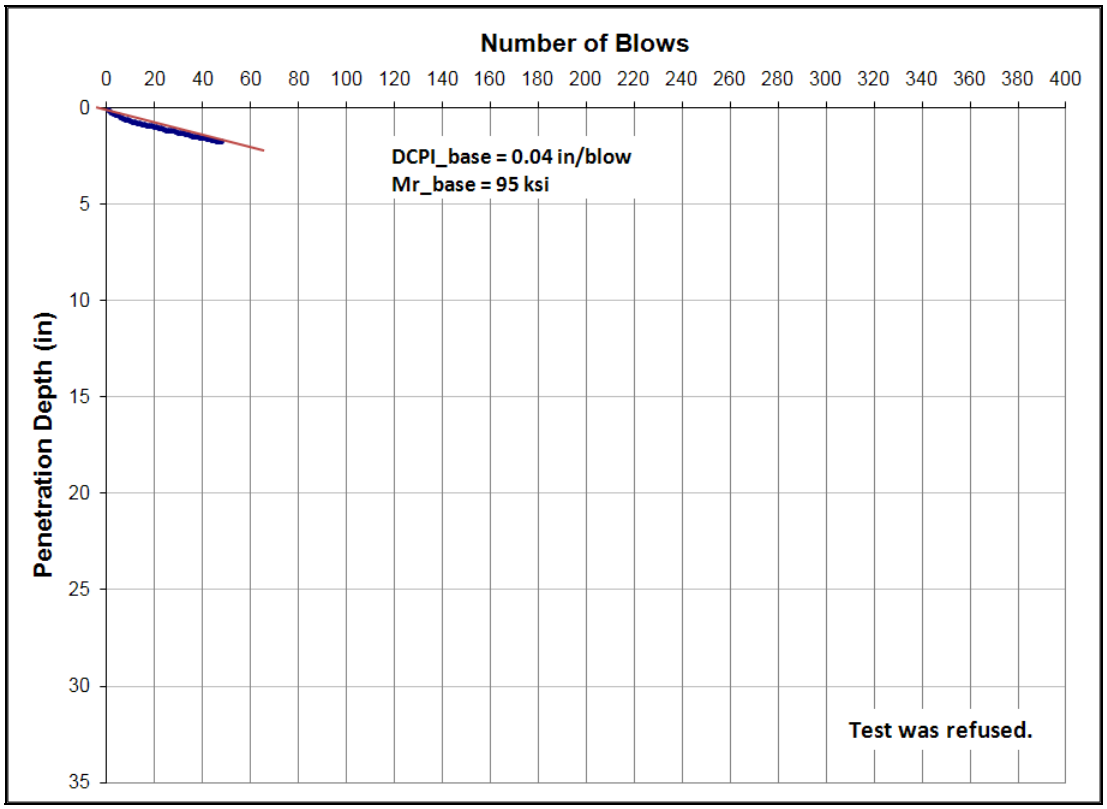

Figure B22. DCP Data Analysis on Section 86190000-3A.

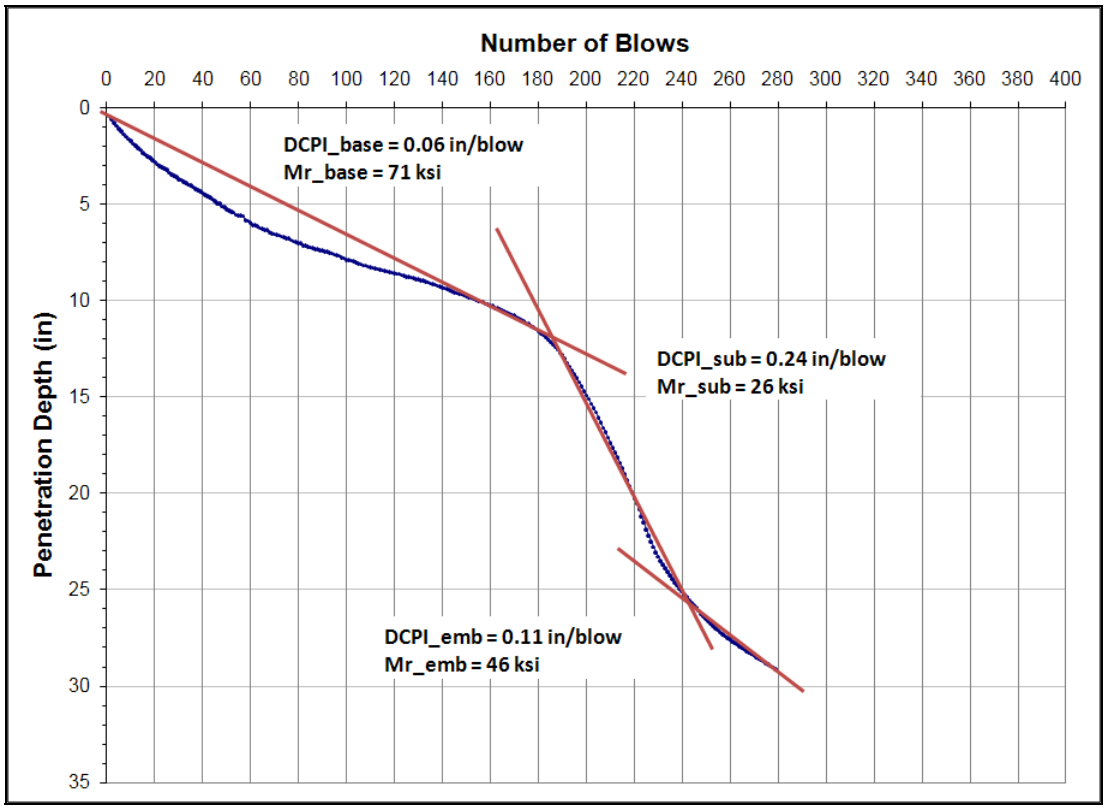

Figure B23. DCP Data Analysis on Section 93100000-2A.

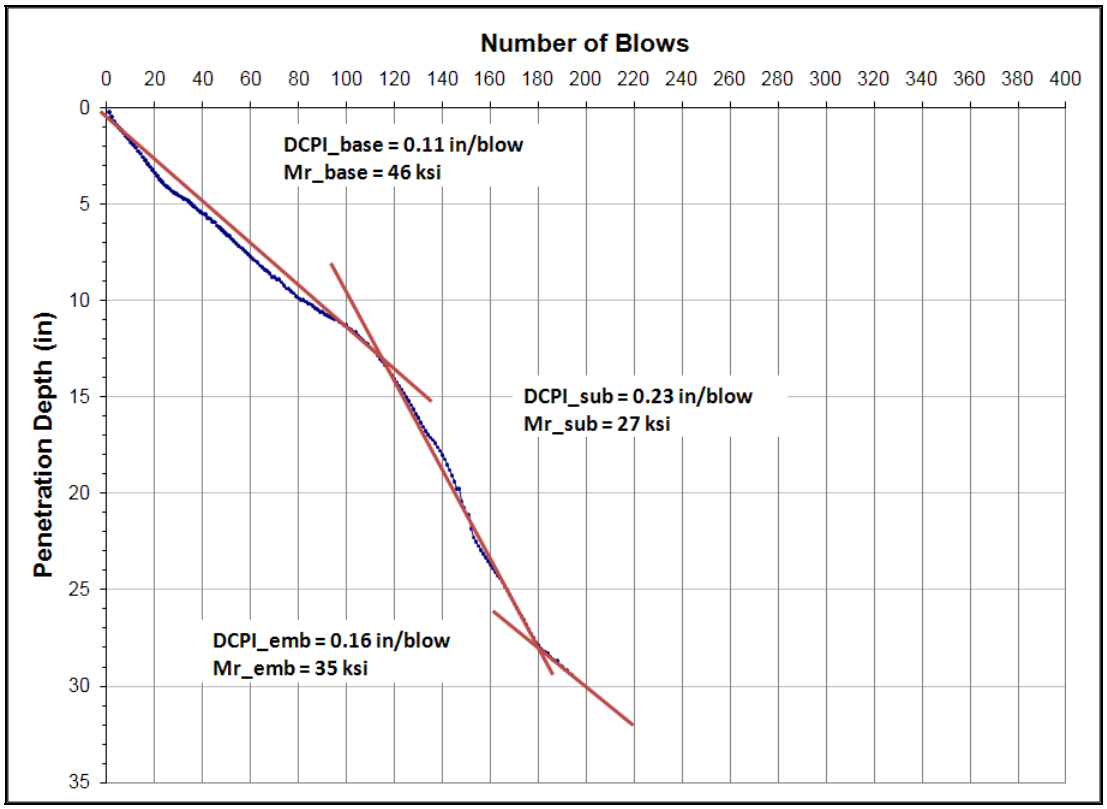

Figure B24. DCP Data Analysis on Section 93100000-3A.

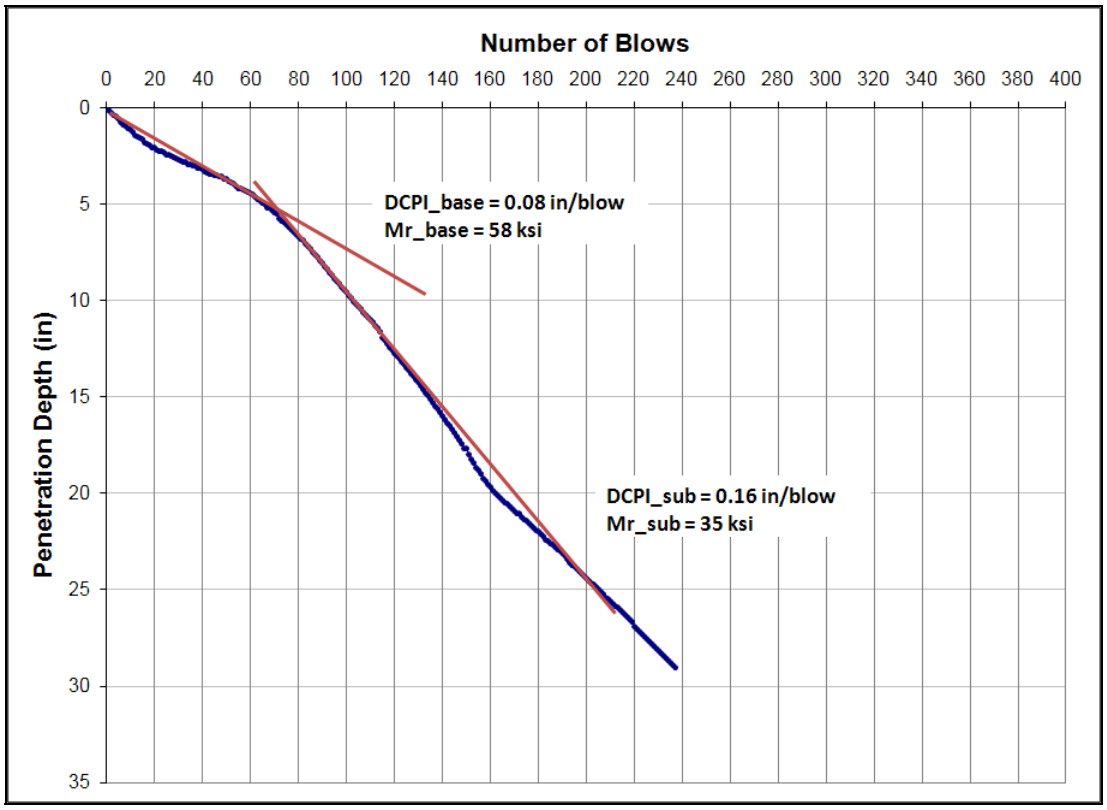

Figure B25. DCP Data Analysis on Section 77002000-2A.

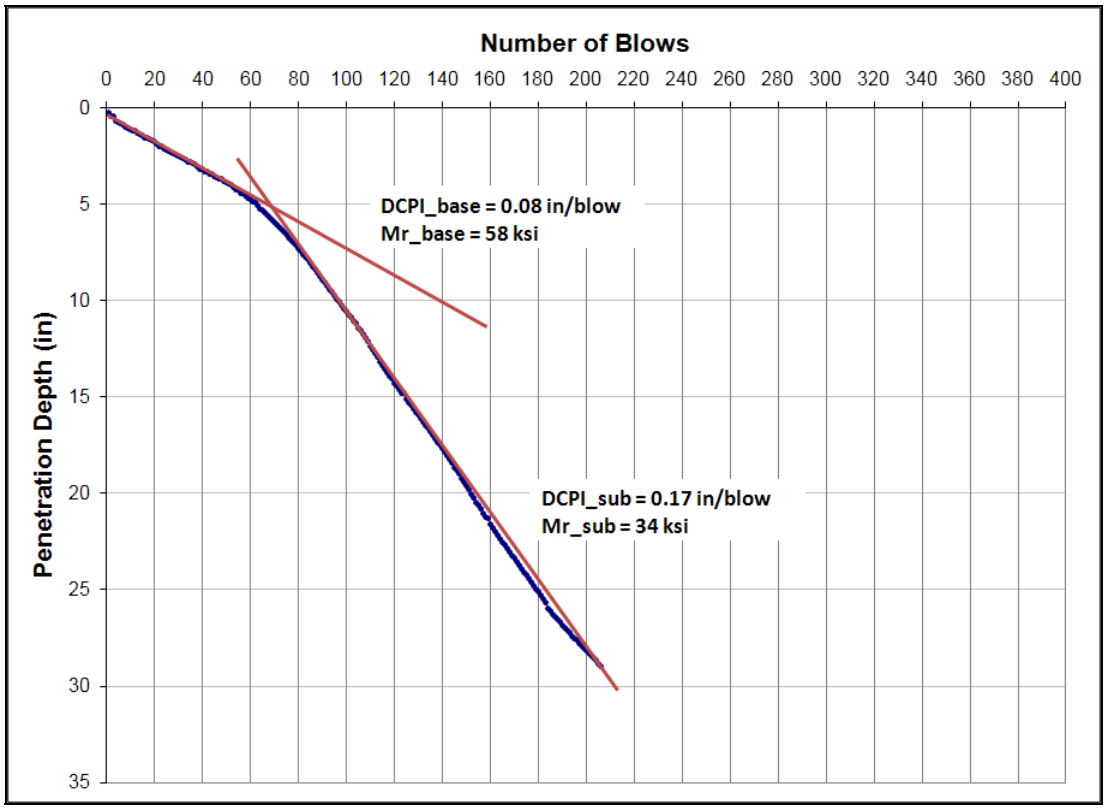

Figure B26. DCP Data Analysis on Section 77002000-3A.

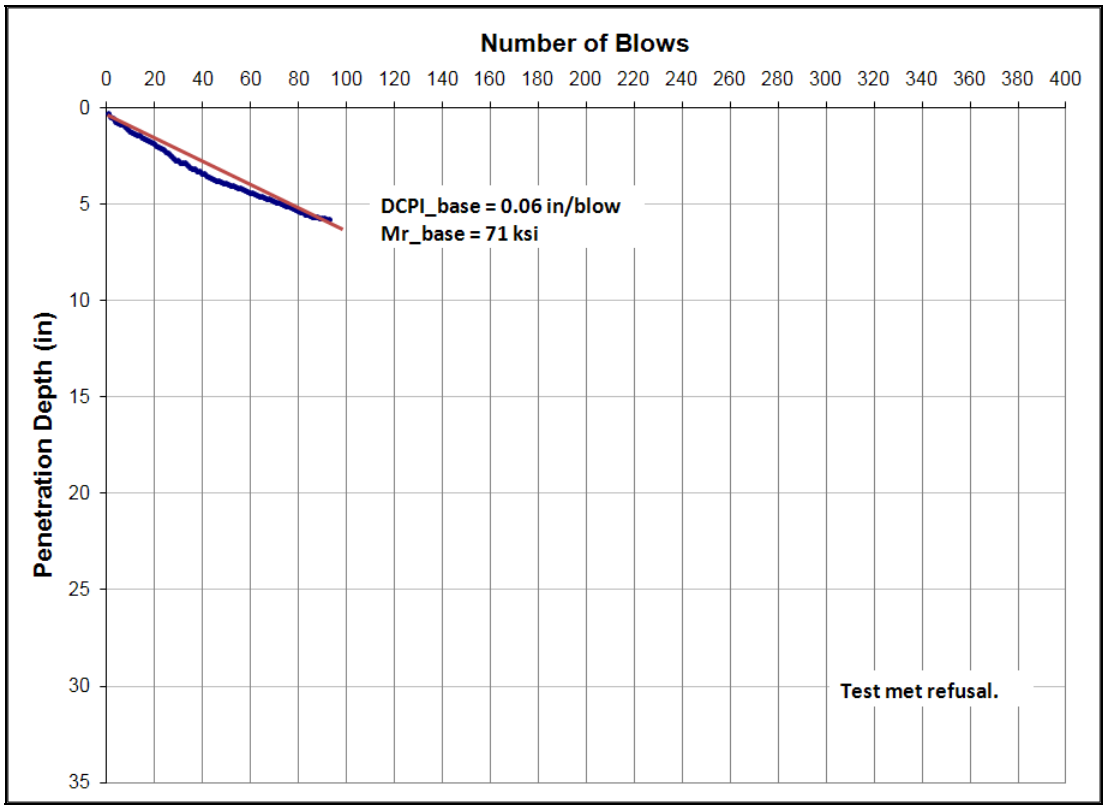

Figure B27. DCP Data Analysis on Section 92060000-2A.

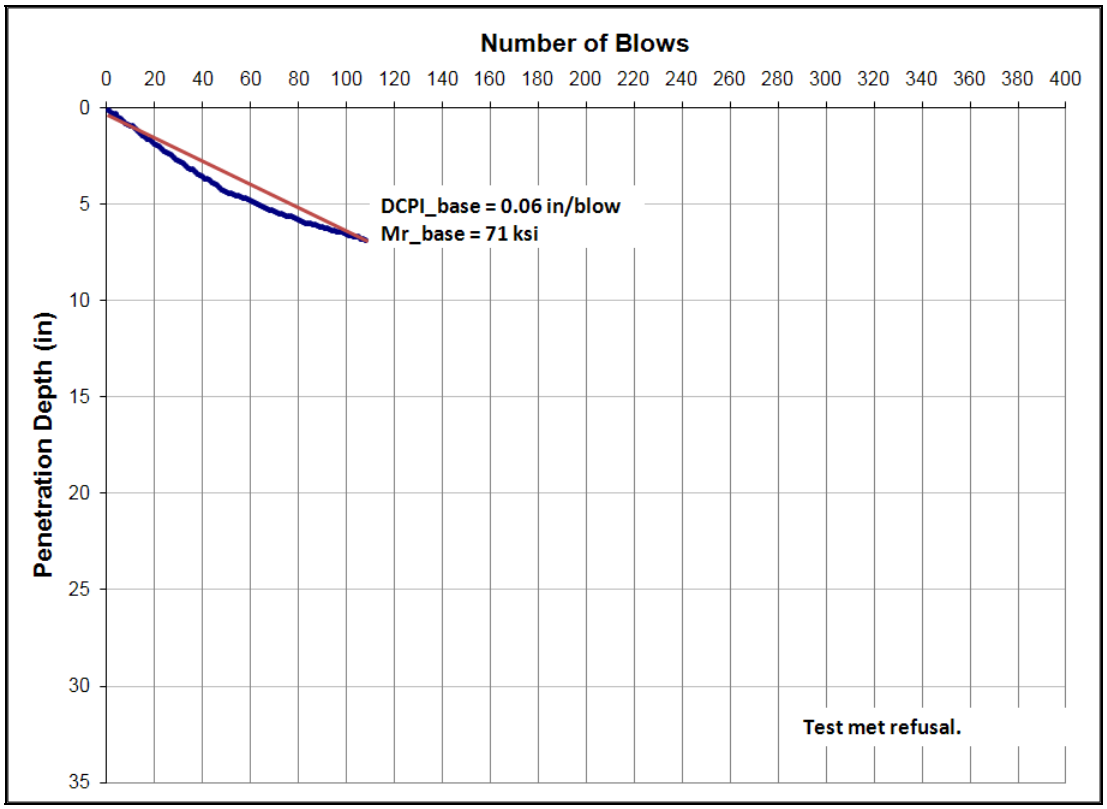

Figure B28. DCP Data Analysis on Section 92060000-3A.

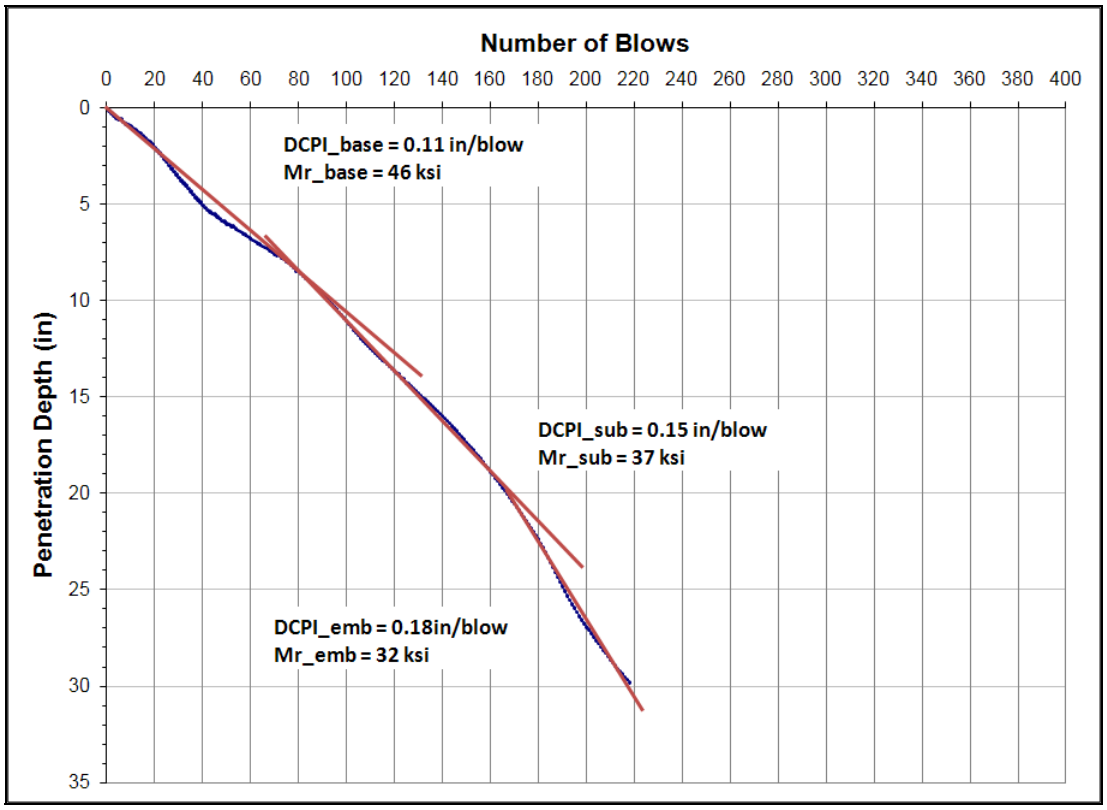

Figure B29. DCP Data Analysis on Section 79270000-2A.

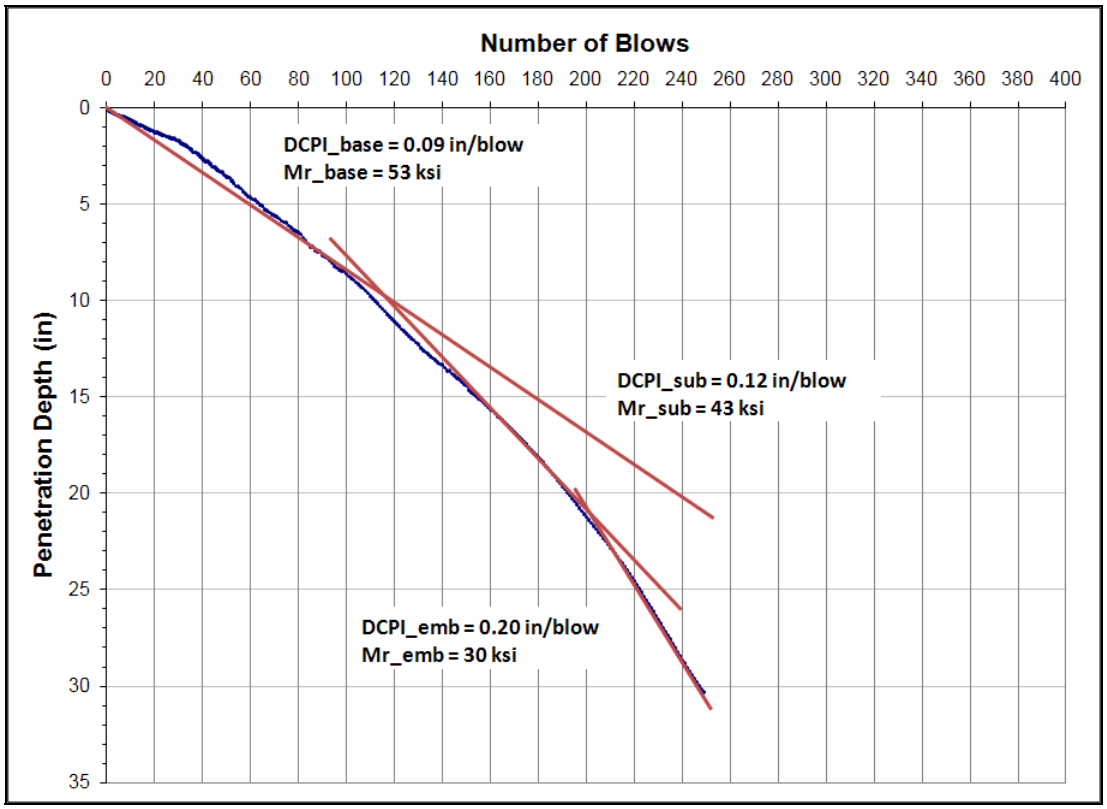

Figure B30. DCP Data Analysis on Section 79270000-3A.

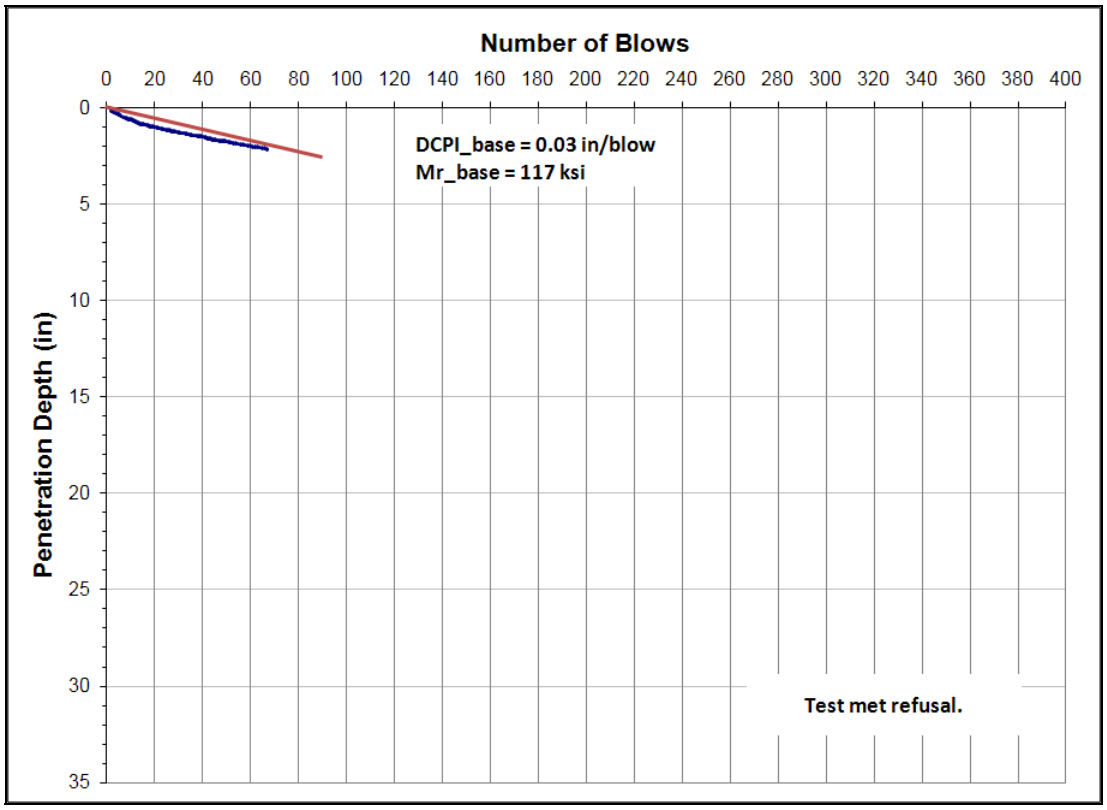

Figure B31. DCP Data Analysis on Section 87120000-2A.

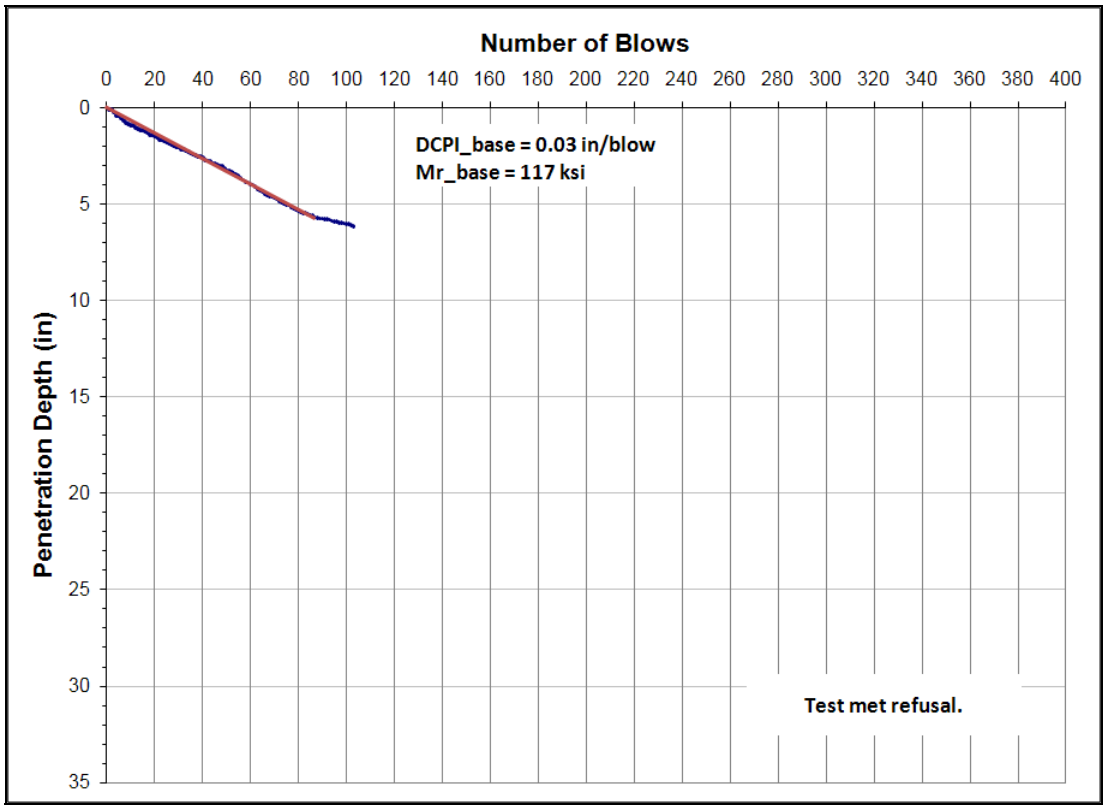

Figure B32. DCP Data Analysis on Section 87120000-3A.

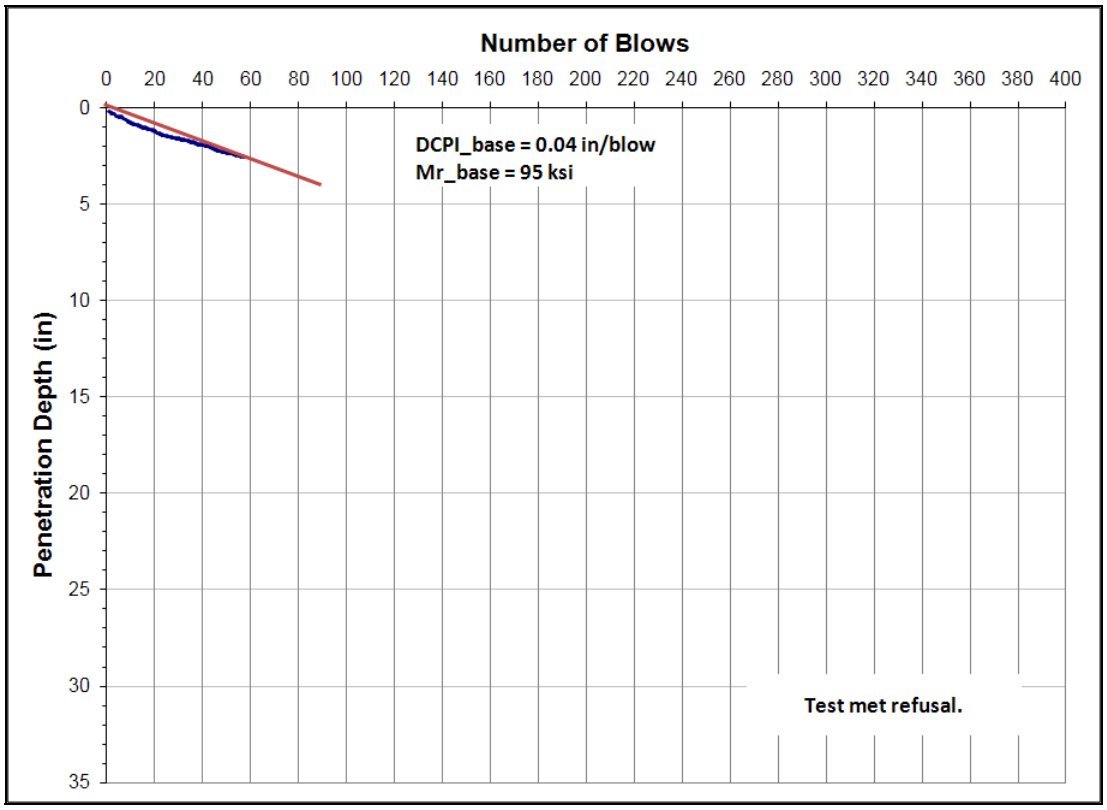

Figure B33. DCP Data Analysis on Section 87060000-2A.

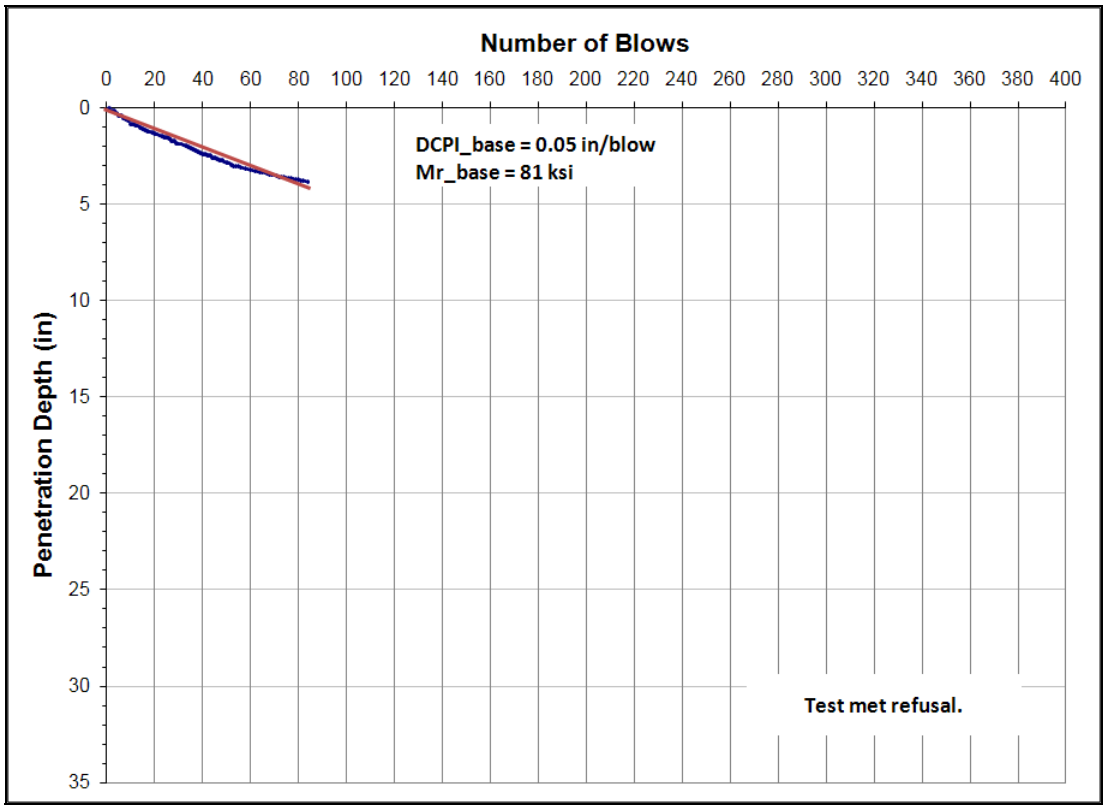

Figure B34. DCP Data Analysis on Section 87060000-3A.

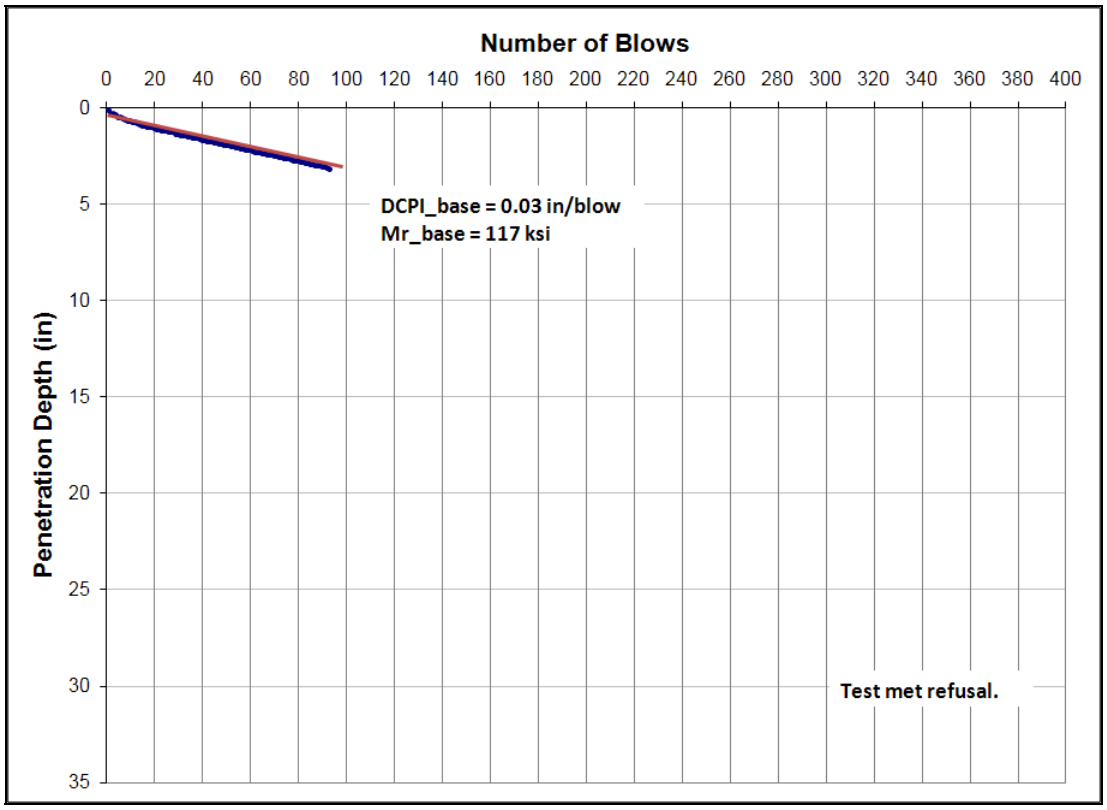

Figure B35. DCP Data Analysis on Section 90060000-2A.

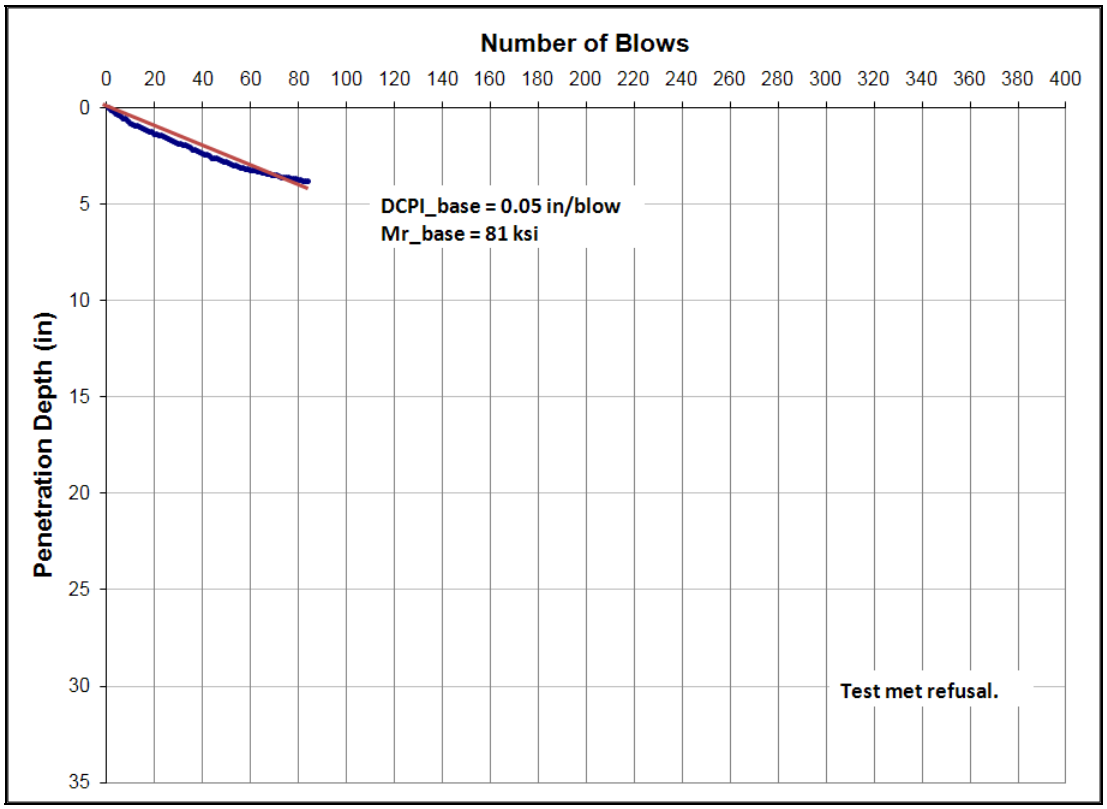

Figure B36. DCP Data Analysis on Section 90060000-3A.

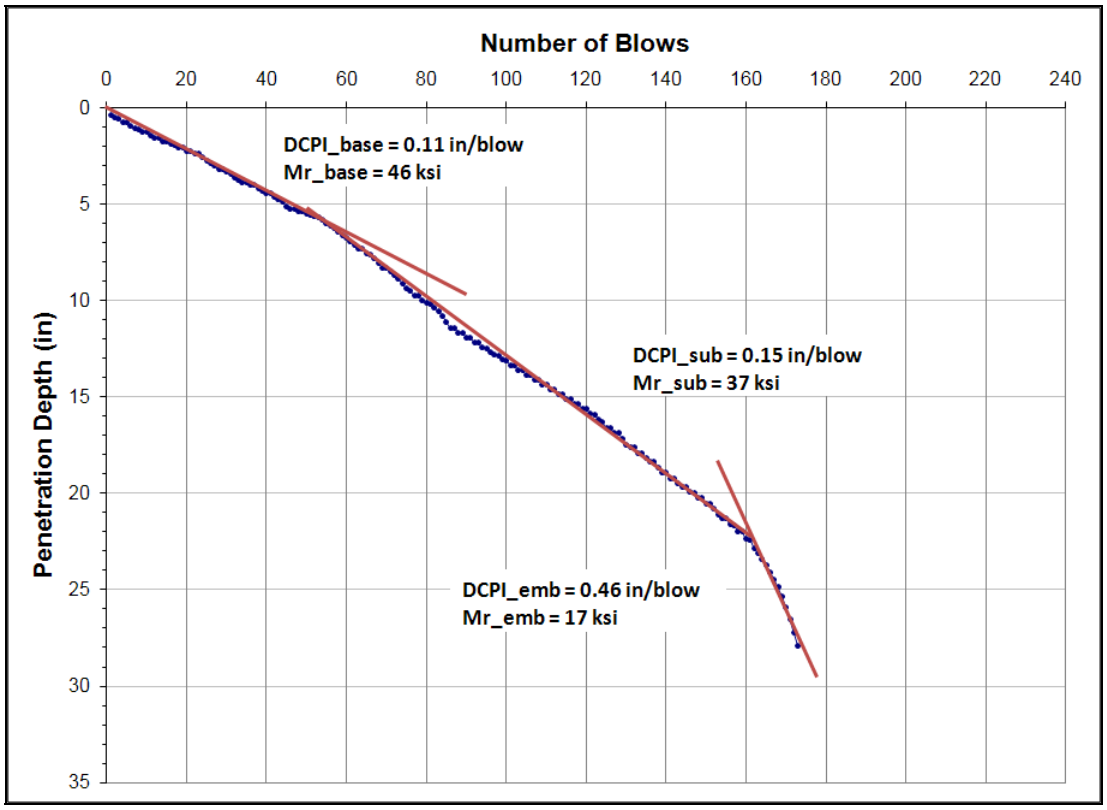

Figure B37. DCP Data Analysis on Section 10060000-2A.

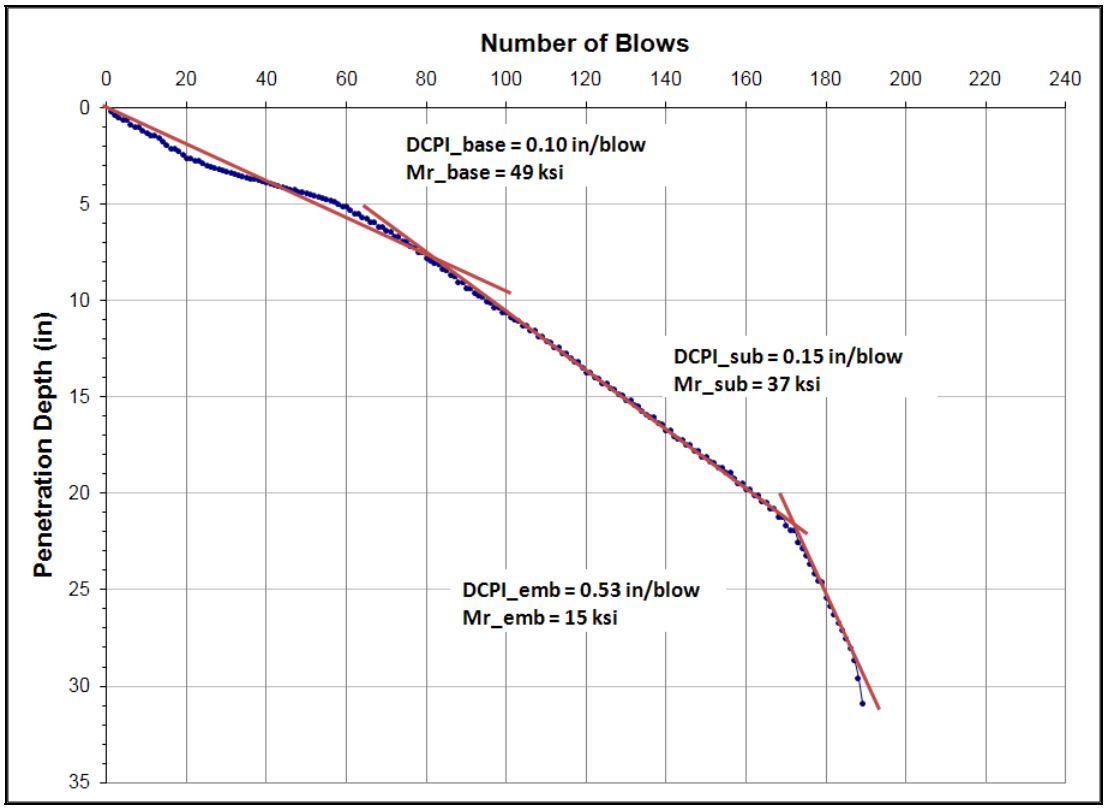

Figure B38. DCP Data Analysis on Section 10060000-3A.

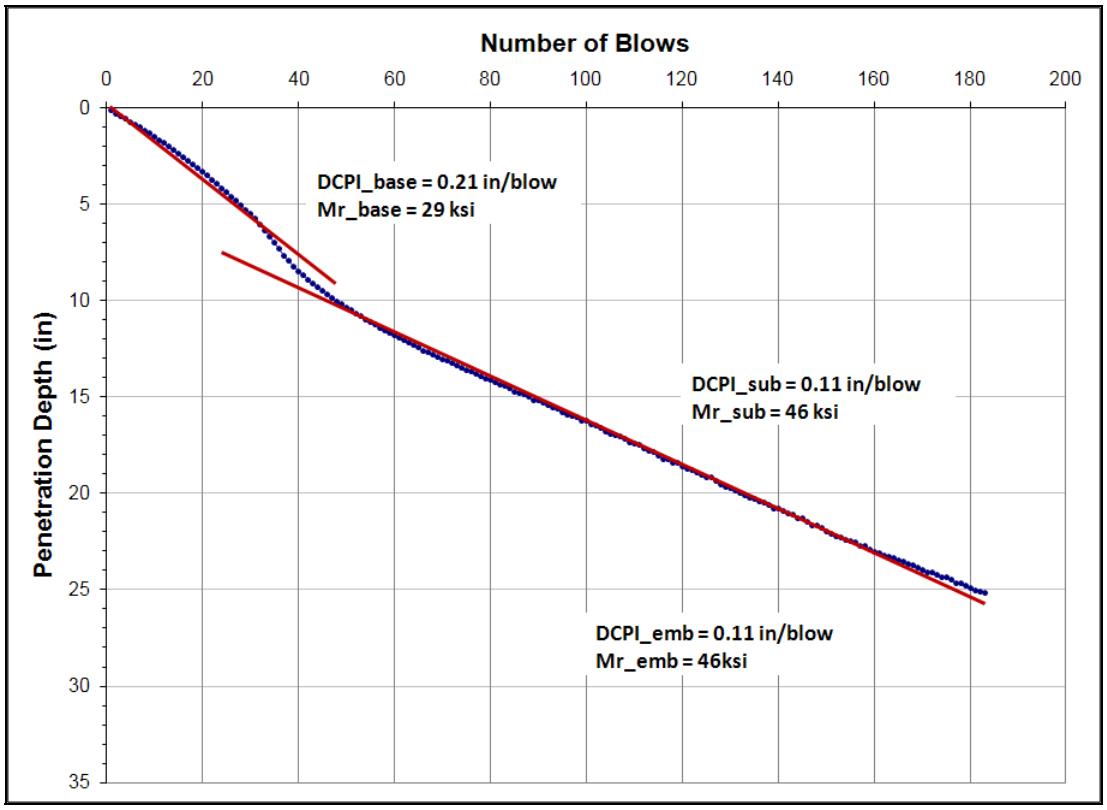

Figure B39. DCP Data Analysis on Section 10160000-2A.

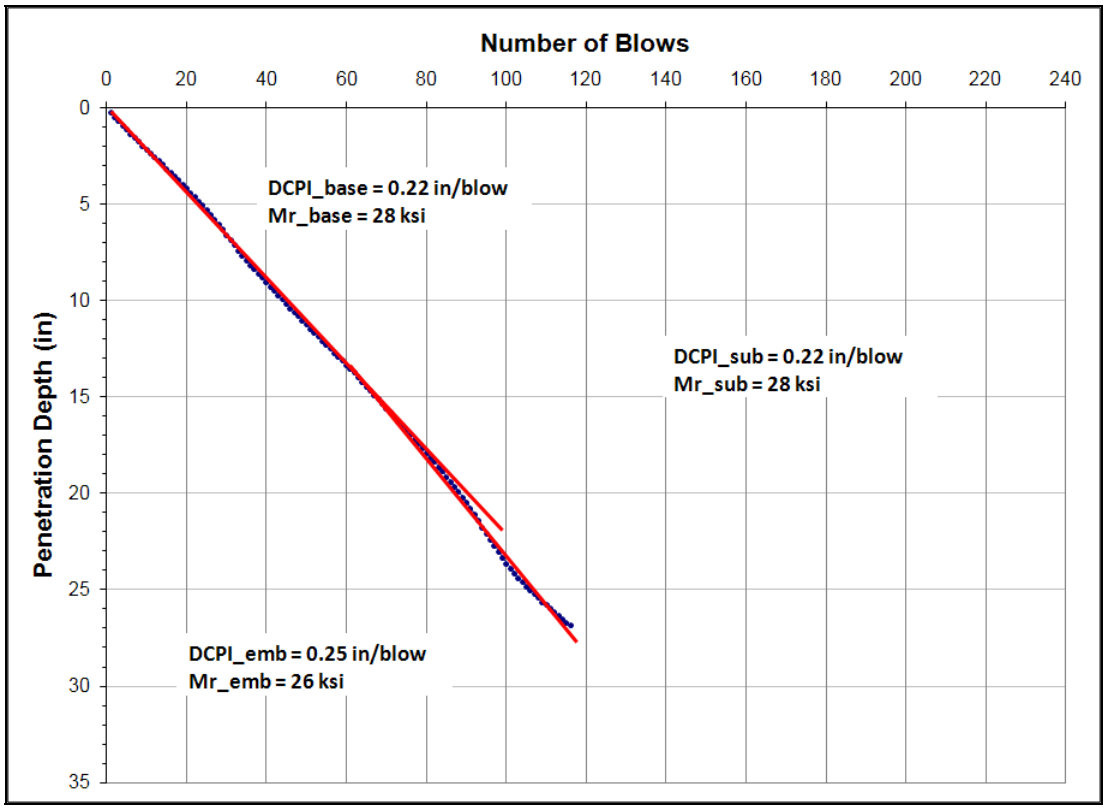

Figure B40. DCP Data Analysis on Section 10160000-3A.

APPENDIX C

SOIL-WATER CHARACTERISTIC CURVE COEFFICIENTS

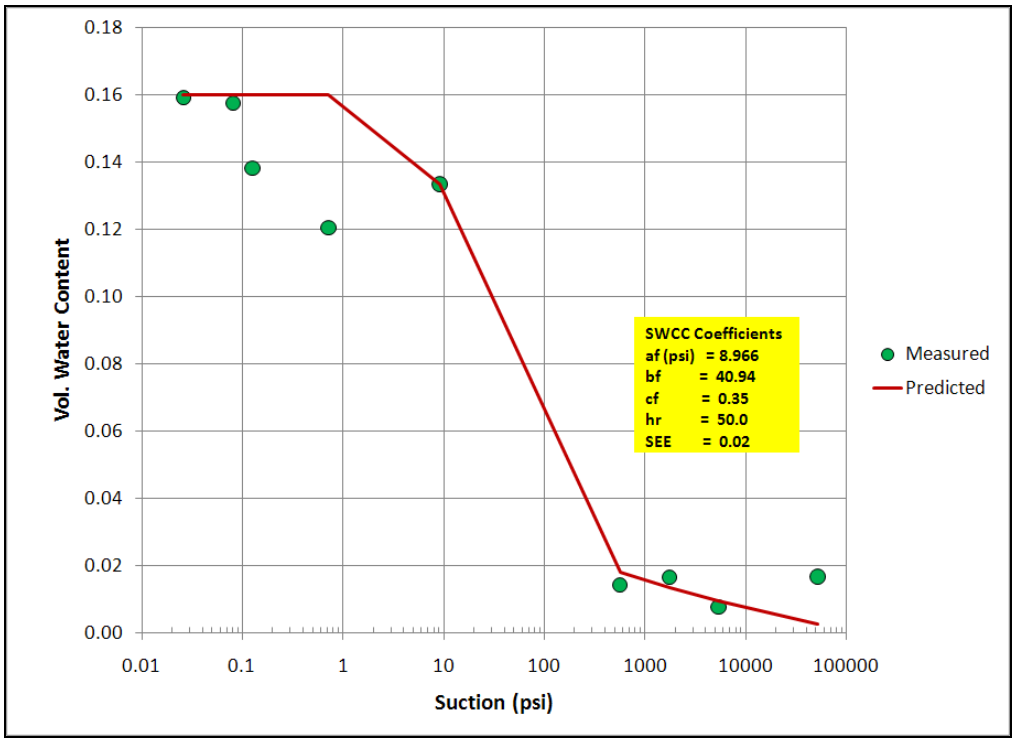

Figure C1. SWCC of LR Base Material on Section 86190000 in Broward County.

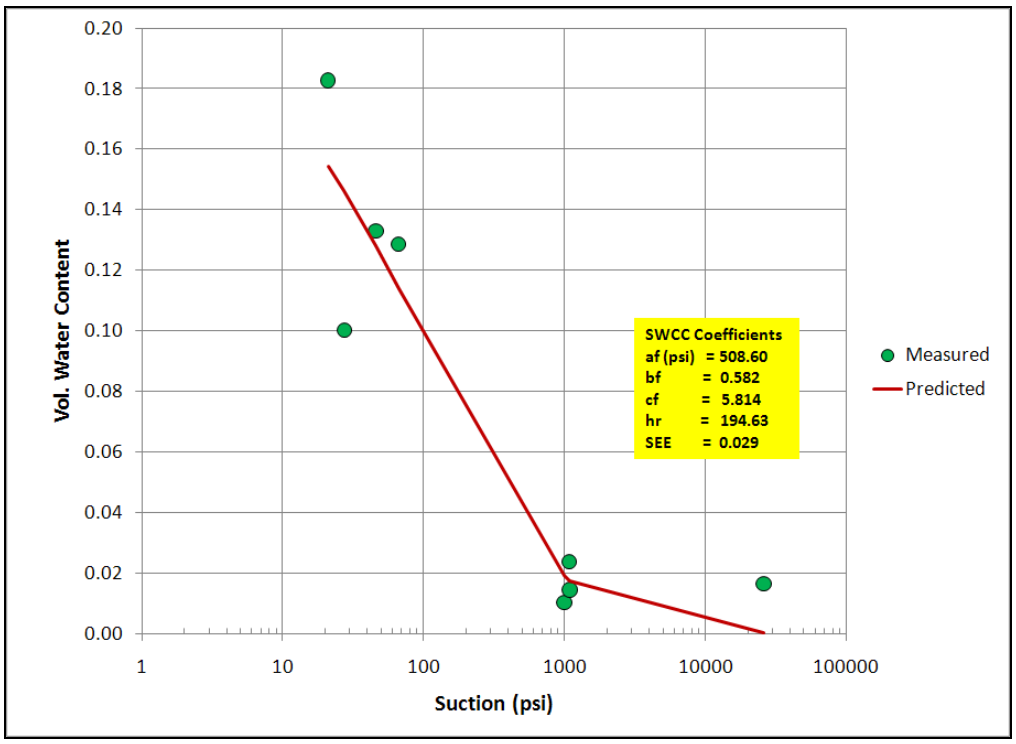

Figure C2. SWCC of Subgrade Material on Section 86190000 in Broward County.

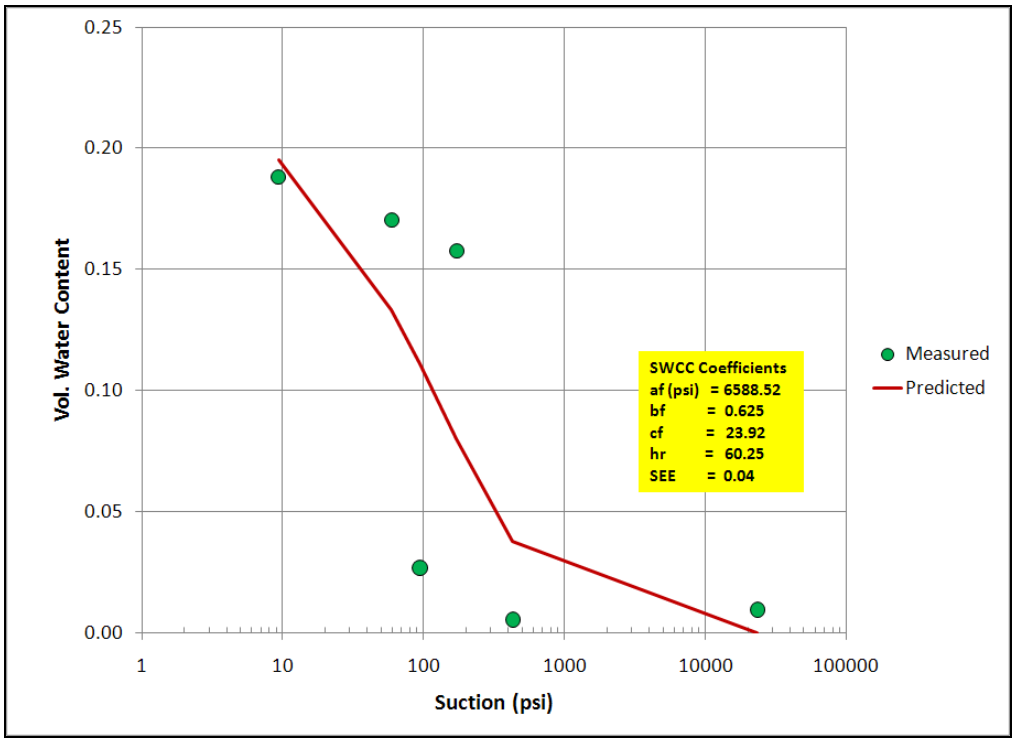

Figure C3. SWCC of Embankment Material on Section 86190000 in Broward County.

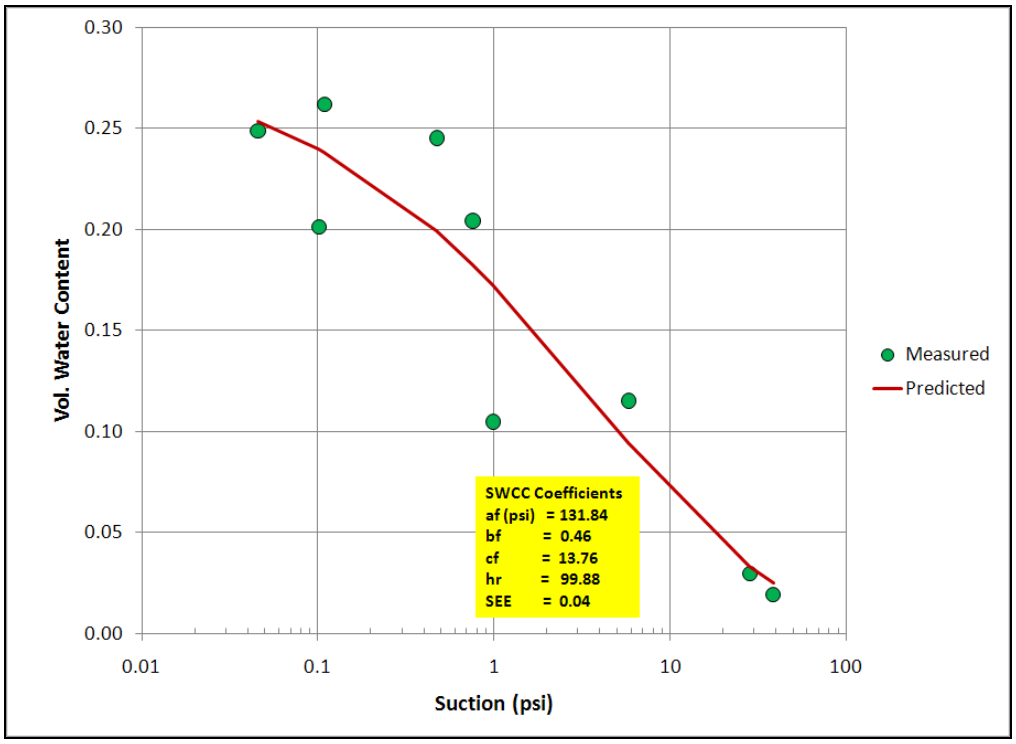

Figure C4. SWCC of LR Base Material on Section 26005000 in Alachua County.

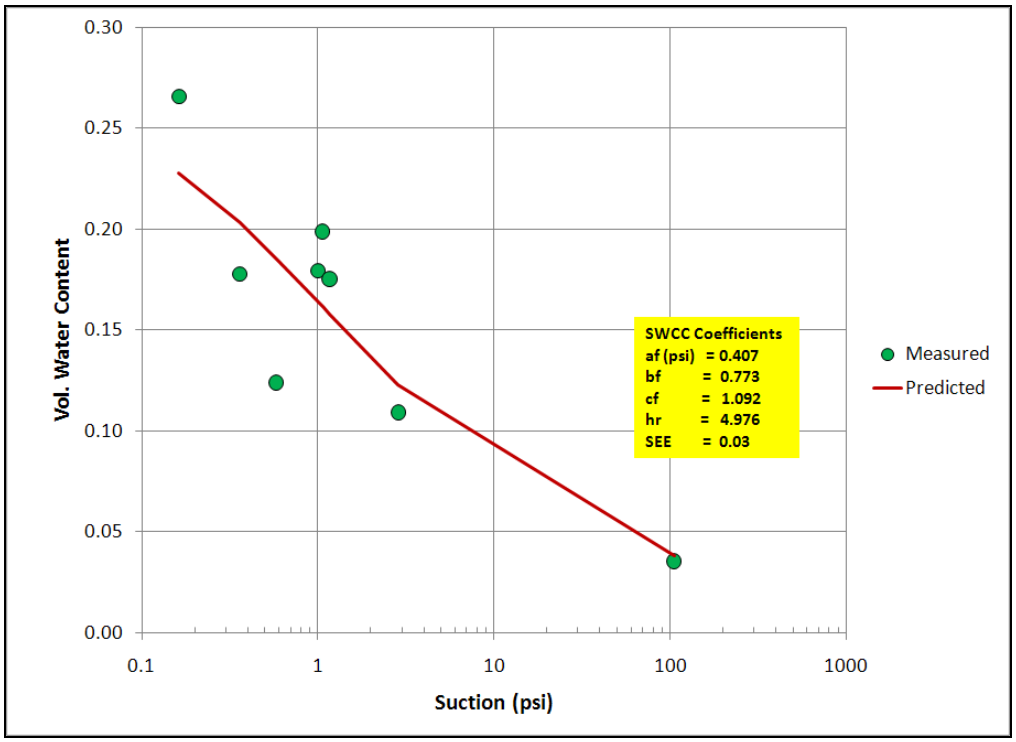

Figure C5. SWCC of Subgrade Material on Section 26005000 in Alachua County.

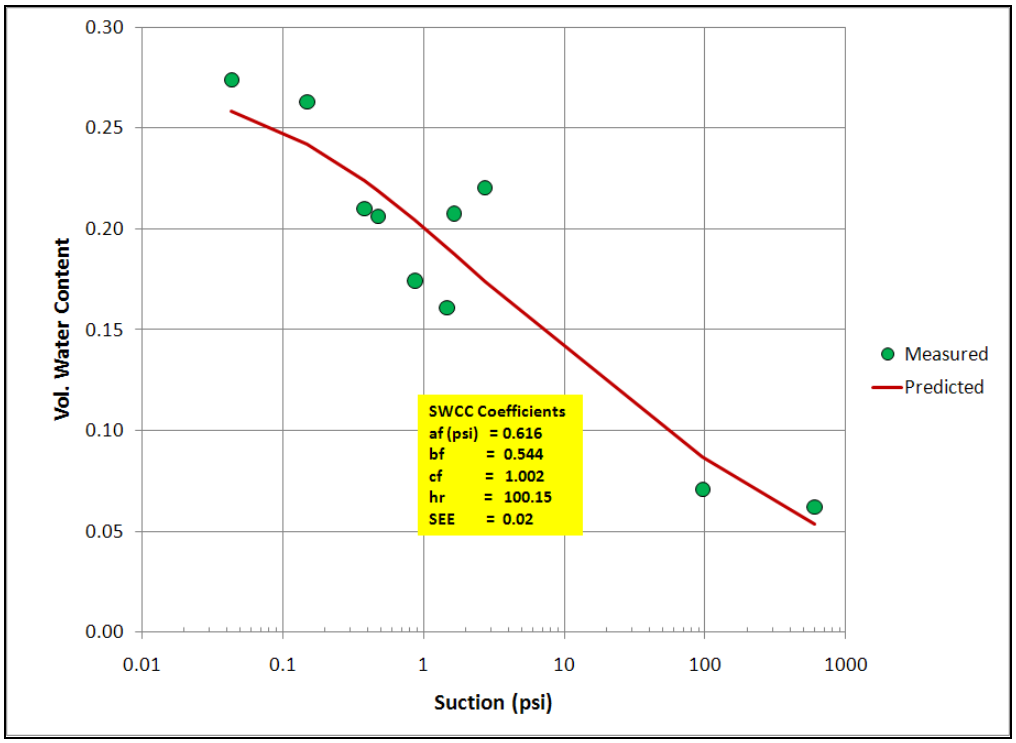

Figure C6. SWCC of Embankment Material on Section 26005000 in Alachua County.

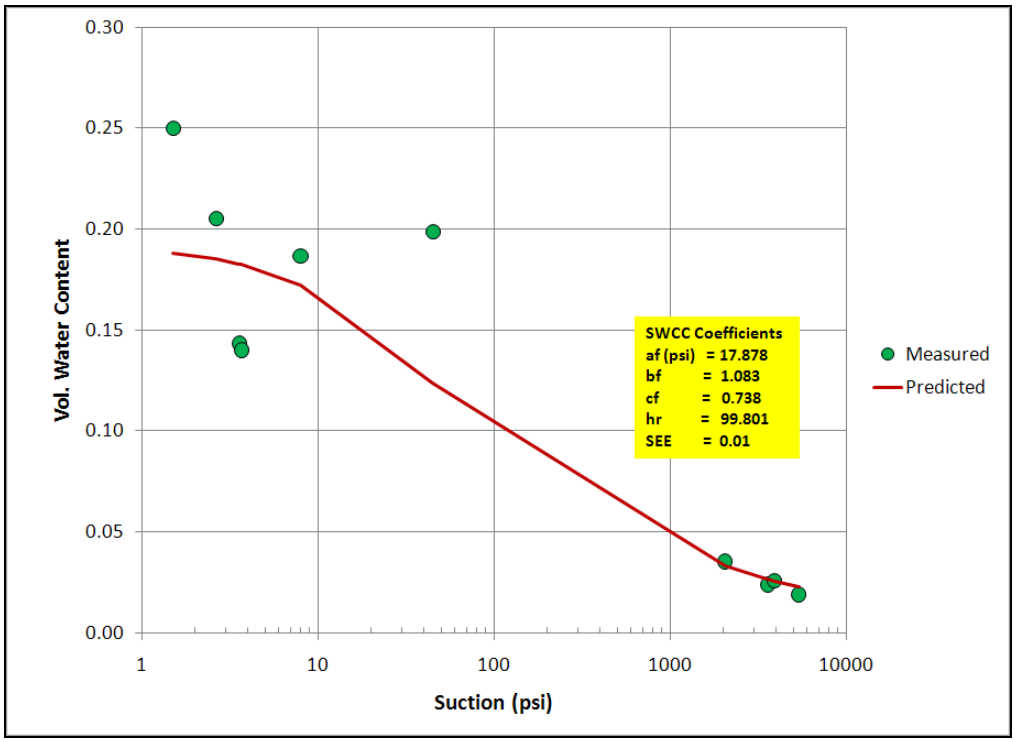

Figure C7. SWCC of Sandy Clay Base Material on Section 58060000 in Santa Rosa County.

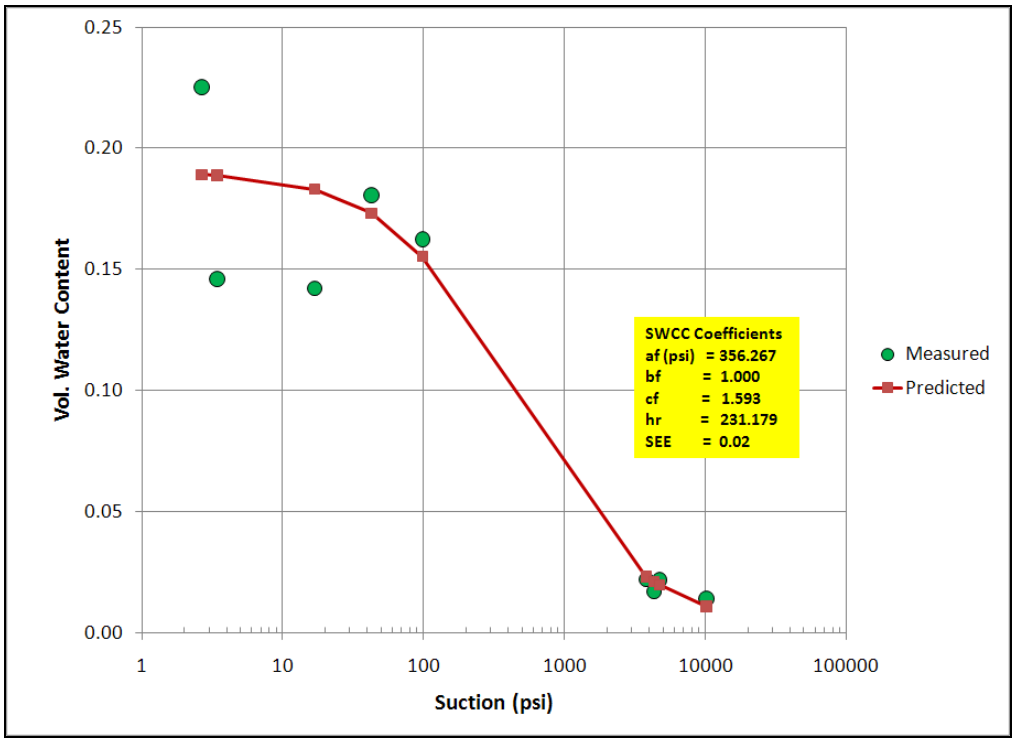

Figure C8. SWCC of Subgrade Material on Section 58060000 in Santa Rosa County.

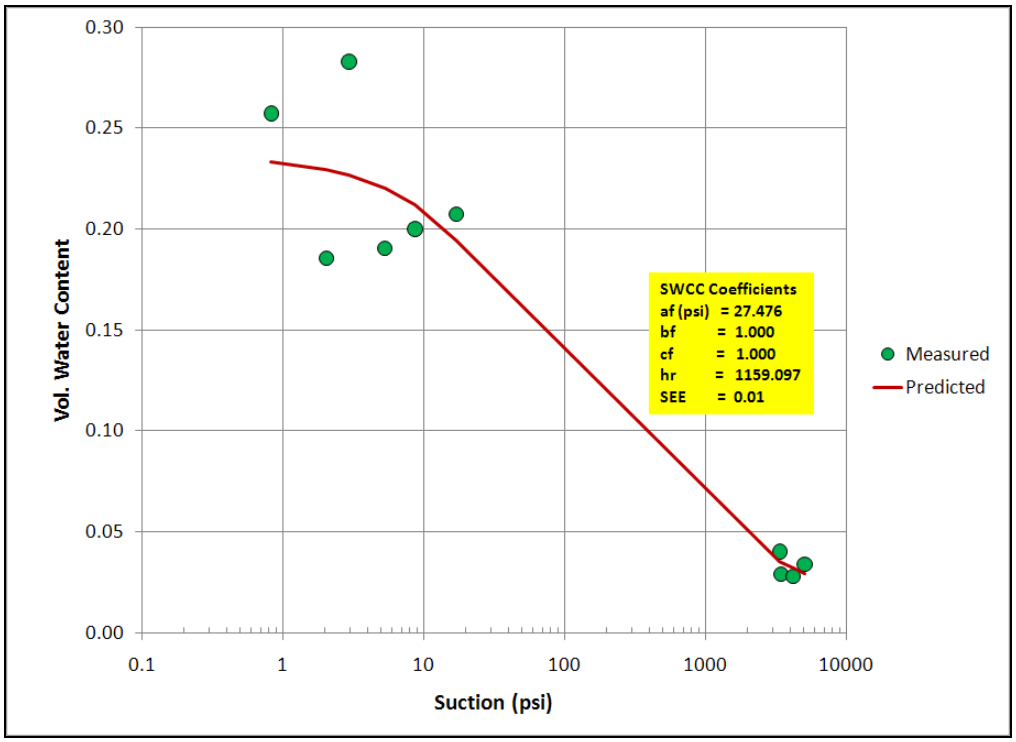

Figure C9. SWCC of Embankment Material on Section 58060000 in Santa Rosa County.

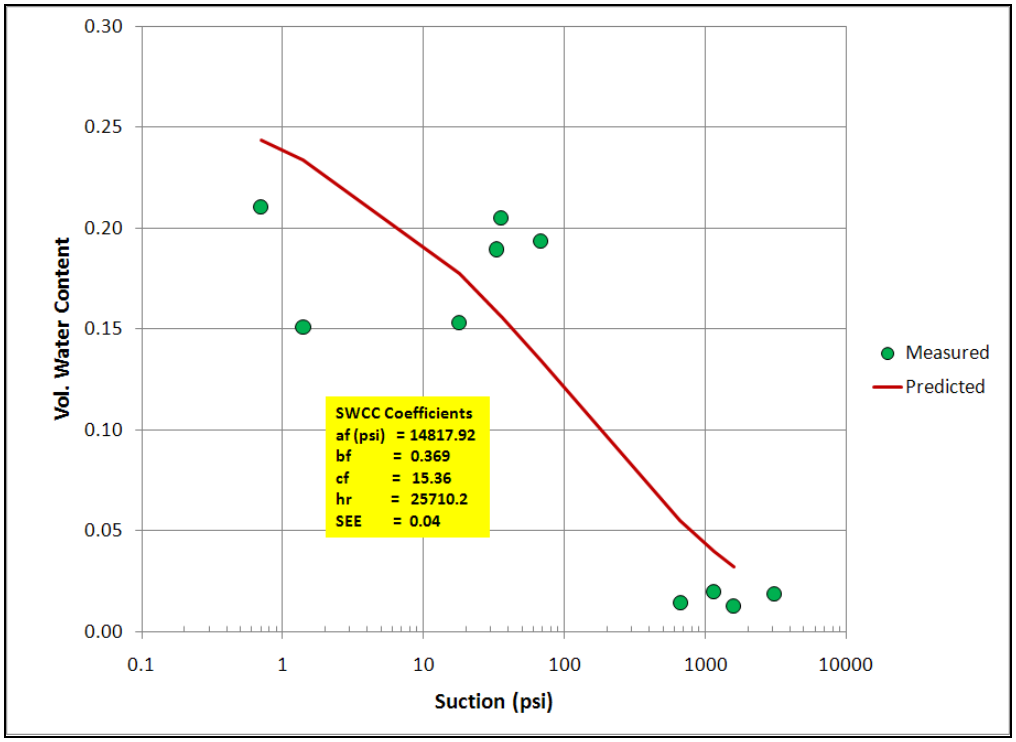

Figure C10. SWCC of Subgrade Material on Section 28040000 in Bradford County.

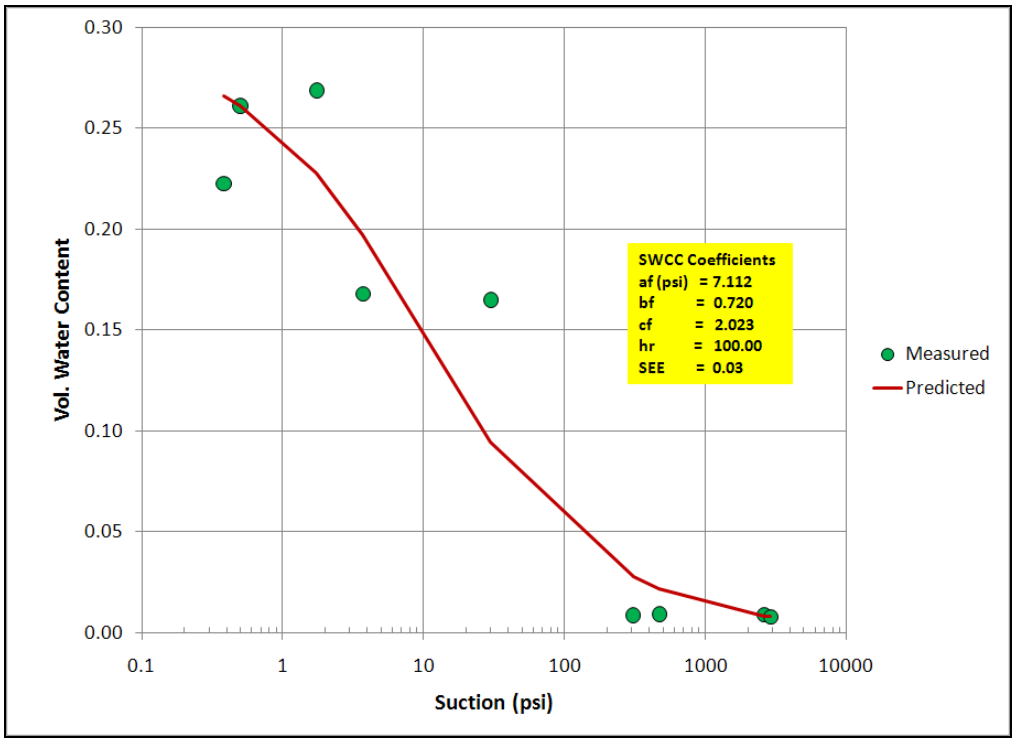

Figure C11. SWCC of Embankment Material on Section 28040000 in Bradford County.

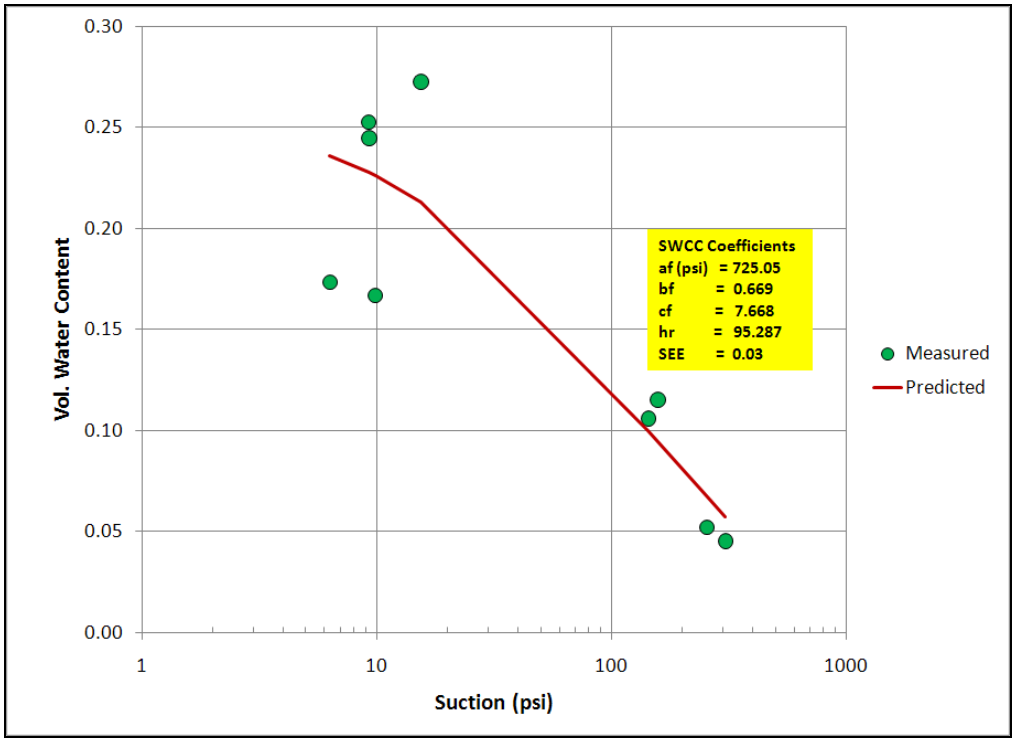

Figure C12. SWCC of LR Base Material on Section 16003000 in Polk County.

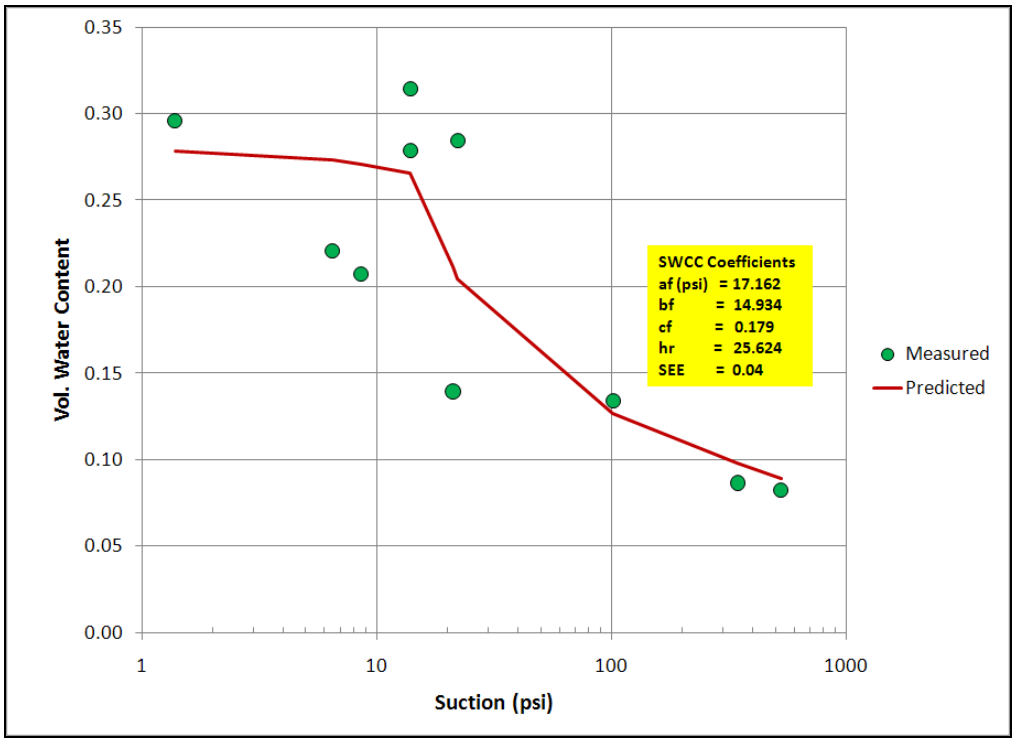

Figure C13. SWCC of Embankment Material on Section 10060000 in Hillsborough County.

APPENDIX D

SUMMARY OF RESILIENT MODULUS DATA ON UNDERLYING MATERIALS

K1	770.26
K2	1.06
K3	-0.77
K4	4.06

$$M_R = K_1 P_a \left(\frac{\theta + 3K_4 SV_W}{P_a} \right)^{K_2} \left(\frac{\tau_{OCT}}{P_a} + 1 \right)^{K_3}$$

	Axial stress	Test sequence	Confining pressure (psi)	Bulk stress (psi)	M_R_Tested (psi)	Oct. shear stress (psi)	Soil suction (psi)	Vol. water content	M_R_Pred. (psi)	Error
OPTIMUM	5.8	1.0	3.0	11.8	15994.1	1.3	5.607	0.199	18939.1	8672681.6
	8.3	2.0	3.0	14.3	16907.8	2.5	5.607	0.199	19825.6	8513563.9
	11.0	3.0	3.0	17.0	18343.0	3.8	5.607	0.199	20688.7	5501915.7
	9.6	4.0	5.0	19.6	21577.6	2.2	5.607	0.199	24179.0	6767399.8
	14.1	5.0	5.0	24.1	23063.4	4.3	5.607	0.199	25241.1	4742159.3
	18.8	6.0	5.0	28.8	24323.6	6.5	5.607	0.199	26254.3	3727487.8
	19.2	7.0	10.0	39.2	32122.9	4.3	5.607	0.199	36030.5	15269389.3
	28.4	8.0	10.0	48.4	34011.1	8.7	5.607	0.199	36444.5	5921282.6
	37.6	9.0	10.0	57.6	35886.9	13.0	5.607	0.199	37001.5	1242273.4
	24.2	10.0	15.0	54.2	38065.0	4.3	5.607	0.199	46987.7	79614673.4
	28.7	11.0	15.0	58.7	39242.1	6.5	5.607	0.199	46343.3	50427667.8
	42.5	12.0	15.0	72.5	42483.0	13.0	5.607	0.199	45330.0	8105526.0
	33.7	13.0	20.0	73.7	44967.6	6.5	5.607	0.199	56612.1	135594791.8
	38.3	14.0	20.0	78.3	46447.7	8.6	5.607	0.199	55430.6	80693263.2
	56.6	15.0	20.0	96.6	50147.0	17.2	5.607	0.199	52696.5	6499884.1
FIELD	30.1	1.0	20.0	70.1	68994.6	4.7	5.732	0.197	57887.3	123372068.3
	40.1	2.0	20.0	80.1	61931.0	9.5	5.732	0.197	55128.2	46278005.3
	50.1	3.0	20.0	90.1	57015.9	14.2	5.732	0.197	53486.0	12459936.1
	25.1	4.0	15.0	55.1	52398.7	4.8	5.732	0.197	46952.8	29657643.5
	35.3	5.0	15.0	65.3	49166.2	9.6	5.732	0.197	45822.3	11181723.7
	45.2	6.0	15.0	75.2	49067.1	14.2	5.732	0.197	45329.3	13971070.6
	15.1	7.0	10.0	35.1	45354.8	2.4	5.732	0.197	36066.0	86282571.4
	20.1	8.0	10.0	40.1	40203.7	4.8	5.732	0.197	36182.2	16172604.3
	30.4	9.0	10.0	50.4	39091.9	9.6	5.732	0.197	36660.1	5913505.3
	40.4	10.0	10.0	60.4	40022.2	14.3	5.732	0.197	37278.9	7525443.4
	10.1	11.0	5.0	20.1	28493.2	2.4	5.732	0.197	24450.0	16347275.2
	15.1	12.0	5.0	25.1	25978.5	4.8	5.732	0.197	25601.5	142118.1
	20.5	13.0	5.0	30.5	27246.2	7.3	5.732	0.197	26702.3	295892.1
	8.1	14.0	3.0	14.1	22379.6	2.4	5.732	0.197	19877.1	6262506.0
	10.1	15.0	3.0	16.1	21631.2	3.4	5.732	0.197	20531.3	1209792.2
	12.1	16.0	3.0	18.1	21737.1	4.3	5.732	0.197	21130.2	368289.8
									SSE	798734405
									SEE	5075.99

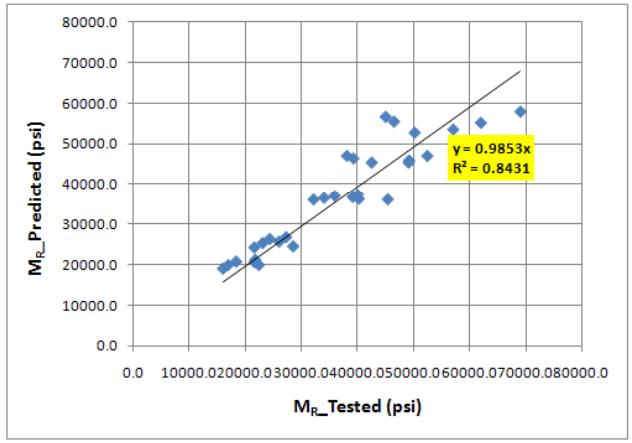

Figure D1. Resilient Modulus Properties of Base Material on Section 16020000.

K1	1439.32
K2	0.52
K3	-0.24
K4	-0.08

$$M_R = K_1 P_a \left(\frac{\theta + 3K_4 SV_W}{P_a} \right)^{K_2} \left(\frac{\tau_{OCT}}{P_a} + 1 \right)^{K_3}$$

	Axial stress	Test sequence	Confining pressure (psi)	Bulk stress (psi)	M_R_Tested (psi)	Oct. shear stress (psi)	Soil suction (psi)	Vol. water content	M_R_Pred. (psi)	Error
OPTIMUM	21.7	1.0	15.0	51.7	41659.8	3.2	43.00	0.20	37840.0	14590990.8
	24.7	2.0	15.0	54.7	41468.7	4.6	43.00	0.20	38294.5	10075482.1
	29.8	3.0	15.0	59.8	41329.3	7.0	43.00	0.20	39034.2	5267351.5
	14.7	4.0	10.0	34.7	31816.4	2.2	43.00	0.20	30793.9	1045588.1
	16.7	5.0	10.0	36.7	31752.0	3.2	43.00	0.20	31346.5	164444.1
	19.7	6.0	10.0	39.7	32021.6	4.6	43.00	0.20	32130.0	11738.0
	24.7	7.0	10.0	44.7	33541.5	6.9	43.00	0.20	33338.1	41381.6
	7.7	8.0	5.0	17.7	22536.9	1.3	43.00	0.20	21241.0	1679281.2
	9.7	9.0	5.0	19.7	22140.8	2.2	43.00	0.20	22308.1	28001.1
	11.7	10.0	5.0	21.7	22420.6	3.2	43.00	0.20	23285.9	748710.1
	14.7	11.0	5.0	24.7	23748.9	4.6	43.00	0.20	24625.5	768508.9
	4.7	12.0	2.0	8.7	15162.2	1.3	43.00	0.20	13533.6	2652148.7
	6.7	13.0	2.0	10.7	16114.1	2.2	43.00	0.20	15341.0	597715.4
	8.8	14.0	2.0	12.8	17191.2	3.2	43.00	0.20	16910.7	78655.6
FIELD	21.7	1.0	15.0	51.7	34178.7	3.2	137.59	0.14	36739.8	6559370.3
	24.7	2.0	15.0	54.7	35298.0	4.6	137.59	0.14	37239.4	3769085.5
	29.7	3.0	15.0	59.7	37133.5	6.9	137.59	0.14	38053.3	846040.9
	14.7	4.0	10.0	34.7	27146.6	2.2	137.59	0.14	29420.3	5169690.4
	16.7	5.0	10.0	36.7	28037.5	3.2	137.59	0.14	30028.4	3963871.1
	19.7	6.0	10.0	39.7	29340.5	4.6	137.59	0.14	30889.7	2400038.9
	24.7	7.0	10.0	44.7	31420.5	6.9	137.59	0.14	32202.9	612263.3
	7.7	8.0	5.0	17.7	18399.6	1.3	137.59	0.14	19211.4	658992.2
	9.7	9.0	5.0	19.7	19571.1	2.2	137.59	0.14	20425.3	729536.5
	11.7	10.0	5.0	21.7	20701.6	3.2	137.59	0.14	21534.6	693957.7
	14.7	11.0	5.0	24.7	22307.6	4.6	137.59	0.14	23020.5	508162.0
	4.7	12.0	2.0	8.7	12216.7	1.3	137.59	0.14	10263.4	3815254.0
	6.7	13.0	2.0	10.7	13757.7	2.2	137.59	0.14	12564.2	1424443.2
	8.7	14.0	2.0	12.7	15197.8	3.2	137.59	0.14	14462.2	541165.4
									SSE	69441868.5
									SEE	1496.68

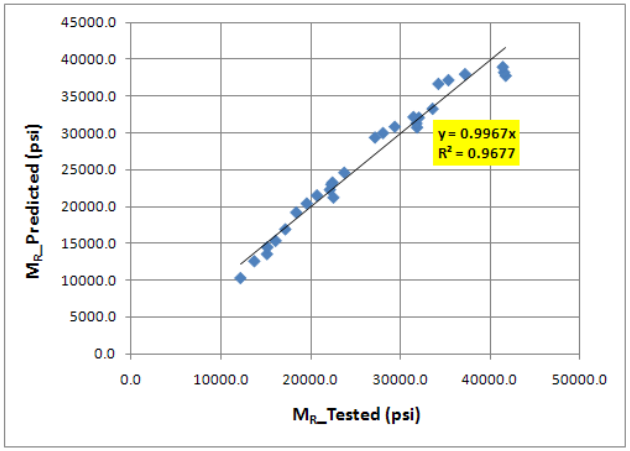

Figure D2. Resilient Modulus Properties of Subgrade Material on Section 16020000.

K1	1114.26
K2	0.69
K3	-0.27
K4	0.16

$$M_R = K_1 P_a \left(\frac{\theta + 3K_4 SV_w}{P_a} \right)^{K_2} \left(\frac{\tau_{OCT}}{P_a} + 1 \right)^{K_3}$$

	Axial stress	Test sequence	Confining pressure (psi)	Bulk stress (psi)	M_R_Tested (psi)	Oct. shear stress (psi)	Soil suction (psi)	Vol. water content	M_R_Pred. (psi)	Error
OPTIMUM	21.8	1.0	15.0	51.8	39982.2	3.2	52.46	0.19	39188.6	629703.2
	24.8	2.0	15.0	54.8	39974.6	4.6	52.46	0.19	39792.5	33159.2
	29.7	3.0	15.0	59.7	40435.1	6.9	52.46	0.19	40785.9	123039.7
	14.7	4.0	10.0	34.7	31984.4	2.2	52.46	0.19	31035.1	901177.9
	16.7	5.0	10.0	36.7	31478.0	3.2	52.46	0.19	31653.7	30861.7
	19.7	6.0	10.0	39.7	32067.9	4.6	52.46	0.19	32544.6	227232.5
	24.7	7.0	10.0	44.7	33206.2	6.9	52.46	0.19	33967.2	579080.3
	7.7	8.0	5.0	17.7	22763.5	1.3	52.46	0.19	21324.3	2071112.4
	9.7	9.0	5.0	19.7	22701.7	2.2	52.46	0.19	22299.0	162139.1
	11.7	10.0	5.0	21.7	23002.9	3.2	52.46	0.19	23205.6	41080.6
	14.7	11.0	5.0	24.7	23866.5	4.6	52.46	0.19	24488.7	387109.8
	4.7	12.0	2.0	8.7	15650.8	1.3	52.46	0.19	14981.4	448139.7
	6.7	13.0	2.0	10.7	16335.4	2.2	52.46	0.19	16237.5	9591.9
	8.8	14.0	2.0	12.8	16928.5	3.2	52.46	0.19	17438.1	259705.8
FIELD	21.7	1.0	15.0	51.7	37879.5	3.2	45.75	0.20	38939.5	1123737.1
	24.7	2.0	15.0	54.7	39104.5	4.6	45.75	0.20	39547.4	196180.6
	29.7	3.0	15.0	59.7	41112.3	6.9	45.75	0.20	40566.2	298208.8
	14.7	4.0	10.0	34.7	30171.3	2.2	45.75	0.20	30764.9	352379.3
	16.7	5.0	10.0	36.7	31149.0	3.2	45.75	0.20	31386.5	56419.5
	19.7	6.0	10.0	39.7	32578.5	4.6	45.75	0.20	32292.4	81829.4
	24.7	7.0	10.0	44.7	34858.6	6.9	45.75	0.20	33729.3	1275323.2
	7.7	8.0	5.0	17.7	20547.7	1.3	45.75	0.20	21017.0	220251.3
	9.7	9.0	5.0	19.7	21839.4	2.2	45.75	0.20	21980.4	19868.5
	11.7	10.0	5.0	21.7	23084.9	3.2	45.75	0.20	22903.0	33081.5
	14.7	11.0	5.0	24.7	24853.0	4.6	45.75	0.20	24201.3	424716.0
	4.7	12.0	2.0	8.7	13711.8	1.3	45.75	0.20	14597.5	784443.5
	6.7	13.0	2.0	10.7	15418.9	2.2	45.75	0.20	15868.6	202253.0
	8.7	14.0	2.0	12.7	17012.1	3.2	45.75	0.20	17065.9	2897.0
									SSE	10974722.3
									SEE	595.00

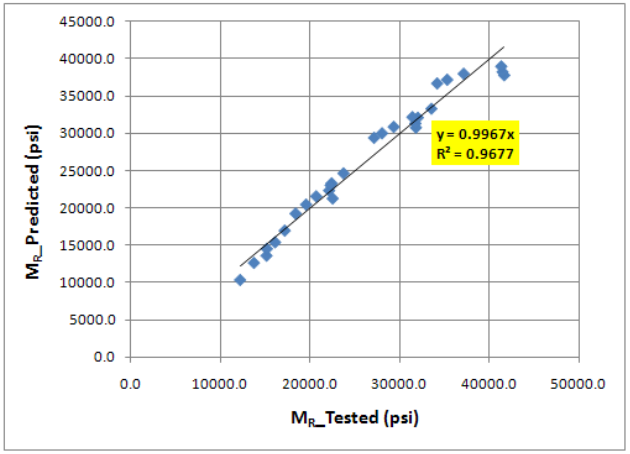

Figure D3. Resilient Modulus Properties of Embankment Material on Section 16020000.

K1	923.33
K2	0.89
K3	-0.72
K4	2.62

$$M_R = K_1 P_a \left(\frac{\theta + 3K_4 SV_w}{P_a} \right)^{K_2} \left(\frac{\tau_{OCT}}{P_a} + 1 \right)^{K_3}$$

	Axial stress	Test sequence	Confining pressure (psi)	Bulk stress (psi)	M_R_Tested (psi)	Oct. shear stress (psi)	Soil suction (psi)	Vol. water content	M_R_Pred. (psi)	Error
OPTIMUM	5.6	1.0	3	11.77	15994.15	1.2	5.607	0.199	17241	1555592
	8.2	2.0	3	14.34	16907.78	2.5	5.607	0.199	18102	1426280
	11.0	3.0	3	17.05	18343.04	3.8	5.607	0.199	18937	353328
	9.5	4.0	5	19.56	21577.56	2.1	5.607	0.199	22020	195632
	14.2	5.0	5	24.06	23063.43	4.3	5.607	0.199	22957	11413
	19.0	6.0	5	28.78	24323.59	6.6	5.607	0.199	23825	248950
	19.2	7.0	10	39.20	32122.93	4.3	5.607	0.199	32179	3197
	28.8	8.0	10	48.38	34011.10	8.9	5.607	0.199	32184	3338369
	38.2	9.0	10	57.58	35886.91	13.3	5.607	0.199	32407	12107597
	24.2	10.0	15	54.16	38064.97	4.3	5.607	0.199	40992	8566989
	28.9	11.0	15	58.69	39242.10	6.5	5.607	0.199	40236	988105
	43.2	12.0	15	72.52	42482.99	13.3	5.607	0.199	38823	13394916
	33.9	13.0	20	73.68	44967.62	6.5	5.607	0.199	48139	10057208
	38.6	14.0	20	78.29	46447.66	8.7	5.607	0.199	46997	301371
	57.4	15.0	20	96.59	50146.97	17.6	5.607	0.199	44059	37065449
FIELD	29.9	1.0	20	69.86	49166.75	4.7	0.080	0.269	44536	21439586
	39.9	2.0	20	79.86	43821.90	9.4	0.080	0.269	42769	1107841
	49.9	3.0	20	89.87	37348.67	14.1	0.080	0.269	41685	18804981
	24.9	4.0	15	54.90	36350.34	4.7	0.080	0.269	35923	182242
	34.9	5.0	15	64.90	33740.63	9.4	0.080	0.269	35546	3258393
	44.9	6.0	15	74.92	31413.82	14.1	0.080	0.269	35436	16178902
	14.9	7.0	10	34.88	30525.55	2.3	0.080	0.269	26423	16831065
	19.9	8.0	10	39.92	26475.26	4.7	0.080	0.269	27063	345735
	29.9	9.0	10	49.93	26108.99	9.4	0.080	0.269	28147	4151641
	39.9	10.0	10	59.91	23970.10	14.1	0.080	0.269	29054	25843367
	9.9	11.0	5	19.88	18413.41	2.3	0.080	0.269	16060	5536573
	14.9	12.0	5	24.93	16749.82	4.7	0.080	0.269	17826	1157926
	19.9	13.0	5	29.93	17463.08	7.0	0.080	0.269	19271	3268762
	7.9	14.0	3	13.89	14106.18	2.3	0.080	0.269	11704	5772570
	9.9	15.0	3	15.88	14022.52	3.2	0.080	0.269	12663	1846972
	11.9	16.0	3	17.90	14474.92	4.2	0.080	0.269	13551	853329
									SSE	216194281
									SEE	2640.83

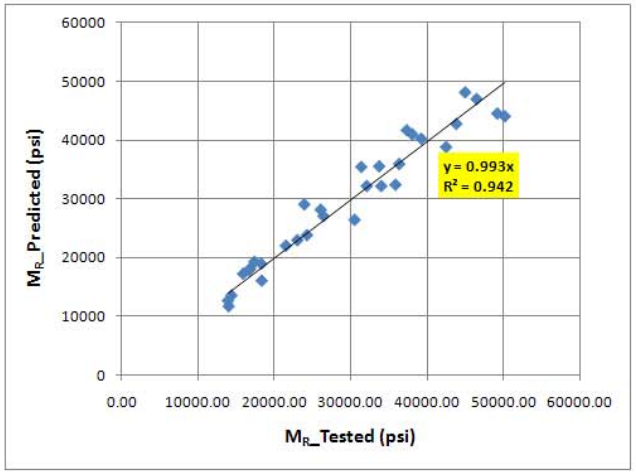

Figure D4. Resilient Modulus Properties of Base Material on Section 12500000.

K1	1264.07
K2	0.54
K3	-0.22
K4	-0.01

$$M_R = K_1 P_a \left(\frac{\theta + 3K_4 SV_W}{P_a} \right)^{K_2} \left(\frac{\tau_{OCT}}{P_a} + 1 \right)^{K_3}$$

	Axial stress	Test sequence	Confining pressure (psi)	Bulk stress (psi)	M_R_Tested (psi)	Oct. shear stress (psi)	Soil suction (psi)	Vol. water content	M_R_Pred. (psi)	Error
OPTIMUM	21.7	1.0	15.0	51.7	35440.2	3.2	42.62	0.20	34666.7	598321.6
	24.7	2.0	15.0	54.7	35459.2	4.6	42.62	0.20	35139.9	101997.6
	29.8	3.0	15.0	59.8	36127.9	7.0	42.62	0.20	35908.0	48326.4
	14.7	4.0	10.0	34.7	28992.2	2.2	42.62	0.20	28277.7	510564.3
	16.7	5.0	10.0	36.7	28878.9	3.2	42.62	0.20	28798.4	6487.4
	19.7	6.0	10.0	39.7	28627.0	4.6	42.62	0.20	29544.1	841163.9
	24.8	7.0	10.0	44.8	29972.7	7.0	42.62	0.20	30708.6	541578.8
	7.7	8.0	5.0	17.7	21082.1	1.3	42.62	0.20	19852.9	1511048.9
	9.7	9.0	5.0	19.7	20685.5	2.2	42.62	0.20	20788.4	10600.9
	11.7	10.0	5.0	21.7	20869.8	3.2	42.62	0.20	21645.7	602046.3
	14.7	11.0	5.0	24.7	21620.7	4.6	42.62	0.20	22839.6	1485738.1
	4.7	12.0	2.0	8.7	14577.5	1.3	42.62	0.20	13414.3	1353035.0
	6.7	13.0	2.0	10.7	15120.1	2.2	42.62	0.20	14876.3	59457.4
	8.8	14.0	2.0	12.8	15963.4	3.2	42.62	0.20	16160.4	38796.2
FIELD	21.7	1.0	15.0	51.7	33651.7	3.2	468.93	0.07	34329.1	458847.8
	24.7	2.0	15.0	54.7	34683.5	4.6	468.93	0.07	34809.3	15830.9
	29.7	3.0	15.0	59.7	36370.9	6.9	468.93	0.07	35598.7	596442.2
	14.7	4.0	10.0	34.7	27117.8	2.2	468.93	0.07	27860.1	551020.4
	16.7	5.0	10.0	36.7	27950.9	3.2	468.93	0.07	28396.0	198097.1
	19.7	6.0	10.0	39.7	29166.6	4.6	468.93	0.07	29163.8	7.4
	24.7	7.0	10.0	44.7	31100.0	6.9	468.93	0.07	30353.2	557695.5
	7.7	8.0	5.0	17.7	18834.9	1.3	468.93	0.07	19269.4	188831.3
	9.7	9.0	5.0	19.7	19956.6	2.2	468.93	0.07	20231.9	75792.8
	11.7	10.0	5.0	21.7	21034.9	3.2	468.93	0.07	21129.6	8973.7
	14.7	11.0	5.0	24.7	22560.6	4.6	468.93	0.07	22357.5	41240.3
	4.7	12.0	2.0	8.7	12831.7	1.3	468.93	0.07	12603.3	52189.2
	6.7	13.0	2.0	10.7	14342.9	2.2	468.93	0.07	14126.1	46997.8
	8.7	14.0	2.0	12.7	15745.4	3.2	468.93	0.07	15479.0	70995.2
									SSE	10572124
									SEE	583.98

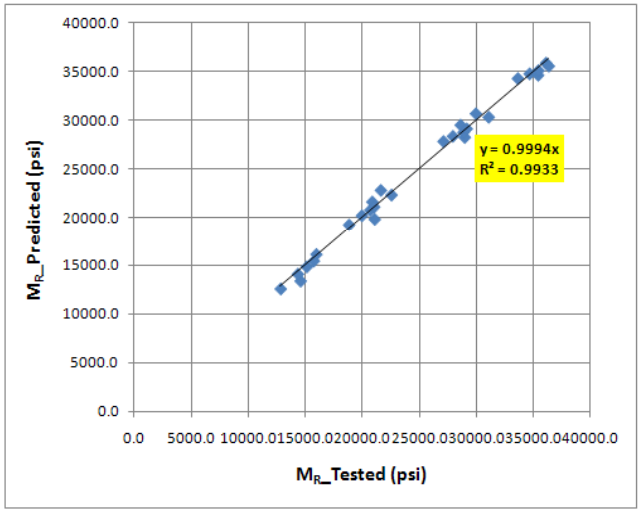

Figure D5. Resilient Modulus Properties of Subgrade Material on Section 12500000.

K1	1.68
K2	2.93
K3	-0.33
K4	4.01

$$M_R = K_1 P_a \left(\frac{\theta + 3K_4 SV_W}{P_a} \right)^{K_2} \left(\frac{\tau_{OCT}}{P_a} + 1 \right)^{K_3}$$

	Axial stress	Test sequence	Confining pressure (psi)	Bulk stress (psi)	M_R_Tested (psi)	Oct. shear stress (psi)	Soil suction (psi)	Vol. water content	M_R_Pred. (psi)	Error
OPTIMUM	21.7	1.0	15.0	51.7	40482.3	3.2	58.554	0.187	38611.3	3500407.6
	24.7	2.0	15.0	54.7	40525.6	4.6	58.554	0.187	39491.7	1069086.0
	29.7	3.0	15.0	59.7	41731.1	6.9	58.554	0.187	41084.1	418513.5
	14.7	4.0	10.0	34.7	33509.3	2.2	58.554	0.187	29559.4	15601477.6
	16.7	5.0	10.0	36.7	33086.7	3.2	58.554	0.187	30067.3	9116451.0
	19.7	6.0	10.0	39.7	33333.1	4.6	58.554	0.187	30887.5	5981013.0
	24.7	7.0	10.0	44.7	35022.8	6.9	58.554	0.187	32346.0	7165156.7
	7.7	8.0	5.0	17.7	24419.8	1.3	58.554	0.187	21964.5	6028487.6
	9.7	9.0	5.0	19.7	24470.4	2.2	58.554	0.187	22407.1	4257491.1
	11.8	10.0	5.0	21.8	24417.8	3.2	58.554	0.187	22881.6	2359858.2
	14.7	11.0	5.0	24.7	25388.5	4.6	58.554	0.187	23613.6	3150506.4
	4.7	12.0	2.0	8.7	17011.9	1.3	58.554	0.187	18302.7	1666108.8
	6.7	13.0	2.0	10.7	17576.4	2.2	58.554	0.187	18726.0	1321561.1
	8.7	14.0	2.0	12.7	18663.3	3.2	58.554	0.187	19163.6	250335.1
FIELD	21.7	1.0	15.0	51.7	30062.2	3.2	53.643	0.191	33538.3	12083420.2
	24.7	2.0	15.0	54.7	30935.0	4.6	53.643	0.191	34370.6	11803290.1
	29.7	3.0	15.0	59.7	32359.7	6.9	53.643	0.191	35897.7	12517432.1
	14.7	4.0	10.0	34.7	24500.2	2.2	53.643	0.191	25295.8	632983.5
	16.7	5.0	10.0	36.7	25213.0	3.2	53.643	0.191	25781.1	322700.4
	19.7	6.0	10.0	39.7	26251.1	4.6	53.643	0.191	26551.7	90389.0
	24.7	7.0	10.0	44.7	27897.5	6.9	53.643	0.191	27932.6	1231.3
	7.7	8.0	5.0	17.7	17344.2	1.3	53.643	0.191	18455.2	1234311.6
	9.7	9.0	5.0	19.7	18321.6	2.2	53.643	0.191	18873.1	304150.7
	11.7	10.0	5.0	21.7	19258.5	3.2	53.643	0.191	19312.6	2931.0
	14.7	11.0	5.0	24.7	20579.9	4.6	53.643	0.191	20000.4	335850.2
	4.7	12.0	2.0	8.7	12055.7	1.3	53.643	0.191	15208.6	9940993.8
	6.7	13.0	2.0	10.7	13397.2	2.2	53.643	0.191	15595.1	4831087.6
	8.7	14.0	2.0	12.7	14635.7	3.2	53.643	0.191	16002.4	1868026.8
									SSE	117855252
									SEE	1949.82

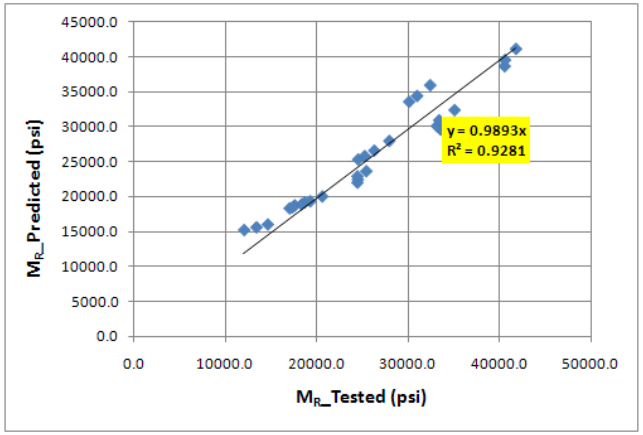

Figure D6. Resilient Modulus Properties of Embankment Material on Section 12500000.

K1	944.46
K2	0.76
K3	-0.39
K4	0.53

$$M_R = K_1 P_a \left(\frac{\theta + 3K_4 SV_W}{P_a} \right)^{K_2} \left(\frac{\tau_{OCT}}{P_a} + 1 \right)^{K_3}$$

	Axial stress	Test sequence	Confining pressure (psi)	Bulk stress (psi)	M_R_Tested (psi)	Oct. shear stress (psi)	Soil suction (psi)	Vol. water content	M_R_Pred. (psi)	Error
OPTIMUM	5.6	1.0	3.0	11.6	15585.3	1.2	21.96931	0.20	15984	159148.13
	8.2	2.0	3.0	14.2	15815.6	2.5	21.96931	0.20	17190	1889143
	11.0	3.0	3.0	17.0	17085.7	3.8	21.96931	0.20	18325	1536681.3
	9.5	4.0	5.0	19.5	20986.1	2.1	21.96931	0.20	20505	231484.39
	14.2	5.0	5.0	24.2	22029.9	4.3	21.96931	0.20	22087	3270.8081
	19.0	6.0	5.0	29.0	22641.3	6.6	21.96931	0.20	23565	853306.81
	19.2	7.0	10.0	39.2	31136.3	4.3	21.96931	0.20	29748	1927873
	28.8	8.0	10.0	48.8	31733.4	8.9	21.96931	0.20	31569	27052.357
	38.2	9.0	10.0	58.2	32423.6	13.3	21.96931	0.20	33206	612790.86
	24.2	10.0	15.0	54.2	37372.4	4.3	21.96931	0.20	36814	311882.69
	28.9	11.0	15.0	58.9	37225.6	6.5	21.96931	0.20	37290	4152.4585
	43.2	12.0	15.0	73.2	39252.9	13.3	21.96931	0.20	38851	161517.78
	33.9	13.0	20.0	73.9	44566.3	6.5	21.96931	0.20	43560	1011707.9
	38.6	14.0	20.0	78.6	44926.1	8.7	21.96931	0.20	43730	1430738
	57.4	15.0	20.0	97.4	46850.9	17.6	21.96931	0.20	44841	4041233.6
FIELD	5.6	1.0	3.0	11.6	22490	1.2	51.65864	0.16	19772	7391201.4
	8.2	2.0	3.0	14.2	20967	2.5	51.65864	0.16	20728	57114.276
	11.0	3.0	3.0	17.0	21349	3.8	51.65864	0.16	21677	107820.1
	9.4	4.0	5.0	19.4	25643	2.1	51.65864	0.16	23876	3125259
	14.0	5.0	5.0	24.0	25092	4.2	51.65864	0.16	25166	5381.2142
	18.6	6.0	5.0	28.6	25845	6.4	51.65864	0.16	26366	271187.72
	19.1	7.0	10.0	39.1	33300	4.3	51.65864	0.16	32592	501578.87
	28.3	8.0	10.0	48.3	33461	8.6	51.65864	0.16	34014	306387.24
	37.8	9.0	10.0	57.8	34007	13.1	51.65864	0.16	35421	1997971.1
	24.1	10.0	15.0	54.1	38382	4.3	51.65864	0.16	39494	1235270.3
	28.7	11.0	15.0	58.7	38125	6.5	51.65864	0.16	39804	2816223.7
	42.6	12.0	15.0	72.6	40407	13.0	51.65864	0.16	40964	310155.48
	33.7	13.0	20.0	73.7	44755	6.5	51.65864	0.16	45971	1478308.9
	38.3	14.0	20.0	78.3	45378	8.6	51.65864	0.16	46014	404795.24
	57.0	15.0	20.0	97.0	46991	17.4	51.65864	0.16	46743	61687.907
									SSE	34272325.4
									SEE	1068.8

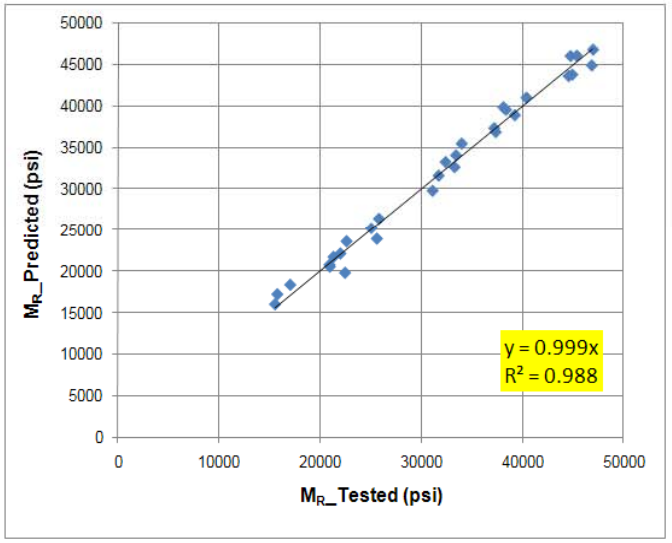

Figure D7. Resilient Modulus Properties of Base Material on Section 16003000.

K1	1223.20
K2	0.68
K3	-1.12
K4	0.06

$$M_R = K_1 P_a \left(\frac{\theta + 3K_4 SV_W}{P_a} \right)^{K_2} \left(\frac{\tau_{OCT}}{P_a} + 1 \right)^{K_3}$$

	Axial stress	Test sequence	Confining pressure (psi)	Bulk stress (psi)	M_R_Tested (psi)	Oct. shear stress (psi)	Soil suction (psi)	Vol. water content	M_R_Pred. (psi)	Error
OPTIMUM	7.9	1.0	6.0	19.9	21483.2	0.9	32.25257	0.17	21237	60550.574
	9.7	2.0	6.0	21.7	21295.4	1.7	32.25257	0.17	21161	18185.946
	11.6	3.0	6.0	23.6	21039.2	2.6	32.25257	0.17	21055	246.55025
	13.4	4.0	6.0	25.4	20959.3	3.5	32.25257	0.17	20930	880.54724
	15.2	5.0	6.0	27.2	21308.1	4.3	32.25257	0.17	20791	267160.78
	5.9	6.0	4.0	13.9	17282.0	0.9	32.25257	0.17	16831	203637.25
	7.7	7.0	4.0	15.7	16716.3	1.7	32.25257	0.17	17143	181862.66
	9.6	8.0	4.0	17.6	16945.8	2.6	32.25257	0.17	17374	183162.37
	11.4	9.0	4.0	19.4	17571.1	3.5	32.25257	0.17	17538	1117.7173
	13.2	10.0	4.0	21.2	18347.3	4.3	32.25257	0.17	17648	488564.59
	3.9	11.0	2.0	7.9	12149.6	0.9	32.25257	0.17	11784	133806.17
	5.7	12.0	2.0	9.7	12151.6	1.7	32.25257	0.17	12618	217409.47
	7.5	13.0	2.0	11.5	12595.9	2.6	32.25257	0.17	13281	469730.37
	9.4	14.0	2.0	13.4	13723.3	3.5	32.25257	0.17	13804	6472.6331
	11.2	15.0	2.0	15.2	14565.1	4.3	32.25257	0.17	14219	119498.45
FIELD	7.9	1.0	6.0	19.9	21920.0	0.9	65.4312	0.14	21675	60129.876
	9.7	2.0	6.0	21.7	21555.2	1.7	65.4312	0.14	21563	60.978384
	11.5	3.0	6.0	23.5	21082.8	2.6	65.4312	0.14	21427	118596.53
	13.4	4.0	6.0	25.4	20899.6	3.5	65.4312	0.14	21273	139572.47
	15.2	5.0	6.0	27.2	21197.0	4.3	65.4312	0.14	21109	7724.9762
	5.8	6.0	4.0	13.8	17618.3	0.9	65.4312	0.14	17309	95594.225
	7.6	7.0	4.0	15.6	16988.3	1.7	65.4312	0.14	17573	341740.35
	9.5	8.0	4.0	17.5	17054.2	2.6	65.4312	0.14	17768	508927.48
	11.3	9.0	4.0	19.3	17534.3	3.5	65.4312	0.14	17903	135852.91
	13.2	10.0	4.0	21.2	18194.8	4.3	65.4312	0.14	17988	42687.955
	3.8	11.0	2.0	7.8	13291.4	0.8	65.4312	0.14	12328	927660.07
	5.6	12.0	2.0	9.6	13015.9	1.7	65.4312	0.14	13082	4413.8188
	7.4	13.0	2.0	11.4	13269.5	2.6	65.4312	0.14	13697	182699.77
	9.3	14.0	2.0	13.3	14198.7	3.4	65.4312	0.14	14190	83.493647
	11.1	15.0	2.0	15.1	14953.8	4.3	65.4312	0.14	14576	142799.18
									SSE	5060830.2
									SEE	410.7

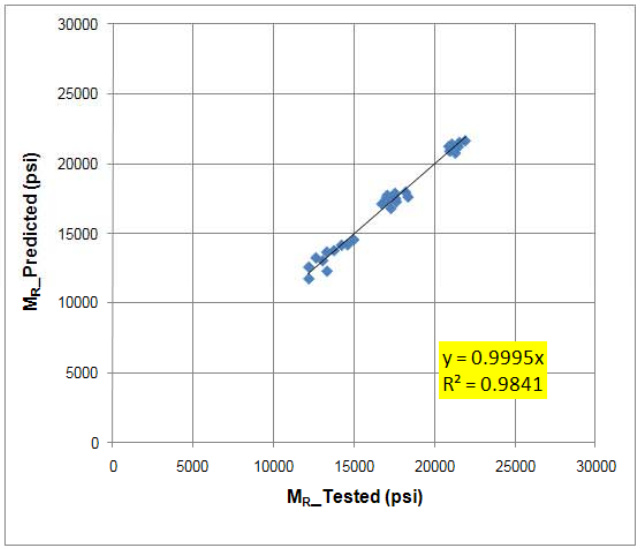

Figure D8. Resilient Modulus Properties of Subgrade Material on Section 16003000.

K1	1175.54
K2	0.71
K3	-1.53
K4	5.19

$$M_R = K_1 P_a \left(\frac{I_1 + 3K_4 S\theta_W}{P_a} \right)^{K_2} \left(\frac{\tau_{OCT}}{P_a} + 1 \right)^{K_3}$$

	Axial stress	Test sequence	Confining pressure (psi)	Bulk stress (psi)	M_R_Tested (psi)	Oct. shear stress (psi)	Soil suction (psi)	Vol. water content	M_R_Pred. (psi)	Error
OPTIMUM	7.9	1.0	6	19.8905	19856	0.9	0.01	0.20	19492	132306.67
	9.7	2.0	6	21.7054	19023	1.7	0.01	0.20	19086	3939.779
	11.5	3.0	6	23.513	18236	2.6	0.01	0.20	18677	194431.8
	13.3	4.0	6	25.3233	17857	3.5	0.01	0.20	18269	169875.61
	15.1	5.0	6	27.1469	18106	4.3	0.01	0.20	17864	58816.404
	5.9	6.0	4	13.8818	15779	0.9	0.01	0.20	15111	446789.03
	7.7	7.0	4	15.7049	14811	1.7	0.01	0.20	15173	130637.71
	9.5	8.0	4	17.5287	14593	2.6	0.01	0.20	15155	315812.82
	11.3	9.0	4	19.3383	15032	3.5	0.01	0.20	15079	2213.9118
	13.1	10.0	4	21.1186	15408	4.3	0.01	0.20	14965	195912.77
	3.8	11.0	2	7.83997	11033	0.9	0.01	0.20	10102	865944.45
	5.6	12.0	2	9.63605	10553	1.7	0.01	0.20	10767	45866.26
	7.4	13.0	2	11.4281	10780	2.6	0.01	0.20	11239	210529.61
	9.2	14.0	2	13.1743	11314	3.4	0.01	0.20	11563	62124.287
	11.0	15.0	2	14.9863	11912	4.2	0.01	0.20	11794	14058.425
FIELD	7.9	1.0	6.0	19.8529	20686	0.9	0.77	0.16	20801	13211.357
	9.7	2.0	6.0	21.6891	20225	1.7	0.77	0.16	20256	984.05356
	11.5	3.0	6.0	23.5278	19726	2.6	0.77	0.16	19727	0.9125285
	13.4	4.0	6.0	25.392	19322	3.5	0.77	0.16	19208	13079.187
	15.3	5.0	6.0	27.2917	19472	4.4	0.77	0.16	18700	595982.54
	5.8	6.0	4.0	13.8131	16672	0.9	0.77	0.16	16545	16225.15
	7.6	7.0	4.0	15.647	15935	1.7	0.77	0.16	16451	266381.61
	9.5	8.0	4.0	17.4742	15792	2.6	0.77	0.16	16302	259583.87
	11.4	9.0	4.0	19.3532	16079	3.5	0.77	0.16	16109	930.24704
	13.2	10.0	4.0	21.1919	16456	4.3	0.77	0.16	15895	314426.31
	3.8	11.0	2.0	7.76504	12530	0.8	0.77	0.16	11749	610540.71
	5.5	12.0	2.0	9.51894	12005	1.7	0.77	0.16	12199	38003.526
	7.4	13.0	2.0	11.3631	12012	2.5	0.77	0.16	12518	256106.72
	9.2	14.0	2.0	13.1708	12592	3.4	0.77	0.16	12716	15450.432
	10.9	15.0	2.0	14.9129	12583	4.2	0.77	0.16	12827	59749.635
									SSE	5309915.8
									SEE	420.7

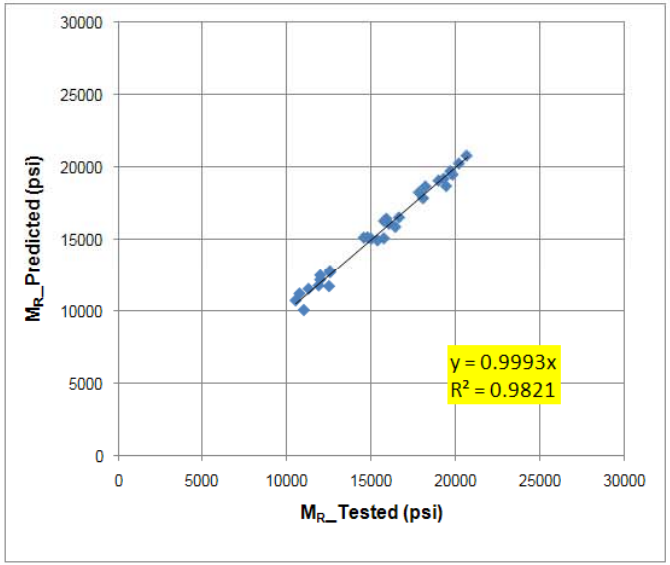

Figure D9. Resilient Modulus Properties of Embankment Material on Section 16003000.

K1	1545.30
K2	0.46
K3	-0.29
K4	-11.93

$$M_R = K_1 P_a \left(\frac{\theta + 3K_4 SV_W}{P_a} \right)^{K_2} \left(\frac{\tau_{OCT}}{P_a} + 1 \right)^{K_3}$$

	Axial stress	Test sequence	Confining pressure (psi)	Bulk stress (psi)	M_R_Tested (psi)	Oct. shear stress (psi)	Soil suction (psi)	Vol. water content	M_R_Pred. (psi)	Error
OPTIMUM	21.7	1.0	15.0	51.7	41288.8	3.2	0.35	0.20	37139.1	17220463.0
	24.7	2.0	15.0	54.7	40917.1	4.6	0.35	0.20	37323.8	12911959.5
	29.7	3.0	15.0	59.7	41250.0	6.9	0.35	0.20	37640.9	13025276.2
	14.7	4.0	10.0	34.7	33459.4	2.2	0.35	0.20	31026.9	5917177.9
	16.7	5.0	10.0	36.7	32590.9	3.2	0.35	0.20	31399.9	1418419.2
	19.7	6.0	10.0	39.7	32376.7	4.6	0.35	0.20	31923.1	205736.3
	24.8	7.0	10.0	44.8	34068.7	7.0	0.35	0.20	32715.9	1830174.6
	7.7	8.0	5.0	17.7	24568.5	1.3	0.35	0.20	22292.6	5179714.3
	9.7	9.0	5.0	19.7	24008.9	2.2	0.35	0.20	23222.3	618679.2
	11.7	10.0	5.0	21.7	23849.7	3.2	0.35	0.20	24044.8	38075.2
	14.8	11.0	5.0	24.8	24849.0	4.6	0.35	0.20	25159.5	96396.2
	4.7	12.0	2.0	8.7	16950.7	1.3	0.35	0.20	14709.8	5021684.6
	6.7	13.0	2.0	10.7	17307.3	2.2	0.35	0.20	16480.5	683590.1
	8.8	14.0	2.0	12.8	18239.7	3.2	0.35	0.20	17973.4	70874.0
FIELD	21.7	1.0	15.0	51.7	32154.4	3.2	1.16	0.16	35717.4	12694895.5
	24.7	2.0	15.0	54.7	33171.1	4.6	1.16	0.16	35977.3	7874952.0
	29.7	3.0	15.0	59.7	34836.0	6.9	1.16	0.16	36405.0	2461758.1
	14.7	4.0	10.0	34.7	25739.2	2.2	1.16	0.16	29187.4	11890014.8
	16.7	5.0	10.0	36.7	26554.8	3.2	1.16	0.16	29649.5	9577744.3
	19.7	6.0	10.0	39.7	27746.1	4.6	1.16	0.16	30291.8	6480816.6
	24.7	7.0	10.0	44.7	29644.0	6.9	1.16	0.16	31245.3	2564013.1
	7.7	8.0	5.0	17.7	17677.4	1.3	1.16	0.16	19360.8	2833691.2
	9.7	9.0	5.0	19.7	18763.7	2.2	1.16	0.16	20541.9	3162128.5
	11.7	10.0	5.0	21.7	19809.7	3.2	1.16	0.16	21588.4	3163982.9
	14.7	11.0	5.0	24.7	21292.5	4.6	1.16	0.16	22945.2	2731373.4
	4.7	12.0	2.0	8.7	11901.5	1.3	1.16	0.16	9062.7	8058535.6
	6.7	13.0	2.0	10.7	13348.8	2.2	1.16	0.16	12058.8	1664107.5
	8.7	14.0	2.0	12.7	14696.4	3.2	1.16	0.16	14247.8	201215.7
									SSE	139597449.5
									SEE	2122.06

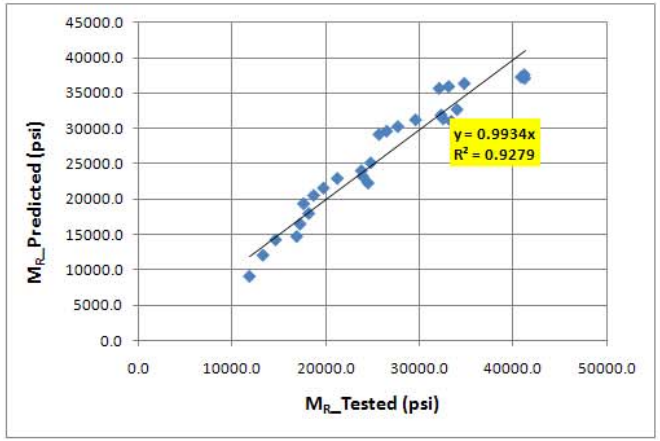

Figure D10. Resilient Modulus Properties of Subgrade Material on Section 26060000.

K1	28.04
K2	2.35
K3	-1.14
K4	24.38

$$M_R = K_1 P_a \left(\frac{\theta + 3K_4 SV_W}{P_a} \right)^{K_2} \left(\frac{\tau_{OCT}}{P_a} + 1 \right)^{K_3}$$

	Axial stress	Test sequence	Confining pressure (psi)	Bulk stress (psi)	M_R_Tested (psi)	Oct. shear stress (psi)	Soil suction (psi)	Vol. water content	M_R_Pred. (psi)	Error
OPTIMUM	5.6	1.0	3.0	11.6	15414.8	1.2	3.60	0.23	15387.7	736.2
	8.2	2.0	3.0	14.0	15288.1	2.5	3.60	0.23	15231.5	3202.3
	11.0	3.0	3.0	16.7	16238.2	3.8	3.60	0.23	15204.7	1068165.9
	9.5	4.0	5.0	19.4	19639.2	2.1	3.60	0.23	18394.4	1549688.5
	14.2	5.0	5.0	23.8	20434.7	4.3	3.60	0.23	18102.0	5441405.8
	19.0	6.0	5.0	28.4	21125.1	6.6	3.60	0.23	18055.4	9423190.5
	19.2	7.0	10.0	39.0	28657.5	4.3	3.60	0.23	26852.8	3256748.8
	28.8	8.0	10.0	48.2	29863.5	8.9	3.60	0.23	25883.5	15840985.2
	38.2	9.0	10.0	57.4	30799.3	13.3	3.60	0.23	25718.0	25819308.7
	24.2	10.0	15.0	54.1	34379.1	4.3	3.60	0.23	37553.1	10074007.2
	28.9	11.0	15.0	58.5	34722.1	6.5	3.60	0.23	36214.2	2226476.9
	43.2	12.0	15.0	72.3	37264.9	13.3	3.60	0.23	34120.5	9887754.4
	33.9	13.0	20.0	73.6	40815.6	6.5	3.60	0.23	48024.7	51971068.4
	38.6	14.0	20.0	78.2	41961.2	8.7	3.60	0.23	46389.6	19610522.8
	57.4	15.0	20.0	96.3	45137.7	17.6	3.60	0.23	42812.7	5405857.4
FIELD	29.9	1.0	20.0	69.9	76218.2	4.7	5.24	0.21	72061.8	17275976.8
	39.9	2.0	20.0	79.9	64886.6	9.4	5.24	0.21	65126.3	57453.3
	49.9	3.0	20.0	89.9	58427.5	14.1	5.24	0.21	61045.8	6855786.6
	24.9	4.0	15.0	54.9	57426.5	4.7	5.24	0.21	56364.6	1127738.6
	34.9	5.0	15.0	64.9	51226.9	9.4	5.24	0.21	51776.9	302455.3
	44.9	6.0	15.0	74.9	49412.2	14.1	5.24	0.21	49214.4	39153.8
	14.9	7.0	10.0	34.9	53250.5	2.3	5.24	0.21	45115.6	66177178.9
	19.9	8.0	10.0	39.9	43658.2	4.7	5.24	0.21	42854.1	646562.2
	29.9	9.0	10.0	49.9	40159.9	9.4	5.24	0.21	40146.9	168.5
	39.9	10.0	10.0	59.9	40067.3	14.1	5.24	0.21	38824.0	1545601.7
	9.9	11.0	5.0	19.9	32369.5	2.3	5.24	0.21	32602.6	54335.9
	14.9	12.0	5.0	24.9	27672.2	4.7	5.24	0.21	31416.6	14020516.7
	19.9	13.0	5.0	29.9	27823.6	7.0	5.24	0.21	30657.5	8030731.3
	7.9	14.0	3.0	13.9	25297.3	2.3	5.24	0.21	28240.2	8660636.5
	9.9	15.0	3.0	15.9	23789.7	3.2	5.24	0.21	27857.0	16542702.2
	11.9	16.0	3.0	17.9	23599.8	4.2	5.24	0.21	27543.0	15549084.2
									SSE	318465202
									SEE	3205.16

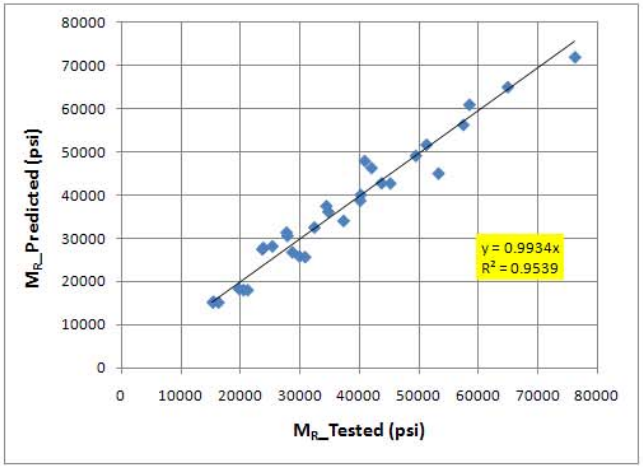

Figure D11. Resilient Modulus Properties of Base Material on Section 71020000.

K1	840.70
K2	0.60
K3	-0.19
K4	0.40

$$M_R = K_1 P_a \left(\frac{\theta + 3K_4 SV_W}{P_a} \right)^{K_2} \left(\frac{\tau_{OCT}}{P_a} + 1 \right)^{K_3}$$

	Axial stress	Test sequence	Confining pressure (psi)	Bulk stress (psi)	M_R_Tested (psi)	Oct. shear stress (psi)	Soil suction (psi)	Vol. water content	M_R_Pred. (psi)	Error
OPTIMUM	21.7	1.0	15.0	51.7	24898.0	3.2	1.77	0.23	25434.0	287264.1
	24.7	2.0	15.0	54.7	24850.3	4.6	1.77	0.23	25920.3	1145024.4
	29.8	3.0	15.0	59.8	25810.2	7.0	1.77	0.23	26706.4	803260.9
	14.7	4.0	10.0	34.7	20601.0	2.2	1.77	0.23	20262.6	114541.4
	16.7	5.0	10.0	36.7	20298.2	3.2	1.77	0.23	20733.3	189291.1
	19.7	6.0	10.0	39.7	20479.2	4.6	1.77	0.23	21400.3	848331.4
	24.7	7.0	10.0	44.7	21558.5	6.9	1.77	0.23	22459.6	812039.2
	7.7	8.0	5.0	17.7	15116.7	1.3	1.77	0.23	13758.1	1845716.2
	9.7	9.0	5.0	19.7	14953.6	2.2	1.77	0.23	14489.9	215053.8
	11.7	10.0	5.0	21.7	14941.3	3.2	1.77	0.23	15183.8	58808.9
	14.7	11.0	5.0	24.7	15420.2	4.6	1.77	0.23	16149.0	531173.7
	4.7	12.0	2.0	8.7	10501.5	1.3	1.77	0.23	9110.2	1935689.4
	6.7	13.0	2.0	10.7	10683.5	2.2	1.77	0.23	10153.6	280766.6
	8.7	14.0	2.0	12.7	11120.8	3.2	1.77	0.23	11097.3	553.2
FIELD	21.7	1.0	15.0	51.7	26616.2	3.2	16.87	0.18	26350.5	70589.4
	24.7	2.0	15.0	54.7	27454.1	4.6	16.87	0.18	26795.8	433403.7
	29.7	3.0	15.0	59.7	28826.0	6.9	16.87	0.18	27533.4	1670988.8
	14.7	4.0	10.0	34.7	21326.4	2.2	16.87	0.18	21338.6	148.6
	16.7	5.0	10.0	36.7	21999.1	3.2	16.87	0.18	21770.0	52500.3
	19.7	6.0	10.0	39.7	22981.7	4.6	16.87	0.18	22397.2	341665.6
	24.7	7.0	10.0	44.7	24546.8	6.9	16.87	0.18	23388.8	1340963.6
	7.7	8.0	5.0	17.7	14670.4	1.3	16.87	0.18	15148.8	228820.2
	9.7	9.0	5.0	19.7	15567.9	2.2	16.87	0.18	15810.6	58899.1
	11.7	10.0	5.0	21.7	16431.9	3.2	16.87	0.18	16442.9	120.8
	14.7	11.0	5.0	24.7	17656.4	4.6	16.87	0.18	17330.4	106255.2
	4.7	12.0	2.0	8.7	9893.8	1.3	16.87	0.18	10888.4	989329.0
	6.7	13.0	2.0	10.7	11091.5	2.2	16.87	0.18	11783.0	478118.9
	8.7	14.0	2.0	12.7	12206.2	3.2	16.87	0.18	12619.5	170838.4
									SSE	15010156.1
									SEE	695.84

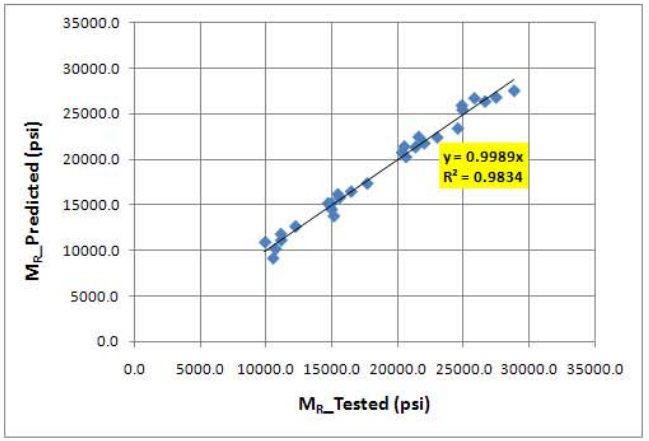

Figure D12. Resilient Modulus Properties of Subgrade Material on Section 71020000.

K1	1123.84
K2	0.55
K3	-0.20
K4	0.81

$$M_R = K_1 P_a \left(\frac{\theta + 3K_4 SV_W}{P_a} \right)^{K_2} \left(\frac{\tau_{OCT}}{P_a} + 1 \right)^{K_3}$$

	Axial stress	Test sequence	Confining pressure (psi)	Bulk stress (psi)	M_R_Tested (psi)	Oct. shear stress (psi)	Soil suction (psi)	Vol. water content	M_R_Pred. (psi)	Error
OPTIMUM	21.7	1.0	15.0	51.7	32106.8	3.2	3.21	0.20	32004.8	10400.0
	24.7	2.0	15.0	54.7	31824.0	4.6	3.21	0.20	32469.3	416539.8
	29.8	3.0	15.0	59.8	32907.3	7.0	3.21	0.20	33223.8	100229.6
	14.7	4.0	10.0	34.7	26891.9	2.2	3.21	0.20	26208.1	467592.7
	16.7	5.0	10.0	36.7	26498.4	3.2	3.21	0.20	26694.3	38370.9
	19.8	6.0	10.0	39.8	26283.1	4.6	3.21	0.20	27390.7	1226647.0
	24.7	7.0	10.0	44.7	27753.4	7.0	3.21	0.20	28477.5	524316.9
	7.7	8.0	5.0	17.7	20080.1	1.3	3.21	0.20	18736.2	1805902.7
	9.7	9.0	5.0	19.7	19841.0	2.2	3.21	0.20	19552.4	83298.9
	11.7	10.0	5.0	21.7	19716.9	3.2	3.21	0.20	20317.8	361136.0
	14.8	11.0	5.0	24.8	20578.9	4.6	3.21	0.20	21384.1	648462.9
	4.7	12.0	2.0	8.7	14269.8	1.3	3.21	0.20	13270.7	998107.1
	6.7	13.0	2.0	10.7	14537.4	2.2	3.21	0.20	14454.8	6822.1
	8.7	14.0	2.0	12.7	15507.7	3.2	3.21	0.20	15546.3	1490.1
FIELD	21.7	1.0	15.0	51.7	32233.9	3.2	8.55	0.15	32481.8	61475.2
	24.7	2.0	15.0	54.7	33122.0	4.6	8.55	0.15	32920.4	40631.6
	29.7	3.0	15.0	59.7	34569.0	6.9	8.55	0.15	33648.5	847286.1
	14.7	4.0	10.0	34.7	26541.8	2.2	8.55	0.15	26778.7	56161.7
	16.7	5.0	10.0	36.7	27274.6	3.2	8.55	0.15	27240.8	1139.5
	19.7	6.0	10.0	39.7	28339.9	4.6	8.55	0.15	27909.5	185249.9
	24.7	7.0	10.0	44.7	30025.4	6.9	8.55	0.15	28959.8	1135414.1
	7.7	8.0	5.0	17.7	19118.7	1.3	8.55	0.15	19502.5	147288.0
	9.7	9.0	5.0	19.7	20140.5	2.2	8.55	0.15	20270.7	16947.8
	11.7	10.0	5.0	21.7	21117.4	3.2	8.55	0.15	20998.6	14121.3
	14.7	11.0	5.0	24.7	22491.1	4.6	8.55	0.15	22010.7	230811.0
	4.7	12.0	2.0	8.7	13534.4	1.3	8.55	0.15	14273.5	546191.8
	6.7	13.0	2.0	10.7	14960.9	2.2	8.55	0.15	15371.2	168318.0
	8.7	14.0	2.0	12.7	16271.4	3.2	8.55	0.15	16383.8	12615.5
									SSE	10152968.3
									SEE	572.29

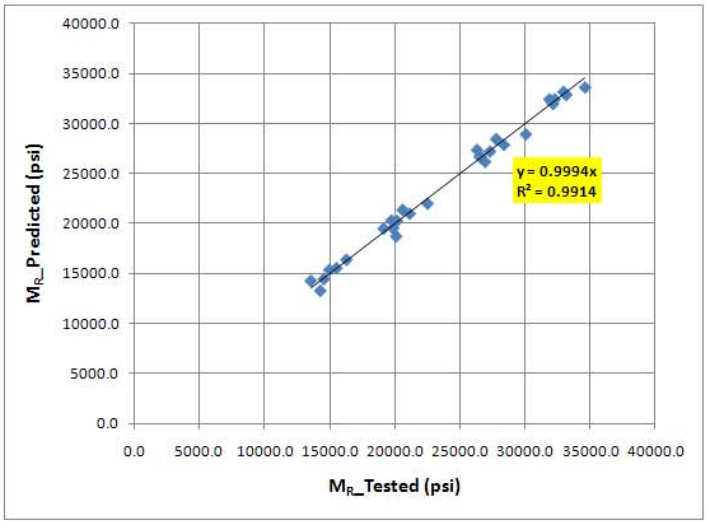

Figure D13. Resilient Modulus Properties of Embankment Material on Section 71020000.

K1	943.95
K2	0.76
K3	-0.34
K4	13.52

$$M_R = K_1 P_a \left(\frac{\theta + 3K_4 SV_W}{P_a} \right)^{K_2} \left(\frac{\tau_{OCT}}{P_a} + 1 \right)^{K_3}$$

	Axial stress	Test sequence	Confining pressure (psi)	Bulk stress (psi)	M_R_Tested (psi)	Oct. shear stress (psi)	Soil suction (psi)	Vol. water content	M_R_Pred. (psi)	Error
OPTIMUM	5.6	1.0	3.0	11.6	14866	1.2	0.45914	0.20011	13875	982752.96
	8.3	2.0	3.0	14.3	15679	2.5	0.45914	0.20011	15285	154902.82
	11.2	3.0	3.0	17.2	16793	3.9	0.45914	0.20011	16702	8371.2291
	9.5	4.0	5.0	19.5	19365	2.1	0.45914	0.20011	18686	460143.13
	14.3	5.0	5.0	24.3	21442	4.4	0.45914	0.20011	20652	624797.39
	19.5	6.0	5.0	29.5	20591	6.8	0.45914	0.20011	22557	3864719.6
	19.3	7.0	10.0	39.3	28108	4.4	0.45914	0.20011	28645	287645.94
	29.1	8.0	10.0	49.1	30319	9.0	0.45914	0.20011	31099	608673.39
	38.4	9.0	10.0	58.4	31311	13.4	0.45914	0.20011	33197	3558580.9
	24.3	10.0	15.0	54.3	33912	4.4	0.45914	0.20011	35979	4273036
	29.1	11.0	15.0	59.1	35815	6.6	0.45914	0.20011	36774	919398.91
	43.3	12.0	15.0	73.3	39650	13.3	0.45914	0.20011	39115	285939.64
	34.1	13.0	20.0	74.1	42864	6.6	0.45914	0.20011	43297	187141.75
	38.9	14.0	20.0	78.9	45146	8.9	0.45914	0.20011	43775	1881556.2
	57.4	15.0	20.0	97.4	48210	17.6	0.45914	0.20011	45844	5599052.4
FIELD	6.0	1.0	3.0	12.0	14191.0	1.4	0.09855	0.24179	12150	4167431.7
	9.1	2.0	3.0	15.1	14222.4	2.9	0.09855	0.24179	13916	94205.973
	12.3	3.0	3.0	18.3	15261.1	4.4	0.09855	0.24179	15556	87109.24
	10.1	4.0	5.0	20.1	18907.9	2.4	0.09855	0.24179	17259	2718137.7
	15.4	5.0	5.0	25.4	19812.8	4.9	0.09855	0.24179	19550	68977.754
	21.5	6.0	5.0	31.5	20571.1	7.8	0.09855	0.24179	21837	1603220.2
	20.4	7.0	10.0	40.4	28834.9	4.9	0.09855	0.24179	27556	1634898.6
	31.2	8.0	10.0	51.2	29946.4	10.0	0.09855	0.24179	30375	183520.28
	41.2	9.0	10.0	61.2	31041.4	14.7	0.09855	0.24179	32694	2732183.1
	25.5	10.0	15.0	55.5	35449.6	5.0	0.09855	0.24179	34897	305851.93
	30.9	11.0	15.0	60.9	35643.9	7.5	0.09855	0.24179	35869	50751.872
	45.6	12.0	15.0	75.6	37713.6	14.4	0.09855	0.24179	38449	540466.41
	35.7	13.0	20.0	75.7	42599.5	7.4	0.09855	0.24179	42301	89280.689
	40.7	14.0	20.0	80.7	43376.5	9.8	0.09855	0.24179	42870	256395.21
	60.2	15.0	20.0	100.2	45660.6	18.9	0.09855	0.24179	45234	182164.09
									SSE	38411307.0
									SEE	1131.5

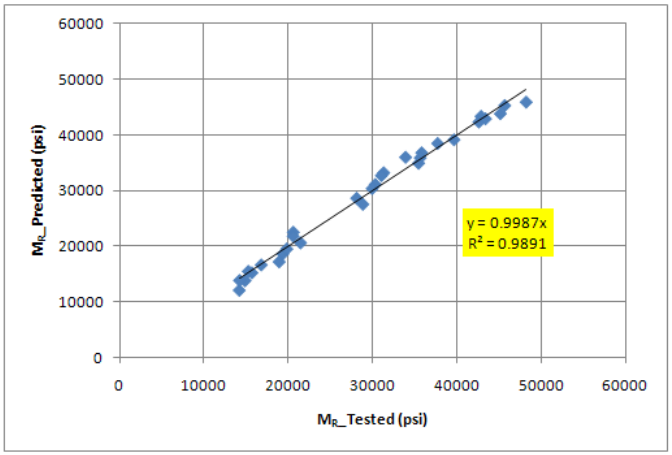

Figure D14. Resilient Modulus Properties of Base Material on Section 26005000.

K1	286.12
K2	1.45
K3	-0.77
K4	31.19

$$M_R = K_1 P_a \left(\frac{\theta + 3K_4 SV_W}{P_a} \right)^{K_2} \left(\frac{\tau_{OCT}}{P_a} + 1 \right)^{K_3}$$

	Axial stress	Test sequence	Confining pressure (psi)	Bulk stress (psi)	M_R_Tested (psi)	Oct. shear stress (psi)	Soil suction (psi)	Vol. water content	M_R_Pred. (psi)	Error
OPTIMUM	7.9	1.0	6.0	19.9	14554.2	0.9	0.99275	0.16442	14265	83808.411
	9.8	2.0	6.0	21.8	14626.5	1.8	0.99275	0.16442	14744	13861.481
	11.7	3.0	6.0	23.7	14828.3	2.7	0.99275	0.16442	15217	151173.55
	13.6	4.0	6.0	25.6	15184.7	3.6	0.99275	0.16442	15686	251716.68
	15.8	5.0	6.0	27.8	15692.8	4.6	0.99275	0.16442	16199	256564.04
	5.8	6.0	4.0	13.8	11372.0	0.9	0.99275	0.16442	10872	249623.34
	7.7	7.0	4.0	15.7	12090.1	1.8	0.99275	0.16442	11405	469613.51
	9.7	8.0	4.0	17.7	12658.4	2.7	0.99275	0.16442	11942	513106.7
	11.6	9.0	4.0	19.6	13426.2	3.6	0.99275	0.16442	12471	913186.53
	13.9	10.0	4.0	21.9	13583.5	4.6	0.99275	0.16442	13058	276516.88
	3.8	11.0	2.0	7.8	7687.8	0.9	0.99275	0.16442	7780	8435.073
	5.7	12.0	2.0	9.7	8100.3	1.7	0.99275	0.16442	8341	57964.671
	7.6	13.0	2.0	11.6	8772.3	2.6	0.99275	0.16442	8912	19413.689
	9.7	14.0	2.0	13.7	8415.8	3.6	0.99275	0.16442	9523	1226095.3
	11.9	15.0	2.0	15.9	9219.4	4.7	0.99275	0.16442	10137	842636.92
FIELD	7.9	1.0	6.0	19.9	17776.4	0.9	1.57482	0.14572	18041	70016.838
	9.7	2.0	6.0	21.7	17999.5	1.8	1.57482	0.14572	18428	183353.31
	11.6	3.0	6.0	23.6	18672.0	2.6	1.57482	0.14572	18812	19711.503
	13.5	4.0	6.0	25.5	19160.4	3.5	1.57482	0.14572	19199	1478.1734
	15.3	5.0	6.0	27.3	19673.2	4.4	1.57482	0.14572	19585	7701.9112
	5.9	6.0	4.0	13.9	14686.0	0.9	1.57482	0.14572	14378	94641.575
	7.7	7.0	4.0	15.7	14695.9	1.8	1.57482	0.14572	14845	22206.601
	9.6	8.0	4.0	17.6	15242.4	2.6	1.57482	0.14572	15308	4285.2161
	11.5	9.0	4.0	19.5	16197.8	3.5	1.57482	0.14572	15761	190775.38
	13.4	10.0	4.0	21.4	16998.0	4.4	1.57482	0.14572	16205	628422.05
	3.8	11.0	2.0	7.8	10882.4	0.9	1.57482	0.14572	10975	8597.5119
	5.7	12.0	2.0	9.7	11163.3	1.8	1.57482	0.14572	11506	117605.71
	7.6	13.0	2.0	11.6	11868.1	2.7	1.57482	0.14572	12032	26743.312
	9.4	14.0	2.0	13.4	12822.1	3.5	1.57482	0.14572	12497	105521.05
	11.2	15.0	2.0	15.2	12928.1	4.4	1.57482	0.14572	12998	4895.7241
									SSE	6819672.7
									SEE	476.8

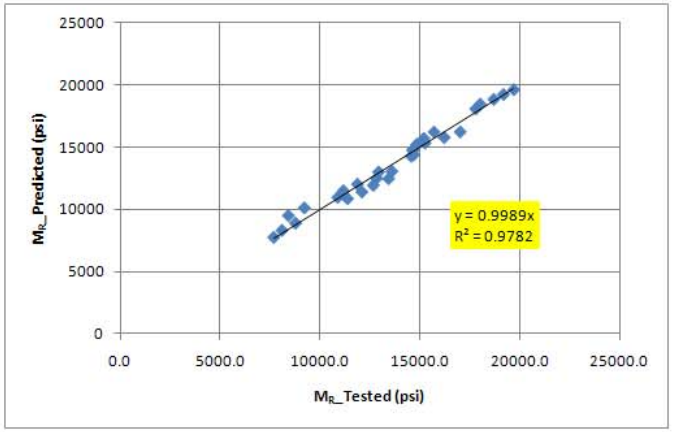

Figure D15. Resilient Modulus Properties of Subgrade Material on Section 26005000.

K1	299.60
K2	1.34
K3	-1.19
K4	18.12

$$M_R = K_1 P_a \left(\frac{\theta + 3K_4 SV_W}{P_a} \right)^{K_2} \left(\frac{\tau_{OCT}}{P_a} + 1 \right)^{K_3}$$

	Axial stress	Test sequence	Confining pressure (psi)	Bulk stress (psi)	M_R_Tested (psi)	Oct. shear stress (psi)	Soil suction (psi)	Vol. water content	M_R_Pred. (psi)	Error
OPTIMUM	7.8	1.0	6.0	19.81143	14702.2	0.9	1.6571	0.18749	14140	315815.77
	9.7	2.0	6.0	21.6524	14622.8	1.7	1.6571	0.18749	14142	230676.14
	11.7	3.0	6.0	23.69337	14293.4	2.7	1.6571	0.18749	14151	20336.769
	13.7	4.0	6.0	25.68602	13946.2	3.6	1.6571	0.18749	14164	47292.215
	15.6	5.0	6.0	27.59691	14247.1	4.5	1.6571	0.18749	14179	4575.6153
	5.8	6.0	4.0	13.76187	10752.7	0.8	1.6571	0.18749	11119	134445.61
	7.6	7.0	4.0	15.6231	10390.7	1.7	1.6571	0.18749	11263	760500.73
	9.7	8.0	4.0	17.73687	10700.1	2.7	1.6571	0.18749	11415	511491.72
	11.7	9.0	4.0	19.71006	11470.3	3.6	1.6571	0.18749	11549	6199.8622
	13.5	10.0	4.0	21.54297	12175.6	4.5	1.6571	0.18749	11667	259051.18
	3.7	11.0	2.0	7.691534	7804.7	0.8	1.6571	0.18749	8286	231703.22
	5.6	12.0	2.0	9.639577	7824.7	1.7	1.6571	0.18749	8563	545818.52
	7.8	13.0	2.0	11.77672	8479.4	2.7	1.6571	0.18749	8844	132725.34
	9.7	14.0	2.0	13.65506	9473.4	3.6	1.6571	0.18749	9072	161176.61
	11.5	15.0	2.0	15.51567	11124.9	4.5	1.6571	0.18749	9283	3391521.1
FIELD	7.8	1.0	6.0	19.84	13403.5	0.9	1.3247	0.19348	12632	595074.63
	9.7	2.0	6.0	21.72	13084.6	1.8	1.3247	0.19348	12706	142997.59
	11.7	3.0	6.0	23.71	12452.5	2.7	1.3247	0.19348	12783	109468.21
	13.5	4.0	6.0	25.55	12313.8	3.6	1.3247	0.19348	12853	290421.32
	15.3	5.0	6.0	27.34	12477.1	4.4	1.3247	0.19348	12918	194718.25
	5.8	6.0	4.0	13.82	9858.5	0.9	1.3247	0.19348	9709	22438.844
	7.8	7.0	4.0	15.80	9536.9	1.8	1.3247	0.19348	9927	152011.51
	9.7	8.0	4.0	17.72	9688.6	2.7	1.3247	0.19348	10124	189396.89
	11.5	9.0	4.0	19.52	10095.6	3.5	1.3247	0.19348	10296	40111.823
	13.3	10.0	4.0	21.26	10254.1	4.4	1.3247	0.19348	10452	39271.271
	3.8	11.0	2.0	7.80	7749.1	0.8	1.3247	0.19348	6994	570500.57
	5.8	12.0	2.0	9.79	7381.6	1.8	1.3247	0.19348	7330	2659.6818
	7.7	13.0	2.0	11.68	7681.0	2.7	1.3247	0.19348	7625	3130.4837
	9.4	14.0	2.0	13.43	7992.7	3.5	1.3247	0.19348	7880	12765.453
	11.1	15.0	2.0	15.12	8293.4	4.3	1.3247	0.19348	8111	33376.247
									SSE	9151673.2
									SEE	552.3

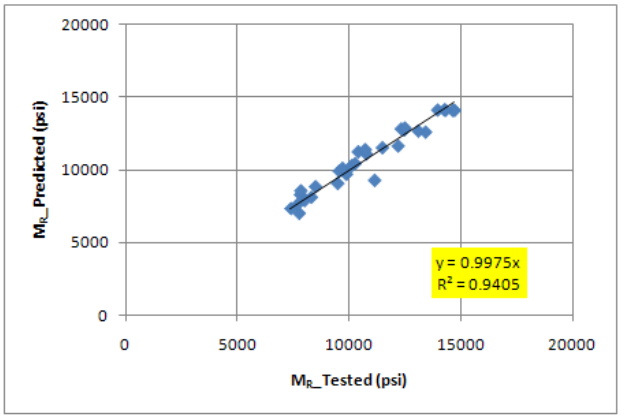

Figure D16. Resilient Modulus Properties of Embankment Material on Section 26005000.

K1	1653.33
K2	0.77
K3	-0.89
K4	-0.65

$$M_R = K_1 P_a \left(\frac{\theta + 3K_4 SV_W}{P_a} \right)^{K_2} \left(\frac{\tau_{OCT}}{P_a} + 1 \right)^{K_3}$$

	Axial stress	Test sequence	Confining pressure (psi)	Bulk stress (psi)	M_R_Tested (psi)	Oct. shear stress (psi)	Soil suction (psi)	Vol. water content	M_R_Pred. (psi)	Error
OPTIMUM	5.8	1.0	3	11.7867	16657.68954	1.3	12.2842	0.170	13618	9238498
	8.7	2.0	3	14.6774	16199.48649	2.7	12.2842	0.170	16166	1102
	11.4	3.0	3	17.3975	17005.17911	4.0	12.2842	0.170	18075	1143455
	9.8	4.0	5	19.8477	20502.67574	2.3	12.2842	0.170	22411	3641952
	14.3	5.0	5	24.3278	21081.17462	4.4	12.2842	0.170	24436	11255738
	18.9	6.0	5	28.92	22045.81717	6.6	12.2842	0.170	25955	15283517
	19.4	7.0	10	39.3913	30078.30332	4.4	12.2842	0.170	37436	54140131
	28.6	8.0	10	48.5543	31112.23994	8.7	12.2842	0.170	37198	37040187
	37.6	9.0	10	57.5784	32193.43049	13.0	12.2842	0.170	36895	22100160
	24.4	10.0	15	54.3582	36530.89829	4.4	12.2842	0.170	49168	159695910
	28.9	11.0	15	58.9182	36455.56618	6.6	12.2842	0.170	47738	127292494
	42.6	12.0	15	72.643	39102.16013	13.0	12.2842	0.170	44608	30318967
	33.9	13.0	20	73.8783	43427.13301	6.5	12.2842	0.170	57517	198530359
	38.6	14.0	20	78.5642	44208.80128	8.8	12.2842	0.170	55300	123012600
	56.6	15.0	20	96.5976	47018.30069	17.3	12.2842	0.170	49442	5875194
FIELD	29.9	1.0	20	69.915	75486.13	4.7	8.39586	0.220	60075	237490983
	39.9	2.0	20	79.917	68286.155	9.4	8.39586	0.220	54984	176953114
	49.9	3.0	20	89.921	60224.735	14.1	8.39586	0.220	51453	76945273
	25.0	4.0	15	54.968	55639.4	4.7	8.39586	0.220	49303	40143986
	35.0	5.0	15	64.987	52838.87	9.4	8.39586	0.220	46450	40817469
	44.9	6.0	15	74.923	50246.995	14.1	8.39586	0.220	44427	33866612
	14.9	7.0	10	34.921	46238.905	2.3	8.39586	0.220	37933	68984571
	20.1	8.0	10	40.068	40452.68	4.7	8.39586	0.220	37802	7023979
	30.1	9.0	10	50.119	40464.425	9.5	8.39586	0.220	37443	9131788
	40.1	10.0	10	60.055	39222.5	14.2	8.39586	0.220	37046	4735060
	8.8	11.0	5	18.786	27011.035	1.8	8.39586	0.220	22368	21562318
	15.1	12.0	5	25.134	24968.42	4.8	8.39586	0.220	25168	39893
	20.2	13.0	5	30.235	26216.725	7.2	8.39586	0.220	26684	218151
	8.1	14.0	3	14.049	20181.39	2.4	8.39586	0.220	16244	15506183
	10.0	15.0	3	15.977	20361.335	3.3	8.39586	0.220	17658	7308695
	12.1	16.0	3	18.053	21325.875	4.3	8.39586	0.220	18967	5564378
									SSE	1.545E+09
									SEE	7059.34

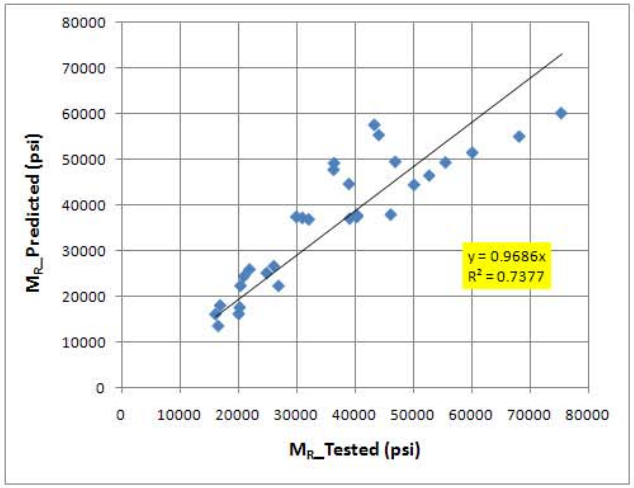

Figure D17. Resilient Modulus Properties of Base Material on Section 54020000.

K1	14.20
K2	2.31
K3	-0.40
K4	0.06

$$M_R = K_1 P_a \left(\frac{\theta + 3K_4 SV_W}{P_a} \right)^{K_2} \left(\frac{\tau_{OCT}}{P_a} + 1 \right)^{K_3}$$

	Axial stress	Test sequence	Confining pressure (psi)	Bulk stress (psi)	M_R_Tested (psi)	Oct. shear stress (psi)	Soil suction (psi)	Vol. water content	M_R_Pred. (psi)	Error
OPTIMUM	21.7	1.0	15.0	51.716	47150.04	3.2	3145.07	0.181	39045	65699514
	24.7	2.0	15.0	54.730	46333.46	4.6	3145.07	0.181	39691	44115696
	29.7	3.0	15.0	59.731	46476.90	6.9	3145.07	0.181	40897	31130477
	14.7	4.0	10.0	34.732	39746.47	2.2	3145.07	0.181	29979	95394745
	16.7	5.0	10.0	36.743	38355.83	3.2	3145.07	0.181	30397	63350256
	19.7	6.0	10.0	39.747	37602.93	4.6	3145.07	0.181	31064	42754938
	24.7	7.0	10.0	44.749	38407.89	7.0	3145.07	0.181	32279	37569410
	7.7	8.0	5.0	17.727	31355.62	1.3	3145.07	0.181	22129	85129478
	9.7	9.0	5.0	19.732	29254.13	2.2	3145.07	0.181	22528	45237461
	11.7	10.0	5.0	21.743	28206.51	3.2	3145.07	0.181	22949	27644871
	14.7	11.0	5.0	24.746	28133.55	4.6	3145.07	0.181	23610	20460422
	4.7	12.0	2.0	8.742	22339.78	1.3	3145.07	0.181	18235	16847856
	6.7	13.0	2.0	10.709	21284.62	2.2	3145.07	0.181	18623	7085746
	8.7	14.0	2.0	12.735	21283.31	3.2	3145.07	0.181	19039	5038364
FIELD	21.7	1.0	15.0	51.722	33778.46	3.2	3501.15	0.150	34768	978943
	24.7	2.0	15.0	54.689	34807.86	4.6	3501.15	0.150	35419	373444
	29.7	3.0	15.0	59.706	36491.16	6.9	3501.15	0.150	36637	21289
	14.7	4.0	10.0	34.711	27254.70	2.2	3501.15	0.150	26275	959090
	16.7	5.0	10.0	36.707	28087.01	3.2	3501.15	0.150	26693	1942889
	19.7	6.0	10.0	39.711	29301.17	4.6	3501.15	0.150	27361	3764857
	24.7	7.0	10.0	44.710	31231.72	6.9	3501.15	0.150	28563	7121919
	7.7	8.0	5.0	17.703	18970.77	1.3	3501.15	0.150	18996	636
	9.7	9.0	5.0	19.700	20093.68	2.2	3501.15	0.150	19391	494236
	11.7	10.0	5.0	21.711	21172.82	3.2	3501.15	0.150	19806	1869302
	14.7	11.0	5.0	24.709	22699.16	4.6	3501.15	0.150	20454	5042170
	4.7	12.0	2.0	8.712	12953.69	1.3	3501.15	0.150	15438	6169909
	6.7	13.0	2.0	10.702	14469.64	2.2	3501.15	0.150	15821	1826459
	8.7	14.0	2.0	12.715	15875.83	3.2	3501.15	0.150	16224	121017
									SSE	618145394
									SEE	4465.44

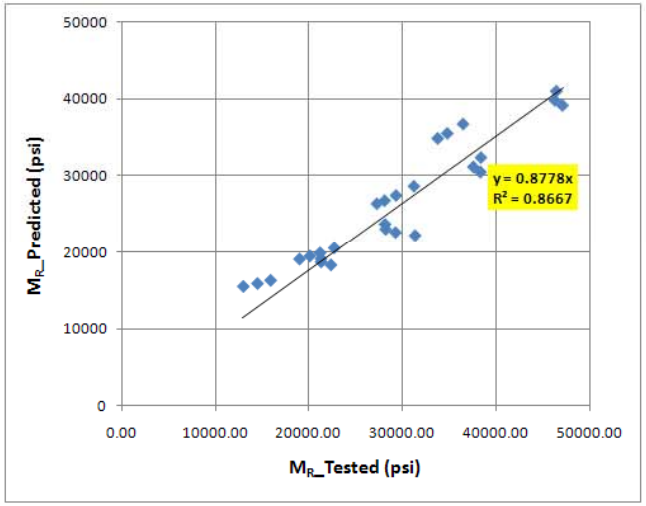

Figure D18. Resilient Modulus Properties of Subgrade Material on Section 54020000.

K1	543.86
K2	0.90
K3	-0.17
K4	0.08

$$M_R = K_1 P_a \left(\frac{\theta + 3K_4 SV_W}{P_a} \right)^{K_2} \left(\frac{\tau_{OCT}}{P_a} + 1 \right)^{K_3}$$

	Axial stress	Test sequence	Confining pressure (psi)	Bulk stress (psi)	M_R_Tested (psi)	Oct. shear stress (psi)	Soil suction (psi)	Vol. water content	M_R_Pred. (psi)	Error
OPTIMUM	21.7	1.0	15	51.712	34433.95	3.2	532.058	0.180	33473	923023
	24.7	2.0	15	54.734	34838.32	4.6	532.058	0.180	34220	382736
	29.7	3.0	15	59.738	36517.59	6.9	532.058	0.180	35462	1113487
	14.7	4.0	10	34.739	28053.05	2.2	532.058	0.180	26820	1519827
	16.7	5.0	10	36.733	27948.34	3.2	532.058	0.180	27387	315535
	19.7	6.0	10	39.730	28484.98	4.6	532.058	0.180	28234	62995
	24.7	7.0	10	44.724	30606.63	6.9	532.058	0.180	29634	945667
	7.7	8.0	5	17.735	20345.63	1.3	532.058	0.180	19828	268183
	9.7	9.0	5	19.727	20111.97	2.2	532.058	0.180	20485	139331
	11.7	10.0	5	21.740	20526.35	3.2	532.058	0.180	21142	379145
	14.7	11.0	5	24.744	21894.80	4.6	532.058	0.180	22109	45868
	4.7	12.0	2	8.732	13927.76	1.3	532.058	0.180	15864	3749162
	6.7	13.0	2	10.732	14803.07	2.2	532.058	0.180	16585	3174702
	8.7	14.0	2	12.732	15973.69	3.2	532.058	0.180	17294	1743335
FIELD	21.7	1.0	15.00	51.722	25696.98	3.2	150.811	0.234	27505	3268621
	24.7	2.0	15.00	54.689	26502.56	4.6	150.811	0.234	28342	3383013
	29.7	3.0	15.00	59.706	27821.30	6.9	150.811	0.234	29745	3701670
	14.7	4.0	10.00	34.711	20608.72	2.2	150.811	0.234	20608	1
	16.7	5.0	10.00	36.707	21256.12	3.2	150.811	0.234	21257	2
	19.7	6.0	10.00	39.711	22201.52	4.6	150.811	0.234	22222	414
	24.7	7.0	10.00	44.710	23706.99	6.9	150.811	0.234	23795	7694
	7.7	8.0	5.00	17.703	14198.73	1.3	150.811	0.234	13286	832897
	9.7	9.0	5.00	19.700	15063.63	2.2	150.811	0.234	14048	1030645
	11.7	10.0	5.00	21.711	15896.10	3.2	150.811	0.234	14802	1198147
	14.7	11.0	5.00	24.709	17075.58	4.6	150.811	0.234	15899	1384175
	4.7	12.0	2.00	8.712	9591.31	1.3	150.811	0.234	9116	225780
	6.7	13.0	2.00	10.702	10747.31	2.2	150.811	0.234	9954	629883
	8.7	14.0	2.00	12.715	11822.69	3.2	150.811	0.234	10780	1088109
									SSE	31514046
									SEE	1008.26

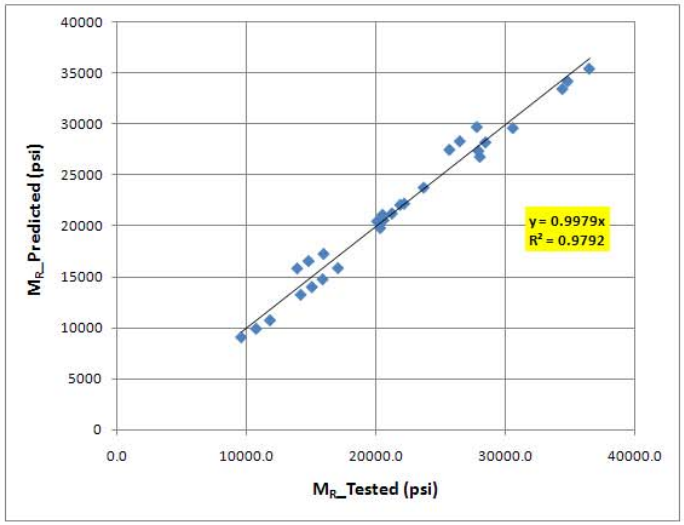

Figure D19. Resilient Modulus Properties of Embankment Material on Section 54020000.

K1	920.68
K2	1.01
K3	-0.94
K4	0.77

$$M_R = K_1 P_a \left(\frac{\theta + 3K_4 SV_W}{P_a} \right)^{K_2} \left(\frac{\tau_{OCT}}{P_a} + 1 \right)^{K_3}$$

	Axial stress	Test sequence	Confining pressure (psi)	Bulk stress (psi)	M_R_Tested (psi)	Oct. shear stress (psi)	Soil suction (psi)	Vol. water content	M_R_Pred. (psi)	Error
OPTIMUM	5.8	1.0	3	11.79	16657.69	1.3	12.2842	0.170	14114	6470515
	8.7	2.0	3	14.68	16199.49	2.7	12.2842	0.170	15353	716572
	11.4	3.0	3	17.40	17005.18	4.0	12.2842	0.170	16368	405835
	9.8	4.0	5	19.85	20502.68	2.3	12.2842	0.170	19899	364504
	14.3	5.0	5	24.33	21081.17	4.4	12.2842	0.170	21062	355
	18.9	6.0	5	28.92	22045.82	6.6	12.2842	0.170	22043	7
	19.4	7.0	10	39.39	30078.30	4.4	12.2842	0.170	32038	3839607
	28.6	8.0	10	48.55	31112.24	8.7	12.2842	0.170	31923	657584
	37.6	9.0	10	57.58	32193.43	13.0	12.2842	0.170	31902	85065
	24.4	10.0	15	54.36	36530.90	4.4	12.2842	0.170	43048	42467884
	28.9	11.0	15	58.92	36455.57	6.6	12.2842	0.170	41920	29861343
	42.6	12.0	15	72.64	39102.16	13.0	12.2842	0.170	39652	302272
	33.9	13.0	20	73.88	43427.13	6.5	12.2842	0.170	51917	72083047
	38.6	14.0	20	78.56	44208.80	8.8	12.2842	0.170	50096	34656192
	56.6	15.0	20	96.60	47018.30	17.3	12.2842	0.170	45507	2285480
FIELD	29.8	1.0	20	69.830	63740.26	4.6	9.3103	0.208	53568	103474909
	39.9	2.0	20	79.920	55042.435	9.4	9.3103	0.208	49416	31658545
	49.9	3.0	20	89.857	47613.94	14.1	9.3103	0.208	46708	821433
	24.8	4.0	15	54.824	45613.955	4.6	9.3103	0.208	42656	8747800
	34.8	5.0	15	64.825	43889.905	9.4	9.3103	0.208	40566	11047228
	43.2	6.0	15	73.218	40255.625	13.3	9.3103	0.208	39397	737606
	14.9	7.0	10	34.878	35377.39	2.3	9.3103	0.208	31867	12323253
	19.9	8.0	10	39.869	31769.79	4.7	9.3103	0.208	31773	8
	29.9	9.0	10	49.926	32929.065	9.4	9.3103	0.208	31708	1491744
	39.9	10.0	10	59.890	30838.165	14.1	9.3103	0.208	31729	794118
	9.9	11.0	5	19.886	19022.985	2.3	9.3103	0.208	19625	362984
	14.9	12.0	5	24.900	18877.405	4.7	9.3103	0.208	20943	4266441
	20.0	13.0	5	29.959	20790.1	7.1	9.3103	0.208	22016	1501819
	7.9	14.0	3	13.853	14674	2.3	9.3103	0.208	14736	3883
	9.9	15.0	3	15.942	15488.9	3.3	9.3103	0.208	15574	7167
	11.9	16.0	3	17.904	16768.38	4.2	9.3103	0.208	16288	230605
									SSE	371665806
									SEE	3462.55

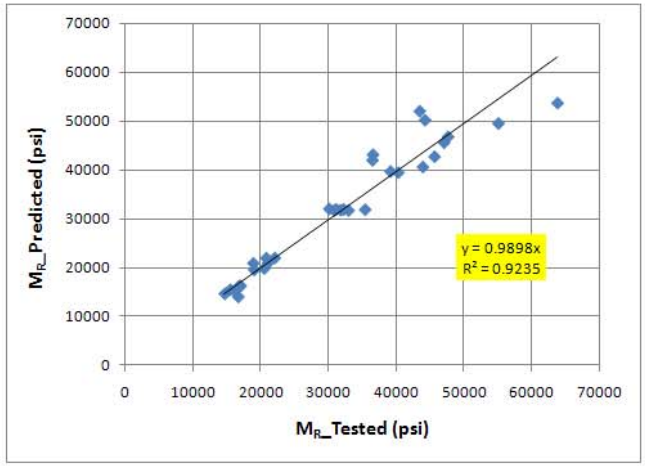

Figure D20. Resilient Modulus Properties of Base Material on Section 50020000.

K1	501.63
K2	1.04
K3	-0.43
K4	0.01

$$M_R = K_1 P_a \left(\frac{\theta + 3K_4 SV_W}{P_a} \right)^{K_2} \left(\frac{\tau_{OCT}}{P_a} + 1 \right)^{K_3}$$

	Axial stress	Test sequence	Confining pressure (psi)	Bulk stress (psi)	M_R_Tested (psi)	Oct. shear stress (psi)	Soil suction (psi)	Vol. water content	M_R_Pred. (psi)	Error
OPTIMUM	21.7	1.0	15	51.713	38418.77	3.2	3144.98	0.181	37170	1558613
	24.7	2.0	15	54.732	37490.95	4.6	3144.98	0.181	37470	426
	29.7	3.0	15	59.729	37748.11	6.9	3144.98	0.181	38037	83354
	14.7	4.0	10	34.734	31422.91	2.2	3144.98	0.181	29120	5305593
	16.7	5.0	10	36.714	31031.31	3.2	3144.98	0.181	29464	2455654
	19.7	6.0	10	39.737	30482.47	4.6	3144.98	0.181	30002	231319
	24.7	7.0	10	44.740	31390.86	6.9	3144.98	0.181	30910	231226
	7.7	8.0	5	17.705	23462.25	1.3	3144.98	0.181	20801	7081244
	9.7	9.0	5	19.723	22356.17	2.2	3144.98	0.181	21328	1057501
	11.7	10.0	5	21.733	22256.39	3.2	3144.98	0.181	21846	168442
	14.8	11.0	5	24.773	22850.62	4.6	3144.98	0.181	22618	54203
	4.7	12.0	2	8.725	15863.60	1.3	3144.98	0.181	16081	47464
	6.7	13.0	2	10.725	15842.57	2.2	3144.98	0.181	16708	749481
	8.7	14.0	2	12.729	16639.57	3.2	3144.98	0.181	17322	465828
FIELD	21.7	1.0	15.00	51.722	33778.46	3.2	3501.15	0.150	36250	6106609
	24.7	2.0	15.00	54.689	34807.86	4.6	3501.15	0.150	36572	3113719
	29.7	3.0	15.00	59.706	36491.16	6.9	3501.15	0.150	37182	477383
	14.7	4.0	10.00	34.711	27254.70	2.2	3501.15	0.150	28186	866464
	16.7	5.0	10.00	36.707	28087.01	3.2	3501.15	0.150	28553	217278
	19.7	6.0	10.00	39.711	29301.17	4.6	3501.15	0.150	29115	34845
	24.7	7.0	10.00	44.710	31231.72	6.9	3501.15	0.150	30062	1367582
	7.7	8.0	5.00	17.703	18970.77	1.3	3501.15	0.150	19862	794912
	9.7	9.0	5.00	19.700	20093.68	2.2	3501.15	0.150	20404	96593
	11.7	10.0	5.00	21.711	21172.82	3.2	3501.15	0.150	20943	53002
	14.7	11.0	5.00	24.709	22699.16	4.6	3501.15	0.150	21731	938090
	4.7	12.0	2.00	8.712	12953.69	1.3	3501.15	0.150	15150	4825894
	6.7	13.0	2.00	10.702	14469.64	2.2	3501.15	0.150	15794	1754673
	8.7	14.0	2.00	12.715	15875.83	3.2	3501.15	0.150	16430	306903
									SSE	40444297
									SEE	1142.21

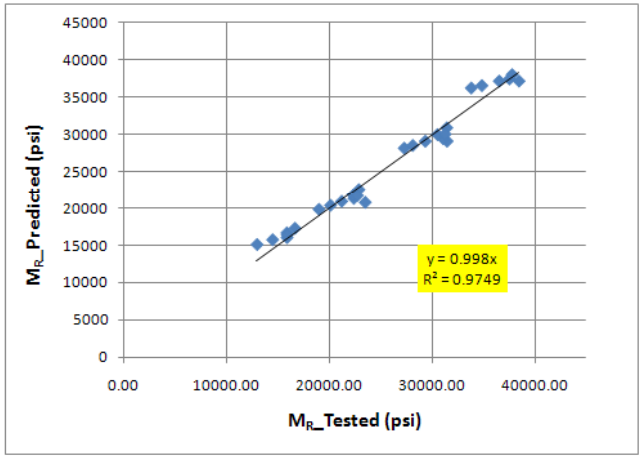

Figure D21. Resilient Modulus Properties of Subgrade Material on Section 50020000.

K1	863.22
K2	1.10
K3	-0.99
K4	5.85

$$M_R = K_1 P_a \left(\frac{\theta + 3K_4 SV_w}{P_a} \right)^{K_2} \left(\frac{\tau_{OCT}}{P_a} + 1 \right)^{K_3}$$

	Axial stress	Test sequence	Confining pressure (psi)	Bulk stress (psi)	M_R_Tested (psi)	Oct. shear stress (psi)	Soil suction (psi)	Vol. water content	M_R_Pred. (psi)	Error
OPTIMUM	5.6	1.0	3	11.6941	15887.8345	1.2	0.010	0.161	9146	45458079
	8.2	2.0	3	14.2535	16001.0206	2.5	0.010	0.161	10524	29997813
	11.0	3.0	3	17.0616	17249.87683	3.8	0.010	0.161	11919	28413184
	9.5	4.0	5	19.4728	19642.70486	2.1	0.010	0.161	15135	20316141
	14.2	5.0	5	24.0681	21286.72374	4.3	0.010	0.161	16901	19235579
	19.0	6.0	5	28.8807	22642.66882	6.6	0.010	0.161	18445	17622660
	19.2	7.0	10	39.0917	29644.54265	4.3	0.010	0.161	28836	653825
	28.8	8.0	10	48.4911	31399.51599	8.9	0.010	0.161	29519	3535352
	38.2	9.0	10	57.6162	33406.0378	13.3	0.010	0.161	30029	11401297
	24.2	10.0	15	54.1205	36230.94536	4.3	0.010	0.161	41276	25455914
	28.9	11.0	15	58.6882	35516.44632	6.5	0.010	0.161	40411	23954311
	43.2	12.0	15	72.5594	39350.48119	13.3	0.010	0.161	38703	419413
	33.9	13.0	20	73.6792	42548.72959	6.5	0.010	0.161	51961	88598898
	38.6	14.0	20	78.3133	43590.1707	8.7	0.010	0.161	50318	45258067
	57.4	15.0	20	96.5638	47382.69519	17.6	0.010	0.161	45944	2071119
FIELD	29.9	1.0	20	69.867	79890.215	4.7	8.995	0.141	72919	48597390
	39.9	2.0	20	79.857	69383.66	9.4	8.995	0.141	65652	13923620
	49.9	3.0	20	89.860	62752.955	14.1	8.995	0.141	60836	3673670
	24.9	4.0	15	54.875	61159.55	4.7	8.995	0.141	59935	1499014
	34.9	5.0	15	64.864	54728.945	9.4	8.995	0.141	55097	135651
	44.9	6.0	15	74.849	53454.83	14.1	8.995	0.141	51927	2334892
	14.9	7.0	10	34.874	55828.77	2.3	8.995	0.141	49050	45948781
	19.9	8.0	10	39.892	45788.97	4.7	8.995	0.141	47216	2036317
	29.9	9.0	10	49.886	42693.365	9.4	8.995	0.141	44732	4156295
	39.9	10.0	10	59.895	43149.68	14.1	8.995	0.141	43151	2
	9.9	11.0	5	19.871	35233.695	2.3	8.995	0.141	35055	32052
	14.9	12.0	5	24.903	29565.065	4.7	8.995	0.141	34815	27561481
	19.9	13.0	5	29.894	29798.515	7.0	8.995	0.141	34672	23746226
	7.9	14.0	3	13.865	28179.445	2.3	8.995	0.141	29592	1994566
	9.9	15.0	3	15.871	26245.87	3.2	8.995	0.141	29745	12242194
	11.9	16.0	3	17.883	25703.28	4.2	8.995	0.141	29892	17545920
									SSE	567819724
									SEE	4279.81

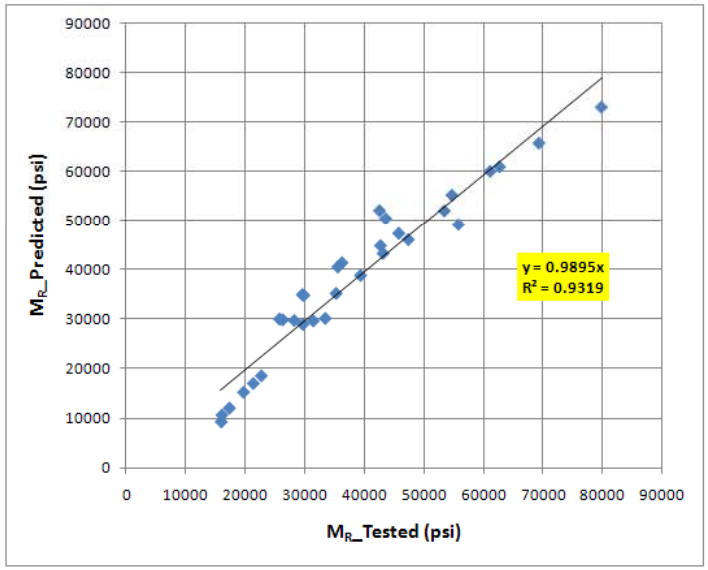

Figure D22. Resilient Modulus Properties of Base Material on Section 89010000.

K1	1806.55
K2	0.51
K3	-0.23
K4	-0.10

$$M_R = K_1 P_a \left(\frac{\theta + 3K_4 SV_W}{P_a} \right)^{K_2} \left(\frac{\tau_{OCT}}{P_a} + 1 \right)^{K_3}$$

	Axial stress	Test sequence	Confining pressure (psi)	Bulk stress (psi)	M_R_Tested (psi)	Oct. shear stress (psi)	Soil suction (psi)	Vol. water content	M_R_Pred. (psi)	Error
OPTIMUM	21.7	1.0	15	51.721	50152.51	3.2	12.4461	0.168	47724	5896292
	24.7	2.0	15	54.725	50253.31	4.6	12.4461	0.168	48289	3859757
	29.7	3.0	15	59.721	51170.98	6.9	12.4461	0.168	49206	3860377
	14.7	4.0	10	34.725	41251.55	2.2	12.4461	0.168	39280	3885407
	16.7	5.0	10	36.731	40268.61	3.2	12.4461	0.168	39946	104227
	19.7	6.0	10	39.717	40339.10	4.6	12.4461	0.168	40888	300854
	24.7	7.0	10	44.743	42458.72	6.9	12.4461	0.168	42360	9721
	7.7	8.0	5	17.711	29438.33	1.3	12.4461	0.168	27937	2255042
	9.7	9.0	5	19.728	29232.81	2.2	12.4461	0.168	29190	1801
	11.7	10.0	5	21.737	29361.03	3.2	12.4461	0.168	30343	964946
	14.7	11.0	5	24.734	30417.50	4.6	12.4461	0.168	31917	2248151
	4.7	12.0	2	8.711	20392.77	1.3	12.4461	0.168	19037	1839080
	6.7	13.0	2	10.717	21028.33	2.2	12.4461	0.168	21048	397
	8.7	14.0	2	12.746	22226.36	3.2	12.4461	0.168	22831	365754
FIELD	21.7	1.0	15.00	51.722	43839.48	3.2	213.621	0.066	45943	4425073
	24.7	2.0	15.00	54.689	45240.80	4.6	213.621	0.066	46581	1794955
	29.7	3.0	15.00	59.706	47536.57	6.9	213.621	0.066	47619	6833
	14.7	4.0	10.00	34.711	35009.10	2.2	213.621	0.066	37060	4206011
	16.7	5.0	10.00	36.707	36130.49	3.2	213.621	0.066	37813	2830233
	19.7	6.0	10.00	39.711	37769.22	4.6	213.621	0.066	38881	1236900
	24.7	7.0	10.00	44.710	40381.53	6.9	213.621	0.066	40515	17913
	7.7	8.0	5.00	17.703	23946.97	1.3	213.621	0.066	24691	553815
	9.7	9.0	5.00	19.700	25434.74	2.2	213.621	0.066	26163	530540
	11.7	10.0	5.00	21.711	26868.29	3.2	213.621	0.066	27513	415279
	14.7	11.0	5.00	24.709	28901.88	4.6	213.621	0.066	29327	180315
	4.7	12.0	2.00	8.712	16054.03	1.3	213.621	0.066	13988	4270205
	6.7	13.0	2.00	10.702	18028.59	2.2	213.621	0.066	16699	1769041
	8.7	14.0	2.00	12.715	19869.15	3.2	213.621	0.066	18965	816639
									SSE	48645557
									SEE	1252.68

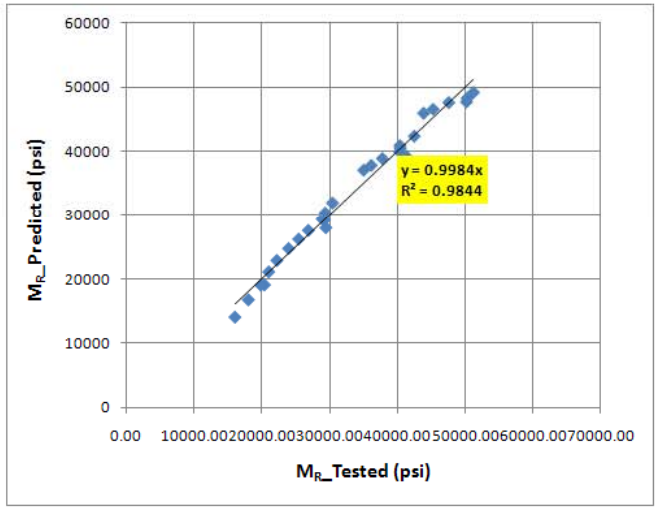

Figure D23. Resilient Modulus Properties of Subgrade Material on Section 89010000.

K1	1275.70
K2	0.56
K3	-0.13
K4	-0.02

$$M_R = K_1 P_a \left(\frac{\theta + 3K_4 SV_W}{P_a} \right)^{K_2} \left(\frac{\tau_{OCT}}{P_a} + 1 \right)^{K_3}$$

	Axial stress	Test sequence	Confining pressure (psi)	Bulk stress (psi)	M_R_Tested (psi)	Oct. shear stress (psi)	Soil suction (psi)	Vol. water content	M_R_Pred. (psi)	Error
OPTIMUM	21.7	1.0	15	51.722	38142.91	3.2	4.84207	0.163	36821	1747351
	24.8	2.0	15	54.761	38364.67	4.6	4.84207	0.163	37636	531461
	29.7	3.0	15	59.744	39342.10	7.0	4.84207	0.163	38928	171485
	14.7	4.0	10	34.722	29685.63	2.2	4.84207	0.163	29637	2354
	16.7	5.0	10	36.744	29688.82	3.2	4.84207	0.163	30375	470225
	19.7	6.0	10	39.735	30487.70	4.6	4.84207	0.163	31424	876482
	24.8	7.0	10	44.759	32641.69	7.0	4.84207	0.163	33089	200236
	7.7	8.0	5	17.719	21441.84	1.3	4.84207	0.163	20447	990464
	9.7	9.0	5	19.732	21180.48	2.2	4.84207	0.163	21559	143035
	11.8	10.0	5	21.752	21634.46	3.2	4.84207	0.163	22610	952552
	14.7	11.0	5	24.734	23054.69	4.6	4.84207	0.163	24064	1010900
	4.7	12.0	2	8.735	14756.95	1.3	4.84207	0.163	13718	1078881
	6.7	13.0	2	10.721	15849.54	2.2	4.84207	0.163	15285	319093
	8.8	14.0	2	12.820	16984.47	3.2	4.84207	0.163	16780	41801
FIELD	21.7	1.0	15.00	51.722	36039.85	3.2	317.94	0.037	36577	288105
	24.7	2.0	15.00	54.689	37179.00	4.6	317.94	0.037	37381	40655
	29.7	3.0	15.00	59.706	39044.41	6.9	317.94	0.037	38695	122261
	14.7	4.0	10.00	34.711	28851.77	2.2	317.94	0.037	29341	239228
	16.7	5.0	10.00	36.707	29765.61	3.2	317.94	0.037	30078	97701
	19.7	6.0	10.00	39.711	31100.49	4.6	317.94	0.037	31145	1967
	24.7	7.0	10.00	44.710	33227.11	6.9	317.94	0.037	32820	165372
	7.7	8.0	5.00	17.703	19817.78	1.3	317.94	0.037	20041	49678
	9.7	9.0	5.00	19.700	21035.07	2.2	317.94	0.037	21166	17104
	11.7	10.0	5.00	21.711	22207.26	3.2	317.94	0.037	22233	646
	14.7	11.0	5.00	24.709	23868.92	4.6	317.94	0.037	23719	22535
	4.7	12.0	2.00	8.712	13344.36	1.3	317.94	0.037	13154	36413
	6.7	13.0	2.00	10.702	14966.55	2.2	317.94	0.037	14777	35974
	8.7	14.0	2.00	12.715	16476.88	3.2	317.94	0.037	16255	49158
									SSE	9711116.1
									SEE	559.70

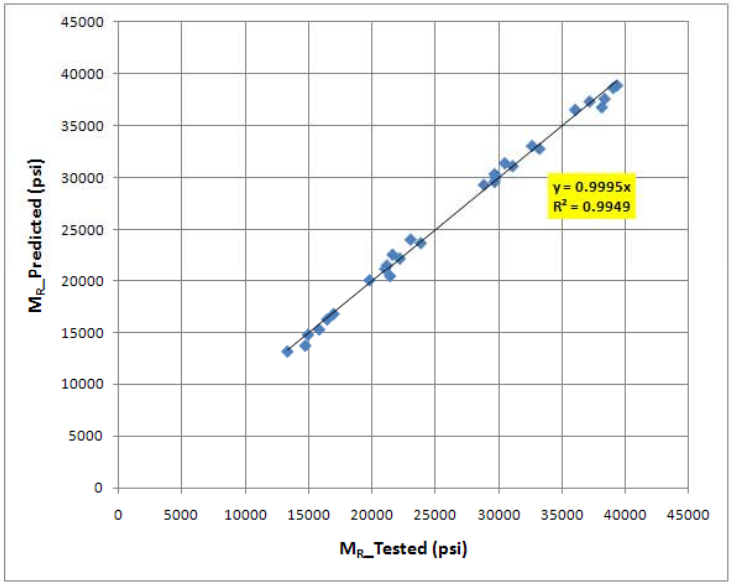

Figure D24. Resilient Modulus Properties of Embankment Material on Section 89010000.

K1	1077.24
K2	0.74
K3	-0.29
K4	0.65

$$M_R = K_1 P_a \left(\frac{\theta + 3K_4 SV_W}{P_a} \right)^{K_2} \left(\frac{\tau_{OCT}}{P_a} + 1 \right)^{K_3}$$

	Axial stress	Test sequence	Confining pressure (psi)	Bulk stress (psi)	M_R_Tested (psi)	Oct. shear stress (psi)	Soil suction (psi)	Vol. water content	M_R_Pred. (psi)	Error
OPTIMUM	5.5	1.0	3.0	11.5	14193.4	1.2	3.18604	0.16538	13695	248489.1893
	8.0	2.0	3.0	14.0	14796.7	2.4	3.18604	0.16538	15373	332247.3166
	11.0	3.0	3.0	17.0	16472.5	3.8	3.18604	0.16538	17138	442686.582
	9.4	4.0	5.0	19.4	19382.6	2.1	3.18604	0.16538	19353	873.3243952
	14.1	5.0	5.0	24.1	21801.1	4.3	3.18604	0.16538	21775	661.4868747
	19.3	6.0	5.0	29.3	23830.8	6.7	3.18604	0.16538	24120	83582.56281
	19.2	7.0	10.0	39.2	32366.9	4.3	3.18604	0.16538	30798	2461685.013
	29.2	8.0	10.0	49.2	34946.8	9.0	3.18604	0.16538	34004	887898.0406
	38.8	9.0	10.0	58.8	36665.7	13.6	3.18604	0.16538	36778	12686.9723
	24.3	10.0	15.0	54.3	38784.4	4.4	3.18604	0.16538	38981	38456.5086
	29.2	11.0	15.0	59.2	40105.2	6.7	3.18604	0.16538	40140	1207.775568
	43.6	12.0	15.0	73.6	43636.0	13.5	3.18604	0.16538	43380	65374.65997
	34.1	13.0	20.0	74.1	46296.8	6.6	3.18604	0.16538	47297	1000301.772
	38.8	14.0	20.0	78.8	47760.4	8.9	3.18604	0.16538	48064	92228.49681
	57.8	15.0	20.0	97.8	51465.2	17.8	3.18604	0.16538	51198	71335.83007
FIELD	5.4	1.0	3.0	11.4	16343	1.2	8.16401	0.13703	14588	3078065.246
	7.9	2.0	3.0	13.9	15708	2.3	8.16401	0.13703	16124	173308.8088
	10.9	3.0	3.0	16.9	16905	3.7	8.16401	0.13703	17883	956120.8395
	9.2	4.0	5.0	19.2	20723	2.0	8.16401	0.13703	20049	454076.6361
	14.0	5.0	5.0	24.0	21450	4.2	8.16401	0.13703	22445	989997.2654
	19.1	6.0	5.0	29.1	23676	6.6	8.16401	0.13703	24719	1088995.939
	19.3	7.0	10.0	39.3	31631	4.4	8.16401	0.13703	31499	17431.91543
	28.7	8.0	10.0	48.7	34115	8.8	8.16401	0.13703	34436	103003.6184
	38.0	9.0	10.0	58.0	37283	13.2	8.16401	0.13703	37093	36025.40395
	24.3	10.0	15.0	54.3	40198	4.4	8.16401	0.13703	39593	366920.1197
	29.1	11.0	15.0	59.1	40561	6.7	8.16401	0.13703	40681	14400.51028
	43.0	12.0	15.0	73.0	43854	13.2	8.16401	0.13703	43734	14386.17693
	34.1	13.0	20.0	74.1	47875	6.6	8.16401	0.13703	47840	1242.865323
	39.0	14.0	20.0	79.0	48580	8.9	8.16401	0.13703	48600	382.2547873
	57.3	15.0	20.0	97.3	51504	17.6	8.16401	0.13703	51557	2876.566186
									SSE	13036949.7
									SEE	659.2

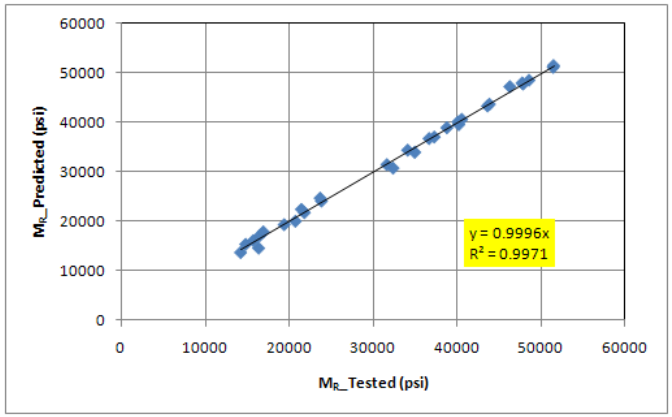

Figure D25. Resilient Modulus Properties of Base Material on Section 93310000.

K1	974.74
K2	0.78
K3	-0.63
K4	0.73

$$M_R = K_1 P_a \left(\frac{\theta + 3K_4 SV_W}{P_a} \right)^{K_2} \left(\frac{\tau_{OCT}}{P_a} + 1 \right)^{K_3}$$

	Axial stress	Test sequence	Confining pressure (psi)	Bulk stress (psi)	M_R_Tested (psi)	Oct. shear stress (psi)	Soil suction (psi)	Vol. water content	M_R_Pred. (psi)	Error
OPTIMUM	7.9	1.0	6.0	19.9	21739.4	0.9	17.2223	0.15988	21435	92882.83846
	9.7	2.0	6.0	21.7	21863.2	1.7	17.2223	0.15988	21846	299.2900023
	11.5	3.0	6.0	23.5	22284.1	2.6	17.2223	0.15988	22233	2662.887934
	13.4	4.0	6.0	25.4	22617.4	3.5	17.2223	0.15988	22617	0.153610116
	15.4	5.0	6.0	27.4	23145.6	4.4	17.2223	0.15988	22978	28255.39634
	5.8	6.0	4.0	13.8	18004.9	0.9	17.2223	0.15988	17429	331606.6812
	7.6	7.0	4.0	15.6	17916.5	1.7	17.2223	0.15988	18032	13272.43602
	9.5	8.0	4.0	17.5	18371.8	2.6	17.2223	0.15988	18613	58361.20422
	11.4	9.0	4.0	19.4	19459.4	3.5	17.2223	0.15988	19161	88754.23706
	13.3	10.0	4.0	21.3	20336.0	4.4	17.2223	0.15988	19667	448253.8071
	3.8	11.0	2.0	7.8	13496.5	0.8	17.2223	0.15988	13124	138583.6666
	5.6	12.0	2.0	9.6	13606.7	1.7	17.2223	0.15988	13956	121820.7747
	7.4	13.0	2.0	11.4	14420.3	2.6	17.2223	0.15988	14762	116554.0667
	9.4	14.0	2.0	13.4	15623.7	3.5	17.2223	0.15988	15527	9397.960013
	11.3	15.0	2.0	15.3	16256.6	4.4	17.2223	0.15988	16198	3474.778347
FIELD	7.9	1.0	6.0	19.9	21394.6	0.9	17.4259	0.15956	21471	5915.396284
	9.7	2.0	6.0	21.7	21608.5	1.7	17.4259	0.15956	21886	76782.42956
	11.6	3.0	6.0	23.6	22028.7	2.6	17.4259	0.15956	22286	65961.81171
	13.5	4.0	6.0	25.5	22379.4	3.6	17.4259	0.15956	22673	86056.65126
	15.4	5.0	6.0	27.4	22906.8	4.4	17.4259	0.15956	23021	13096.97558
	5.8	6.0	4.0	13.8	17781.0	0.9	17.4259	0.15956	17471	96190.0398
	7.7	7.0	4.0	15.7	17764.7	1.7	17.4259	0.15956	18080	99668.81817
	9.5	8.0	4.0	17.5	18224.8	2.6	17.4259	0.15956	18653	183471.5472
	11.5	9.0	4.0	19.5	19211.0	3.5	17.4259	0.15956	19222	119.8361624
	13.4	10.0	4.0	21.4	20078.8	4.4	17.4259	0.15956	19729	122657.5135
	3.8	11.0	2.0	7.8	13457.2	0.8	17.4259	0.15956	13173	80626.72215
	5.6	12.0	2.0	9.6	13755.0	1.7	17.4259	0.15956	14017	68385.22149
	7.5	13.0	2.0	11.5	14503.0	2.6	17.4259	0.15956	14821	101017.076
	9.5	14.0	2.0	13.5	15628.9	3.5	17.4259	0.15956	15580	2429.879035
	11.3	15.0	2.0	15.3	16030.7	4.4	17.4259	0.15956	16245	46057.80635
									SSE	2502617.903
									SEE	288.8

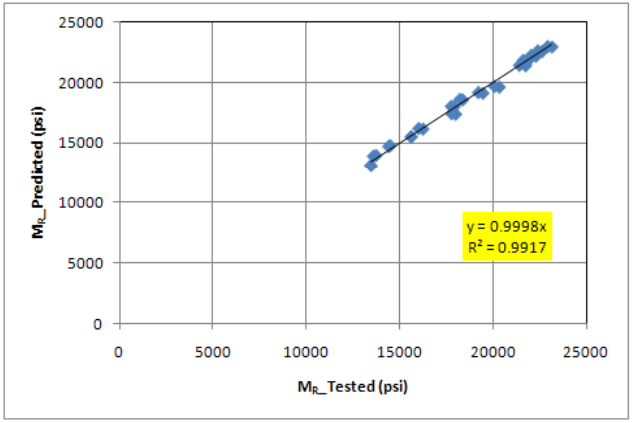

Figure D26. Resilient Modulus Properties of Subgrade Material on Section 93310000.

K1	490.70
K2	1.18
K3	-0.72
K4	48.45

$$M_R = K_1 P_a \left(\frac{\theta + 3K_4 SV_W}{P_a} \right)^{K_2} \left(\frac{\tau_{OCT}}{P_a} + 1 \right)^{K_3}$$

	Axial stress	Test sequence	Confining pressure (psi)	Bulk stress (psi)	M_R_Tested (psi)	Oct. shear stress (psi)	Soil suction (psi)	Vol. water content	M_R_Pred. (psi)	Error
OPTIMUM	7.9	1.0	6.0	19.9	20743.2	0.9	0.68861	0.17342	20691	2774.348324
	9.7	2.0	6.0	21.7	20934.6	1.7	0.68861	0.17342	21050	13222.10126
	11.6	3.0	6.0	23.6	21309.1	2.6	0.68861	0.17342	21416	11399.30518
	13.5	4.0	6.0	25.5	21619.9	3.5	0.68861	0.17342	21783	26665.16974
	15.4	5.0	6.0	27.4	22145.9	4.4	0.68861	0.17342	22139	51.59129405
	5.9	6.0	4.0	13.9	17186.2	0.9	0.68861	0.17342	16819	134869.5641
	7.7	7.0	4.0	15.7	17167.6	1.7	0.68861	0.17342	17292	15465.92631
	9.6	8.0	4.0	17.6	17677.1	2.6	0.68861	0.17342	17774	9473.108132
	11.5	9.0	4.0	19.5	18638.7	3.6	0.68861	0.17342	18242	157060.8021
	13.4	10.0	4.0	21.4	19486.3	4.4	0.68861	0.17342	18690	633410.6517
	3.8	11.0	2.0	7.8	12603.2	0.8	0.68861	0.17342	13063	211726.9029
	5.6	12.0	2.0	9.6	12986.3	1.7	0.68861	0.17342	13639	426253.4633
	7.6	13.0	2.0	11.6	13854.1	2.6	0.68861	0.17342	14229	140671.2781
	9.5	14.0	2.0	13.5	15104.7	3.5	0.68861	0.17342	14793	97115.83397
	11.3	15.0	2.0	15.3	15610.5	4.4	0.68861	0.17342	15309	90923.08532
FIELD	7.9	1.0	6.0	19.9	18647.9	0.9	0.51416	0.18817	18549	9777.89628
	9.7	2.0	6.0	21.7	18929.4	1.7	0.51416	0.18817	18971	1700.4743
	11.6	3.0	6.0	23.6	19284.1	2.6	0.51416	0.18817	19401	13621.90928
	13.5	4.0	6.0	25.5	19475.8	3.6	0.51416	0.18817	19827	123138.5086
	15.4	5.0	6.0	27.4	19796.2	4.5	0.51416	0.18817	20237	194049.36
	5.8	6.0	4.0	13.8	15249.9	0.9	0.51416	0.18817	14740	260378.0352
	7.6	7.0	4.0	15.6	15249.0	1.7	0.51416	0.18817	15261	154.3938472
	9.5	8.0	4.0	17.5	15755.6	2.6	0.51416	0.18817	15794	1509.611177
	11.5	9.0	4.0	19.5	16644.9	3.6	0.51416	0.18817	16342	92015.50898
	13.4	10.0	4.0	21.4	17181.9	4.4	0.51416	0.18817	16825	127052.8704
	3.7	11.0	2.0	7.7	11465.0	0.8	0.51416	0.18817	11055	168213.57
	5.5	12.0	2.0	9.5	11688.6	1.7	0.51416	0.18817	11672	267.2776375
	7.5	13.0	2.0	11.5	12442.4	2.6	0.51416	0.18817	12310	17569.92364
	9.2	14.0	2.0	13.2	12844.3	3.4	0.51416	0.18817	12868	585.7616406
	10.8	15.0	2.0	14.8	12376.8	4.2	0.51416	0.18817	13350	946243.9238
									SSE	3927362.2
									SEE	361.8

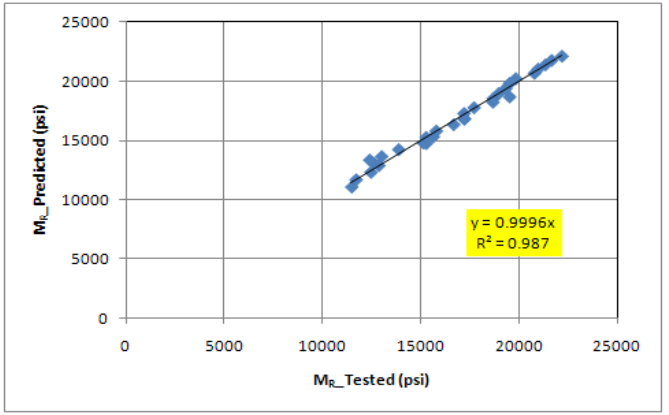

Figure D27. Resilient Modulus Properties of Embankment Material on Section 93310000.

K1	1195.77
K2	0.65
K3	-0.18
K4	0.45

$$M_R = K_1 P_a \left(\frac{\theta + 3K_4 SV_W}{P_a} \right)^{K_2} \left(\frac{\tau_{OCT}}{P_a} + 1 \right)^{K_3}$$

	Axial stress	Test sequence	Confining pressure (psi)	Bulk stress (psi)	M_R_Tested (psi)	Oct. shear stress (psi)	Soil suction (psi)	Vol. water content	M_R_Pred. (psi)	Error
OPTIMUM	5.7	1.0	3.0	11.7	16037.1	1.3	0.00001	0.16547	14830	1456560.1
	8.5	2.0	3.0	14.5	17134.5	2.6	0.00001	0.16547	16825	95516.648
	11.5	3.0	3.0	17.5	18983.8	4.0	0.00001	0.16547	18775	43592.481
	9.6	4.0	5.0	19.6	19924.3	2.1	0.00001	0.16547	20543	383039.69
	14.5	5.0	5.0	24.5	23351.4	4.5	0.00001	0.16547	23249	10389.758
	19.7	6.0	5.0	29.7	25421.6	6.9	0.00001	0.16547	25747	105675.22
	19.5	7.0	10.0	39.5	31907.2	4.5	0.00001	0.16547	31651	65572.858
	29.3	8.0	10.0	49.3	35711.7	9.1	0.00001	0.16547	35152	313739.6
	38.4	9.0	10.0	58.4	37651.1	13.4	0.00001	0.16547	38113	213617.39
	24.5	10.0	15.0	54.5	37897.4	4.5	0.00001	0.16547	39007	1232136.6
	29.4	11.0	15.0	59.4	39969.5	6.8	0.00001	0.16547	40417	200315.43
	43.3	12.0	15.0	73.3	44599.2	13.4	0.00001	0.16547	44177	178335.67
	34.3	13.0	20.0	74.3	46242.4	6.7	0.00001	0.16547	46750	257770.81
	39.1	14.0	20.0	79.1	48479.2	9.0	0.00001	0.16547	47824	429560.24
	57.6	15.0	20.0	97.6	52811.8	17.7	0.00001	0.16547	51805	1014575.4
FIELD	5.4	1.0	3.0	11.4	15870	1.1	10.9815	0.07438	15531	114660.15
	7.8	2.0	3.0	13.8	16430	2.3	10.9815	0.07438	17220	624493.8
	10.7	3.0	3.0	16.7	18175	3.6	10.9815	0.07438	19036	741425.68
	9.2	4.0	5.0	19.2	21164	2.0	10.9815	0.07438	21077	7401.5056
	14.5	5.0	5.0	24.5	23370	4.5	10.9815	0.07438	23917	299608.17
	19.7	6.0	5.0	29.7	24784	6.9	10.9815	0.07438	26381	2549165.8
	19.5	7.0	10.0	39.5	32849	4.5	10.9815	0.07438	32243	366870.76
	29.8	8.0	10.0	49.8	35716	9.3	10.9815	0.07438	35828	12413.648
	39.3	9.0	10.0	59.3	36990	13.8	10.9815	0.07438	38847	3450165.1
	24.7	10.0	15.0	54.7	38934	4.6	10.9815	0.07438	39565	398851.84
	29.8	11.0	15.0	59.8	40668	7.0	10.9815	0.07438	40996	107702.6
	44.3	12.0	15.0	74.3	44568	13.8	10.9815	0.07438	44845	76604.889
	34.6	13.0	20.0	74.6	47039	6.9	10.9815	0.07438	47259	48192.005
	39.8	14.0	20.0	79.8	48808	9.3	10.9815	0.07438	48401	166191.8
	58.7	15.0	20.0	98.7	51870	18.2	10.9815	0.07438	52419	301136.42
									SSE	15265282
									SEE	713.33214

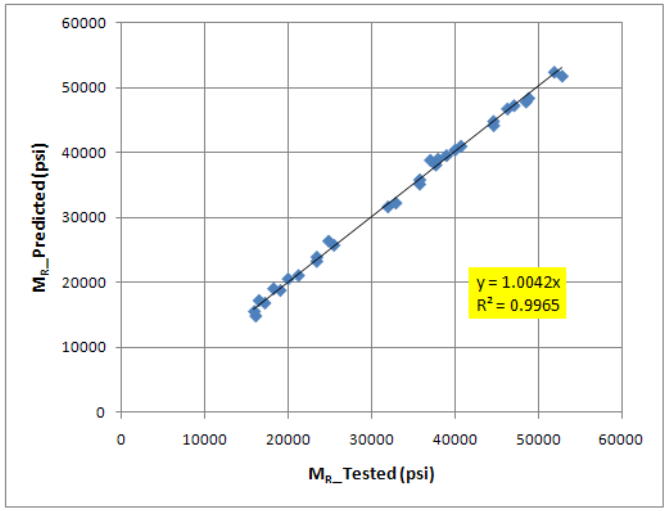

Figure D28. Resilient Modulus Properties of Base Material on Section 86190000.

K1	734.76
K2	1.14
K3	-0.96
K4	1.12

$$M_R = K_1 P_a \left(\frac{\theta + 3K_4 SV_W}{P_a} \right)^{K_2} \left(\frac{\tau_{OCT}}{P_a} + 1 \right)^{K_3}$$

	Axial stress	Test sequence	Confining pressure (psi)	Bulk stress (psi)	M_R_Tested (psi)	Oct. shear stress (psi)	Soil suction (psi)	Vol. water content	M_R_Pred. (psi)	Error
OPTIMUM	8.0	1.0	6.0	20.0	27647.7	0.9	29.5943	0.14352	26701	896820.59
	9.8	2.0	6.0	21.8	27578.0	1.8	29.5943	0.14352	26889	474424.59
	11.6	3.0	6.0	23.6	27472.6	2.6	29.5943	0.14352	27076	157040.37
	13.5	4.0	6.0	25.5	27408.8	3.5	29.5943	0.14352	27266	20491.57
	15.4	5.0	6.0	27.4	27686.5	4.4	29.5943	0.14352	27448	56849.213
	5.9	6.0	4.0	13.9	21527.4	0.9	29.5943	0.14352	21440	7620.9696
	7.7	7.0	4.0	15.7	21376.5	1.7	29.5943	0.14352	21846	220059.81
	9.6	8.0	4.0	17.6	22029.0	2.6	29.5943	0.14352	22248	48017.824
	11.5	9.0	4.0	19.5	23146.7	3.5	29.5943	0.14352	22635	262202.91
	13.4	10.0	4.0	21.4	23855.1	4.4	29.5943	0.14352	22996	738563.07
	3.8	11.0	2.0	7.8	15240.7	0.9	29.5943	0.14352	16298	1118475.8
	5.6	12.0	2.0	9.6	15443.4	1.7	29.5943	0.14352	16927	2201236
	7.5	13.0	2.0	11.5	16444.5	2.6	29.5943	0.14352	17538	1194640.1
	9.4	14.0	2.0	13.4	17842.6	3.5	29.5943	0.14352	18108	70473.595
	11.4	15.0	2.0	15.4	18986.7	4.4	29.5943	0.14352	18665	103372.56
FIELD	7.6	1.0	6.0	19.6	21220.5	0.8	15.9244	0.16183	21695	225396.32
	9.7	2.0	6.0	21.7	21644.6	1.7	15.9244	0.16183	22156	261827.09
	11.5	3.0	6.0	23.5	21715.3	2.6	15.9244	0.16183	22532	666409.35
	13.4	4.0	6.0	25.4	21796.6	3.5	15.9244	0.16183	22918	1257544.3
	15.5	5.0	6.0	27.5	22344.9	4.5	15.9244	0.16183	23289	891950.39
	5.7	6.0	4.0	13.7	17228.1	0.8	15.9244	0.16183	16564	441588.2
	7.5	7.0	4.0	15.5	17219.7	1.7	15.9244	0.16183	17200	370.24238
	9.4	8.0	4.0	17.4	17804.9	2.5	15.9244	0.16183	17776	820.4653
	11.3	9.0	4.0	19.3	18698.4	3.4	15.9244	0.16183	18340	128352.37
	13.3	10.0	4.0	21.3	19285.1	4.4	15.9244	0.16183	18900	148439.32
	3.7	11.0	2.0	7.7	12793.5	0.8	15.9244	0.16183	11611	1397844.6
	5.4	12.0	2.0	9.4	13160.0	1.6	15.9244	0.16183	12390	592232.93
	7.3	13.0	2.0	11.3	13804.0	2.5	15.9244	0.16183	13170	401433.99
	9.3	14.0	2.0	13.3	14538.6	3.4	15.9244	0.16183	13941	356902.12
	11.1	15.0	2.0	15.1	14550.3	4.3	15.9244	0.16183	14596	2096.4921
									SSE	14343497
									SEE	691.45974

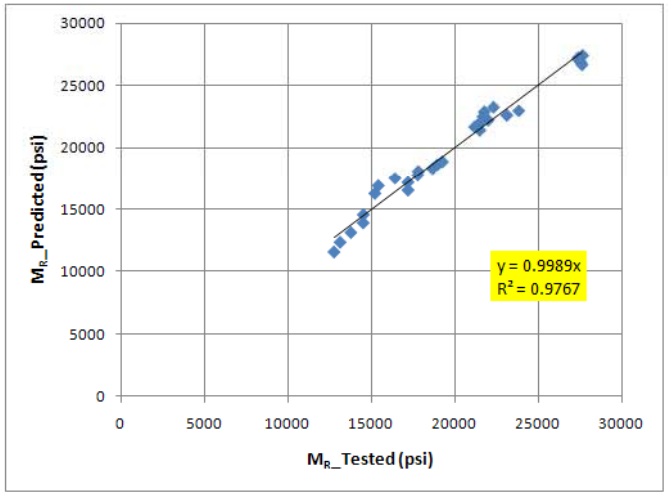

Figure D29. Resilient Modulus Properties of Subgrade Material on Section 86190000.

K1	4.65
K2	3.16
K3	-0.87
K4	36.34

$$M_R = K_1 P_a \left(\frac{\theta + 3K_4 SV_W}{P_a} \right)^{K_2} \left(\frac{\tau_{OCT}}{P_a} + 1 \right)^{K_3}$$

	Axial stress	Test sequence	Confining pressure (psi)	Bulk stress (psi)	M_R_Tested (psi)	Oct. shear stress (psi)	Soil suction (psi)	Vol. water content	M_R_Pred. (psi)	Error
OPTIMUM	8.0	1.0	6.0	20.0	24679.4	0.9	4.28607	0.16154	24624	3056.3985
	9.7	2.0	6.0	21.7	24772.5	1.8	4.28607	0.16154	24923	22727.172
	11.6	3.0	6.0	23.6	24982.8	2.6	4.28607	0.16154	25279	87674.253
	13.5	4.0	6.0	25.5	25039.3	3.5	4.28607	0.16154	25674	403176.12
	15.4	5.0	6.0	27.4	25414.4	4.4	4.28607	0.16154	26110	484000.6
	5.9	6.0	4.0	13.9	20480.1	0.9	4.28607	0.16154	20050	185053.61
	7.7	7.0	4.0	15.7	20391.1	1.7	4.28607	0.16154	20375	245.65197
	9.6	8.0	4.0	17.6	20897.1	2.6	4.28607	0.16154	20745	23024.287
	11.5	9.0	4.0	19.5	21770.9	3.5	4.28607	0.16154	21152	382519.11
	13.4	10.0	4.0	21.4	22511.9	4.4	4.28607	0.16154	21598	834851.56
	3.8	11.0	2.0	7.8	15805.1	0.9	4.28607	0.16154	16088	79828.962
	5.6	12.0	2.0	9.6	15979.5	1.7	4.28607	0.16154	16423	196952.7
	7.5	13.0	2.0	11.5	16738.5	2.6	4.28607	0.16154	16797	3444.4676
	9.4	14.0	2.0	13.4	17911.1	3.5	4.28607	0.16154	17204	499680.55
	11.4	15.0	2.0	15.4	18726.2	4.4	4.28607	0.16154	17648	1162831.1
FIELD	7.9	1.0	6.0	19.9	20904.4	0.9	3.8991	0.16412	20246	432946.47
	9.7	2.0	6.0	21.7	21152.2	1.8	3.8991	0.16412	20581	326123.63
	11.6	3.0	6.0	23.6	21030.7	2.6	3.8991	0.16412	20951	6304.5268
	13.5	4.0	6.0	25.5	20969.4	3.6	3.8991	0.16412	21371	161519.77
	15.5	5.0	6.0	27.5	21381.7	4.5	3.8991	0.16412	21828	198872.67
	5.9	6.0	4.0	13.9	16486.5	0.9	3.8991	0.16412	16264	49488.931
	7.7	7.0	4.0	15.7	16533.8	1.7	3.8991	0.16412	16599	4315.5031
	9.6	8.0	4.0	17.6	17109.8	2.6	3.8991	0.16412	16978	17257.161
	11.6	9.0	4.0	19.6	17855.5	3.6	3.8991	0.16412	17407	201428.73
	13.5	10.0	4.0	21.5	18341.0	4.5	3.8991	0.16412	17844	247445.09
	3.8	11.0	2.0	7.8	12103.0	0.9	3.8991	0.16412	12845	550252.06
	5.6	12.0	2.0	9.6	12443.5	1.7	3.8991	0.16412	13174	533535.37
	7.5	13.0	2.0	11.5	13078.1	2.6	3.8991	0.16412	13549	221680.85
	9.4	14.0	2.0	13.4	13652.8	3.5	3.8991	0.16412	13949	87945.845
	11.3	15.0	2.0	15.3	13590.4	4.4	3.8991	0.16412	14350	577262.5
									SSE	7985445.7
									SEE	515.92783

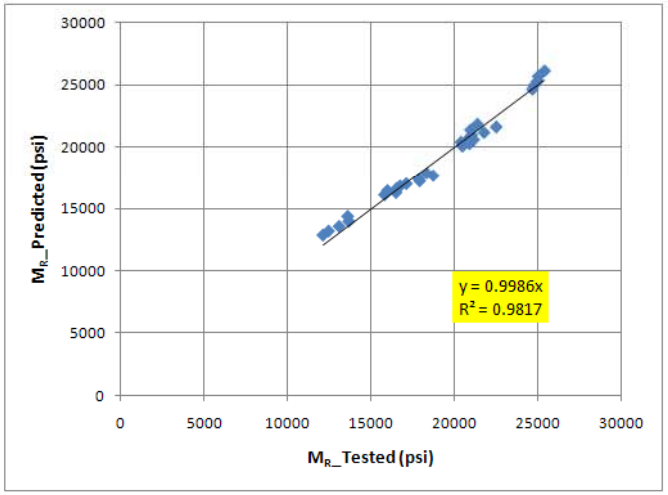

Figure D30. Resilient Modulus Properties of Embankment Material on Section 86190000.

K1	0.66
K2	3.46
K3	-1.06
K4	65.68

$$M_R = K_1 P_a \left(\frac{\theta + 3K_4 SV_W}{P_a} \right)^{K_2} \left(\frac{\tau_{OCT}}{P_a} + 1 \right)^{K_3}$$

	Axial stress	Test sequence	Confining pressure (psi)	Bulk stress (psi)	M_R_Tested (psi)	Oct. shear stress (psi)	Soil suction (psi)	Vol. water content	M_R_Pred. (psi)	Error
OPTIMUM	5.9	1.0	3	11.8818	20720.45385	1.4	2.94424	0.213	19814	821344
	8.3	2.0	3	14.2829	20038.72092	2.5	2.94424	0.213	19573	217285
	10.9	3.0	3	16.8835	20721.65714	3.7	2.94424	0.213	19394	1762918
	9.6	4.0	5	19.591	24786.58944	2.2	2.94424	0.213	22770	4067534
	13.9	5.0	5	23.8916	25007.77115	4.2	2.94424	0.213	22335	7141996
	18.4	6.0	5	28.4396	25876.69496	6.3	2.94424	0.213	22114	14161304
	19.0	7.0	10	39.0419	33921.79048	4.3	2.94424	0.213	31206	7375369
	28.1	8.0	10	48.0841	35097.75589	8.5	2.94424	0.213	30292	23096889
	37.3	9.0	10	57.29	36021.27272	12.9	2.94424	0.213	30224	33609508
	24.1	10.0	15	54.1219	40080.79733	4.3	2.94424	0.213	42325	5038610
	28.5	11.0	15	58.5258	40636.02722	6.4	2.94424	0.213	41227	348726
	42.3	12.0	15	72.2564	43044.77889	12.8	2.94424	0.213	39820	10396118
	33.6	13.0	20	73.599	47065.59509	6.4	2.94424	0.213	54193	50795387
	38.1	14.0	20	78.1125	48065.82841	8.5	2.94424	0.213	52887	23242303
	56.3	15.0	20	96.2916	51109.63664	17.1	2.94424	0.213	50988	14893
FIELD	29.9	1.0	20	69.939	83554.51	4.7	4.42651	0.163	76592	48470926
	39.9	2.0	20	79.906	72320.635	9.4	4.42651	0.163	71177	1307768
	50.0	3.0	20	89.944	65994.285	14.1	4.42651	0.163	68477	6166022
	24.9	4.0	15	54.931	61960.385	4.7	4.42651	0.163	59440	6354113
	34.9	5.0	15	64.925	56612.35	9.4	4.42651	0.163	55883	531575
	45.0	6.0	15	74.949	55574.585	14.1	4.42651	0.163	54352	1495096
	14.9	7.0	10	34.870	49749.355	2.3	4.42651	0.163	47214	6429318
	19.8	8.0	10	39.826	45760.84	4.6	4.42651	0.163	45247	264514
	29.9	9.0	10	49.877	43607.155	9.4	4.42651	0.163	43100	257644
	39.9	10.0	10	59.861	44637.235	14.1	4.42651	0.163	42438	4838142
	9.9	11.0	5	19.884	35033.45	2.3	4.42651	0.163	34760	74546
	15.0	12.0	5	24.949	30026.89	4.7	4.42651	0.163	33585	12657941
	19.9	13.0	5	29.867	30384.17	7.0	4.42651	0.163	32900	6330334
	7.9	14.0	3	13.907	27184.6	2.3	4.42651	0.163	30507	11038661
	9.9	15.0	3	15.909	25767.66	3.3	4.42651	0.163	30088	18668497
	11.9	16.0	3	17.893	25830.3	4.2	4.42651	0.163	29751	15370864
									SSE	3.22E+08
									SEE	3224.63

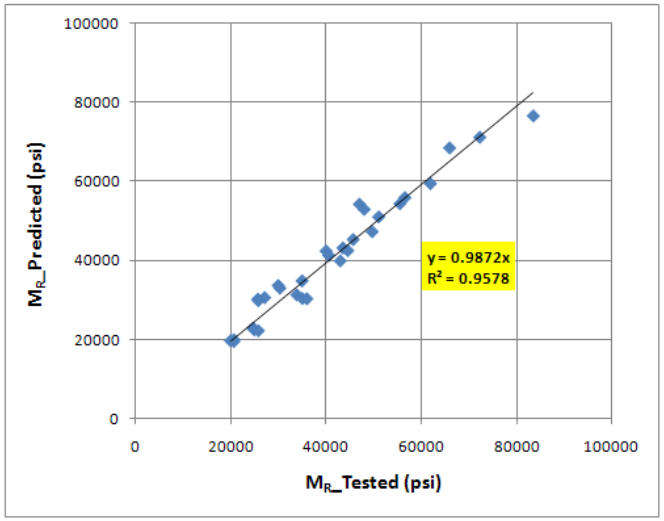

Figure D31. Resilient Modulus Properties of Base Material on Section 77002000.

K1	463.53
K2	1.11
K3	-0.48
K4	0.76

$$M_R = K_1 P_a \left(\frac{\theta + 3K_4 SV_W}{P_a} \right)^{K_2} \left(\frac{\tau_{OCT}}{P_a} + 1 \right)^{K_3}$$

	Axial stress	Test sequence	Confining pressure (psi)	Bulk stress (psi)	M_R_Tested (psi)	Oct. shear stress (psi)	Soil suction (psi)	Vol. water content	M_R_Pred. (psi)	Error
OPTIMUM	21.7	1.0	15	51.749	43927.10	3.2	118.196	0.123	43202	525645
	24.7	2.0	15	54.730	43186.24	4.6	118.196	0.123	43276	8145
	29.8	3.0	15	59.750	43575.96	7.0	118.196	0.123	43525	2554
	14.7	4.0	10	34.746	36715.71	2.2	118.196	0.123	34644	4291372
	16.7	5.0	10	36.721	35598.91	3.2	118.196	0.123	34849	562024
	19.7	6.0	10	39.736	34913.59	4.6	118.196	0.123	35194	78414
	24.7	7.0	10	44.742	35849.25	6.9	118.196	0.123	35829	408
	7.7	8.0	5	17.717	28749.10	1.3	118.196	0.123	25900	8119461
	9.7	9.0	5	19.726	27015.44	2.2	118.196	0.123	26292	523673
	11.7	10.0	5	21.743	26382.92	3.2	118.196	0.123	26690	94135
	14.8	11.0	5	24.756	26332.73	4.6	118.196	0.123	27289	915406
	4.7	12.0	2	8.728	20119.08	1.3	118.196	0.123	20892	597970
	6.7	13.0	2	10.719	19596.64	2.2	118.196	0.123	21395	3234589
	8.7	14.0	2	12.740	19954.46	3.2	118.196	0.123	21901	3787402
FIELD	21.7	1.0	15.00	51.722	36350.39	3.2	85.0549	0.132	38913	6566612
	24.7	2.0	15.00	54.689	37366.12	4.6	85.0549	0.132	39124	3088465
	29.7	3.0	15.00	59.706	39021.81	6.9	85.0549	0.132	39572	302770
	14.7	4.0	10.00	34.711	29850.30	2.2	85.0549	0.132	30350	249241
	16.7	5.0	10.00	36.707	30686.12	3.2	85.0549	0.132	30653	1071
	19.7	6.0	10.00	39.711	31901.81	4.6	85.0549	0.132	31128	598079
	24.7	7.0	10.00	44.710	33826.35	6.9	85.0549	0.132	31953	3508070
	7.7	8.0	5.00	17.703	21403.67	1.3	85.0549	0.132	21628	50176
	9.7	9.0	5.00	19.700	22564.00	2.2	85.0549	0.132	22115	201358
	11.7	10.0	5.00	21.711	23674.10	3.2	85.0549	0.132	22603	1147488
	14.7	11.0	5.00	24.709	25236.36	4.6	85.0549	0.132	23323	3662147
	4.7	12.0	2.00	8.712	15079.13	1.3	85.0549	0.132	16716	2678697
	6.7	13.0	2.00	10.702	16691.73	2.2	85.0549	0.132	17309	381483
	8.7	14.0	2.00	12.715	18175.19	3.2	85.0549	0.132	17898	76806
									SSE	45253663
									SEE	1208.22

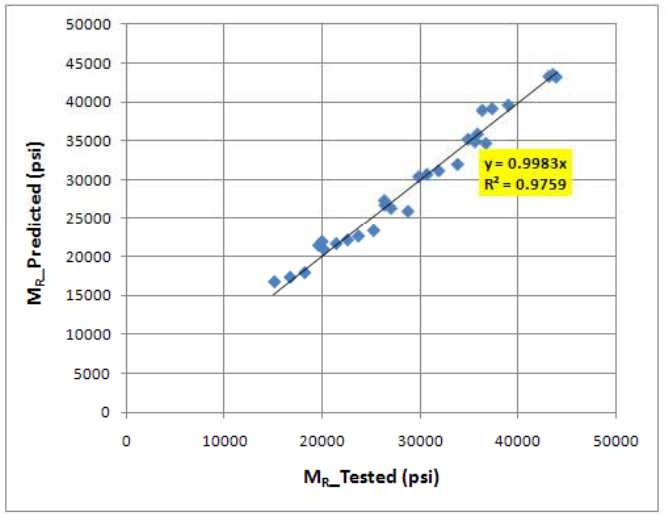

Figure D32. Resilient Modulus Properties of Subgrade Material on Section 77002000.

K1	1210.09
K2	0.60
K3	-0.13
K4	9.14

$$M_R = K_1 P_a \left(\frac{\theta + 3K_4 SV_W}{P_a} \right)^{K_2} \left(\frac{\tau_{OCT}}{P_a} + 1 \right)^{K_3}$$

	Axial stress	Test sequence	Confining pressure (psi)	Bulk stress (psi)	M_R_Tested (psi)	Oct. shear stress (psi)	Soil suction (psi)	Vol. water content	M_R_Pred. (psi)	Error
OPTIMUM	14.8	1.0	5	24.750	23848.05	4.6	0.99378	0.149	25532	2836441
	4.7	2.0	2	8.717	16301.92	1.3	0.99378	0.149	16074	51985
	6.7	3.0	2	10.724	16918.92	2.2	0.99378	0.149	17410	241034
	8.9	4.0	2	12.867	17599.59	3.2	0.99378	0.149	18737	1293177
	21.7	5.0	15	51.722	37349.54	3.2	0.99378	0.149	38359	1019229
	24.7	6.0	15	54.712	37449.04	4.6	0.99378	0.149	39176	2983766
	29.7	7.0	15	59.710	38435.75	6.9	0.99378	0.149	40508	4294307
	14.7	8.0	10	34.731	30528.31	2.2	0.99378	0.149	31069	292489
	16.7	9.0	10	36.729	30013.27	3.2	0.99378	0.149	31787	3144556
	19.7	10.0	10	39.740	30254.62	4.6	0.99378	0.149	32834	6654244
	24.8	11.0	10	44.758	32323.18	7.0	0.99378	0.149	34500	4739743
	7.7	12.0	5	17.717	23060.92	1.3	0.99378	0.149	22140	847505
	9.7	13.0	5	19.712	22631.32	2.2	0.99378	0.149	23157	276201
	11.7	14.0	5	21.735	22553.43	3.2	0.99378	0.149	24141	2520486
FIELD	21.7	1.0	15.00	51.722	38349.38	3.2	1.21403	0.139	38592	58820
	24.7	2.0	15.00	54.689	39460.57	4.6	1.21403	0.139	39396	4160
	29.7	3.0	15.00	59.706	41274.22	6.9	1.21403	0.139	40722	304696
	14.7	4.0	10.00	34.711	31266.58	2.2	1.21403	0.139	31334	4588
	16.7	5.0	10.00	36.707	32174.42	3.2	1.21403	0.139	32044	17062
	19.7	6.0	10.00	39.711	33496.45	4.6	1.21403	0.139	33079	174141
	24.7	7.0	10.00	44.710	35593.08	6.9	1.21403	0.139	34725	753127
	7.7	8.0	5.00	17.703	22149.11	1.3	1.21403	0.139	22478	108410
	9.7	9.0	5.00	19.700	23394.81	2.2	1.21403	0.139	23482	7556
	11.7	10.0	5.00	21.711	24588.77	3.2	1.21403	0.139	24448	19877
	14.7	11.0	5.00	24.709	26272.50	4.6	1.21403	0.139	25815	208882
	4.7	12.0	2.00	8.712	15406.41	1.3	1.21403	0.139	16497	1189439
	6.7	13.0	2.00	10.702	17117.27	2.2	1.21403	0.139	17795	459731
	8.7	14.0	2.00	12.715	18696.47	3.2	1.21403	0.139	19023	106496
									SSE	34612151
									SEE	1056.66

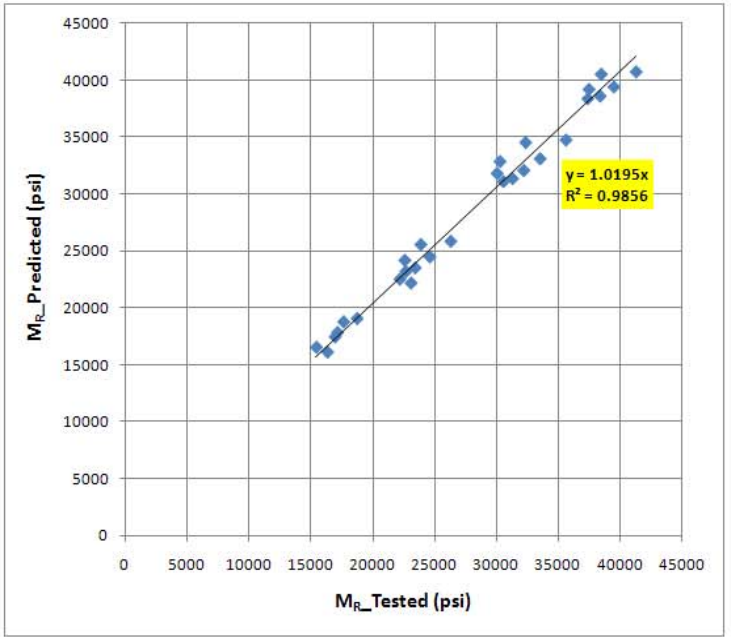

Figure D33. Resilient Modulus Properties of Embankment Material on Section 77002000.

K1	3.06
K2	2.85
K3	-0.66
K4	37.39

$$M_R = K_1 P_a \left(\frac{\theta + 3K_4 SV_W}{P_a} \right)^{K_2} \left(\frac{\tau_{OCT}}{P_a} + 1 \right)^{K_3}$$

	Axial stress	Test sequence	Confining pressure (psi)	Bulk stress (psi)	M_R_Tested (psi)	Oct. shear stress (psi)	Soil suction (psi)	Vol. water content	M_R_Pred. (psi)	Error
OPTIMUM	5.8	1.0	3	11.8337	18026.22009	1.3	8.07559	0.134	23101	25751513
	8.4	2.0	3	14.366	18234.2246	2.5	8.07559	0.134	23238	25034749
	11.1	3.0	3	17.0668	19621.82891	3.8	8.07559	0.134	23442	14596635
	9.6	4.0	5	19.648	23179.21559	2.2	8.07559	0.134	26260	9488657
	14.1	5.0	5	24.0713	24316.398	4.3	8.07559	0.134	26541	4947170
	18.8	6.0	5	28.7686	25807.60696	6.5	8.07559	0.134	27004	1432228
	19.1	7.0	10	39.1373	33531.95863	4.3	8.07559	0.134	35129	2550683
	28.4	8.0	10	48.393	35516.28485	8.7	8.07559	0.134	35932	172995
	37.5	9.0	10	57.4925	37774.61436	13.0	8.07559	0.134	37292	232745
	24.2	10.0	15	54.188	41431.19596	4.3	8.07559	0.134	45334	15235661
	28.7	11.0	15	58.7071	41661.33729	6.5	8.07559	0.134	45423	14146992
	42.5	12.0	15	72.4684	44797.01342	12.9	8.07559	0.134	46925	4530229
	33.7	13.0	20	73.7403	48353.03207	6.5	8.07559	0.134	57075	76076400
	38.3	14.0	20	78.3286	49759.93924	8.6	8.07559	0.134	57172	54932497
	56.6	15.0	20	96.5593	53015.44439	17.2	8.07559	0.134	59578	43072397
FIELD	29.8	1.0	20	69.836	66099.41	4.6	12.5808	0.089	61415	21939799
	39.9	2.0	20	79.848	64864.155	9.4	12.5808	0.089	61231	13200702
	49.9	3.0	20	89.851	64723.65	14.1	12.5808	0.089	62250	6121386
	24.9	4.0	15	54.915	55508.9	4.7	12.5808	0.089	48931	43274565
	34.9	5.0	15	64.848	53890.265	9.4	12.5808	0.089	49349	20624674
	44.8	6.0	15	74.773	55433.065	14.0	12.5808	0.089	50680	22593687
	14.3	7.0	10	34.308	48589.645	2.0	12.5808	0.089	38218	107569141
	19.9	8.0	10	39.926	43052.82	4.7	12.5808	0.089	38232	23242735
	29.9	9.0	10	49.939	43340.355	9.4	12.5808	0.089	39089	18074131
	39.9	10.0	10	59.870	45957.75	14.1	12.5808	0.089	40634	28347393
	9.3	11.0	5	19.324	31364.515	2.0	12.5808	0.089	28880	6174659
	14.9	12.0	5	24.921	29181.25	4.7	12.5808	0.089	29178	9
	19.9	13.0	5	29.935	30257.15	7.0	12.5808	0.089	29668	346764
	8.1	14.0	3	14.084	25530.585	2.4	12.5808	0.089	25645	12995
	9.5	15.0	3	15.536	24058.4	3.1	12.5808	0.089	25728	2788070
	11.5	16.0	3	17.451	24904.62	4.0	12.5808	0.089	25866	924477
									SSE	607436735
									SEE	4426.59

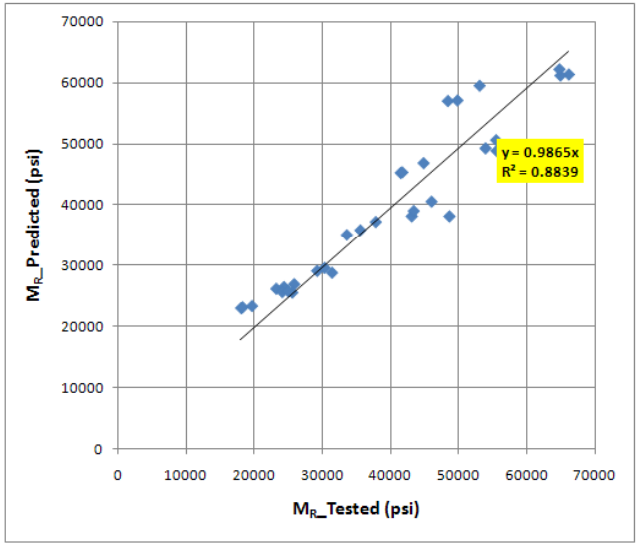

Figure D34. Resilient Modulus Properties of Base Material on Section 92060000.

K1	1565.43
K2	0.61
K3	-0.26
K4	0.14

$$M_R = K_1 P_a \left(\frac{\theta + 3K_4 SV_W}{P_a} \right)^{K_2} \left(\frac{\tau_{OCT}}{P_a} + 1 \right)^{K_3}$$

	Axial stress	Test sequence	Confining pressure (psi)	Bulk stress (psi)	M_R_Tested (psi)	Oct. shear stress (psi)	Soil suction (psi)	Vol. water content	M_R_Pred. (psi)	Error
OPTIMUM	21.7	1.0	15.0	51.724	48427.69	3.2	10.4533	0.172	46988	2072953
	24.7	2.0	15.0	54.731	48348.36	4.6	10.4533	0.172	47632	513280
	29.8	3.0	15.0	59.755	49386.12	7.0	10.4533	0.172	48691	483859
	14.7	4.0	10.0	34.720	39111.34	2.2	10.4533	0.172	37600	2285512
	16.7	5.0	10.0	36.736	38387.59	3.2	10.4533	0.172	38323	4158
	19.7	6.0	10.0	39.723	38239.21	4.6	10.4533	0.172	39350	1233180
	24.7	7.0	10.0	44.730	40154.90	6.9	10.4533	0.172	40964	655396
	7.7	8.0	5.0	17.708	27266.50	1.3	10.4533	0.172	25702	2448658
	9.7	9.0	5.0	19.714	26448.04	2.2	10.4533	0.172	26947	248519
	11.7	10.0	5.0	21.738	26672.71	3.2	10.4533	0.172	28121	2096367
	14.8	11.0	5.0	24.751	27727.15	4.6	10.4533	0.172	29740	4051548
	4.7	12.0	2.0	8.723	18715.67	1.3	10.4533	0.172	17157	2429973
	6.7	13.0	2.0	10.727	18920.90	2.2	10.4533	0.172	18981	3649
	8.7	14.0	2.0	12.719	20045.11	3.2	10.4533	0.172	20617	327608
FIELD	21.7	1.0	15.0	51.722	46248.85	3.2	41.3457	0.132	47812	2442072
	24.7	2.0	15.0	54.689	47592.91	4.6	41.3457	0.132	48414	674050
	29.7	3.0	15.0	59.706	49786.88	6.9	41.3457	0.132	49422	133051
	14.7	4.0	10.0	34.711	37684.53	2.2	41.3457	0.132	38572	788424
	16.7	5.0	10.0	36.707	38781.97	3.2	41.3457	0.132	39255	223761
	19.7	6.0	10.0	39.711	40380.27	4.6	41.3457	0.132	40242	19191
	24.7	7.0	10.0	44.710	42915.41	6.9	41.3457	0.132	41789	1268239
	7.7	8.0	5.0	17.703	26668.61	1.3	41.3457	0.132	26972	92112
	9.7	9.0	5.0	19.700	28173.01	2.2	41.3457	0.132	28144	814
	11.7	10.0	5.0	21.711	29615.14	3.2	41.3457	0.132	29253	131202
	14.7	11.0	5.0	24.709	31649.20	4.6	41.3457	0.132	30791	737240
	4.7	12.0	2.0	8.712	18530.36	1.3	41.3457	0.132	18781	62979
	6.7	13.0	2.0	10.702	20594.48	2.2	41.3457	0.132	20461	17908
	8.7	14.0	2.0	12.715	22500.29	3.2	41.3457	0.132	22007	243014
									SSE	25688718
									SEE	910.31

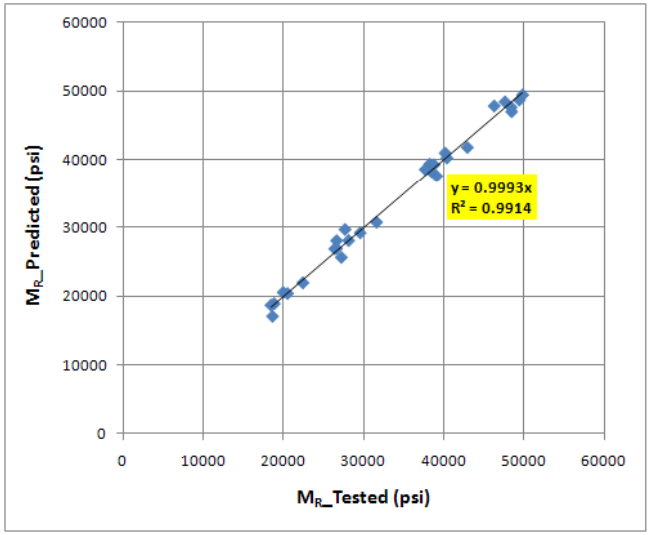

Figure D35. Resilient Modulus Properties of Subgrade Material on Section 92060000.

K1	68.16
K2	1.69
K3	-0.17
K4	366.00

$$M_R = K_1 P_a \left(\frac{\theta + 3K_4 SV_W}{P_a} \right)^{K_2} \left(\frac{\tau_{OCT}}{P_a} + 1 \right)^{K_3}$$

	Axial stress	Test sequence	Confining pressure (psi)	Bulk stress (psi)	M_R_Tested (psi)	Oct. shear stress (psi)	Soil suction (psi)	Vol. water content	M_R_Pred. (psi)	Error
OPTIMUM	21.7	1.0	15.0	51.739	27126.69	3.2	0.22743	0.215	27568	194559
	24.7	2.0	15.0	54.743	27554.26	4.6	0.22743	0.215	28537	965121
	29.7	3.0	15.0	59.739	28842.22	6.9	0.22743	0.215	30199	1840138
	14.7	4.0	10.0	34.730	21876.67	2.2	0.22743	0.215	20651	1502436
	16.7	5.0	10.0	36.730	21719.45	3.2	0.22743	0.215	21250	220123
	19.7	6.0	10.0	39.726	22223.46	4.6	0.22743	0.215	22166	3260
	24.8	7.0	10.0	44.757	23659.65	7.0	0.22743	0.215	23751	8289
	7.7	8.0	5.0	17.734	15273.44	1.3	0.22743	0.215	14523	563201
	9.7	9.0	5.0	19.723	15531.90	2.2	0.22743	0.215	15067	216205
	11.7	10.0	5.0	21.742	15728.86	3.2	0.22743	0.215	15629	10062
	14.8	11.0	5.0	24.750	16760.10	4.6	0.22743	0.215	16482	77163
	4.7	12.0	2.0	8.719	11280.34	1.3	0.22743	0.215	11555	75209
	6.7	13.0	2.0	10.725	11788.71	2.2	0.22743	0.215	12071	79900
	8.8	14.0	2.0	12.772	12353.64	3.2	0.22743	0.215	12608	64820
FIELD	21.7	1.0	15.0	51.722	33840.49	3.2	0.30072	0.207	34328	237998
	24.7	2.0	15.0	54.689	34805.50	4.6	0.30072	0.207	35320	264814
	29.7	3.0	15.0	59.706	36379.64	6.9	0.30072	0.207	37055	455802
	14.7	4.0	10.0	34.711	27678.61	2.2	0.30072	0.207	26742	877961
	16.7	5.0	10.0	36.707	28469.54	3.2	0.30072	0.207	27371	1207800
	19.7	6.0	10.0	39.711	29620.69	4.6	0.30072	0.207	28338	1645732
	24.7	7.0	10.0	44.710	31444.89	6.9	0.30072	0.207	29999	2092028
	7.7	8.0	5.0	17.703	19713.31	1.3	0.30072	0.207	19888	30551
	9.7	9.0	5.0	19.700	20804.22	2.2	0.30072	0.207	20475	108391
	11.7	10.0	5.0	21.711	21848.97	3.2	0.30072	0.207	21077	596601
	14.7	11.0	5.0	24.709	23320.95	4.6	0.30072	0.207	21992	1767108
	4.7	12.0	2.0	8.712	13790.13	1.3	0.30072	0.207	16492	7297970
	6.7	13.0	2.0	10.702	15296.31	2.2	0.30072	0.207	17053	3084574
	8.7	14.0	2.0	12.715	16684.49	3.2	0.30072	0.207	17630	893919
									SSE	26381738
									SEE	922.51

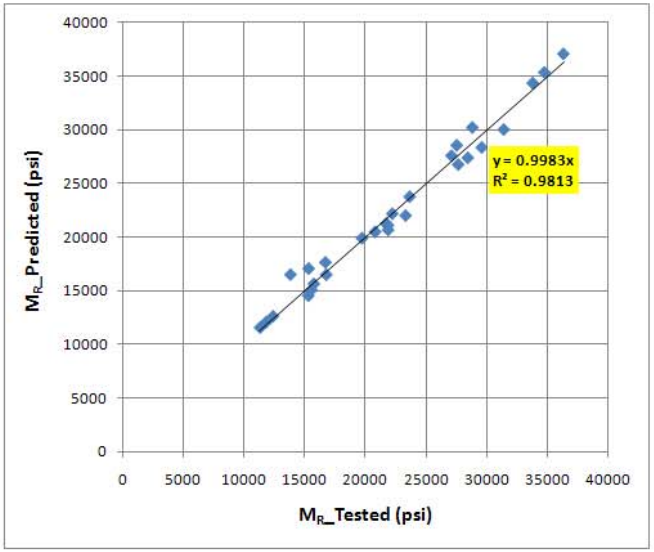

Figure D36. Resilient Modulus Properties of Embankment Material on Section 92060000.

K1	486.06
K2	1.00
K3	-0.24
K4	10.04

$$M_R = K_1 P_a \left(\frac{\theta + 3K_4 SV_W}{P_a} \right)^{K_2} \left(\frac{\tau_{OCT}}{P_a} + 1 \right)^{K_3}$$

	Axial stress	Test sequence	Confining pressure (psi)	Bulk stress (psi)	M_R_Tested (psi)	Oct. shear stress (psi)	Soil suction (psi)	Vol. water content	M_R_Pred. (psi)	Error
OPTIMUM	5.4	1.0	3.0	11.4	14804.5	1.2	3.62154	0.19763	15740	874432
	8.0	2.0	3.0	14.0	14680.2	2.4	3.62154	0.19763	16652	3886910
	10.8	3.0	3.0	16.8	16080.4	3.7	3.62154	0.19763	17653	2471840
	9.3	4.0	5.0	19.3	19490.4	2.0	3.62154	0.19763	19227	69288
	14.0	5.0	5.0	24.0	20780.0	4.2	3.62154	0.19763	20779	1.66107
	18.8	6.0	5.0	28.8	22157.4	6.5	3.62154	0.19763	22342	33902
	19.1	7.0	10.0	39.1	30828.0	4.3	3.62154	0.19763	27685	9880726
	28.6	8.0	10.0	48.6	32368.4	8.8	3.62154	0.19763	30373	3981410
	38.1	9.0	10.0	58.1	33367.8	13.3	3.62154	0.19763	33044	105132
	24.2	10.0	15.0	54.2	37771.5	4.3	3.62154	0.19763	34542	1E+07
	28.8	11.0	15.0	58.8	37726.4	6.5	3.62154	0.19763	35682	4178212
	42.9	12.0	15.0	72.9	40028.8	13.2	3.62154	0.19763	39216	661037
	33.9	13.0	20.0	73.9	44939.8	6.5	3.62154	0.19763	42346	6726913
	38.5	14.0	20.0	78.5	45469.6	8.7	3.62154	0.19763	43351	4490296
	57.4	15.0	20.0	97.4	47966.0	17.6	3.62154	0.19763	47595	137636
FIELD	5.5	1.0	3.0	11.5	9960	1.2	1.89084	0.22115	11495	2357695
	8.3	2.0	3.0	14.3	11579	2.5	1.89084	0.22115	12583	1007079
	11.3	3.0	3.0	17.3	13116	3.9	1.89084	0.22115	13687	325983
	9.4	4.0	5.0	19.4	13269	2.1	1.89084	0.22115	15045	3154504
	14.2	5.0	5.0	24.2	15447	4.3	1.89084	0.22115	16771	1753403
	19.1	6.0	5.0	29.1	16791	6.6	1.89084	0.22115	18481	2854006
	19.3	7.0	10.0	39.3	22382	4.4	1.89084	0.22115	23631	1560668
	28.9	8.0	10.0	48.9	25311	8.9	1.89084	0.22115	26595	1648853
	38.3	9.0	10.0	58.3	27015	13.3	1.89084	0.22115	29366	5529492
	24.2	10.0	15.0	54.2	28200	4.3	1.89084	0.22115	30460	5109442
	29.0	11.0	15.0	59.0	30116	6.6	1.89084	0.22115	31744	2649198
	42.9	12.0	15.0	72.9	34343	13.1	1.89084	0.22115	35487	1310459
	33.9	13.0	20.0	73.9	37097	6.6	1.89084	0.22115	38383	1652188
	38.5	14.0	20.0	78.5	39192	8.7	1.89084	0.22115	39468	76604.6
	57.1	15.0	20.0	97.1	42859	17.5	1.89084	0.22115	43936	1160339
									SSE	8E+07
									SEE	1633.81

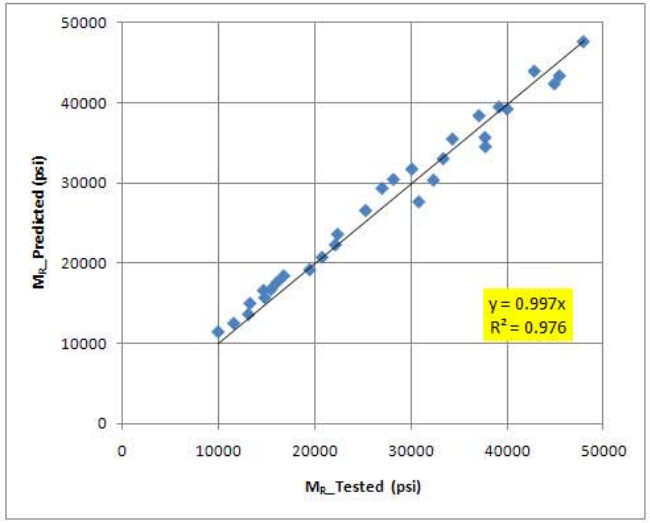

Figure D37. Resilient Modulus Properties of Base Material on Section 79270000.

K1	1076.49
K2	0.73
K3	-0.91
K4	0.04

$$M_R = K_1 P_a \left(\frac{\theta + 3K_4 SV_W}{P_a} \right)^{K_2} \left(\frac{\tau_{OCT}}{P_a} + 1 \right)^{K_3}$$

	Axial stress	Test sequence	Confining pressure (psi)	Bulk stress (psi)	M_R_Tested (psi)	Oct. shear stress (psi)	Soil suction (psi)	Vol. water content	M_R_Pred. (psi)	Error
OPTIMUM	7.9	1.0	6.0	19.9	19800.2	0.9	55.1599	0.14579	19330	221087
	9.7	2.0	6.0	21.7	19733.6	1.7	55.1599	0.14579	19558	30963.3
	11.5	3.0	6.0	23.5	19767.7	2.6	55.1599	0.14579	19747	420.524
	13.3	4.0	6.0	25.3	19944.3	3.5	55.1599	0.14579	19900	1923.83
	15.2	5.0	6.0	27.2	20499.8	4.3	55.1599	0.14579	20029	221489
	5.9	6.0	4.0	13.9	15640.4	0.9	55.1599	0.14579	15097	294862
	7.7	7.0	4.0	15.7	15178.6	1.7	55.1599	0.14579	15630	203828
	9.5	8.0	4.0	17.5	15541.9	2.6	55.1599	0.14579	16091	301772
	11.4	9.0	4.0	19.4	16461.6	3.5	55.1599	0.14579	16486	598.054
	13.2	10.0	4.0	21.2	17408.3	4.3	55.1599	0.14579	16820	346012
	3.8	11.0	2.0	7.8	10575.3	0.8	55.1599	0.14579	10318	66138.8
	5.6	12.0	2.0	9.6	10642.2	1.7	55.1599	0.14579	11260	381133
	7.5	13.0	2.0	11.5	11295.6	2.6	55.1599	0.14579	12077	609951
	9.3	14.0	2.0	13.3	12507.1	3.5	55.1599	0.14579	12772	70353.6
	11.2	15.0	2.0	15.2	13518.0	4.3	55.1599	0.14579	13373	21113.2
FIELD	7.9	1.0	6.0	19.9	19112.3	0.9	35.6918	0.16431	19141	851.375
	9.7	2.0	6.0	21.7	19001.7	1.7	35.6918	0.16431	19379	142206
	11.5	3.0	6.0	23.5	19108.2	2.6	35.6918	0.16431	19579	221734
	13.3	4.0	6.0	25.3	19383.9	3.4	35.6918	0.16431	19743	128956
	15.2	5.0	6.0	27.2	19936.9	4.3	35.6918	0.16431	19881	3152.91
	5.9	6.0	4.0	13.9	15577.5	0.9	35.6918	0.16431	14882	484109
	7.7	7.0	4.0	15.7	15256.3	1.7	35.6918	0.16431	15433	31160.3
	9.5	8.0	4.0	17.5	15557.9	2.6	35.6918	0.16431	15902	118554
	11.3	9.0	4.0	19.3	16369.1	3.4	35.6918	0.16431	16307	3798.97
	13.2	10.0	4.0	21.2	17150.5	4.3	35.6918	0.16431	16658	242851
	3.8	11.0	2.0	7.8	10926.6	0.8	35.6918	0.16431	10081	715026
	5.6	12.0	2.0	9.6	11002.5	1.7	35.6918	0.16431	11037	1187.7
	7.5	13.0	2.0	11.5	11629.8	2.6	35.6918	0.16431	11867	56318.6
	9.3	14.0	2.0	13.3	12708.5	3.4	35.6918	0.16431	12566	20421.4
	11.1	15.0	2.0	15.1	13443.5	4.3	35.6918	0.16431	13167	76667.2
									SSE	5018641
									SEE	409.009

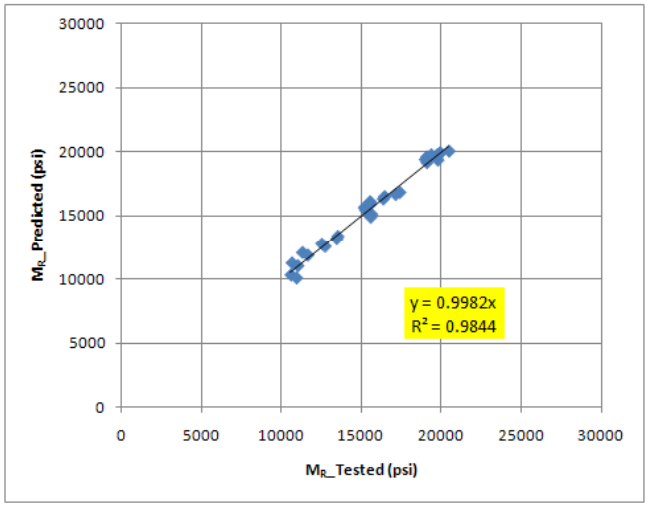

Figure D38. Resilient Modulus Properties of Subgrade Material on Section 79270000.

K1	1035.95
K2	0.79
K3	-1.11
K4	6.76

$$M_R = K_1 P_a \left(\frac{\theta + 3K_4 SV_W}{P_a} \right)^{K_2} \left(\frac{\tau_{OCT}}{P_a} + 1 \right)^{K_3}$$

	Axial stress	Test sequence	Confining pressure (psi)	Bulk stress (psi)	M_R_Tested (psi)	Oct. shear stress (psi)	Soil suction (psi)	Vol. water content	M_R_Pred. (psi)	Error
OPTIMUM	7.9	1.0	6.0	19.9	18965.8	0.9	0.15397	0.22405	18530	190114
	9.8	2.0	6.0	21.8	18787.7	1.8	0.15397	0.22405	18653	18186.1
	11.6	3.0	6.0	23.6	18843.5	2.6	0.15397	0.22405	18735	11707.2
	13.4	4.0	6.0	25.4	18943.0	3.5	0.15397	0.22405	18786	24557.1
	15.2	5.0	6.0	27.2	19370.6	4.4	0.15397	0.22405	18814	310304
	5.9	6.0	4.0	13.9	14268.4	0.9	0.15397	0.22405	14127	20088.6
	7.7	7.0	4.0	15.7	14264.8	1.7	0.15397	0.22405	14595	108917
	9.6	8.0	4.0	17.6	14750.1	2.6	0.15397	0.22405	14979	52609.8
	11.4	9.0	4.0	19.4	15567.7	3.5	0.15397	0.22405	15296	73572.2
	13.2	10.0	4.0	21.2	16257.0	4.4	0.15397	0.22405	15555	492389
	3.8	11.0	2.0	7.8	9489.7	0.8	0.15397	0.22405	9264	51152.9
	5.6	12.0	2.0	9.6	9872.9	1.7	0.15397	0.22405	10156	80237.2
	7.5	13.0	2.0	11.5	10653.0	2.6	0.15397	0.22405	10912	67219.2
	9.3	14.0	2.0	13.3	11464.6	3.4	0.15397	0.22405	11532	4581.32
	11.1	15.0	2.0	15.1	11720.6	4.3	0.15397	0.22405	12053	110449
FIELD	7.9	1.0	6.0	19.9	18499.4	0.9	0.19426	0.21894	18644	20885.7
	9.7	2.0	6.0	21.7	18554.7	1.7	0.19426	0.21894	18756	40519.1
	11.5	3.0	6.0	23.5	18437.8	2.6	0.19426	0.21894	18832	155479
	13.3	4.0	6.0	25.3	18425.6	3.4	0.19426	0.21894	18877	204116
	15.1	5.0	6.0	27.1	18755.2	4.3	0.19426	0.21894	18899	20756.4
	5.9	6.0	4.0	13.9	14482.8	0.9	0.19426	0.21894	14243	57439
	7.6	7.0	4.0	15.6	14272.8	1.7	0.19426	0.21894	14692	175996
	9.5	8.0	4.0	17.5	14665.8	2.6	0.19426	0.21894	15069	162663
	11.3	9.0	4.0	19.3	15380.6	3.4	0.19426	0.21894	15379	2.57239
	13.1	10.0	4.0	21.1	15873.6	4.3	0.19426	0.21894	15631	58971.7
	3.8	11.0	2.0	7.8	10156.0	0.8	0.19426	0.21894	9399	573131
	5.6	12.0	2.0	9.6	10345.0	1.7	0.19426	0.21894	10282	3928.97
	7.4	13.0	2.0	11.4	11020.9	2.6	0.19426	0.21894	11020	0.93836
	9.2	14.0	2.0	13.2	11612.5	3.4	0.19426	0.21894	11620	60.6344
	11.0	15.0	2.0	15.0	11797.9	4.2	0.19426	0.21894	12127	108048
									SSE	3198082
									SEE	326.501

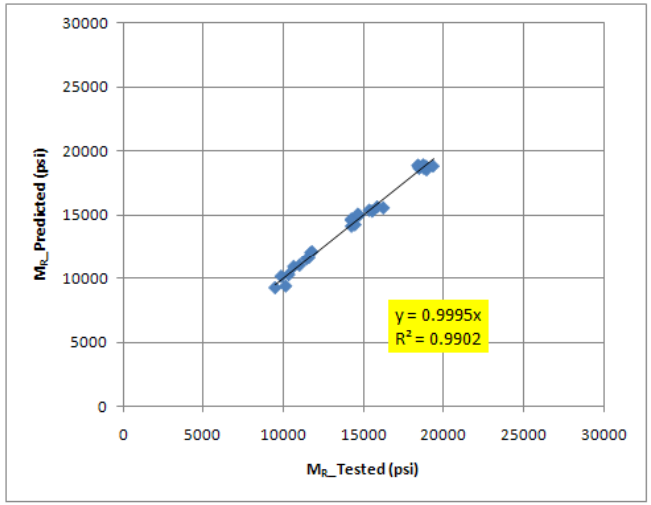

Figure D39. Resilient Modulus Properties of Embankment Material on Section 79270000.

K1	561.78
K2	1.46
K3	-1.21
K4	12.39

$$M_R = K_1 P_a \left(\frac{\theta + 3K_4 SV_W}{P_a} \right)^{K_2} \left(\frac{\tau_{OCT}}{P_a} + 1 \right)^{K_3}$$

	Axial stress	Test sequence	Confining pressure (psi)	Bulk stress (psi)	M_R_Tested (psi)	Oct. shear stress (psi)	Soil suction (psi)	Vol. water content	M_R_Pred. (psi)	Error
OPTIMUM	5.6	1.0	3	11.69409	15887.8345	1.2	0.01	0.161	5448	108993435
	8.2	2.0	3	14.25348	16001.0206	2.5	0.01	0.161	6603	88317433
	11.0	3.0	3	17.06162	17249.8768	3.8	0.01	0.161	7836	88618948
	9.5	4.0	5	19.47283	19642.7049	2.1	0.01	0.161	10637	81106932
	14.2	5.0	5	24.06812	21286.7237	4.3	0.01	0.161	12451	78065829
	19.0	6.0	5	28.8807	22642.6688	6.6	0.01	0.161	14129	72479650
	19.2	7.0	10	39.09174	29644.5427	4.3	0.01	0.161	25185	19889719
	28.8	8.0	10	48.49106	31399.516	8.9	0.01	0.161	26533	23685672
	38.2	9.0	10	57.61622	33406.0378	13.3	0.01	0.161	27610	33593805
	24.2	10.0	15	54.12046	36230.9454	4.3	0.01	0.161	40418	17534270
	28.9	11.0	15	58.68819	35516.4463	6.5	0.01	0.161	39739	17826629
	43.2	12.0	15	72.55943	39350.4812	13.3	0.01	0.161	38588	580726
	33.9	13.0	20	73.67923	42548.7296	6.5	0.01	0.161	55363	164212765
	38.6	14.0	20	78.31329	43590.1707	8.7	0.01	0.161	53593	100051228
	57.4	15.0	20	96.5638	47382.6952	17.6	0.01	0.161	49084	2895824
FIELD	29.9	1.0	20	69.903	123495.485	4.7	9.174052	0.131	117798	32457367
	39.9	2.0	20	79.892	101170.125	9.4	9.174052	0.131	101927	573533
	49.9	3.0	20	89.884	91927.535	14.1	9.174052	0.131	91672	65125
	24.9	4.0	15	54.873	99901.955	4.7	9.174052	0.131	96101	14450742
	34.9	5.0	15	64.877	84421.03	9.4	9.174052	0.131	84591	28815
	44.9	6.0	15	74.913	80263.01	14.1	9.174052	0.131	77177	9526266
	14.9	7.0	10	34.872	88180.735	2.3	9.174052	0.131	81340	46794387
	19.9	8.0	10	39.919	76625.105	4.7	9.174052	0.131	75753	760092
	29.9	9.0	10	49.928	68682.005	9.4	9.174052	0.131	68263	175243
	39.9	10.0	10	59.932	67304.94	14.1	9.174052	0.131	63508	14419896
	9.9	11.0	5	19.903	58176.03	2.3	9.174052	0.131	60012	3372106
	14.9	12.0	5	24.906	51839.24	4.7	9.174052	0.131	57045	27104808
	19.9	13.0	5	29.912	50725.785	7.0	9.174052	0.131	54822	16775768
	7.9	14.0	3	13.911	48128.835	2.3	9.174052	0.131	52085	15647447
	9.9	15.0	3	15.898	45727.2	3.3	9.174052	0.131	51193	29878491
	11.9	16.0	3	17.909	45147.635	4.2	9.174052	0.131	50400	27591243
									SSE	1.137E+09
									SEE	6057.45

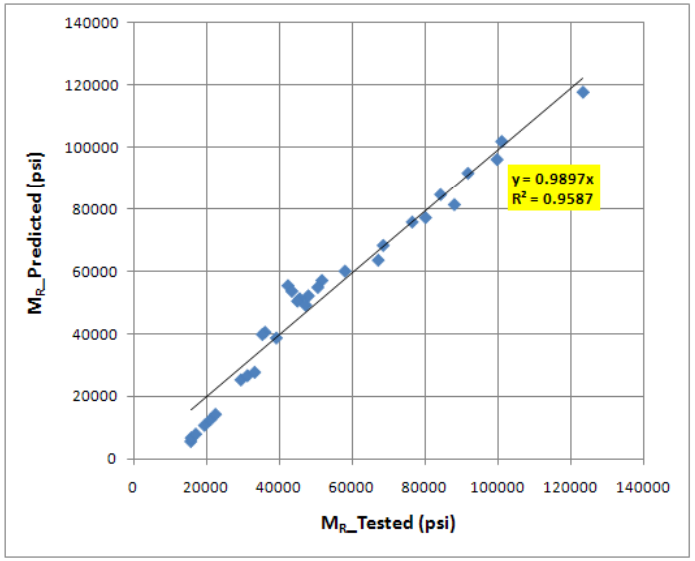

Figure D40. Resilient Modulus Properties of Base Material on Section 87120000.

K1	1372.02
K2	0.63
K3	-0.24
K4	-0.58

$$M_R = K_1 P_a \left(\frac{\theta + 3K_4 SV_W}{P_a} \right)^{K_2} \left(\frac{\tau_{OCT}}{P_a} + 1 \right)^{K_3}$$

	Axial stress	Test sequence	Confining pressure (psi)	Bulk stress (psi)	M_R_Tested (psi)	Oct. shear stress (psi)	Soil suction (psi)	Vol. water content	M_R_Pred. (psi)	Error
OPTIMUM	5.2	1.0	3.0	11.2	15870	1.1	8.95185	0.14309	14479	1935498.8
	7.8	2.0	3.0	13.8	16430	2.3	8.95185	0.14309	16655	50449.362
	10.7	3.0	3.0	16.7	18175	3.6	8.95185	0.14309	18837	438433.77
	9.1	4.0	5.0	19.1	21164	2.0	8.95185	0.14309	21278	13091.434
	14.4	5.0	5.0	24.4	23370	4.4	8.95185	0.14309	24391	1043217.7
	19.6	6.0	5.0	29.6	24784	6.9	8.95185	0.14309	27102	5371850.6
	19.3	7.0	10.0	39.3	32849	4.4	8.95185	0.14309	33825	952825.64
	29.4	8.0	10.0	49.4	35716	9.2	8.95185	0.14309	37323	2581248.8
	38.9	9.0	10.0	58.9	36990	13.6	8.95185	0.14309	40184	10205306
	24.6	10.0	15.0	54.6	38934	4.5	8.95185	0.14309	42028	9577588.6
	29.5	11.0	15.0	59.5	40668	6.8	8.95185	0.14309	43262	6730029.5
	43.4	12.0	15.0	73.4	44568	13.4	8.95185	0.14309	46531	3852598.3
	34.4	13.0	20.0	74.4	47039	6.8	8.95185	0.14309	50118	9477731.2
	39.2	14.0	20.0	79.2	48808	9.0	8.95185	0.14309	50935	4524864.3
	57.7	15.0	20.0	97.7	51870	17.8	8.95185	0.14309	54097	4958476
FIELD	5.4	1.0	3.0	11.4	17011.1	1.1	9.42431	0.11619	14936	4307566.7
	7.8	2.0	3.0	13.8	17409.9	2.3	9.42431	0.11619	16973	190527.72
	10.7	3.0	3.0	16.7	19185.8	3.6	9.42431	0.11619	19095	8212.964
	9.2	4.0	5.0	19.2	22826.9	2.0	9.42431	0.11619	21566	1590254.9
	14.5	5.0	5.0	24.5	25143.7	4.5	9.42431	0.11619	24712	185984.54
	19.7	6.0	5.0	29.7	26979.0	6.9	9.42431	0.11619	27351	138252.2
	19.5	7.0	10.0	39.5	36312.3	4.5	9.42431	0.11619	34104	4876346.4
	29.8	8.0	10.0	49.8	39241.9	9.3	9.42431	0.11619	37597	2706091.4
	39.3	9.0	10.0	59.3	41391.0	13.8	9.42431	0.11619	40459	867994.56
	24.7	10.0	15.0	54.7	44801.0	4.6	9.42431	0.11619	42212	6702742.9
	29.8	11.0	15.0	59.8	45398.8	7.0	9.42431	0.11619	43479	3687089.4
	44.3	12.0	15.0	74.3	49052.3	13.8	9.42431	0.11619	46860	4807080
	34.6	13.0	20.0	74.6	52961.9	6.9	9.42431	0.11619	50290	7137547.1
	39.8	14.0	20.0	79.8	54232.3	9.3	9.42431	0.11619	51179	9321006.3
	58.7	15.0	20.0	98.7	57976.0	18.2	9.42431	0.11619	54380	12929058
									SSE	121168964
									SEE	2009.7178

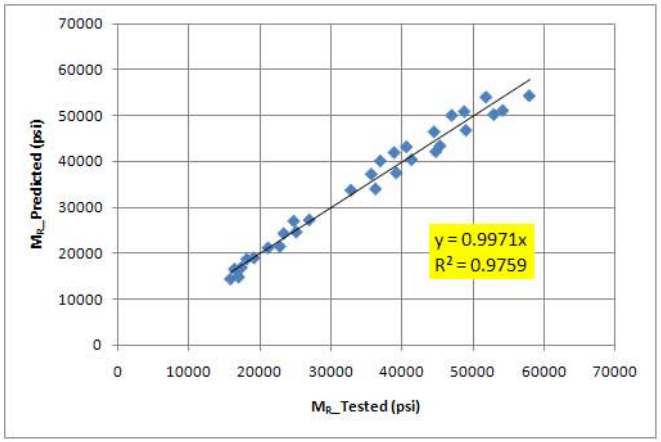

Figure D41. Resilient Modulus Properties of Base Material on Section 87060000.

K1	1696.72
K2	0.74
K3	-1.55
K4	0.15

$$M_R = K_1 P_a \left(\frac{\theta + 3K_4 SV_W}{P_a} \right)^{K_2} \left(\frac{\tau_{OCT}}{P_a} + 1 \right)^{K_3}$$

	Axial stress	Test sequence	Confining pressure (psi)	Bulk stress (psi)	M_R_Tested (psi)	Oct. shear stress (psi)	Soil suction (psi)	Vol. water content	M_R_Pred. (psi)	Error
OPTIMUM	7.7	1.0	6.0	19.7	29544.3	0.8	25.2767	0.14856	30239	481897.38
	9.6	2.0	6.0	21.6	28578.2	1.7	25.2767	0.14856	29506	861639.5
	11.4	3.0	6.0	23.4	27842.1	2.5	25.2767	0.14856	28833	982118.29
	13.2	4.0	6.0	25.2	27331.5	3.4	25.2767	0.14856	28156	679342.32
	15.1	5.0	6.0	27.1	27313.3	4.3	25.2767	0.14856	27477	26723.305
	5.8	6.0	4.0	13.8	23698.1	0.8	25.2767	0.14856	23682	245.97644
	7.5	7.0	4.0	15.5	22483.9	1.7	25.2767	0.14856	23652	1365385.8
	9.3	8.0	4.0	17.3	22351.8	2.5	25.2767	0.14856	23532	1391835.6
	11.2	9.0	4.0	19.2	22872.7	3.4	25.2767	0.14856	23336	214165.91
	13.1	10.0	4.0	21.1	23386.1	4.3	25.2767	0.14856	23089	88035.33
	3.7	11.0	2.0	7.7	16775.9	0.8	25.2767	0.14856	16387	151372.58
	5.4	12.0	2.0	9.4	15983.6	1.6	25.2767	0.14856	17136	1327374.8
	7.1	13.0	2.0	11.1	16274.5	2.4	25.2767	0.14856	17699	2029271.2
	9.0	14.0	2.0	13.0	17521.8	3.3	25.2767	0.14856	18106	341114.1
	10.9	15.0	2.0	14.9	18401.6	4.2	25.2767	0.14856	18368	1096.7645
FIELD	7.8	1.0	6.0	19.8	31361.9	0.8	24.0319	0.15012	30155	1457374.1
	9.8	2.0	6.0	21.8	30275.9	1.8	24.0319	0.15012	29376	810547.92
	11.7	3.0	6.0	23.7	29192.3	2.7	24.0319	0.15012	28672	271206.42
	13.6	4.0	6.0	25.6	28522.8	3.6	24.0319	0.15012	27972	303652.83
	15.5	5.0	6.0	27.5	28172.0	4.5	24.0319	0.15012	27263	827003.82
	5.8	6.0	4.0	13.8	25011.0	0.9	24.0319	0.15012	23607	1970598.1
	7.7	7.0	4.0	15.7	23448.0	1.8	24.0319	0.15012	23575	16072.007
	9.6	8.0	4.0	17.6	23017.0	2.6	24.0319	0.15012	23443	181436.84
	11.5	9.0	4.0	19.5	23525.0	3.6	24.0319	0.15012	23237	83048.181
	13.6	10.0	4.0	21.6	23920.7	4.5	24.0319	0.15012	22965	914258.73
	3.8	11.0	2.0	7.8	18576.6	0.9	24.0319	0.15012	16386	4797797.3
	5.6	12.0	2.0	9.6	17232.1	1.7	24.0319	0.15012	17155	5901.5728
	7.6	13.0	2.0	11.6	17208.8	2.6	24.0319	0.15012	17743	285484.1
	9.8	14.0	2.0	13.8	18406.5	3.7	24.0319	0.15012	18172	54767.663
	11.7	15.0	2.0	15.7	19122.7	4.6	24.0319	0.15012	18395	530166.53
									SSE	22450935
									SEE	865.08063

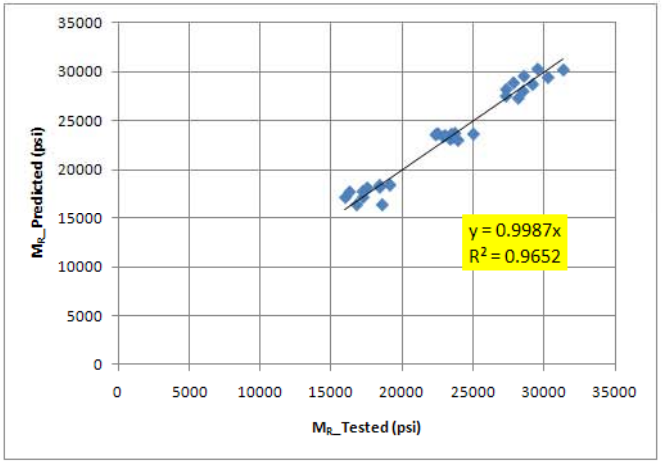

Figure D42. Resilient Modulus Properties of Subgrade Material on Section 87060000.

K1	1634.73
K2	0.78
K3	-1.55
K4	0.18

$$M_R = K_1 P_a \left(\frac{\theta + 3K_4 SV_W}{P_a} \right)^{K_2} \left(\frac{\tau_{OCT}}{P_a} + 1 \right)^{K_3}$$

	Axial stress	Test sequence	Confining pressure (psi)	Bulk stress (psi)	M_R_Tested (psi)	Oct. shear stress (psi)	Soil suction (psi)	Vol. water content	M_R_Pred. (psi)	Error
OPTIMUM	7.7	1.0	6.0	19.7	29544.3	0.8	30.2154	0.14856	30230	470331.26
	9.6	2.0	6.0	21.6	28578.2	1.7	30.2154	0.14856	29510	868939.59
	11.4	3.0	6.0	23.4	27842.1	2.5	30.2154	0.14856	28851	1017277.7
	13.2	4.0	6.0	25.2	27331.5	3.4	30.2154	0.14856	28189	734573.35
	15.1	5.0	6.0	27.1	27313.3	4.3	30.2154	0.14856	27526	45227.923
	5.8	6.0	4.0	13.8	23698.1	0.8	30.2154	0.14856	23662	1328.3279
	7.5	7.0	4.0	15.5	22483.9	1.7	30.2154	0.14856	23624	1300552.3
	9.3	8.0	4.0	17.3	22351.8	2.5	30.2154	0.14856	23504	1326679.4
	11.2	9.0	4.0	19.2	22872.7	3.4	30.2154	0.14856	23313	194096.46
	13.1	10.0	4.0	21.1	23386.1	4.3	30.2154	0.14856	23077	95779.504
	3.7	11.0	2.0	7.7	16775.9	0.8	30.2154	0.14856	16475	90625.038
	5.4	12.0	2.0	9.4	15983.6	1.6	30.2154	0.14856	17170	1406707.9
	7.1	13.0	2.0	11.1	16274.5	2.4	30.2154	0.14856	17698	2026451.5
	9.0	14.0	2.0	13.0	17521.8	3.3	30.2154	0.14856	18084	316500.26
	10.9	15.0	2.0	14.9	18401.6	4.2	30.2154	0.14856	18338	4070.4209
FIELD	7.8	1.0	6.0	19.8	31361.9	0.8	28.997	0.15012	30140	1493992.3
	9.8	2.0	6.0	21.8	30275.9	1.8	28.997	0.15012	29374	812572.49
	11.7	3.0	6.0	23.7	29192.3	2.7	28.997	0.15012	28686	256860.9
	13.6	4.0	6.0	25.6	28522.8	3.6	28.997	0.15012	28002	270993.08
	15.5	5.0	6.0	27.5	28172.0	4.5	28.997	0.15012	27311	741610.3
	5.8	6.0	4.0	13.8	25011.0	0.9	28.997	0.15012	23580	2048752.7
	7.7	7.0	4.0	15.7	23448.0	1.8	28.997	0.15012	23540	8525.4478
	9.6	8.0	4.0	17.6	23017.0	2.6	28.997	0.15012	23410	154417.49
	11.5	9.0	4.0	19.5	23525.0	3.6	28.997	0.15012	23211	98674.474
	13.6	10.0	4.0	21.6	23920.7	4.5	28.997	0.15012	22950	942454.18
	3.8	11.0	2.0	7.8	18576.6	0.9	28.997	0.15012	16462	4469871
	5.6	12.0	2.0	9.6	17232.1	1.7	28.997	0.15012	17178	2970.7049
	7.6	13.0	2.0	11.6	17208.8	2.6	28.997	0.15012	17731	272582.74
	9.8	14.0	2.0	13.8	18406.5	3.7	28.997	0.15012	18141	70426.132
	11.7	15.0	2.0	15.7	19122.7	4.6	28.997	0.15012	18358	585143.52
									SSE	22128988
									SEE	858.8556

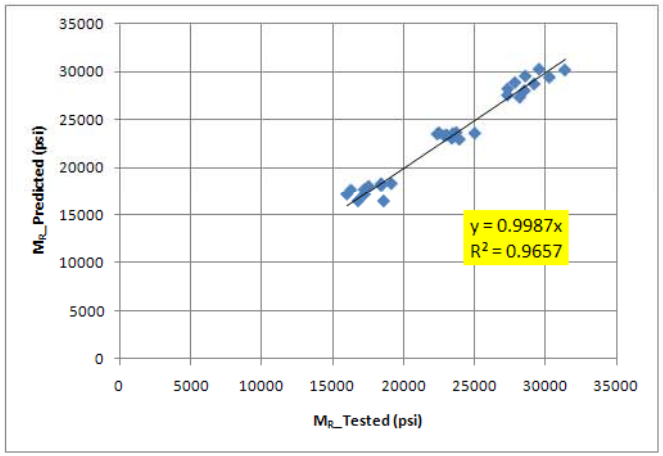

Figure D43. Resilient Modulus Properties of Embankment Material on Section 87060000.

K1	868.69
K2	0.75
K3	-0.17
K4	0.71

$$M_R = K_1 P_a \left(\frac{\theta + 3K_4 SV_W}{P_a} \right)^{K_2} \left(\frac{\tau_{OCT}}{P_a} + 1 \right)^{K_3}$$

	Axial stress	Test sequence	Confining pressure (psi)	Bulk stress (psi)	M_R_Tested (psi)	Oct. shear stress (psi)	Soil suction (psi)	Vol. water content	M_R_Pred. (psi)	Error
OPTIMUM	5.3	1.0	3.0	11.3	12678	1.1	2.2647	0.17908	10901	3158950.646
	7.8	2.0	3.0	13.8	13034	2.3	2.2647	0.17908	12423	373290.9491
	10.7	3.0	3.0	16.7	15159	3.7	2.2647	0.17908	14034	1265339.402
	9.2	4.0	5.0	19.2	16234	2.0	2.2647	0.17908	15709	275966.9927
	13.9	5.0	5.0	23.9	18434	4.2	2.2647	0.17908	18008	181900.1154
	19.2	6.0	5.0	29.2	21434	6.7	2.2647	0.17908	20404	1061078.513
	19.1	7.0	10.0	39.1	25672	4.3	2.2647	0.17908	25755	6883.313438
	29.1	8.0	10.0	49.1	29599	9.0	2.2647	0.17908	29343	65888.71993
	38.4	9.0	10.0	58.4	32930	13.4	2.2647	0.17908	32437	243034.3818
	24.2	10.0	15.0	54.2	32214	4.3	2.2647	0.17908	32734	270625.3876
	29.1	11.0	15.0	59.1	32787	6.7	2.2647	0.17908	34256	2156963.257
	43.2	12.0	15.0	73.2	37577	13.3	2.2647	0.17908	38349	595459.1453
	34.0	13.0	20.0	74.0	38791	6.6	2.2647	0.17908	40460	2784724.32
	38.9	14.0	20.0	78.9	40100	8.9	2.2647	0.17908	41701	2563291.279
	57.4	15.0	20.0	97.4	44910	17.6	2.2647	0.17908	46240	1770428.472
FIELD	5.3	1.0	3.0	11.3	14279.1	1.1	26.441	0.11526	14466	34961.79164
	7.8	2.0	3.0	13.8	14587.7	2.3	26.441	0.11526	15790	1445151.037
	11.0	3.0	3.0	17.0	15784.3	3.8	26.441	0.11526	17359	2479803.541
	9.1	4.0	5.0	19.1	18268.9	1.9	26.441	0.11526	18850	338034.9586
	14.1	5.0	5.0	24.1	20105.9	4.3	26.441	0.11526	21066	921083.1513
	19.2	6.0	5.0	29.2	21914.2	6.7	26.441	0.11526	23198	1648596.424
	19.4	7.0	10.0	39.4	29373.7	4.4	26.441	0.11526	28536	702049.5735
	28.8	8.0	10.0	48.8	32314.9	8.9	26.441	0.11526	31693	386229.6036
	38.1	9.0	10.0	58.1	34565.4	13.3	26.441	0.11526	34613	2251.144009
	24.4	10.0	15.0	54.4	36276.9	4.4	26.441	0.11526	35265	1023285.047
	29.2	11.0	15.0	59.2	37195.8	6.7	26.441	0.11526	36627	324106.1436
	43.1	12.0	15.0	73.1	40888.8	13.2	26.441	0.11526	40449	192993.3664
	34.2	13.0	20.0	74.2	44174.9	6.7	26.441	0.11526	42741	2056505.465
	38.9	14.0	20.0	78.9	45305.8	8.9	26.441	0.11526	43870	2061084.787
	57.3	15.0	20.0	97.3	49454.3	17.6	26.441	0.11526	48187	1607246.774
									SSE	31997207.70
									SEE	1032.750497

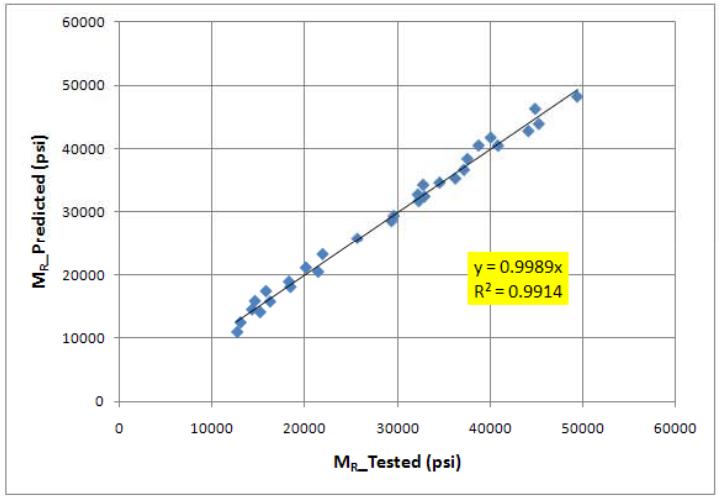

Figure D44. Resilient Modulus Properties of Base Material on Section 90060000.

K1	746.57
K2	0.82
K3	-0.18
K4	13.48

$$M_R = K_1 P_a \left(\frac{\theta + 3K_4 SV_W}{P_a} \right)^{K_2} \left(\frac{\tau_{OCT}}{P_a} + 1 \right)^{K_3}$$

	Axial stress	Test sequence	Confining pressure (psi)	Bulk stress (psi)	M_R_Tested (psi)	Oct. shear stress (psi)	Soil suction (psi)	Vol. water content	M_R_Pred. (psi)	Error
OPTIMUM	5.3	1.0	3.0	11.3	12678	1.1	0.6301	0.17908	11494	1403506.39
	7.8	2.0	3.0	13.8	13034	2.3	0.6301	0.17908	12820	45781.41762
	10.7	3.0	3.0	16.7	15159	3.7	0.6301	0.17908	14253	820785.4908
	9.2	4.0	5.0	19.2	16234	2.0	0.6301	0.17908	15854	144078.5439
	13.9	5.0	5.0	23.9	18434	4.2	0.6301	0.17908	17965	220113.6142
	19.2	6.0	5.0	29.2	21434	6.7	0.6301	0.17908	20209	1500651.957
	19.1	7.0	10.0	39.1	25672	4.3	0.6301	0.17908	25519	23409.33258
	29.1	8.0	10.0	49.1	29599	9.0	0.6301	0.17908	29020	335573.1971
	38.4	9.0	10.0	58.4	32930	13.4	0.6301	0.17908	32093	699727.1796
	24.2	10.0	15.0	54.2	32214	4.3	0.6301	0.17908	32566	124009.02
	29.1	11.0	15.0	59.1	32787	6.7	0.6301	0.17908	34076	1659866.952
	43.2	12.0	15.0	73.2	37577	13.3	0.6301	0.17908	38197	383459.1606
	34.0	13.0	20.0	74.0	38791	6.6	0.6301	0.17908	40518	2982344.353
	38.9	14.0	20.0	78.9	40100	8.9	0.6301	0.17908	41775	2807924.978
	57.4	15.0	20.0	97.4	44910	17.6	0.6301	0.17908	46441	2346021.552
FIELD	5.3	1.0	3.0	11.3	14279.1	1.1	2.2072	0.11526	14798	269470.8903
	7.8	2.0	3.0	13.8	14587.7	2.3	2.2072	0.11526	15991	1969826.043
	11.0	3.0	3.0	17.0	15784.3	3.8	2.2072	0.11526	17426	2695658.115
	9.1	4.0	5.0	19.1	18268.9	1.9	2.2072	0.11526	18897	394823.203
	14.1	5.0	5.0	24.1	20105.9	4.3	2.2072	0.11526	20969	744942.2445
	19.2	6.0	5.0	29.2	21914.2	6.7	2.2072	0.11526	22996	1170337.886
	19.4	7.0	10.0	39.4	29373.7	4.4	2.2072	0.11526	28360	1028508.881
	28.8	8.0	10.0	48.8	32314.9	8.9	2.2072	0.11526	31464	723600.4671
	38.1	9.0	10.0	58.1	34565.4	13.3	2.2072	0.11526	34381	34186.51978
	24.4	10.0	15.0	54.4	36276.9	4.4	2.2072	0.11526	35221	1114313.893
	29.2	11.0	15.0	59.2	37195.8	6.7	2.2072	0.11526	36578	381984.3286
	43.1	12.0	15.0	73.1	40888.8	13.2	2.2072	0.11526	40442	199393.5197
	34.2	13.0	20.0	74.2	44174.9	6.7	2.2072	0.11526	42966	1460881.924
	38.9	14.0	20.0	78.9	45305.8	8.9	2.2072	0.11526	44113	1422002.051
	57.3	15.0	20.0	97.3	49454.3	17.6	2.2072	0.11526	48561	797569.1275
									SSE	29904752.2
									SEE	998.4

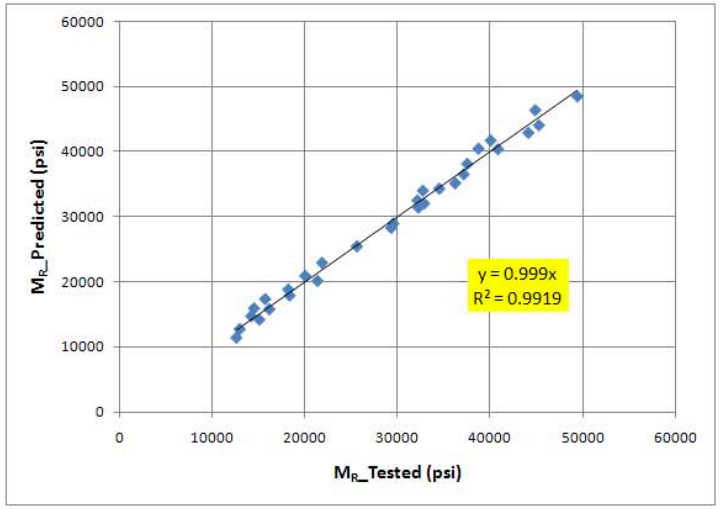

Figure D45. Resilient Modulus Properties of Embankment Material on Section 90060000.

K1	720.33
K2	0.90
K3	-0.39
K4	1.60

$$M_R = K_1 P_a \left(\frac{\theta + 3K_4 SV_W}{P_a} \right)^{K_2} \left(\frac{\tau_{OCT}}{P_a} + 1 \right)^{K_3}$$

	Axial stress	Test sequence	Confining pressure (psi)	Bulk stress (psi)	M_R_Tested (psi)	Oct. shear stress (psi)	Soil suction (psi)	Vol. water content	M_R_Pred. (psi)	Error
OPTIMUM	5.7	1.0	3.0	11.7	19249.4	1.3	26.4128	0.192468	23095	14785374.19
	8.4	2.0	3.0	14.4	19729.2	2.5	26.4128	0.192468	23908	17464895.59
	11.1	3.0	3.0	17.1	21419.9	3.8	26.4128	0.192468	24730	10955980.4
	9.5	4.0	5.0	19.5	25937.6	2.1	26.4128	0.192468	27018	1168193.52
	14.1	5.0	5.0	24.1	27156.6	4.3	26.4128	0.192468	28178	1042839.088
	18.7	6.0	5.0	28.7	29058.3	6.5	26.4128	0.192468	29326	71634.41853
	19.1	7.0	10.0	39.1	38255.5	4.3	26.4128	0.192468	35965	5246040.216
	28.4	8.0	10.0	48.4	39802.6	8.7	26.4128	0.192468	37503	5287325.453
	37.7	9.0	10.0	57.7	40205.9	13.1	26.4128	0.192468	39092	1240619.532
	24.2	10.0	15.0	54.2	44748.7	4.3	26.4128	0.192468	43565	1401865.571
	28.7	11.0	15.0	58.7	45208.5	6.5	26.4128	0.192468	43958	1563174.858
	42.6	12.0	15.0	72.6	47379.4	13.0	26.4128	0.192468	45487	3580165.931
	33.7	13.0	20.0	73.7	52036.1	6.5	26.4128	0.192468	51074	925676.1425
	38.3	14.0	20.0	78.3	52865.7	8.6	26.4128	0.192468	51238	2650293.785
	56.8	15.0	20.0	96.8	54524.8	17.4	26.4128	0.192468	52565	3841799.287
FIELD	5.6	1.0	3.0	11.6	22490	1.2	16.1029	0.211327	18345	17185750.57
	8.2	2.0	3.0	14.2	20967	2.5	16.1029	0.211327	19312	2738424.971
	11.0	3.0	3.0	17.0	21349	3.8	16.1029	0.211327	20295	1110342.323
	9.4	4.0	5.0	19.4	25643	2.1	16.1029	0.211327	22453	10179506.67
	14.0	5.0	5.0	24.0	25092	4.2	16.1029	0.211327	23872	1488864.626
	18.6	6.0	5.0	28.6	25845	6.4	16.1029	0.211327	25231	376968.1651
	19.1	7.0	10.0	39.1	33300	4.3	16.1029	0.211327	31788	2286083.012
	28.3	8.0	10.0	48.3	33461	8.6	16.1029	0.211327	33697	55609.8883
	37.8	9.0	10.0	57.8	34007	13.1	16.1029	0.211327	35613	2579634.198
	24.1	10.0	15.0	54.1	38382	4.3	16.1029	0.211327	39485	1215572.303
	28.7	11.0	15.0	58.7	38125	6.5	16.1029	0.211327	40072	3787648.784
	42.6	12.0	15.0	72.6	40407	13.0	16.1029	0.211327	42050	2701837.721
	33.7	13.0	20.0	73.7	44755	6.5	16.1029	0.211327	47255	6251274.186
	38.3	14.0	20.0	78.3	45378	8.6	16.1029	0.211327	47578	4843487.051
	57.0	15.0	20.0	97.0	46991	17.4	16.1029	0.211327	49400	5804372.546
									SSE	133831255.0
									SEE	2112.1

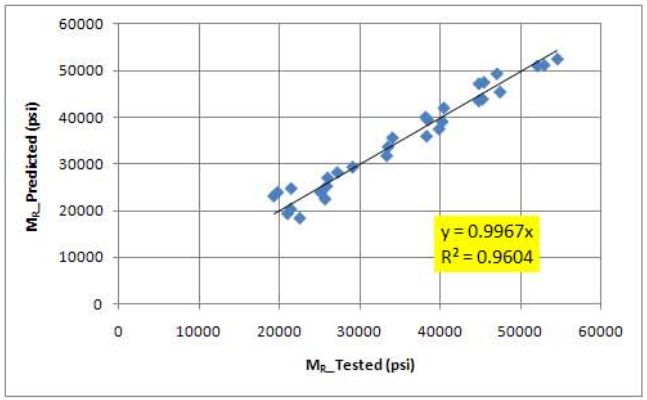

Figure D46. Resilient Modulus Properties of Base Material on Section 10060000.

K1	1298.81
K2	0.47
K3	-0.76
K4	-0.25

$$M_R = K_1 P_a \left(\frac{\theta + 3K_4 SV_W}{P_a} \right)^{K_2} \left(\frac{\tau_{OCT}}{P_a} + 1 \right)^{K_3}$$

	Axial stress	Test sequence	Confining pressure (psi)	Bulk stress (psi)	M_R_Tested (psi)	Oct. shear stress (psi)	Soil suction (psi)	Vol. water content	M_R_Pred. (psi)	Error
OPTIMUM	7.9	1.0	6.0	19.9	19741.1	0.9	21.2512	0.210649	19149	350191.2379
	9.7	2.0	6.0	21.7	19791.6	1.7	21.2512	0.210649	19312	230419.1591
	11.6	3.0	6.0	23.6	19998.5	2.6	21.2512	0.210649	19426	327214.0193
	13.4	4.0	6.0	25.4	20138.5	3.5	21.2512	0.210649	19502	404994.3045
	15.3	5.0	6.0	27.3	20499.4	4.4	21.2512	0.210649	19547	906471.8952
	5.8	6.0	4.0	13.8	15833.2	0.9	21.2512	0.210649	15456	142517.0241
	7.7	7.0	4.0	15.7	15772.8	1.7	21.2512	0.210649	16003	53148.11279
	9.5	8.0	4.0	17.5	16250.2	2.6	21.2512	0.210649	16439	35676.16467
	11.4	9.0	4.0	19.4	17049.8	3.5	21.2512	0.210649	16784	70694.68845
	13.3	10.0	4.0	21.3	17819.2	4.4	21.2512	0.210649	17053	586298.8691
	3.8	11.0	2.0	7.8	11947.7	0.8	21.2512	0.210649	10310	2681820.417
	5.6	12.0	2.0	9.6	12169.7	1.7	21.2512	0.210649	11638	283110.8387
	7.5	13.0	2.0	11.5	12838.5	2.6	21.2512	0.210649	12651	35217.75263
	9.4	14.0	2.0	13.4	13920.4	3.5	21.2512	0.210649	13435	235882.2023
	11.2	15.0	2.0	15.2	14492.6	4.3	21.2512	0.210649	14037	207395.4267
FIELD	7.8	1.0	6.0	19.8	18195.3	0.9	33.6217	0.167574	18663	218516.8472
	9.7	2.0	6.0	21.7	18550.9	1.7	33.6217	0.167574	18871	102395.1108
	11.5	3.0	6.0	23.5	18540.8	2.6	33.6217	0.167574	19024	233738.9375
	13.4	4.0	6.0	25.4	18699.5	3.5	33.6217	0.167574	19134	188704.6791
	15.2	5.0	6.0	27.2	19148.6	4.4	33.6217	0.167574	19207	3442.877525
	5.8	6.0	4.0	13.8	14317.2	0.8	33.6217	0.167574	14824	257121.0929
	7.6	7.0	4.0	15.6	14293.6	1.7	33.6217	0.167574	15449	1336015.353
	9.5	8.0	4.0	17.5	14811.4	2.6	33.6217	0.167574	15953	1302922.218
	11.4	9.0	4.0	19.4	15676.4	3.5	33.6217	0.167574	16344	445646.5366
	13.2	10.0	4.0	21.2	16450.2	4.4	33.6217	0.167574	16650	40067.89292
	3.8	11.0	2.0	7.8	10162.9	0.8	33.6217	0.167574	9259	817875.5355
	5.6	12.0	2.0	9.6	10465.0	1.7	33.6217	0.167574	10815	122612.3234
	7.5	13.0	2.0	11.5	11155.5	2.6	33.6217	0.167574	11983	685506.6024
	9.3	14.0	2.0	13.3	12168.1	3.5	33.6217	0.167574	12852	467733.9281
	11.1	15.0	2.0	15.1	12592.7	4.3	33.6217	0.167574	13504	830959.8431
									SSE	13604311.9
									SEE	673.4

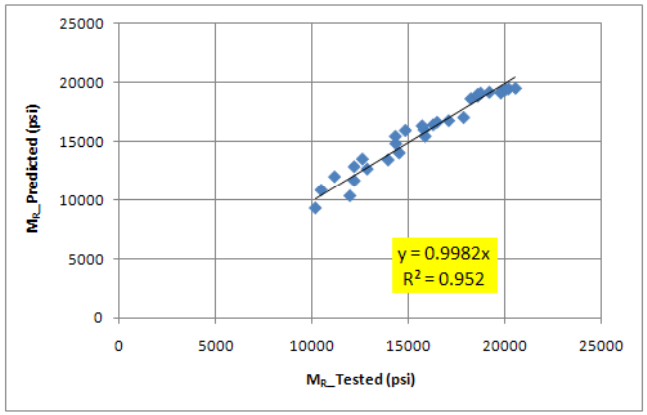

Figure D47. Resilient Modulus Properties of Subgrade Material on Section 10060000.

K1	1022.36
K2	0.72
K3	-2.22
K4	0.06

$$M_R = K_1 P_a \left(\frac{\theta + 3K_4 SV_W}{P_a} \right)^{K_2} \left(\frac{\tau_{OCT}}{P_a} + 1 \right)^{K_3}$$

	Axial stress	Test sequence	Confining pressure (psi)	Bulk stress (psi)	M_R_Tested (psi)	Oct. shear stress (psi)	Soil suction (psi)	Vol. water content	M_R_Pred. (psi)	Error
OPTIMUM	7.9	1.0	6.0	19.9	16391.2	0.9	21.3185	0.210128	16796	163575.217
	9.7	2.0	6.0	21.7	15258.3	1.7	21.3185	0.210128	15824	320369.5408
	11.5	3.0	6.0	23.5	13924.7	2.6	21.3185	0.210128	14932	1013709.087
	13.3	4.0	6.0	25.3	12839.1	3.5	21.3185	0.210128	14122	1645211.443
	15.2	5.0	6.0	27.2	12699.6	4.3	21.3185	0.210128	13361	438069.0971
	5.9	6.0	4.0	13.9	12816.9	0.9	21.3185	0.210128	13120	91699.91124
	7.7	7.0	4.0	15.7	11735.9	1.7	21.3185	0.210128	12653	841342.6158
	9.5	8.0	4.0	17.5	11252.2	2.6	21.3185	0.210128	12174	848991.2596
	11.3	9.0	4.0	19.3	11130.4	3.5	21.3185	0.210128	11693	316664.5745
	13.2	10.0	4.0	21.2	11068.6	4.3	21.3185	0.210128	11226	24646.36385
	3.8	11.0	2.0	7.8	9122.6	0.9	21.3185	0.210128	8972	22729.74158
	5.7	12.0	2.0	9.7	8611.2	1.7	21.3185	0.210120	9132	270932.6041
	7.5	13.0	2.0	11.5	8277.1	2.6	21.3185	0.210128	9145	752803.0427
	9.3	14.0	2.0	13.3	8616.7	3.5	21.3185	0.210128	9062	197892.6256
	11.1	15.0	2.0	15.1	9096.4	4.3	21.3185	0.210128	8919	31578.99459
FIELD	7.9	1.0	6.0	19.9	17609.3	0.9	18.9051	0.233096	16789	672792.023
	9.7	2.0	6.0	21.7	16581.7	1.7	18.9051	0.233096	15834	558529.9126
	11.5	3.0	6.0	23.5	15506.5	2.6	18.9051	0.233096	14932	330093.1226
	13.3	4.0	6.0	25.3	14773.4	3.4	18.9051	0.233096	14128	415957.2459
	15.1	5.0	6.0	27.1	14448.8	4.3	18.9051	0.233096	13383	1135946.741
	5.8	6.0	4.0	13.8	13735.2	0.9	18.9051	0.233096	13118	380423.6376
	7.7	7.0	4.0	15.7	12841.0	1.7	18.9051	0.233096	12658	33367.15283
	9.5	8.0	4.0	17.5	12513.6	2.6	18.9051	0.233096	12181	110292.0231
	11.3	9.0	4.0	19.3	12568.7	3.4	18.9051	0.233096	11699	756238.8642
	13.1	10.0	4.0	21.1	12333.2	4.3	18.9051	0.233096	11243	1188066.316
	3.8	11.0	2.0	7.8	9835.3	0.8	18.9051	0.233096	8959	768527.3189
	5.6	12.0	2.0	9.6	9148.2	1.7	18.9051	0.233096	9121	752.7921598
	7.4	13.0	2.0	11.4	8933.2	2.5	18.9051	0.233096	9140	42753.69794
	9.2	14.0	2.0	13.2	9233.7	3.4	18.9051	0.233096	9064	28901.5528
	11.0	15.0	2.0	15.0	9427.5	4.2	18.9051	0.233096	8927	250677.9291
									SSE	13653536.4
									SEE	674.6

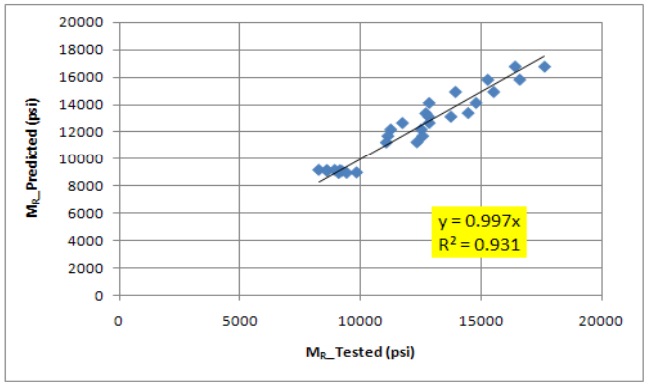

Figure D48. Resilient Modulus Properties of Embankment Material on Section 10060000.

K1	121.38
K2	1.64
K3	-0.53
K4	16.13

$$M_R = K_1 P_a \left(\frac{\theta + 3K_4 SV_W}{P_a} \right)^{K_2} \left(\frac{\tau_{OCT}}{P_a} + 1 \right)^{K_3}$$

	Axial stress	Test sequence	Confining pressure (psi)	Bulk stress (psi)	M_R_Tested (psi)	Oct. shear stress (psi)	Soil suction (psi)	Vol. water content	M_R_Pred. (psi)	Error
OPTIMUM	5.5	1.0	3.0	11.5	16971.8	1.2	4.70411	0.21862	18026	1111093.81
	8.0	2.0	3.0	14.0	16445.9	2.4	4.70411	0.21862	18526	4325926.13
	10.8	3.0	3.0	16.8	17690.5	3.7	4.70411	0.21862	19078	1925452.06
	9.4	4.0	5.0	19.4	22320.7	2.1	4.70411	0.21862	21349	943328.565
	13.9	5.0	5.0	23.9	22775.0	4.2	4.70411	0.21862	22206	324197.38
	18.7	6.0	5.0	28.7	24164.3	6.4	4.70411	0.21862	23166	996020.964
	19.1	7.0	10.0	39.1	33824.2	4.3	4.70411	0.21862	30147	13518615.5
	28.6	8.0	10.0	48.6	34744.8	8.8	4.70411	0.21862	31778	8799675.87
	38.5	9.0	10.0	58.5	35505.2	13.4	4.70411	0.21862	33733	3140076.43
	24.2	10.0	15.0	54.2	41324.2	4.3	4.70411	0.21862	38960	5590934.16
	28.8	11.0	15.0	58.8	41196.9	6.5	4.70411	0.21862	39472	2974898.91
	43.3	12.0	15.0	73.3	42778.8	13.3	4.70411	0.21862	41718	1124930.4
	33.8	13.0	20.0	73.8	48240.7	6.5	4.70411	0.21862	48823	338610.592
	38.5	14.0	20.0	78.5	48466.3	8.7	4.70411	0.21862	49202	541529.859
	57.8	15.0	20.0	97.8	50182.3	17.8	4.70411	0.21862	51904	2965670.19
FIELD	5.5	1.0	3.0	11.5	12324	1.2	3.83284	0.2382	15411	9527181.83
	8.2	2.0	3.0	14.2	13524	2.4	3.83284	0.2382	15965	5958466.51
	11.0	3.0	3.0	17.0	15075	3.8	3.83284	0.2382	16562	2210936.03
	9.4	4.0	5.0	19.4	18118	2.1	3.83284	0.2382	18598	230272.622
	14.0	5.0	5.0	24.0	19869	4.3	3.83284	0.2382	19540	107986.752
	18.7	6.0	5.0	28.7	20277	6.5	3.83284	0.2382	20534	66219.675
	19.1	7.0	10.0	39.1	27912	4.3	3.83284	0.2382	27097	664340.883
	28.5	8.0	10.0	48.5	29888	8.7	3.83284	0.2382	28849	1077919.26
	38.0	9.0	10.0	58.0	30796	13.2	3.83284	0.2382	30817	442.545545
	24.1	10.0	15.0	54.1	34079	4.3	3.83284	0.2382	35574	2237244.29
	28.7	11.0	15.0	58.7	35818	6.5	3.83284	0.2382	36178	129279.394
	42.9	12.0	15.0	72.9	39326	13.2	3.83284	0.2382	38574	566276.193
	33.8	13.0	20.0	73.8	43252	6.5	3.83284	0.2382	45248	3981585.16
	38.4	14.0	20.0	78.4	44929	8.7	3.83284	0.2382	45716	619884.201
	57.1	15.0	20.0	97.1	47423	17.5	3.83284	0.2382	48592	1366370.67
									SSE	77365366.9
									SEE	1605.9

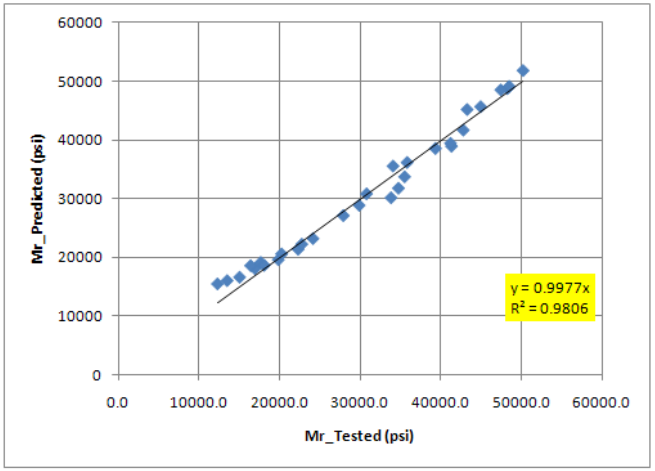

Figure D49. Resilient Modulus Properties of Base Material on Section 10160000.

K1	849.33
K2	0.88
K3	-0.99
K4	21.75

$$M_R = K_1 P_a \left(\frac{\theta + 3K_4 SV_W}{P_a} \right)^{K_2} \left(\frac{\tau_{OCT}}{P_a} + 1 \right)^{K_3}$$

	Axial stress	Test sequence	Confining pressure (psi)	Bulk stress (psi)	M_R_Tested (psi)	Oct. shear stress (psi)	Soil suction (psi)	Vol. water content	M_R_Pred. (psi)	Error
OPTIMUM	7.9	1.0	6.0	19.9	19272.7	0.9	0.500	0.17365	19155	13793.7873
	9.7	2.0	6.0	21.7	19017.2	1.7	0.500	0.17365	19289	74013.4435
	11.5	3.0	6.0	23.5	19034.4	2.6	0.500	0.17365	19405	137035.717
	13.4	4.0	6.0	25.4	19234.2	3.5	0.500	0.17365	19501	71327.1131
	15.3	5.0	6.0	27.3	19691.1	4.4	0.500	0.17365	19582	11824.9286
	5.8	6.0	4.0	13.8	15703.2	0.9	0.500	0.17365	15109	353370.298
	7.7	7.0	4.0	15.7	15502.8	1.7	0.500	0.17365	15490	165.220839
	9.5	8.0	4.0	17.5	15797.6	2.6	0.500	0.17365	15830	1034.26325
	11.4	9.0	4.0	19.4	16470.6	3.5	0.500	0.17365	16131	115187.684
	13.2	10.0	4.0	21.2	16981.3	4.4	0.500	0.17365	16388	352324.094
	3.8	11.0	2.0	7.8	11166.4	0.8	0.500	0.17365	10892	75226.2764
	5.6	12.0	2.0	9.6	11421.1	1.7	0.500	0.17365	11547	15911.9248
	7.5	13.0	2.0	11.5	11998.4	2.6	0.500	0.17365	12136	18880.2667
	9.2	14.0	2.0	13.2	12464.7	3.4	0.500	0.17365	12617	23127.521
	10.8	15.0	2.0	14.8	11995.3	4.2	0.500	0.17365	13013	1035410.73
FIELD	7.9	1.0	6.0	19.9	18781.9	0.9	0.454	0.17618	18862	6460.60848
	9.7	2.0	6.0	21.7	18650.6	1.7	0.454	0.17618	19013	131496.744
	11.5	3.0	6.0	23.5	18773.5	2.6	0.454	0.17618	19143	136856.245
	13.4	4.0	6.0	25.4	19103.7	3.5	0.454	0.17618	19256	23088.8085
	15.3	5.0	6.0	27.3	19658.1	4.4	0.454	0.17618	19350	94863.7738
	5.8	6.0	4.0	13.8	15191.2	0.9	0.454	0.17618	14804	149719.717
	7.6	7.0	4.0	15.6	15128.0	1.7	0.454	0.17618	15205	5880.48636
	9.5	8.0	4.0	17.5	15617.1	2.6	0.454	0.17618	15562	2986.1288
	11.4	9.0	4.0	19.4	16399.8	3.5	0.454	0.17618	15879	271024.409
	13.2	10.0	4.0	21.2	16998.0	4.4	0.454	0.17618	16149	721055.365
	3.8	11.0	2.0	7.8	10712.2	0.8	0.454	0.17618	10570	20299.0461
	5.6	12.0	2.0	9.6	11084.7	1.7	0.454	0.17618	11246	26137.731
	7.5	13.0	2.0	11.5	11805.7	2.6	0.454	0.17618	11861	3019.69291
	9.2	14.0	2.0	13.2	12422.0	3.4	0.454	0.17618	12362	3573.69895
	10.8	15.0	2.0	14.8	11979.4	4.2	0.454	0.17618	12766	618558.315
									SSE	4513654.0
									SEE	387.9

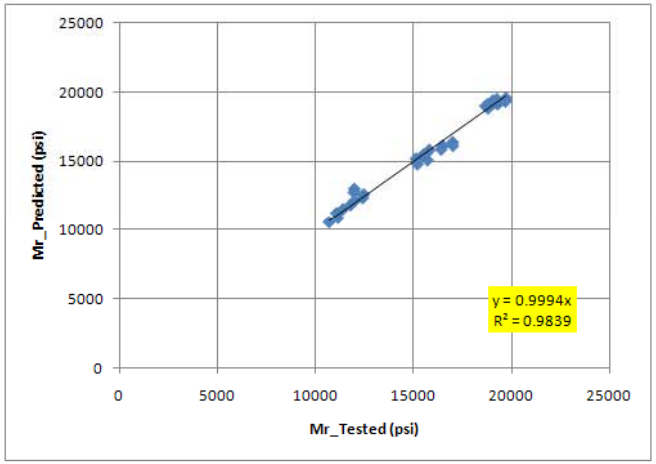

Figure D50. Resilient Modulus Properties of Subgrade Material on Section 10160000.

K1	639.70
K2	0.97
K3	-0.81
K4	0.48

$$M_R = K_1 P_a \left(\frac{\theta + 3K_4 SV_W}{P_a} \right)^{K_2} \left(\frac{\tau_{OCT}}{P_a} + 1 \right)^{K_3}$$

	Axial stress	Test sequence	Confining pressure (psi)	Bulk stress (psi)	M_R_Tested (psi)	Oct. shear stress (psi)	Soil suction (psi)	Vol. water content	M_R_Pred. (psi)	Error
OPTIMUM	7.9	1.0	6.0	19.9	16919.0	0.9	34.5389	0.16607	16788	17040.5272
	9.7	2.0	6.0	21.7	17001.6	1.8	34.5389	0.16607	17076	5538.9389
	11.5	3.0	6.0	23.5	17224.0	2.6	34.5389	0.16607	17339	13296.5739
	13.4	4.0	6.0	25.4	17583.2	3.5	34.5389	0.16607	17594	105.81399
	15.2	5.0	6.0	27.2	18003.0	4.4	34.5389	0.16607	17836	27877.8089
	5.8	6.0	4.0	13.8	13680.6	0.9	34.5389	0.16607	13298	146257.799
	7.6	7.0	4.0	15.6	13705.0	1.7	34.5389	0.16607	13733	759.810464
	9.5	8.0	4.0	17.5	14130.2	2.6	34.5389	0.16607	14154	578.276116
	11.4	9.0	4.0	19.4	14840.9	3.5	34.5389	0.16607	14553	82839.7251
	13.3	10.0	4.0	21.3	15513.2	4.4	34.5389	0.16607	14914	359546.721
	3.8	11.0	2.0	7.8	9729.4	0.8	34.5389	0.16607	9762	1046.75215
	5.6	12.0	2.0	9.6	10050.6	1.7	34.5389	0.16607	10364	97948.2363
	7.4	13.0	2.0	11.4	10636.8	2.6	34.5389	0.16607	10936	89295.0985
	9.3	14.0	2.0	13.3	11468.3	3.4	34.5389	0.16607	11448	418.870459
	11.0	15.0	2.0	15.0	11616.4	4.2	34.5389	0.16607	11897	78705.0235
FIELD	7.9	1.0	6.0	19.9	15797.2	0.9	18.6766	0.23562	15673	15469.3985
	9.7	2.0	6.0	21.7	15888.0	1.7	18.6766	0.23562	16007	14041.0527
	11.5	3.0	6.0	23.5	16159.4	2.6	18.6766	0.23562	16319	25356.5521
	13.4	4.0	6.0	25.4	16369.2	3.5	18.6766	0.23562	16624	64867.7494
	15.2	5.0	6.0	27.2	16770.6	4.4	18.6766	0.23562	16902	17234.5646
	5.8	6.0	4.0	13.8	12628.3	0.9	18.6766	0.23562	12173	207618.627
	7.7	7.0	4.0	15.7	12659.7	1.7	18.6766	0.23562	12675	244.771004
	9.5	8.0	4.0	17.5	13100.9	2.6	18.6766	0.23562	13130	831.430499
	11.3	9.0	4.0	19.3	13790.8	3.5	18.6766	0.23562	13562	52437.0303
	13.2	10.0	4.0	21.2	14392.8	4.3	18.6766	0.23562	13966	182208.379
	3.7	11.0	2.0	7.7	8831.5	0.8	18.6766	0.23562	8616	46574.0292
	5.6	12.0	2.0	9.6	9287.4	1.7	18.6766	0.23562	9277	108.841032
	7.4	13.0	2.0	11.4	9855.0	2.6	18.6766	0.23562	9898	1848.85591
	9.3	14.0	2.0	13.3	10563.2	3.4	18.6766	0.23562	10459	10820.5702
	11.0	15.0	2.0	15.0	10589.0	4.2	18.6766	0.23562	10946	127720.081
									SSE	1688637.9
									SEE	237.3

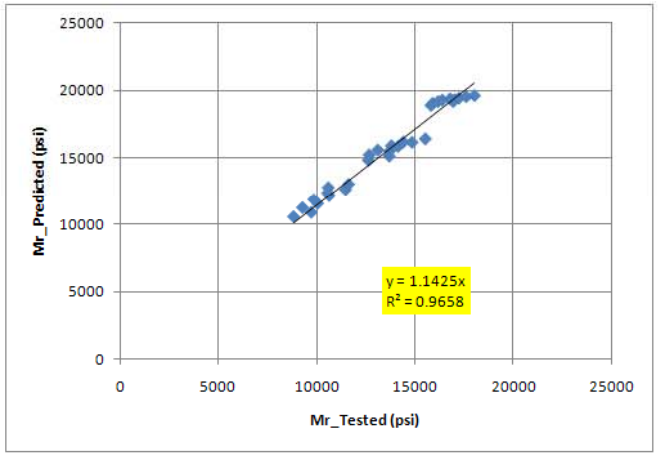

Figure D51. Resilient Modulus Properties of Embankment Material on Section 10160000.

APPENDIX E

SUMMARY OF DM, DSR, AND EXTRACTION DATA ON AC CORES

Table E1. AC Properties Determined on Core Samples from Section 16002000.

Temp. (°F)	Lift 2 - Core A		Lift 2 - Core B		Lift 3 - Core A	
	Complex Modulus G* (Pa)	Phase Angle δ (°)	Complex Modulus G* (Pa)	Phase Angle δ (°)	Complex Modulus G* (Pa)	Phase Angle δ (°)
70	1,829,000	52.71	4,190,100	52.01	3,750,400	52.76
80	1,075,000	55.88	1,758,000	57.24	1,589,000	57.39
90	511,311	59.54	759,527	61.18	661,574	61.65
100	238,572	63.40	301,434	65.10	273,213	65.49
110	102,654	67.54	122,182	69.05	104,587	69.05
120	48,391	72.72	53,127	73.52	44,805	73.33
130	20,381	77.48	23,358	78.30	20,932	78.36
A-VTS	9.108	-2.995	9.975	-3.310	9.920	-3.288

	Gradation				Air Void %	Vol. binder Content (%)	Average Thickness (in)
Core A	Retain 3/4"	Retain 3/8"	Retain #4	#200P			
Lift 2	0.00	9.15	37.20	6.12	0.9	12.64	0.9
Lift 3	0.00	10.37	36.36	6.84	2.3	12.53	2.0
	Gradation				Air Void %	Vol. binder Content (%)	Average Thickness (in)
Core B	Retain 3/4"	Retain 3/8"	Retain #4	#200P			
Lift 2	0.00	3.43	33.12	6.93	2.3	15.4	1.0
Lift 3	1.03	9.19	36.77	5.95	3.4	12.7	2.1

Table E2. AC Properties Determined on Core Samples from Section 12005000.

Temp. (°F)	Lift 1 - Core A		Lift 1 - Core B		Lift 2 - Core B		Lift 3 - Core B	
	Complex Modulus G* (Pa)	Phase Angle δ (°)	Complex Modulus G* (Pa)	Phase Angle δ (°)	Complex Modulus G* (Pa)	Phase Angle δ (°)	Complex Modulus G* (Pa)	Phase Angle δ (°)
70	22,920,000	33.82	10,590,000	36.81	11,690,000	36.93	10,100,000	36.85
80	11,980,000	38.80	5,521,000	41.60	6,126,000	41.45	5,251,000	41.36
90	6,039,000	43.79	2,689,960	46.40	2,994,000	46.19	2,675,000	45.56
100	2,762,000	49.30	1,228,000	51.27	1,431,800	50.28	1,277,000	49.95
110	1,346,000	53.10	566,681	55.74	687,345	54.00	611,576	53.92
120	475,072	59.16	258,329	61.26	294,193	58.81	268,615	59.00
130	236,142	61.30	121,765	64.38	146,262	61.49	128,388	62.35
A-VTS	9.418	-3.080	9.329	-3.055	8.946	-2.914	9.014	-2.940

	Gradation				Air Void %	Vol. binder Content (%)	Average Thickness (in)
Core A	Retain 3/4"	Retain 3/8"	Retain #4	#200P			
Lift 1	0.0	1.6	25.2	6.0	8.4	16.1	1.6
	Gradation				Air Void %	Vol. binder Content (%)	Average Thickness (in)
Core B	Retain 3/4"	Retain 3/8"	Retain #4	#200P			
Lift 1	0.0	0.8	25.0	4.6	10.0	16.3	1.5
Lift 2	0.0	0.4	11.0	18.7	12.3	16.9	0.9
Lift 3	0.0	1.4	24.6	4.9	12.8	14.5	1.8

Table E3. AC Properties Determined on Core Samples from Section 26060000.

Temp. (°F)	Lift 1 - Core A		Lift 1 - Core B		Lift 2 - Core A		Lift 2 - Core B		Lift 3 - Core A&B	
	Complex Modulus G* (Pa)	Phase Angle δ (°)	Complex Modulus G* (Pa)	Phase Angle δ (°)	Complex Modulus G* (Pa)	Phase Angle δ (°)	Complex Modulus G* (Pa)	Phase Angle δ (°)	Complex Modulus G* (Pa)	Phase Angle δ (°)
50	66,609,000	29.32	26,380,000	42.23	35,390,000	32.90	42,750,000	34.48	32,323,000	33.91
60	37,571,000	35.68	12,110,000	48.75	20,517,000	38.59	22,010,000	41.35	17,348,000	38.80
70	19,200,000	42.05	5,275,000	54.36	10,630,000	45.03	10,470,000	48.11	8,505,800	44.22
80	9,164,000	48.12	2,200,000	58.98	5,343,000	50.48	4,768,000	53.99	3,887,900	49.56
90	4,211,000	53.20	917,760	62.49	2,390,000	55.51	2,021,000	59.02	1,731,300	54.51
100	1,688,000	58.15	368,809	65.94	962,237	61.28	954,452	63.59	734,120	59.03
110	762,941	61.55	163,339	68.26	424,387	64.75	390,924	66.84	331,140	62.88
A-VTS	9.088	-2.967	9.068	-2.976	8.954	-2.924	9.090	-2.976	8.998	-2.942

	Gradation				Air Void %	Vol. binder Content (%)	Average Thickness (in)
Core A	Retain 3/4"	Retain 3/8"	Retain #4	#200P			
Lift 1	0.0	0.0	16.3	13.0	8.8	17.7	1.1
Lift 2	0.0	9.2	18.7	10.4	9.6	15.7	1.5
Lift 3	0.0	5.3	21.8	7.9	7.0	14.0	0.8
	Gradation				Air Void %	Vol. binder Content (%)	Average Thickness (in)
Core B	Retain 3/4"	Retain 3/8"	Retain #4	#200P			
Lift 1	0.0	0.0	16.3	13.0	2.5	17.6	1.0
Lift 2	0.0	5.9	20.8	9.6	5.4	15.8	1.5
Lift 3	0.0	5.3	21.8	7.9	1.7	14.0	1.0

Table E4. AC Properties Determined on Core Samples from Section 71020000.

Temp. (°F)	Lift 2 - Core A		Lift 3 - Core B	
	Complex Modulus G* (Pa)	Phase Angle δ (°)	Complex Modulus G* (Pa)	Phase Angle δ (°)
70	15,340,000	40.08	13,961,000	39.26
80	7,928,000	45.12	6,990,000	44.71
90	3,705,000	50.57	3,329,000	49.99
100	1,606,470	55.85	1,484,000	54.73
110	717,705	60.27	663,668	59.00
120	266,239	65.24	299,871	63.84
130	114,284	68.36	131,270	66.71
A-VTS	9.661	-3.176	9.297	-3.044

	Gradation				Air Void %	Vol. binder Content (%)	Average Thickness (in)
Core A	Retain 3/4"	Retain 3/8"	Retain #4	#200P			
Lift 2	0.0	2.0	23.7	5.9	7.9	14.0	1.4
Lift 3	0.0	6.9	28.9	6.2	6.5	13.4	1.5
	Gradation				Air Void %	Vol. binder Content (%)	Average Thickness (in)
Core B	Retain 3/4"	Retain 3/8"	Retain #4	#200P			
Lift 2	0.5	3.0	24.9	5.9	7.1	14.1	1.5
Lift 3	0.0	8.2	28.8	6.2	6.7	13.3	1.7

Table E5. AC Properties Determined on Core Samples from Section 26005000.

Temp. (°F)	Lift 1 - Core A		Lift 2 - Core A		Lift 3 - Core A		Lift 4 - Core A	
	Complex Modulus G* (Pa)	Phase Angle δ (°)	Complex Modulus G* (Pa)	Phase Angle δ (°)	Complex Modulus G* (Pa)	Phase Angle δ (°)	Complex Modulus G* (Pa)	Phase Angle δ (°)
70	13,980,000	30.77	9,305,000	34.88	10,440,000	36.49	14,920,000	35.36
80	8,362,000	34.08	4,952,000	39.14	5,829,000	40.27	8,290,000	39.82
90	4,818,000	37.21	2,475,000	43.75	3,123,000	43.48	4,404,000	43.86
100	2,680,000	40.01	1,874,000	46.62	1,571,000	47.35	2,278,000	47.58
110	1,498,000	42.47	900,340	51.15	803,430	50.51	1,595,740	51.05
120	755,689	48.92	306,918	55.41	382,002	56.25	484,122	56.27
130	463,908	49.30	160,993	57.74	202,019	58.06	254,951	58.05
A-VTS	7.438	-2.354	8.430	-2.725	8.191	-2.637	8.276	-2.665

	Gradation				Air Void %	Vol. binder Content (%)	Average Thickness (in)
Core A	Retain 3/4"	Retain 3/8"	Retain #4	#200P			
Lift 1	0.0	0.2	9.1	5.5	13.5	13.1	1.0
Lift 2	0.0	14.6	35.2	9.5	9.4	12.6	1.2
Lift 3	0.0	6.0	26.9	11.6	6.4	15.0	1.5
Lift 4	0.0	5.5	26.4	10.2	9.7	14.8	1.3
	Gradation				Air Void %	Vol. binder Content (%)	Average Thickness (in)
Core B	Retain 3/4"	Retain 3/8"	Retain #4	#200P			
Lift 1	0.0	0.2	9.1	5.5	15.5	13.1	0.9
Lift 2	0.0	14.6	35.2	9.5	11.1	12.6	1.2
Lift 3	0.0	4.4	25.0	10.3	5.1	15.3	1.4
Lift 4	0.0	5.5	26.4	10.2	7.6	14.8	1.3

Table E6. AC Properties Determined on Core Samples from Section 54020000.

Temp. (°F)	Lift 2 - Core A		Lift 3 - Core A		Lift 2 - Core B		Lift 3 - Core B	
	Complex Modulus G* (Pa)	Phase Angle δ (°)	Complex Modulus G* (Pa)	Phase Angle δ (°)	Complex Modulus G* (Pa)	Phase Angle δ (°)	Complex Modulus G* (Pa)	Phase Angle δ (°)
50	16,430,000	43.12	33,080,000	30.76	85,630,000	25.63	17,474,000	37.55
60	6,164,000	50.41	17,760,000	35.93	47,520,000	32.09	8,640,000	42.54
70	3,064,000	55.00	8,964,000	41.17	24,270,000	38.67	4,062,000	47.45
80	1,201,000	59.86	4,221,000	46.45	11,320,000	44.96	1,806,000	52.08
90	468,485	63.95	1,976,000	50.95	5,007,300	51.24	829,754	55.84
100	182,379	67.84	869,697	55.57	2,680,000	56.03	346,157	59.94
110	73,192	71.20	387,895	59.46	1,141,000	60.29	157,415	63.27
A-VTS	9.674	-3.204	8.947	-2.921	9.266	-3.028	8.927	-2.923

	Gradation				Air Void %	Vol. binder Content (%)	Average Thickness (in)
Core A	Retain 3/4"	Retain 3/8"	Retain #4	#200P			
Lift 2	N/A	N/A	N/A	N/A	3.2	15.1	0.8
Lift 3	0.0	6.0	26.1	10.4	2.7	15.1	1.4
	Gradation				Air Void %	Vol. binder Content (%)	Average Thickness (in)
Core B	Retain 3/4"	Retain 3/8"	Retain #4	#200P			
Lift 2	N/A	N/A	N/A	N/A	12.1	12.5	1.0
Lift 3	0.0	7.2	28.4	8.3	7.0	14.0	1.6

Table E7. AC Properties Determined on Core Samples from Section 50020000.

Temp. (°F)	Lift 1 - Core A		Lift 2 - Core A		Lift 1 - Core B		Lift 2 - Core B	
	Complex Modulus G* (Pa)	Phase Angle δ (°)	Complex Modulus G* (Pa)	Phase Angle δ (°)	Complex Modulus G* (Pa)	Phase Angle δ (°)	Complex Modulus G* (Pa)	Phase Angle δ (°)
50	34,960,000	32.90	16,020,000	36.28	49,020,000	30.35	41,890,000	32.70
60	19,710,000	37.51	9,092,000	40.20	27,876,000	35.21	22,870,000	38.56
70	9,710,000	42.92	4,689,000	44.27	13,870,000	40.88	10,730,000	44.96
80	4,652,000	47.62	2,418,000	47.32	6,596,000	46.28	4,915,000	50.55
90	2,158,000	52.21	1,204,000	50.75	3,105,000	50.89	2,149,000	55.44
100	875,439	57.29	533,320	55.20	1,085,000	56.41	1,002,000	60.87
110	412,737	60.31	252,332	57.90	508,249	59.58	437,325	64.66
A-VTS	8.773	-2.857	7.962	-2.565	9.135	-2.987	9.099	-2.977

	Gradation				Air Void %	Vol. binder Content (%)	Average Thickness (in)
Core A	Retain 3/4"	Retain 3/8"	Retain #4	#200P			
Lift 1	0.0	7.5	26.9	6.0	9.5	10.9	1.7
Lift 2	7.6	33.7	51.7	6.6	2.3	10.9	2.0
	Gradation				Air Void %	Vol. binder Content (%)	Average Thickness (in)
Core B	Retain 3/4"	Retain 3/8"	Retain #4	#200P			
Lift 1	0.0	7.5	26.9	6.0	9.5	10.9	1.7
Lift 2	7.6	33.7	51.7	6.6	2.3	10.9	1.8

Table E8. AC Properties Determined on Core Samples from Section 58060000.

Temp. (°F)	Lift 1 - Core B		Lift 2 - Core B		Lift 3 - Core B	
	Complex Modulus G* (Pa)	Phase Angle δ (°)	Complex Modulus G* (Pa)	Phase Angle δ (°)	Complex Modulus G* (Pa)	Phase Angle δ (°)
50	26,280,000	33.01	27,500,000	32.77	708,000	46.10
60	14,521,000	37.78	15,250,000	37.40	360,667	52.77
70	7,257,000	42.88	7,487,000	42.52	153,333	58.92
80	3,488,000	47.71	3,552,000	47.47	60,700	64.89
90	1,671,000	51.78	1,655,000	51.86	26,300	69.97
100	690,976	56.14	674,630	56.67	12,250	74.19
110	323,879	59.04	319,465	59.86	5,110	78.56
A-VTS	8.672	-2.822	8.858	-2.890	9.36	-3.06

	Gradation				Air Void %	Vol. binder Content (%)	Average Thickness (in)
Core A	Retain 3/4"	Retain 3/8"	Retain #4	#200P			
Lift 1	0.0	1.2	19.2	4.0	10.1	11.5	0.8
Lift 2	0.0	11.5	37.0	3.3	6.8	8.9	1.2
Lift 3	0.0	1.4	30.4	4.2	4.7	10.4	1.0
	Gradation				Air Void %	Vol. binder Content (%)	Average Thickness (in)
Core B	Retain 3/4"	Retain 3/8"	Retain #4	#200P			
Lift 1	0.0	1.2	19.2	4.0	10.1	11.5	1.0
Lift 2	0.0	11.5	37.0	3.3	6.8	8.9	1.3
Lift 3	0.0	1.4	30.4	4.2	4.7	10.4	1.0

Table E9. AC Properties Determined on Core Samples from Section 89010000.

Temp. (°F)	Lift 2 - Core B		Lift 3 - Core B	
	Complex Modulus G* (Pa)	Phase Angle δ (°)	Complex Modulus G* (Pa)	Phase Angle δ (°)
50	18,380,000	40.16	20,710,000	37.82
60	9,030,000	46.10	10,410,000	43.57
70	4,148,000	51.98	4,938,000	49.50
80	1,770,800	57.73	2,188,200	55.21
90	747,804	62.67	954,360	60.23
100	304,414	67.57	394,218	65.46
110	124,651	71.43	167,851	69.49
A-VTS	9.813	-3.231	9.680	-3.180

	Gradation				Air Void %	Vol. binder Content (%)	Average Thickness (in)
Core A	Retain 3/4"	Retain 3/8"	Retain #4	#200P			
Lift 2	0.0	0.6	25.5	5.2	4.4	15.8	0.8
Lift 3	0.0	0.6	25.5	5.2	5.3	15.8	1.0
	Gradation				Air Void %	Vol. binder Content (%)	Average Thickness (in)
Core B	Retain 3/4"	Retain 3/8"	Retain #4	#200P			
Lift 2	0.0	0.6	25.5	5.2	4.4	15.8	0.9
Lift 3	0.0	0.6	25.5	5.2	5.3	15.8	1.0

Table E10. AC Properties Determined on Core Samples from Section 93310000.

Temp. (°F)	Lift 1 - Core B		Lift 2 - Core B		Lift 3 - Core B		Lift 4 - Core B	
	Complex Modulus G* (Pa)	Phase Angle δ (°)	Complex Modulus G* (Pa)	Phase Angle δ (°)	Complex Modulus G* (Pa)	Phase Angle δ (°)	Complex Modulus G* (Pa)	Phase Angle δ (°)
70	4,278,000	53.81	4,933,700	43.25	5,394,000	45.83	10,600,000	35.67
80	1,827,000	58.97	2,656,000	46.39	2,670,000	49.60	5,911,000	39.21
90	740,201	63.51	1,337,000	49.89	1,264,000	53.30	3,103,000	43.02
100	284,788	67.41	639,604	53.32	568,106	56.93	1,562,000	46.69
110	108,366	70.77	305,475	56.78	254,592	60.70	792,113	50.00
120	45,113	74.62	130,635	61.61	93,175	65.34	375,884	55.99
130	19,031	76.95	62,429	64.36	42,999	68.25	191,943	58.56
A-VTS	10.167	-3.380	8.734	-2.846	9.398	-3.090	8.405	-2.715

	Gradation				Air Void %	Vol. binder Content (%)	Average Thickness (in)
Core A	Retain 3/4"	Retain 3/8"	Retain #4	#200P			
Lift 1	0.0	11.3	28.2	2.8	4.0	13.4	2.1
Lift 2	0.0	6.3	29.6	7.9	6.0	13.7	0.6
Lift 3	0.0	0.7	27.1	4.1	8.7	13.6	1.8
Lift 4	0.0	5.5	29.7	7.3	10.3	14.3	0.9
	Gradation				Air Void %	Vol. binder Content (%)	Average Thickness (in)
Core B	Retain 3/4"	Retain 3/8"	Retain #4	#200P			
Lift 1	0.0	11.3	28.2	2.8	4.0	13.4	2.2
Lift 2	0.0	6.3	29.6	7.9	6.0	13.7	0.6
Lift 3	0.0	0.7	27.1	4.1	8.7	13.6	1.9
Lift 4	0.0	5.5	29.7	7.3	10.3	14.3	0.8

Table E11. AC Properties Determined on Core Samples from Section 86190000.

Temp. (°F)	Lift 1 - Core B		Lift 2 - Core B		Lift 3 - Core B	
	Complex Modulus G* (Pa)	Phase Angle δ (°)	Complex Modulus G* (Pa)	Phase Angle δ (°)	Complex Modulus G* (Pa)	Phase Angle δ (°)
70	5,165,000	50.74	6,700,000	49.91	11,340,000	37.57
80	2,349,000	55.70	3,021,000	55.43	6,043,000	42.00
90	1,000,200	60.38	1,271,000	60.52	3,115,900	46.06
100	393,918	64.78	502,609	65.18	1,489,800	50.37
110	154,679	68.39	196,155	69.15	701,549	54.62
120	57,759	72.47	70,652	73.02	189,479	60.47
130	23,971	74.86	29,028	75.40	95,309	63.21
A-VTS	10.182	-3.382	10.248	-3.404	9.663	-3.176

	Gradation				Air Void %	Vol. binder Content (%)	Average Thickness (in)
Core A	Retain 3/4"	Retain 3/8"	Retain #4	#200P			
Lift 1	0.0	2.3	34.4	4.0	8.9	13.5	0.9
Lift 2	0.0	2.2	33.5	5.2	4.9	13.7	1.4
Lift 3	0.0	8.5	35.6	7.8	5.8	11.9	1.5
	Gradation				Air Void %	Vol. binder Content (%)	Average Thickness (in)
Core B	Retain 3/4"	Retain 3/8"	Retain #4	#200P			
Lift 1	0.0	2.3	34.4	4.0	8.9	13.5	0.9
Lift 2	0.0	2.2	33.5	5.2	4.9	13.7	1.4
Lift 3	0.0	8.5	35.6	7.8	5.8	11.9	1.4

Table E12. AC Properties Determined on Core Samples from Section 93100000.

Temp. (°F)	Lift 1 - Core B		Lift 2 - Core B	
	Complex Modulus G* (Pa)	Phase Angle δ (°)	Complex Modulus G* (Pa)	Phase Angle δ (°)
70	6,500,000	44.78	123,333	64.02
80	3,223,000	48.52	54,400	68.50
90	1,513,000	51.90	24,200	73.16
100	666,415	55.17	11,633	76.38
110	298,784	57.89	5,143	80.41
120	125,489	60.97	2,443	82.81
130	59,249	61.86	1,097	85.13
A-VTS	8.830	-2.881	9.78	-3.23

	Gradation				Air Void %	Vol. binder Content (%)	Average Thickness (in)
Core A	Retain 3/4"	Retain 3/8"	Retain #4	#200P			
Lift 1	0.0	5.4	25.1	4.9	7.8	11.8	1.4
Lift 2	4.5	10.9	20.3	6.5	6.6	8.5	1.1
	Gradation				Air Void %	Vol. binder Content (%)	Average Thickness (in)
Core B	Retain 3/4"	Retain 3/8"	Retain #4	#200P			
Lift 1	0.0	5.4	25.1	4.9	7.8	11.8	1.4
Lift 2	4.5	10.9	20.3	6.5	6.6	8.5	1.0

Table E13. AC Properties Determined on Core Samples from Section 77002000.

Temp. (°F)	Lift 1 - Core A		Lift 2 - Core A		Lift 3 - Core A		Lift 4 - Core A	
	Complex Modulus G* (Pa)	Phase Angle δ (°)	Complex Modulus G* (Pa)	Phase Angle δ (°)	Complex Modulus G* (Pa)	Phase Angle δ (°)	Complex Modulus G* (Pa)	Phase Angle δ (°)
70	5,647,000	50.77	7,439,000	42.35	5,755,000	37.73	11,450,000	36.18
80	2,603,000	56.14	3,770,000	46.64	3,348,000	41.62	6,422,000	40.40
90	1,107,000	61.20	1,829,000	50.76	1,788,000	45.81	3,397,000	44.52
100	436,402	65.84	842,628	54.52	922,833	49.70	1,712,000	48.23
110	172,306	69.68	388,452	58.08	452,036	53.51	849,501	51.76
120	74,729	73.46	126,873	63.06	181,762	59.04	549,626	57.13
130	26,642	75.62	60,243	65.76	91,860	62.11	285,965	59.15
A-VTS	10.033	-3.326	9.446	-3.104	8.819	-2.872	7.881	-2.523

Temp. (°F)	Lift 1 - Core B		Lift 2 - Core B		Lift 3 - Core B		Lift 4 - Core B	
	Complex Modulus G* (Pa)	Phase Angle δ (°)	Complex Modulus G* (Pa)	Phase Angle δ (°)	Complex Modulus G* (Pa)	Phase Angle δ (°)	Complex Modulus G* (Pa)	Phase Angle δ (°)
70	7,992,200	47.84	5,942,700	40.37	10,550,000	37.37	14,850,000	36.49
80	3,651,000	53.84	3,610,000	44.03	5,589,000	41.67	8,102,000	40.76
90	1,548,000	59.35	1,873,000	47.66	2,822,000	45.82	4,304,000	44.36
100	619,010	64.16	909,887	51.35	1,356,000	49.93	2,143,000	47.88
110	250,109	68.12	444,757	54.67	641,419	53.51	1,112,000	50.36
120	95,319	72.21	145,110	59.54	243,194	59.06	502,128	55.48
130	42,103	74.93	83,029	61.89	119,652	61.58	266,295	56.90
A-VTS	10.011	-3.315	8.809	-2.869	9.103	-2.972	8.050	-2.583

Table E13. AC Properties Determined on Core Samples from Section 77002000 (continued).

	Gradation				Air Void %	Vol. binder Content (%)	Average Thickness (in)
Core A	Retain 3/4"	Retain 3/8"	Retain #4	#200P			
Lift 1	0.0	6.4	28.1	3.1	5.7	14.9	1.3
Lift 2	0.0	2.7	25.0	6.9	8.6	12.7	1.3
Lift 3	0.0	11.4	42.7	5.3	7.2	11.2	1.4
Lift 4	0.0	9.4	42.7	6.8	10.1	11.5	1.6
	Gradation				Air Void %	Vol. binder Content (%)	Average Thickness (in)
Core B	Retain 3/4"	Retain 3/8"	Retain #4	#200P			
Lift 1	0.0	6.4	27.3	2.8	9.1	14.4	1.3
Lift 2	0.0	3.0	23.5	6.2	12.8	12.8	1.5
Lift 3	0.0	12.0	44.0	5.1	7.3	11.0	1.4
Lift 4	0.0	7.5	37.8	6.3	11.7	11.5	1.6

Table E14. AC Properties Determined on Core Samples from Section 92060000.

Temp. (°F)	Lift 1 - Core A		Lift 2 - Core A		Lift 3 - Core A		Lift 4 - Core A		Lift 5 - Core A	
	Complex Modulus G* (Pa)	Phase Angle δ (°)	Complex Modulus G* (Pa)	Phase Angle δ (°)	Complex Modulus G* (Pa)	Phase Angle δ (°)	Complex Modulus G* (Pa)	Phase Angle δ (°)	Complex Modulus G* (Pa)	Phase Angle δ (°)
70	7,905,000	41.59	7,950,000	43.47	6,013,000	50.75	4,668,000	51.36	3,706,000	51.46
80	3,954,800	46.17	3,856,000	48.30	2,609,000	56.44	2,043,000	56.62	1,652,000	56.24
90	1,857,000	50.85	1,760,000	52.96	1,057,300	61.65	860,173	61.52	712,018	60.71
100	831,318	55.20	762,592	57.44	403,176	66.57	339,699	66.04	283,051	65.19
110	370,526	59.28	333,391	61.46	161,850	70.85	130,805	70.10	108,292	69.40
120	156,365	63.44	141,098	65.61	61,806	75.06	52,886	72.23	43,003	73.70
130	67,659	67.12	60,212	69.52	24,377	79.46	22,177	73.06	17,676	78.59
A-VTS	9.436	-3.100	9.546	-3.141	10.421	-3.468	10.073	-3.343	10.344	-3.444
Temp. (°F)	Lift 1 - Core B		Lift 2 - Core B		Lift 3 - Core B		Lift 4 - Core B		Lift 5 - Core B	
	Complex Modulus G* (Pa)	Phase Angle δ (°)	Complex Modulus G* (Pa)	Phase Angle δ (°)	Complex Modulus G* (Pa)	Phase Angle δ (°)	Complex Modulus G* (Pa)	Phase Angle δ (°)	Complex Modulus G* (Pa)	Phase Angle δ (°)
70	10,100,000	40.53	10,300,000	40.88	5,851,000	49.90	2,552,000	52.36	5,040,000	48.09
80	5,042,500	45.35	5,181,000	45.53	2,547,000	55.65	1,150,000	56.62	2,318,000	53.01
90	2,380,000	50.21	2,417,000	50.32	1,065,700	60.88	494,908	60.94	1,022,000	57.69
100	1,071,000	54.62	1,069,200	54.93	413,563	65.83	205,547	65.25	439,404	62.17
110	489,423	58.49	473,509	59.12	163,934	69.96	83,416	69.54	180,030	66.24
120	210,145	62.73	197,719	63.55	62,036	73.95	33,247	74.06	74,486	70.53
130	93,835	66.02	85,971	67.32	24,067	78.07	13,870	79.17	30,193	74.94
A-VTS	9.262	-3.033	9.472	-3.110	10.424	-3.469	10.235	-3.407	9.905	-3.279

Table E14. AC Properties Determined on Core Samples from Section 92060000 (continued).

	Gradation				Air Void %	Vol. binder Content (%)	Average Thickness (in)
Core A	Retain 3/4"	Retain 3/8"	Retain #4	#200P			
Lift 1	0.0	12.0	29.8	5.0	4.4	13.9	1.5
Lift 2	0.0	12.0	32.0	4.2	6.1	17.8	1.5
Lift 3	0.0	7.5	28.0	4.3	4.7	15.0	1.4
Lift 4	0.0	8.8	30.1	4.7	1.8	14.9	1.3
Lift 5	0.0	9.0	33.4	3.8	2.3	14.8	1.9
	Gradation				Air Void %	Vol. binder Content (%)	Average Thickness (in)
Core B	Retain 3/4"	Retain 3/8"	Retain #4	#200P			
Lift 1	0.0	12.0	29.8	5.0	7.3	13.9	1.7
Lift 2	0.0	12.0	32.0	4.2	8.4	17.8	1.5
Lift 3	0.0	9.1	31.6	4.7	3.0	17.0	1.6
Lift 4	0.0	3.7	26.5	5.9	1.7	15.7	1.3
Lift 5	0.0	8.0	30.6	3.7	3.9	15.2	1.9

Table E15. Dynamic Modulus (ksi) of Core Samples from Section 92060000.

Core	Temp (°F)	Frequency (Hz)			
		0.1	1	10	25
92060-2A	40.1	1023.4	1463.8	1931.1	2120.4
	70.2	265.8	529.1	902.7	1075.1
	99.5	39.2	105.5	275.7	372.7
	130.1	16.6	39.0	102.2	138.1
92060-3A	40.1	1061.5	1494.6	1955.5	2139.5
	69.8	280.6	538.7	908.3	1081.1
	100.8	46.1	114.9	277.0	368.1
	130.6	9.6	21.7	58.4	86.7
92060-2B	39.9	804.5	1121.5	1462.8	1603.8
	70.3	264.7	484.8	787.1	919.9
	101.1	32.4	80.3	188.7	253.8
	130.3	7.5	23.0	59.0	84.3
92060-3B	39.9	712.8	1008.0	1335.0	1465.4
	70.0	179.0	342.1	586.5	703.1
	99.1	35.4	82.5	183.2	244.8
	129.6	9.2	18.5	44.3	63.3

Table E16. AC Properties Determined on Core Samples from Section 79270000.

Temp. (°F)	Lift 1 - Core A		Lift 2 - Core A	
	Complex Modulus G* (Pa)	Phase Angle δ (°)	Complex Modulus G* (Pa)	Phase Angle δ (°)
70	6,776,000	47.29	121,333	71.11
80	3,114,000	52.31	50,433	71.40
90	1,394,000	56.55	22,833	73.76
100	593,339	60.16	10,500	76.87
110	430,283	63.61	5,087	79.84
120	181,777	65.08	2,357	82.26
130	82,252	66.37	1,090	84.75
A-VTS	8.156	-2.636	9.74	3.21

	Gradation				Air Void %	Vol. binder Content (%)	Average Thickness (in)
Core A	Retain 3/4"	Retain 3/8"	Retain #4	#200P			
Lift 1	1.2	19.9	42.3	4.8	8.0	11.8	1.2
Lift 2	0.9	7.1	33.1	6.9	6.7	8.8	1.0
	Gradation				Air Void %	Vol. binder Content (%)	Average Thickness (in)
Core B	Retain 3/4"	Retain 3/8"	Retain #4	#200P			
Lift 1	1.2	19.9	42.3	4.8	8.0	11.8	1.3
Lift 2	0.0	7.1	33.1	6.9	6.7	8.8	1.0

Table E17. AC Properties Determined on Core Samples from Section 87120000.

Temp. (°F)	Lift 1 - Core A		Lift 2 - Core A		Lift 3 - Core A	
	Complex Modulus G* (Pa)	Phase Angle δ (°)	Complex Modulus G* (Pa)	Phase Angle δ (°)	Complex Modulus G* (Pa)	Phase Angle δ (°)
70	29,630,000	31.45	6,671,000	43.11	17,339,000	33.63
80	17,070,000	35.66	3,251,000	47.96	9,464,000	37.98
90	9,420,000	39.80	1,477,000	52.88	4,898,000	42.71
100	4,978,000	43.72	630,420	57.53	2,392,000	47.54
110	2,662,000	46.79	272,922	61.79	1,142,000	52.25
120	1,260,800	51.19	112,177	66.07	457,377	58.70
130	681,056	53.03	47,122	70.25	214,278	62.45
A-VTS	7.862	-2.506	9.820	-3.243	9.321	-3.046

Temp. (°F)	Lift 1 - Core B		Lift 2 - Core B		Lift 3 - Core B	
	Complex Modulus G* (Pa)	Phase Angle δ (°)	Complex Modulus G* (Pa)	Phase Angle δ (°)	Complex Modulus G* (Pa)	Phase Angle δ (°)
70	51,750,000	28.01	6,846,300	44.57	39,760,000	26.56
80	30,260,000	33.25	3,284,000	49.43	24,360,000	30.23
90	16,750,000	38.20	1,471,000	54.20	14,060,000	34.34
100	8,704,000	43.00	624,371	58.88	7,695,000	38.82
110	4,449,000	47.25	260,090	63.18	4,101,000	43.28
120	2,120,200	51.71	105,939	67.47	1,771,000	50.27
130	1,055,000	54.86	43,609	71.96	846,179	55.05
A-VTS	8.469	-2.722	9.904	-3.274	8.773	-2.832

Table E17. AC Properties Determined on Core Samples from Section 87120000 (continued).

	Gradation				Air Void %	Vol. binder Content (%)	Average Thickness (in)
Core A	Retain 3/4"	Retain 3/8"	Retain #4	#200P			
Lift 1	0.0	0.0	53.6	8.6	13.2	12.4	0.6
Lift 2	0.0	6.1	34.7	7.3	2.3	13.6	1.4
Lift 3	14.5	43.9	57.4	7.4	8.2	11.9	1.6
	Gradation				Air Void %	Vol. binder Content (%)	Average Thickness (in)
Core B	Retain 3/4"	Retain 3/8"	Retain #4	#200P			
Lift 1	0.0	0.0	53.6	8.6	12.8	12.4	0.6
Lift 2	0.6	8.5	35.9	7.4	4.3	13.2	1.5
Lift 3	8.5	43.8	58.1	7.2	4.9	12.1	1.6

Table E18. AC Properties Determined on Core Samples from Section 87060000.

Temp. (°F)	Lift 1 - Core A		Lift 2 - Core A		Lift 3 - Core A		Lift 4 - Core A	
	Complex Modulus G* (Pa)	Phase Angle δ (°)	Complex Modulus G* (Pa)	Phase Angle δ (°)	Complex Modulus G* (Pa)	Phase Angle δ (°)	Complex Modulus G* (Pa)	Phase Angle δ (°)
70	4,605,000	49.43	3,602,000	51.90	6,155,000	45.14	47,300	69.82
80	2,192,000	53.64	1,628,000	56.23	3,064,000	49.70	19,300	74.29
90	981,626	57.90	700,969	60.47	1,431,000	54.26	8,780	78.07
100	399,575	62.14	282,075	64.72	642,024	58.56	3,917	81.27
110	166,848	65.76	113,272	68.45	271,095	62.79	1,907	83.87
120	62,003	70.01	48,336	72.45	107,699	67.52	914	85.73
130	26,069	72.80	20,032	75.03	43,479	70.56	476	88.05
A-VTS	9.925	-3.287	9.941	-3.297	9.663	-3.186	10.19	3.38

Table E18. AC Properties Determined on Core Samples from Section 87060000 (continued).

Temp. (°F)	Lift 1 - Core B		Lift 2 - Core B		Lift 3 - Core B		Lift 4 - Core B	
	Complex Modulus G* (Pa)	Phase Angle δ (°)	Complex Modulus G* (Pa)	Phase Angle δ (°)	Complex Modulus G* (Pa)	Phase Angle δ (°)	Complex Modulus G* (Pa)	Phase Angle δ (°)
70	3,959,000	50.10	3,180,000	52.04	6,301,000	43.28	47,300	69.82
80	1,949,000	53.72	1,390,000	57.06	3,098,000	48.10	19,300	74.29
90	859,892	58.13	592,923	61.54	1,462,000	52.77	8,780	78.07
100	359,637	62.25	236,438	65.69	653,181	57.13	3,917	81.27
110	149,884	65.93	93,520	69.40	301,362	61.11	1,907	83.87
120	56,483	69.52	38,775	73.16	113,580	66.29	914	85.73
130	23,321	72.22	16,673	75.68	47,996	69.48	476	88.05
A-VTS	9.854	-3.263	10.120	-3.364	9.646	-3.179	10.19	3.38

	Gradation				Air Void %	Vol. binder Content (%)	Average Thickness (in)
Core A	Retain 3/4"	Retain 3/8"	Retain #4	#200P			
Lift 1	0.0	1.4	25.7	6.6	4.4	11.1	1.3
Lift 2	0.0	9.4	30.2	7.0	4.4	10.8	2.1
Lift 3	0.0	13.2	34.3	8.0	2.2	12.9	1.7
Lift 4	0.0	13.2	34.3	8.0	3.9	15.2	1.7
	Gradation				Air Void %	Vol. binder Content (%)	Average Thickness (in)
Core B	Retain 3/4"	Retain 3/8"	Retain #4	#200P			
Lift 1	0.0	1.4	25.7	6.6	4.4	11.1	1.3
Lift 2	0.0	9.4	30.2	7.0	4.4	10.8	2.2
Lift 3	0.0	13.2	34.3	8.0	2.2	12.9	1.5
Lift 4	0.0	13.2	34.3	8.0	3.9	15.2	1.7

Table E19. Dynamic Modulus (ksi) of Core Samples from Section 87060000.

Core	Temp (°F)	Frequency (Hz)			
		0.1	1	10	25
87060-2A	39.2	1373.5	1835.2	2307.3	2496.6
	68	443.7	769.3	1208.7	1411.5
	104	101.4	236.8	480.9	605.5
	130	19.7	58.4	135.6	202.2
87060-3A	39.2	1344.3	1769.0	2200.3	2371.4
	68	420.4	735.5	1156.2	1343.6
	104	96.2	220.2	448.4	569.5
	130	18.6	56.7	111.4	161.6
87060-4A	39.2	1229.0	1626.4	2029.4	2186.8
	68	377.2	663.8	1045.7	1209.6
	104	88.6	204.2	415.1	526.8
	130	18.3	52.5	99.9	146.8
87060-2B	39.2	1063.4	1485.6	1918.6	2087.7
	68	276.7	527.3	896.0	1075.0
	104	54.6	144.3	318.6	418.9
	130	9.1	37.2	71.6	112.8
87060-3B	39.2	1092.4	1452.2	1820.6	1966.4
	68	322.7	584.9	938.5	1095.7
	104	67.9	169.8	361.6	467.2
	130	13.5	45.3	93.5	140.5
87060-4B	39.2	1302.2	1768.1	2251.3	2448.2
	68	342.6	637.4	1054.8	1254.4
	104	65.0	164.2	364.6	477.4
	130	13.1	40.6	76.9	118.3

Table E20. AC Properties Determined on Core Samples from Section 90060000.

Temp. (°F)	Lift 1 - Core A		Lift 2 - Core A		Lift 3 - Core A	
	Complex Modulus G* (Pa)	Phase Angle δ (°)	Complex Modulus G* (Pa)	Phase Angle δ (°)	Complex Modulus G* (Pa)	Phase Angle δ (°)
70	8,683,000	42.73	8,967,000	45.00	7,950,000	45.36
80	4,371,000	46.90	4,344,000	49.85	3,904,000	49.93
90	2,091,000	50.79	2,039,600	54.03	1,819,000	53.96
100	965,866	53.92	899,050	57.70	798,791	57.50
110	454,234	56.27	404,520	60.38	355,870	60.08
120	231,663	58.77	171,452	62.72	150,961	62.71
130	114,524	59.56	79,227	63.89	73,387	63.54
A-VTS	8.156	-2.631	8.322	-2.693	8.804	-2.870

Temp. (°F)	Lift 1 - Core B		Lift 2 - Core B		Lift 3 - Core B	
	Complex Modulus G* (Pa)	Phase Angle δ (°)	Complex Modulus G* (Pa)	Phase Angle δ (°)	Complex Modulus G* (Pa)	Phase Angle δ (°)
70	7,159,000	43.52	19,200,000	35.76	17,920,000	36.75
80	3,631,000	47.52	10,230,000	41.12	9,493,000	42.01
90	1,779,000	50.98	5,272,000	45.92	4,854,000	46.67
100	827,095	53.97	2,479,000	50.80	2,371,000	50.99
110	402,557	56.07	1,206,000	54.52	1,115,000	55.21
120	163,008	58.87	573,780	60.49	350,654	61.64
130	85,251	59.43	276,030	63.21	166,707	64.32
A-VTS	8.784	-2.851	8.779	-2.861	9.413	-3.082

Table E20. AC Properties Determined on Core Samples from Section 90060000 (continued).

	Gradation				Air Void %	Vol. binder Content (%)	Average Thickness (in)
Core A	Retain 3/4"	Retain 3/8"	Retain #4	#200P			
Lift 1	0.0	20.9	66.0	6.0	10.2	12.1	0.9
Lift 2	0.0	8.8	29.6	5.6	8.9	12.7	1.5
Lift 3	0.0	7.1	35.6	6.8	8.9	13.9	1.3
	Gradation				Air Void %	Vol. binder Content (%)	Average Thickness (in)
Core B	Retain 3/4"	Retain 3/8"	Retain #4	#200P			
Lift 1	0.0	20.9	66.0	6.0	9.9	12.1	0.9
Lift 2	0.0	11.8	32.1	5.2	8.4	12.2	1.6
Lift 3	0.0	5.5	32.1	6.8	7.4	14.4	1.3

Table E21. AC Properties Determined on Core Samples from Section 10060000.

Temp. (°F)	Lift 1 - Core A		Lift 2 - Core A		Lift 3 - Core A	
	Complex Modulus G* (Pa)	Phase Angle δ (°)	Complex Modulus G* (Pa)	Phase Angle δ (°)	Complex Modulus G* (Pa)	Phase Angle δ (°)
70	50,128,000	26.93	6,462,000	44.50	24,190,000	28.47
80	27,750,000	31.01	3,171,000	48.98	14,830,000	31.96
90	14,750,000	36.18	1,485,000	53.31	8,374,000	36.27
100	7,708,600	41.53	655,917	57.65	4,451,000	40.85
110	4,119,000	45.16	289,881	61.54	2,377,000	45.04
120	2,905,000	48.60	111,439	66.08	724,691	53.51
130	1,482,000	51.67	48,494	69.15	393,760	56.08
A-VTS	7.929	-2.524	9.560	-3.148	9.249	-3.011

Table E21. AC Properties Determined on Core Samples from Section 10060000 (continued).

Temp. (°F)	Lift 1 - Core B		Lift 2 - Core B		Lift 3 - Core B	
	Complex Modulus G* (Pa)	Phase Angle δ (°)	Complex Modulus G* (Pa)	Phase Angle δ (°)	Complex Modulus G* (Pa)	Phase Angle δ (°)
70	50,128,000	26.93	6,459,000	43.90	13,940,000	34.30
80	27,750,000	31.01	3,329,000	48.09	7,981,000	38.31
90	14,750,000	36.18	1,598,000	52.32	4,397,000	42.12
100	7,708,600	41.53	719,696	56.57	2,207,200	46.60
110	4,119,000	45.16	317,543	60.48	1,099,000	50.93
120	2,905,000	48.60	128,648	65.55	365,668	57.94
130	1,482,000	51.67	57,148	68.70	182,159	61.01
A-VTS	7.929	-2.524	9.362	-3.075	9.182	-2.996

	Gradation				Air Void %	Vol. binder Content (%)	Average Thickness (in)
Core A	Retain 3/4"	Retain 3/8"	Retain #4	#200P			
Lift 1	0.0	21.6	70.6	5.0	10.6	11.9	0.8
Lift 2	0.0	8.9	33.2	4.5	4.7	11.1	1.7
Lift 3	11.4	36.5	61.8	2.8	9.2	9.6	1.4
	Gradation				Air Void %	Vol. binder Content (%)	Average Thickness (in)
Core B	Retain 3/4"	Retain 3/8"	Retain #4	#200P			
Lift 1	0.0	21.6	70.6	5.0	11.0	11.9	0.8
Lift 2	0.0	8.9	33.0	4.4	6.7	11.1	1.9
Lift 3	4.2	32.8	59.8	2.9	6.0	10.6	1.5

Table E22. AC Properties Determined on Core Samples from Section 10160000.

Temp. (°F)	Lift 1 - Core A		Lift 2 - Core A		Lift 1 - Core B		Lift 2 - Core B	
	Complex Modulus G* (Pa)	Phase Angle δ (°)	Complex Modulus G* (Pa)	Phase Angle δ (°)	Complex Modulus G* (Pa)	Phase Angle δ (°)	Complex Modulus G* (Pa)	Phase Angle δ (°)
50	33,990,000	32.64	34,880,000	35.94	35,590,000	35.34	33,850,000	35.09
60	17,590,000	38.73	17,280,000	42.54	19,160,000	40.73	17,090,000	41.51
70	8,279,000	45.05	7,695,000	49.23	9,200,000	46.98	7,794,000	48.24
80	3,526,000	51.47	3,177,000	55.28	4,072,000	52.79	2,944,000	55.16
90	1,500,000	56.56	1,278,000	60.67	1,748,900	57.79	1,316,000	60.18
100	618,782	60.82	495,239	65.23	736,055	61.72	522,532	64.96
110	260,254	64.00	196,151	69.15	319,390	64.70	216,563	68.95
A-VTS	9.592	-3.160	9.829	-3.250	9.084	-2.974	9.789	-3.235

	Gradation				Air Void %	Vol. binder Content (%)	Average Thickness (in)
Core A	Retain 3/4"	Retain 3/8"	Retain #4	#200P			
Lift 1	0.0	5.8	28.4	4.0	7.7	11.7	1.4
Lift 2	0.0	6.2	29.2	7.9	5.5	12.9	1.5
	Gradation				Air Void %	Vol. binder Content (%)	Average Thickness (in)
Core B	Retain 3/4"	Retain 3/8"	Retain #4	#200P			
Lift 1	0.0	7.8	31.6	4.6	8.7	11.4	1.4
Lift 2	0.0	8.9	31.8	7.5	6.1	12.7	1.4

Table E23. AC Properties Determined on Core Samples from Section 16250000.

Temp. (°F)	Lift 1 - Core B		Lift 2 - Core B	
	Complex Modulus G* (Pa)	Phase Angle δ (°)	Complex Modulus G* (Pa)	Phase Angle δ (°)
70	8,406,000	43.76	9,995,000	42.56
80	3,971,000	48.94	4,914,000	47.71
90	1,736,000	54.24	2,218,000	52.85
100	762,291	58.26	979,182	56.97
110	339,932	61.67	423,751	60.67
120	141,608	64.83	143,703	64.76
130	61,522	67.64	58,827	66.84
A-VTS	9.424	-3.097	9.802	-3.233

	Gradation				Air Void %	Vol. binder Content (%)	Average Thickness (in)
Core A	Retain 3/4"	Retain 3/8"	Retain #4	#200P			
Lift 1	0.0	12.1	34.4	4.4	6.2	12.4	1.3
Lift 2	0.0	6.2	30.8	5.8	7.1	12.7	0.9
	Gradation				Air Void %	Vol. binder Content (%)	Average Thickness (in)
Core B	Retain 3/4"	Retain 3/8"	Retain #4	#200P			
Lift 1	0.0	12.1	34.4	4.4	6.2	12.4	1.2
Lift 2	0.0	6.2	30.8	5.8	7.1	12.7	1.1

Table E24. Dynamic Modulus (ksi) of Core Samples from Section 16250000.

Core	Temp (°F)	Frequency (Hz)			
		0.1	1	10	25
16250-2A	39.2	40.28	125.2	143.2	144.0
	68	69.8	94.8	106.4	123.1
	104	100.76	47.6	64.9	93.9
	130	129.92	25.3	46.5	69.2
16250-3A	40.6	525.6	618.1	702.1	735.0
	70.3	307.9	424.4	532.1	570.0
	100.2	80.5	140.5	245.5	294.4
	129.9	24.5	51.8	99.9	132.7
16250-2B	39.9	1433.9	1760.3	2070.1	2185.4
	70.2	622.5	933.0	1289.5	1435.2
	100.2	164.3	320.4	569.8	688.2
	129.9	42.9	103.8	215.1	286.6
16250-3B	40.3	1424.5	1746.6	2049.2	2165.8
	70.0	567.7	866.4	1208.0	1350.0
	99.7	150.5	304.4	551.7	666.9
	129.7	36.9	99.6	203.6	278.2

Table E25. AC Properties Determined on Core Samples from Section 50010000.

Temp. (°F)	Lift 2&3 - Core B		Lift 5&6- Core B	
	Complex Modulus G* (Pa)	Phase Angle δ (°)	Complex Modulus G* (Pa)	Phase Angle δ (°)
50	16,850,000	44.56	438,700	48.70
60	8,106,000	49.90	218,090	54.50
70	3,503,000	55.05	101,370	60.20
80	1,447,000	59.65	45,832	65.50
90	586,503	63.49	21,087	70.60
100	212,086	67.42	9,699	75.00
110	88,270	70.21	4,611	78.70
A-VTS	9.406	-3.104	8.84	-2.87

	Gradation				Air Void %	Vol. binder Content (%)	Average Thickness (in)
Core A	Retain 3/4"	Retain 3/8"	Retain #4	#200P			
Lift 2&3	0.0	7.6	30.4	8.4	4.7	14.6	1.6
Lift 5&6	0.4	10.2	28.2	6.4	4.4	9.9	2.1
	Gradation				Air Void %	Vol. binder Content (%)	Average Thickness (in)
Core B	Retain 3/4"	Retain 3/8"	Retain #4	#200P			
Lift 2&3	0.0	7.6	30.4	8.4	4.7	14.6	1.7
Lift 5&6	0.4	10.2	28.2	6.4	4.4	9.9	2.4

Table E26. Dynamic Modulus (ksi) of Core Samples from Section 50010000.

Core	Temp (°F)	Frequency (Hz)			
		0.1	1	10	25
50010-1A	40.1	991.3	1300.2	1628.6	1761.7
	70.0	348.5	574.8	874.7	1001.5
	100.0	156.5	282.4	512.8	627.8
	129.9	32.1	59.3	127.9	168.7
50010-2A	39.4	902.0	1174.5	1464.2	1592.0
	69.6	313.1	515.4	773.5	885.7
	99.5	79.9	163.0	320.7	403.0
	129.9	24.9	62.6	124.5	165.5
50010-3A	40.5	863.8	1132.1	1424.5	1571.9
	70.3	305.9	515.9	789.1	999.6
	100.9	82.1	168.2	337.5	427.8
	130.3	28.1	65.9	122.3	159.1
50010-4A	40.1	232.8	273.1	349.5	382.7
	70.0	110.4	160.4	219.1	253.2
	100.4	41.8	64.0	109.9	140.9
	129.7	19.4	33.7	61.0	79.4

Table E27. AC Properties Determined on Core Samples from Section 77040000.

Temp. (°F)	Lift 2 - Core A		Lift 3- Core A	
	Complex Modulus G* (Pa)	Phase Angle δ (°)	Complex Modulus G* (Pa)	Phase Angle δ (°)
70	7,382,000	46.19	999,000	44.26
80	3,415,000	51.47	468,333	51.14
90	1,515,000	56.19	238,333	53.87
100	635,232	60.69	121,000	56.69
110	274,191	64.71	60,733	59.93
120	107,410	68.55	32,800	62.62
130	44,717	72.28	18,400	65.75
A-VTS	9.781	-3.230	7.36	-2.33

	Gradation				Air Void %	Vol. binder Content (%)	Average Thickness (in)
Core A	Retain 3/4"	Retain 3/8"	Retain #4	#200P			
Lift 2	1.6	13.1	45.5	6.5	9.4	14.6	1.4
Lift 3	0.0	2.6	11.8	9.6	13.4	11.7	1.3
	Gradation				Air Void %	Vol. binder Content (%)	Average Thickness (in)
Core B	Retain 3/4"	Retain 3/8"	Retain #4	#200P			
Lift 2	1.6	13.1	45.5	6.5	9.4	14.6	1.5
Lift 3	0.0	2.6	11.8	9.6	13.4	11.7	1.2

Table E28. Dynamic Modulus (ksi) of Core Samples from Section 77040000.

Core	Temp (°F)	Frequency (Hz)			
		0.1	1	10	25
77040-2B	39.9	1158.8	1593.8	2029.0	2200.9
	69.8	335.9	631.5	1035.1	1211.0
	100.0	52.2	146.2	342.0	451.6
	130.1	8.3	18.3	59.7	104.4
77040-3B	39.9	1149.8	1554.0	1956.3	2111.8
	69.8	355.6	637.3	1008.7	1181.6
	100.4	67.4	168.2	364.2	467.7
	129.6	19.5	52.1	117.4	173.9

Texas Transportation Institute
The Texas A&M University System
College Station, TX 77843-3135
979-845-1734
http://tti.tamu.edu